

**Seismic Retrofitting of Local Contemporary Unreinforced  
Masonry Buildings with Soft Storey Basements subjected to  
Seismic Loading**

Sarah Chetcuti

Dissertation submitted to the Faculty for the Built Environment, University of Malta in part fulfilment of the requirements for the attainment of the degree of Master of Engineering (Structural Engineering)

July 2023



L-Università  
ta' Malta

## **University of Malta Library – Electronic Thesis & Dissertations (ETD) Repository**

The copyright of this thesis/dissertation belongs to the author. The author's rights in respect of this work are as defined by the Copyright Act (Chapter 415) of the Laws of Malta or as modified by any successive legislation.

Users may access this full-text thesis/dissertation and can make use of the information contained in accordance with the Copyright Act provided that the author must be properly acknowledged. Further distribution or reproduction in any format is prohibited without the prior permission of the copyright holder.

*To my parents*

## **Acknowledgements**

I want to begin by expressing my gratitude towards Professor Marc Bonello, B.E.&A.(Hons)(Melit.), M.Sc.(Lond.), Ph.D.(Lond.), D.I.C., M.A.S.C.E., M.S.E.I., Eur.Ing. (FEANI), Perit for his unwavering presence and invaluable guidance throughout the course of this dissertation.

Furthermore, I would also like to express my sincere appreciation to Gruppo Sismica, who has generously granted me a full license for the 3D Macro software package, which allowed me to conduct this study.

Additionally, I extend my sincere appreciation to the personnel at the Faculty for the Built Environment who provided me with a PC laptop to run the analyses required for this research.

Lastly, I would also like to express my heartfelt gratitude to my parents, Pio and Jacqueline Chetcuti, who made this opportunity possible for me. Their unwavering support has been instrumental in my journey.

I take full responsibility for any shortcomings in this dissertation.



**L-Università  
ta' Malta**

**FACULTY/INSTITUTE/CENTRE/SCHOOL** Faculty for the Built Environment

## **DECLARATIONS BY POSTGRADUATE STUDENTS**

### **(a) Authenticity of Dissertation**

I hereby declare that I am the legitimate author of this Dissertation and that it is my original work.

No portion of this work has been submitted in support of an application for another degree or qualification of this or any other university or institution of higher education.

I hold the University of Malta harmless against any third party claims with regard to copyright violation, breach of confidentiality, defamation and any other third party right infringement.

### **(b) Research Code of Practice and Ethics Review Procedures**

I declare that I have abided by the University's Research Ethics Review Procedures. Research Ethics & Data Protection form code BEN-2022-00072.

As a Master's student, as per Regulation 77 of the General Regulations for University Postgraduate Awards 2021, I accept that should my dissertation be awarded a Grade A, it will be made publicly available on the University of Malta Institutional Repository.

## **Abstract**

One of the main problems, which is often encountered within local methods of unreinforced masonry (URM) construction for masonry buildings is the Soft Storey Effect. A soft storey may be described as the abrupt reduced sway stiffness experienced by one level in a structure compared to the sway stiffness of the floors above and below. When considering the local context, this soft storey is generally found at Ground Floor or at basement level. In order to provide sufficient space for car parking within these buildings, the internal masonry partition shear walls and piers are often removed in the soft storey level. When these URM buildings are subjected to seismic forces, they may be unable to dissipate the earthquake energy due to a lack of robustness and structural ductility. The primary objective of this dissertation is to identify the adverse effects of seismic events upon the local contemporary URM building typology and to propose structural retrofitting strategies to mitigate these negative effects.

In addition, the proposed research study will allow the determination of how many storeys may be sustained during the design earthquake for the Maltese Islands by URM buildings with a typical floor plan layout, and which have been retrofitted to obtain the necessary horizontal sway stiffness and strength to resist the applied seismic forces. It is intended to determine whether such retrofitting interventions are feasible and whether they effectively provide the required seismic resistance enhancement.

The research methodology used in this dissertation involved both an analytical and a numerical approach. Throughout the first part of the seismic analysis, the EFM (Equivalent Force Method) was used in order to obtain the sway stiffness of each URM transverse wall within the URM building models considered. This sway stiffness was then replaced within the basement level using either structural steelwork or reinforced concrete transverse plane frames within the basement level, which were used as a seismic retrofitting technique to eliminate the Soft Storey Effect. Secondly, a more accurate numerical method, 3D Macro, was then utilised to carry out parametric Non-Linear Static Pushover Seismic Analyses of the URM building models, from which the building seismic vulnerability safety factors were then obtained.

The results showed that the negative impact seismic resistance of having an asymmetrical plan was very evident as several differences were observed in the seismic performance of masonry walls in the transverse direction of the URM buildings. In this research study, the comparison of seismic resistance between different URM buildings was carried out mainly with reference to the integer number of floors that can be safely carried by the buildings when subjected to the design earthquake for the Maltese Islands. Although this is a rather coarse yardstick for comparison, since it is not sensitive to subtle differences in structural behaviour between different URM buildings, the use of the building safety factors allowed a more refined comparison to be carried out.

The seismic analysis results also showed that a decrease in seismic performance occurred within those URM buildings, which were retrofitted with excessively stiff transverse plane frames at basement level, causing failure to occur within the ground floor rather than at basement level. Within single unit retrofitted URM buildings, the transverse structural steelwork plane frames at basement level experienced local buckling. This was not observed in the transverse structural steelwork plane frames at basement level within retrofitted URM building aggregates. However, generally, the retrofitted URM single unit buildings and URM building aggregates exhibited similar behaviour irrespective of the structural material used for the transverse plane frames at basement level. It was also observed that, as the number of single units within URM building aggregates increased, there was little additional benefit to the aggregate seismic resistance, since the benefit of additional sway stiffness was cancelled out by

the adverse effect of additional seismic weight. Furthermore, it was also observed that weaker subsoils gave rise to larger seismic amplifications, rendering the retrofitting techniques futile in certain cases.

**Keywords:** Seismic Retrofitting, Soft Storey, Non-Linear Static Pushover Analysis, Moment-Resisting Frames, Permissible Safe Building Height, Safety Factor

## Table of Contents

Acknowledgements.....	iii
Abstract.....	iv
List of Figures.....	xi
List of Equations.....	xiv
List of Tables.....	xv
Glossary.....	xvi
List of Symbols.....	xviii
Chapter 1: Introduction.....	18
1.1 Motivation Behind Research.....	18
1.2 Scope and Objectives.....	19
1.3 Layout of Dissertation.....	19
Chapter 2: Literature Review.....	20
2.1 Introduction.....	20
2.2 General Considerations.....	21
2.2.1 Background on Malta’s Seismology.....	21
2.2.2 Seismic Hazard, Seismic Risk and Seismic Vulnerability.....	22
2.2.3 Structural Vulnerability in Maltese URM Buildings.....	23
2.2.4 Earthquake Ground Motion Parameters.....	23
2.2.5 Factors affecting seismic activity.....	26
Chapter 3: Failure Modes of Unreinforced Masonry Buildings.....	30
3.1 Introduction.....	30
3.2 Walls.....	32
3.2.1 Wall Openings.....	33
3.2.2 In- Plane Loading.....	34
3.2.3 Out-of-Plane Loading.....	35
3.3 Diaphragms.....	36
3.4 Foundations.....	38
Chapter 4: Retrofitting Techniques.....	39
4.1 Introduction.....	39
4.2 Ties & Tie Rods.....	39
4.3 Steel Frames & Trusses.....	40
4.4 Seismic Bands (Ring Beams).....	41
4.4 Base Isolation.....	41



4.5 Jacketing .....	42
4.6 Wall-to-floor/roof connections .....	42
4.7 Grout Epoxy Injections .....	43
4.8 FRP/GFRP Systems .....	44
4.9 Post-tensioning Tendons .....	45
4.10 Ring Beams .....	45
Chapter 5: Seismic Vulnerability of Local URM Building Aggregates .....	46
5.1 Introduction.....	46
5.2 Building Configuration of Local URM Building Aggregates and their Seismic Response.....	47
5.2.1 Local Building Typologies and Characteristics .....	47
Chapter 6: Research Methodology.....	49
6.1 Lateral Stiffness of Masonry Walls .....	49
6.2 Retrofitting Plane Frames in the Soft Storey Basement.....	59
6.3 Non-Linear Static Pushover Analysis .....	63
6.3.1 General Introduction .....	63
6.3.2 3DMacro .....	64
6.4 Building Plans, General Layouts and Building Aggregate Combinations.....	67
6.4.1 Introduction.....	67
6.4.2 Plan Definition .....	70
6.5 Method of Seismic Analysis .....	71
6.5.1 Definition of Material Properties .....	71
6.5.2 Definition of Geometrical Properties .....	72
6.5.3 Numerical Model Build Up.....	73
6.5.4 Seismic Analysis .....	74
6.5.5 Limitations .....	76
Chapter 7: Discussion of Results .....	77
7.1 Introduction.....	77
7.2 One Unit.....	83
7.3 Two-Unit Aggregate .....	87
7.4 Three-Unit Aggregate .....	92
7.5 Four Unit Aggregate .....	96
7.6 Comparing across Ground Type A .....	100
7.7 Comparing across Ground Type B.....	105
7.8 Comparing across Ground Type C.....	110

Chapter 8: Conclusions and Recommendations for Future Research Work.....	115
8.1 Conclusions.....	115
8.2 Recommendations for Further Research Work.....	117
Bibliography .....	118
Appendix A: Design Parameters for 3DMacro Numerical Modelling .....	123
Appendix A.1 3DMacro General Settings & Geometric Settings .....	123
Appendix A.2 Material Definition .....	127
Appendix A.3 Section Design.....	130
Appendix B: Plans and Drawings of All Building Aggregates.....	136
Appendix B.1 Two-Unit Aggregate.....	136
Appendix B.2 Three-Unit Aggregate.....	137
Appendix B.3 Four-Unit Aggregate.....	138
Appendix C: Screenshots Showing Failure Mechanism at Failing Load Case.....	139
Appendix C.1 Single Unit, Ground Type A.....	139
No Retrofitting .....	139
Repeated Ground Floor.....	139
35% of $K_m$ Sway Stiffness in RC Frames .....	140
50% of $K_m$ Sway Stiffness in RC Frames .....	140
35% of $K_m$ Sway Stiffness in Steel Frames .....	141
50% of $K_m$ Sway Stiffness in Steel Frames .....	142
Appendix C.2 Single Unit, Ground Type B.....	143
No Retrofitting .....	143
Repeated Ground Floor.....	144
35% of $K_m$ Sway Stiffness in RC Frames .....	145
50% of $K_m$ Sway Stiffness in RC Frames .....	146
35% of $K_m$ Sway Stiffness in Steel Frames .....	147
50% of $K_m$ Sway Stiffness in Steel Frames .....	148
Appendix C.3 Single Unit, Ground Type C.....	150
No Retrofitting .....	150
Repeated Ground Floor.....	151
35% of $K_m$ Sway Stiffness in RC Frames .....	152
50% of $K_m$ Sway Stiffness in RC Frames .....	152
35% of $K_m$ Sway Stiffness in Steel Frames .....	153
50% of $K_m$ Sway Stiffness in Steel Frames .....	154

Appendix C.4 Two-Unit Aggregate, Type A.....	156
No Retrofitting .....	156
Repeated Ground Floor .....	157
35% of $K_m$ Sway Stiffness in RC Frames .....	158
50% of $K_m$ Sway Stiffness in RC Frames .....	159
35% of $K_m$ Sway Stiffness in Steel Frames .....	160
50% of $K_m$ Sway Stiffness in Steel Frames .....	161
Appendix C.5 Three-Unit Aggregate, Type A.....	162
No Retrofitting .....	162
35% of $K_m$ Sway Stiffness in RC Frames .....	163
50% of $K_m$ Sway Stiffness in RC Frames .....	164
35% of $K_m$ Sway Stiffness in Steel Frames .....	166
50% of $K_m$ Sway Stiffness in Steel Frames .....	167
Appendix C.6 Four-Unit Aggregate, Type A .....	169
No Retrofitting .....	169
Repeated Ground Floor .....	171
35% of $K_m$ Sway Stiffness in RC Frames .....	175
50% of $K_m$ Sway Stiffness in RC Frames .....	177
35% of $K_m$ Sway Stiffness in Steel Frames .....	178
50% of $K_m$ Sway Stiffness in Steel Frames .....	179
Appendix D: Typical Example of how all $\alpha$ – values were extracted from 3DMacro.....	180
Appendix D.1 Single-Unit Type A .....	180
No Retrofitting .....	180
Repeated Ground Floor .....	183
35% of $K_m$ Sway Stiffness in RC Frames .....	187
50% of $K_m$ Sway Stiffness in RC Frames .....	191
35% of $K_m$ Sway Stiffness in Steel Frames .....	193
50% of $K_m$ Sway Stiffness in Steel Frames .....	196

## List of Figures

<b>Figure 1</b> List of felt earthquakes in the Maltese Islands Source: (Galea, 2007) .....	21
<b>Figure 2</b> Accelerogram Comparison .....	25
<b>Figure 3</b> Acceleration Response Spectra for different local site conditions Source: Eurocode 8 (EN 1998) .....	27
<b>Figure 4</b> Subduction Zones Source: Hyndman & Wang, 1995 .....	28
<b>Figure 5</b> Mechanisms of motion of tectonic plates at their boundaries Source: (Tomazevic,1999) ....	28
<b>Figure 6</b> Propagation of seismic waves from the rock to the surface Source: (Tomazevic, 1999) .....	29
<b>Figure 7</b> Effect of soil-structure interaction Source: (Mylonakis & Gazetas, 2000) .....	30
<b>Figure 8</b> Deformation of the building and typical damage to structural wall Source: (Tomazevic, 1999) .....	30
<b>Figure 9</b> Masonry building during earthquake shaking a) loosely connected walls without slab at roof level, and b) a building with well-connected walls and a roof slab Source: (Tomazevic, 1999).....	32
<b>Figure 10</b> a) horizontal irregularity, b) vertical irregularity, c) offset irregularity, and d) variable openings number irregularity Source: (Parisi & Augenti, 2012) .....	33
<b>Figure 11</b> Diagonal Cracking due to different opening heights for (a,b) rightward and (c,d) leftward orientation of seismic action Source: (Parisi & Augenti, 2012) .....	34
<b>Figure 12</b> In-plane damage of stone masonry walls: a) typical wall with openings b) rocking failure, and c) diagonal shear cracking (adapted from Murty 2005) Source: (Bothara & Brzev, 2011) .....	34
<b>Figure 13</b> Typical failure modes of masonry piers a) rocking, b) sliding shear failure, and c) diagonal cracking Source: (Calderini et al., 2008) .....	35
<b>Figure 14</b> Collapse mechanisms due to out-of-plane action Source: (Ferreira et al., 2015) .....	35
<b>Figure 15</b> Rigid diaphragm action Source: (Murty et al., 2012) .....	36
<b>Figure 16</b> Load distribution across diaphragms Source: (Piazza et al., 2008) .....	37
<b>Figure 17</b> Pounding action on a) same-storey levels, b) different storey levels Source: (Brincat, 2020) .....	37
<b>Figure 18</b> Strengthening existing foundation a) underpinning the foundation, and b) external RC belt Source: (Bothara & Brzev, 2011) .....	38
<b>Figure 19</b> Plan view showing use of steel ties connected through anchor plates Source: Source: (Bothara & Brzev, 2011) adapted from (Tomazevic, 1999) .....	39
<b>Figure 20</b> Retrofitting of Moorhouse Avenue using Vertical Trusses Source: (Abeling, Dizhur, & Ingham, 2018) .....	40
<b>Figure 21</b> Base shear-to-weight ratio for varying storey levels in comparison to existing Source: (Ismail, 2019) .....	40
<b>Figure 22</b> Application of seismic bands Source: (Bothara & Brzev, 2011) adapted from (Murty, 2005) .....	41
<b>Figure 23</b> Jacketing layered process Source: (Bothara & Brzev, 2011) .....	42
<b>Figure 24</b> Steel straps for wall-to-floor anchorage: a) floor beams perpendicular to wall and b) floor beams parallel to wall Source: (Bothara & Brzev, 2011) adapted from (UNIDO, 1983).....	43
<b>Figure 25</b> Grout Procedure Source: (Elsayed & Ghanem, 2017).....	43
<b>Figure 26</b> Strengthening of walls through GFRP Source: (Triller et al., 2017) .....	44
<b>Figure 27</b> Use of RC ring beams Source: (Brincat, 2020) adapted from (Ferreira et. al., 2015) .....	45

<b>Figure 28</b> (left) Two skins of 230mm soft stone with a 50mm cavity, total 510mm and (right) Two skins of 160mm soft stone, typically with no cavity, total 360mm Source: (Buhagiar & Tonna, 2012)	47
<b>Figure 29</b> left) Fixed-fixed Sway Column, (right) Pinned-fixed Sway Column Source: (Alexander, 2010)	50
<b>Figure 30</b> Shear Wall with openings Source: (Taly, 2010)	55
<b>Figure 31</b> Typical locations of hinges within a structural model Source: (Leslie, 2012)	63
<b>Figure 32</b> (left) Modelling of a typical edge panel in its deformed state, (right) Wall modelled using a mesh of inter-connected macro-element quadrilaterals Source: (Brincat, 2020) adapted from Left: (Formisano & Chieffo, 2018) Right: 3DMacro Manuale Teorico	64
<b>Figure 33</b> Equivalent mechanical representation of the macro-element (left) The plane macro-element (right) The spatial macro-element Source: Panto et al. (2016)	65
<b>Figure 34</b> (a) Simplification of numerical model using 3D Macro (b) Resulting collapse mechanism Source: 3D Macro Manuale Teorico	66
<b>Figure 35</b> Typical layout plan (left) basement level (right) all upper floors Source: (Author, 2023) 225mm thick Cast-in-situ Concrete Slab	69
<b>Figure 36</b> Typical layout plan (left) basement level (right) all upper floors Source: (Author, 2023)	73
<b>Figure 37</b> Extract from NTC 2018 Cl. 3.2.1	74
<b>Figure 38</b> Comparison between No Retrofitting vs Repeated GF in SLC	77
<b>Figure 39</b> Comparison between No Retrofitting vs 35% of $K_m$ sway stiffness in RC in SLC	79
<b>Figure 40</b> Comparison between No Retrofitting vs 50% of $K_m$ sway stiffness in RC in SLC	80
<b>Figure 41</b> Comparison between No Retrofitting vs 35% of $K_m$ sway stiffness in Steel in SLC	81
<b>Figure 42</b> Comparison between No Retrofitting vs 50% of $K_m$ sway stiffness in Steel in SLC	82
<b>Figure 43</b> Results indicating number of floors sustained by each retrofitting technique in a One Unit building	85
<b>Figure 44</b> Results indicating alpha values of each retrofitting technique in a One Unit building	86
<b>Figure 45</b> Results indicating alpha values of each retrofitting technique in a Two-Unit aggregate	89
<b>Figure 46</b> Results indicating number of floors sustained by each retrofitting technique in a Two-Unit aggregate	90
<b>Figure 47</b> Results indicating alpha values of each retrofitting technique in a Two-Unit aggregate	91
<b>Figure 48</b> Results indicating number of floors sustained by each retrofitting technique in a Three-Unit aggregate	94
<b>Figure 49</b> Results indicating alpha values of each retrofitting technique in a Three-Unit aggregate	95
<b>Figure 50</b> Results indicating number of floors sustained by each retrofitting technique in a Four-Unit aggregate	98
<b>Figure 51</b> Results indicating alpha values of each retrofitting technique in a Four-Unit aggregate	99
<b>Figure 52</b> Results indicating number of floors sustained by each retrofitting technique across the 1 unit building and all building aggregates for Ground Type A	103
<b>Figure 53</b> Results indicating the safety factor in terms of alpha by each retrofitting technique across the 1 unit building and all building aggregates for Ground Type A	104
<b>Figure 54</b> Results indicating number of floors sustained by each retrofitting technique across the 1 unit building and all building aggregates for Ground Type B	108
<b>Figure 55</b> Results indicating the safety factor in terms of alpha by each retrofitting technique across the 1 unit building and all building aggregates for Ground Type B	109
<b>Figure 56</b> Results indicating number of floors sustained by each retrofitting technique across the 1 unit building and all building aggregates for Ground Type C	113

**Figure 57** Results indicating the safety factor in terms of alpha by each retrofitting technique across the 1 unit building and all building aggregates for Ground Type C ..... 114

## List of Equations

<b>Equation 1</b> Seismic Risk.....	22
<b>Equation 2</b> Duration.....	24
<b>Equation 3</b> Acceleration Spectra .....	25
<b>Equation 4</b> Velocity Spectra .....	25
<b>Equation 5</b> Damping Force .....	26
<b>Equation 6</b> Sway Stiffness of Pinned-Base Columns .....	49
<b>Equation 7</b> Sway Stiffness of Fixed-Base Columns .....	49
<b>Equation 8</b> Seismic Mass.....	52
<b>Equation 9</b> Factor for combination value of a variable action.....	52
<b>Equation 10</b> Fundamental Period of Vibration .....	54
<b>Equation 11</b> Base Shear Force.....	54
<b>Equation 12</b> Base Shear Force in terms of seismic weight of the building .....	54
<b>Equation 13</b> Horizontal Distribution of Base Shear Force .....	54
<b>Equation 14</b> Total Deflection of the Wall.....	55
<b>Equation 15</b> Rigidity of the wall.....	55
<b>Equation 16</b> Rigidity of a cantilever wall .....	56
<b>Equation 17</b> Rigidity of a fixed pier .....	56
<b>Equation 18</b> Moment of Inertia for a pinned-fixed column.....	59
<b>Equation 19</b> Moment of Inertia of fixed-pinned column.....	59
<b>Equation 20</b> Stiffness of masonry wall.....	59
<b>Equation 21</b> Smearred property equation Source: Borg (2021) adapted from Brincat (2020) .....	71

## List of Tables

<b>Table 1</b> Site seismic history for the Maltese Islands since 1500, showing EMS-98 intensity $\geq$ IV Source: (Borg et al., 2010).....	22
<b>Table 2</b> Wave propagation in various types of soil Source: (Tomazevic, 1999).....	29
<b>Table 3</b> Compressive Strength of Masonry Source: (Camilleri, 1988) .....	31
<b>Table 4</b> Recommended maximum distance between structural walls Source: (Tomazevic, 1999) .....	32
<b>Table 5</b> Accumulation of Dead Load Source: (Author, 2023) .....	51
<b>Table 6</b> Final Dead Load & Live Load values Source: (Author, 2023) .....	52
<b>Table 7</b> Result values for seismic weight Source: (Author, 2023).....	53
<b>Table 8</b> EN1990:2002 Annex A1, Table A1.1 .....	53
<b>Table 9</b> Division of each wall segment into solid, strip and pier Source: (Author, 2023) .....	57
<b>Table 10</b> Continuation of Table 9 Source: (Author, 2023) .....	58
<b>Table 11</b> Rigidity of each wall Source: (Author, 2023) .....	58
<b>Table 12</b> Required structural steelwork column sections for plane frame with equivalent sway stiffness of the stone masonry walls Source: (Author, 2023) .....	62
<b>Table 13</b> Mechanical Properties of Masonry Blocks and Mortar Source: Borg (2021) adapted from Brincat (2020) .....	71
<b>Table 14</b> Smeared Properties of Masonry Source: Borg (2021) in Brincat (2020).....	72
<b>Table 15</b> Results for One Unit, Ground Type A, B and C respectively .....	84
<b>Table 16</b> Results for Two Unit, Ground Types A, B and C respectively.....	89
<b>Table 17</b> Results for Three-Unit aggregates, Ground Type A, B and C respectively .....	93
<b>Table 18</b> Results for Four-Unit aggregate, Ground Types A, B and C respectively.....	97
<b>Table 19</b> Results for Ground Type A, No Retrofitting.....	101
<b>Table 20</b> Results for Ground Type A, Repeated Ground Floor .....	101
<b>Table 21</b> Results for Ground Type A, 35% of $K_m$ sway stiffness in RC Frames .....	101
<b>Table 22</b> Results for Ground Type A, 50% of $K_m$ sway stiffness in RC Frames .....	102
<b>Table 23</b> Results for Ground Type A, 35% of $K_m$ sway stiffness in Steel Frames .....	102
<b>Table 24</b> Results for Ground Type A, 50% of $K_m$ sway stiffness in Steel Frames .....	102
<b>Table 25</b> Results for Ground Type B, No Retrofitting.....	106
<b>Table 26</b> Results for Ground Type B, Repeated Ground Floor.....	106
<b>Table 27</b> Results for Ground Type B, 35% of $K_m$ sway stiffness in RC Frames .....	106
<b>Table 28</b> Results for Ground Type B, 50% of $K_m$ sway stiffness in RC Frames .....	107
<b>Table 29</b> Results for Ground Type B, 35% of $K_m$ sway stiffness in Steel Frames.....	107
<b>Table 30</b> Results for Ground Type B, 50% of $K_m$ sway stiffness in Steel Frames.....	107
<b>Table 31</b> Results for Ground Type C, No Retrofitting.....	111
<b>Table 32</b> Results for Ground Type C, Repeated Ground Floor.....	111
<b>Table 33</b> Results for Ground Type C, 35% of $K_m$ sway stiffness in RC Frames .....	111
<b>Table 34</b> Results for Ground Type C, 50% of $K_m$ sway stiffness in RC Frames .....	112
<b>Table 35</b> Results for Ground Type C, 35% of $K_m$ sway stiffness in Steel Frames.....	112
<b>Table 36</b> Results for Ground Type C, 50% of $K_m$ sway stiffness in Steel Frames.....	112



## **Glossary**

3D	Three Dimensional
AG	Aggregate System
DLR	Damage Limitation Requirement
DRS	Design Response Spectra
DS	Displacement Spectra
EC8	Eurocode 8
ELF	Equivalent Lateral Force
ERS	Elastic Response Spectra
EN1991-1-1	Eurocode 1 Part 1
EN1998-1	Eurocode 8 Part 1 or Part 3
FRP	Fiber Reinforced Polymer
GF	Ground Floor
GFRP	Glass Fiber Reinforced Polymer
HCB	hollow concrete blockwork
MDOF	Multi Degree of Freedom
NCR	No Collapse Requirement
NTC 2018	Ministerial Decree of 17 January 2018 Technical Standards for Construction
PC	Personal Computer
PGA	Peak Ground Acceleration
PGD	Peak Ground Displacement
PGV	Peak Ground Velocity
PHA	Peak Horizontal Acceleration
PHV	Peak Horizontal Velocity
PSA	Acceleration Spectra
PSV	Velocity Spectra
RC	Reinforced Concrete
SD	Significant Damage Limit State
SDOF	Single Degree of Freedom
SLC	Collapse Prevention Limit State

SLD	Damage Limit State
SLE	Service Limit State
SLO	Operational Limit State
SLV	Life Protection Limit State
SU	Single Unit
ULS	Ultimate Limit State
URM	Unreinforced Masonry

## List of Symbols

$A_b$	Area of one singular masonry block
$A_m$	Area filled with mortar taken at elevation
$E$	Young's Modulus of Elasticity
$E_b$	Young's Modulus of Elasticity of Limestone Block
$E_m$	Young's Modulus of Elasticity of Mortar
$E_{\text{masonry}}$	Young's Modulus of Elasticity of Masonry
$E_{\text{steel}}$	Young's Modulus of Elasticity of Steel
$F$	Damping force
$F_b$ (or $V_b$ )	Base Shear Force
$f_{mk}$	Characteristic Strength of Masonry
$F_{k_{bm}}$	Compressive strength
$F_{t_{bm}}$	Tensile strength
$F_i$	Horizontal force at the seismic level
$g$	Acceleration due to gravity
$G_b$	Shear Modulus of Elasticity of Block
$G_{bm}$	Shear Modulus of the Smeared Properties of the Masonry Unit and Mortar
$G_m$	Shear Modulus of Elasticity of Mortar
$G_{k,j}$	Dead Load
$H$	Height of the building
$h/I_w$	Aspect Ratio
$I$	Moment of Inertia
$K_m$	Sway Stiffness of Masonry
$K_s$	Sway Stiffness of Steel
$L$	Length of column
$M$	Mass
$M_i$	Mass at each seismic level
$M_s$	Magnitude
$Q_{k,j}$	Live Load
$R_c$	Rigidity of a cantilever wall

$R_f$	Rigidity of a fixed pier
$R_w$	Rigidity of Wall
$S_e$	Peak acceleration
$S_d(T_1)$	Design spectrum at time period, $T_1$
$t$	Wall thickness
$T$	Fundamental period of vibration
$T_n$	natural period of vibration
$w$	Cumulative Seismic Load
$X_b$	Material property of masonry block
$X_m$	Material property of mortar block
$X_t$	Final smeared material property value
$\zeta$	Damping ratio
$\Psi$	Live Load reduction factor
$\varphi$	Dynamic magnification factor
$\Psi_{2,1}$	factor for combination value of a variable action
$\lambda$	Correction factor
$\tau_{bm}$	Shear strength of the Smeared Properties of the Masonry Unit and Mortar
$\alpha$	Safety Factor at a particular limit state (SLV, S

## **Chapter 1: Introduction**

### **1.1 Motivation Behind Research**

Historical records with regards to earthquakes that occurred in the Maltese Islands go as far back as the year 1530. There are no records of any casualties caused by these earthquakes, however, there is considerable data available with regards to the structural damage sustained by the local buckling stock due to earthquake action. One must also bear in mind that some of the available records are insufficient and lack certain detailed technical information. Malta is also located at the centre of a complex system of seismic faults. In fact, some of these faults are still active. Thus, structural retrofitting of existing unreinforced masonry (URM) buildings would be of great benefit and importance in order to re-instate the corresponding seismic resistance of these buildings.

Unreinforced masonry construction in Malta has been widely used for both historic and contemporary buildings due to its versatile qualities as a building material. Over the past few years, Malta has seen an unprecedented increase in building floor heights due to the relaxation of planning regulations, and yet there has not been any tangible improvement in the local URM construction methods in use. A rather worrying factor, which has been observed in recent years is the increase in wall slenderness due to the use of 180mm thick masonry partition walls instead of the traditional 230mm thick walls. Furthermore, the recent increase in the demand for housing, has brought about the phenomenon of having a large cluster of construction sites ongoing at the same time. In this respect, this could imply that several adjacent structures may need retrofitting so as to provide adequate sway resistance, which may be compromised during the construction stage. The current local construction system seems to lack the required information of how local URM buildings would respond to any ground shaking and, thus it is unfortunately often disregarded at the design and construction stages.

The primary objective of this dissertation would be to ultimately identify the adverse effects of seismic events upon the local contemporary URM building typology and to propose structural retrofitting strategies to mitigate these effects. Furthermore, various building typologies and configurations may be considered when retrofitting such URM buildings, such as using buckling restrained-braced frames and fluid viscous dampers.

In addition, the proposed research study will allow the determination of how many storeys may be sustained during the design earthquake for the Maltese Islands by URM buildings with a typical floor plan layout, and which have been retrofitted in order to obtain the necessary horizontal sway stiffness and strength so as to resist the applied seismic forces.

The structural efficiency of such retrofitting techniques may then be determined by comparing the seismic resistance of retrofitted and unretrofitted URM buildings, with the seismic resistance of the latter buildings being obtained from the results of several past research studies on local URM buildings. It is intended to determine whether such retrofitting interventions are economical, whether they provide the required seismic resistance enhancement and whether they impose any form of risk to the URM structure itself and, possibly, to adjacent URM structures.

## 1.2 Scope and Objectives

This study aims to determine the number of additional floors that an existing URM building can withstand once seismic retrofitting interventions are implemented into the URM structure. Furthermore, it seeks to obtain knowledge on which of these seismic retrofitting interventions are deemed to be the most structurally effective. The layout typologies chosen all have the soft storey effect at basement level. This dissertation shall also be taking into consideration a mortar strength of  $2\text{N/mm}^2$  together with one of the main building materials, namely Globigerina Limestone.

Legislation in Malta does not yet pose an obligation on local Periti to consider seismic action in the design of buildings. By means of a numerical research methodology, this research study aims to investigate whether local URM buildings with soft storey basements are capable of withstanding the effects of an earthquake in addition to vertical gravity loading, and how to implement effective strength retrofitting techniques in order to enhance the seismic resistance of these buildings. In this respect, the research questions considered in this dissertation as stated below:

1. What is the seismic resistance of local URM buildings with soft storey basements?
2. What is the effectiveness of strength retrofitting techniques in enhancing the seismic resistance of local URM buildings with soft storey basements?

## 1.3 Layout of Dissertation

In this first chapter, a brief introduction was provided with respect to the local URM construction and its seismic vulnerability to earthquake events. The research methodology and the research questions considered in this study are also presented. Chapter 2 provides a literature review, while Chapter 3 discusses the principal failure modes encountered in local unreinforced masonry (URM) construction. Chapter 4 provides an overview of the most common types of strength retrofitting techniques available, while Chapter 5 focuses upon the seismic vulnerability of local URM building aggregates. Chapter 6 presents the research methodology employed in this dissertation, namely numerical seismic analysis using a proprietary macro-element software program, 3D Macro. Chapter 7 presents the seismic analysis results and the corresponding interpretation of these results. Finally, Chapter 8 gathers the main conclusions derived from this dissertation and also provides recommendations for future research work within this field of study.

## **Chapter 2: Literature Review**

### **2.1 Introduction**

Masonry is a building material, which is widely used across the Maltese Islands in unreinforced masonry (URM) building construction. It is commonly used, since it conveys a satisfactory ability to withstand compressive loads. However, it does not perform as well when it experiences tensile loads due to overturning moments caused by seismic actions (Vella, 2018).

A previous study by (Galdes, 2013) concluded that a local unreinforced masonry (URM) building, should be able to maintain its structural integrity during an earthquake with a Peak Ground Acceleration (PGA) of 0.10g if it has 3 storeys when constructed on rock or if it has two storeys if it is built on a clay subsoil. Marmara' (2016) concluded that any two-storey building, whose ground strata is either rock or clay, and which is composed of only 3 transverse shear walls to withstand lateral seismic loading, would collapse in the event of an earthquake. Marmara' (2016) then proceeded to carry out a study on the same URM structures including reinforced concrete transverse plane frames at basement level situated underneath transverse masonry shear walls at Ground Floor level that were not brought down to the basement level, in order to mitigate the soft storey effect. However, the results obtained showed that additional transverse sway stiffness was required to provide satisfactory structural performance of the URM building during an earthquake.

In addition, Borg (2017) determined that, retrofitting an open plan basement using sway resisting plane frames may only be considered to be beneficial up to a particular number of storeys above the ground. It was also concluded that the design variable, which was deemed to be the most critical with respect to seismic resistance of URM buildings, was the mortar strength.

In view of the above, it was decided that this research study would focus upon several different retrofitting methods with the aim of providing the necessary anti-seismic sway stiffness to the local URM building typology. This research work shall, therefore, also attempt to highlight the inherent weaknesses associated with local URM buildings subjected to seismic loading.

## 2.2 General Considerations

### 2.2.1 Background on Malta's Seismology

Malta's earthquake catalogue dates back to 1530. Information which has been collected over a number of years provide a relatively detailed description of the structural damages sustained by certain building stock in the Maltese Islands. As stated by Galea (2007), *"In this catalogue time period, the islands experienced EMS-98 intensity VII-VIII once (11 January 1693) and intensity VII, or VI-VII five times."*

It is important to note that there are no historical records of any deaths due to seismic events locally and, thus this fact has generally tended to a lack of public awareness of the possible dangerous effects of the local seismic hazard and a general complacency in the implementation of seismic building regulations by local authorities in the local building construction industry. Seismicity in Malta is primarily brought about by the northern segment of the Malta Escarpment, the seismic zones of plate boundaries and the active faults, which lie within the Sicily Channel Rift Zone. (Borg et al., 2008). Earthquakes emerging from the large Hellenic Arc also seem to impose a level of Seismic Hazard. (Galea, 2007)

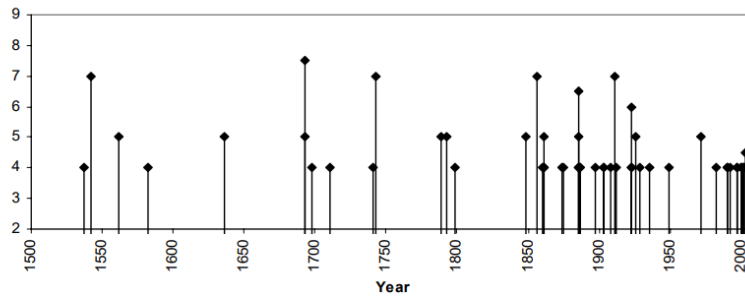


*Figure 1 List of felt earthquakes in the Maltese Islands*  
Source: (Galea, 2007)



Table 1 provides an accurate account of intensities and the magnitude of all seismic events, which were felt in the Maltese Islands since 1530. Galea (2007) suggested that buildings in the Maltese Islands should be designed to withstand an earthquake with a Peak Ground Acceleration (PGA) of 0.10g with a return period of 475 years to Eurocode 8 (EN 1998).

**Table I.** Subset of felt earthquake catalogue, showing only events that produced EMS-98  $I=V$  and over on the Maltese islands.

Year	Month	Day	Hour	Lat	Long	Region	$I_{max}$ on Maltese islands	$I_o$	$M$	Parameter reference
1542	12	10	15:15	37.20	14.90	E. Sicily	VII	XI	$M_w$ 6.6	Gruppo di Lavoro CPTI (2004)
1562	3	8	Morning			Sicily Channel?	V?			
1636	9	1				Sicily Channel(?)	V?			
1693	1	11	13:30	37.18	15.02	E. Sicily	VII-VIII	XI	$M_w$ 7.4	Boschi <i>et al.</i> (2000)
1743	2	20	16:30	39.87	18.78	Ionian Sea	VII	IX	$M_w$ 6.9	Gruppo di Lavoro CPTI (2004)
1789	1	19	Morning			Sicily Channel(?)	V?			
1793	2	26	Morning			Sicily Channel?	V?			
1848	1	11	12:00	37.20	15.20	E. Sicily	V	VIII-IX	$M_w$ 5.5	Gruppo di Lavoro CPTI (2004)
1856	10	12	00:45	35.60	26.00	Crete	VII		$M_w$ 7.7	Papazachos <i>et al.</i> (2000)
1861	2	8	23:45			Sicily Channel(?)	V?			
1886	8	15	02:45			Sicily Channel(?)	V			
1886	8	27	22:00	37.00	27.20	Aegean Sea	VI-VII	XI	$M_w$ 7.3	Papazachos <i>et al.</i> (2000)
1911	9	30	09:25	36.4?	13.5?	Sicily Channel	VII			
1923	9	18	07:30	35.5?	14.5?	Sicily Channel	VI			ISC (2001)
1926	6	26	19:46	36.50	27.50	Aegean Sea	V		$M_w$ 7.6	Papazachos <i>et al.</i> (2000)
1972	3	21	23:06	35.80	15.00	Sicily Channel	V		$M_b$ 4.5	ISC (2001)

**Table I** Site seismic history for the Maltese Islands since 1500, showing EMS-98 intensity  $\geq IV$   
Source: (Borg *et al.*, 2010)

### 2.2.2 Seismic Hazard, Seismic Risk and Seismic Vulnerability

Seismic risk and seismic hazard provide two entirely distinct ideas. Seismic hazard may be defined as the probability of harmful occurrences caused due to seismic action, leading to numerous socio-economic concerns. Therefore, it encompasses parameters, such as resultant ground motions, their frequencies, fault rupture, soil liquefaction and ground vibration. On the other hand, seismic risk is the possibility of exposure to seismic hazard within a stipulated time (return) period. The principal outcomes of seismic risk would be structural damage sustained by buildings. Both parameters are not necessarily directly proportional to one another, and thus low seismic risk may not necessarily mean low seismic hazard (Wang, 2006). Seismic vulnerability deals with the fragility or robustness of a particular structure. Low seismic vulnerability would result in high seismic resistance.

$$\text{Seismic Risk} = \text{Seismic Hazard} \times \text{Vulnerability}$$

**Equation 1** Seismic Risk

Over the years, the Maltese Islands have been categorised as a low-to-moderate seismicity region, however, earthquakes of large magnitudes took place in the vicinity of the Maltese Islands, and thus it is important to consider the seismic risk of local buildings in Malta. In addition, the islands have also witnessed an increasing population, which results in a higher demand for housing and a consequent trend for constructing higher buildings due to the scarcity of land.

### **2.2.3 Structural Vulnerability in Maltese URM Buildings**

A local URM building with an irregular plan layout gives rise to torsion as the centre of stiffness and the centre of mass (which is the point through which the resultant horizontal seismic inertial forces act at each floor of the URM building) do not act at the same point on plan. In such buildings, the plan eccentricities between these two centres in both plan directions would lead to irregular deformation and sway displacements. Furthermore, any imperfections in the design and construction of local URM buildings may lead to catastrophic structural damage under the influence of seismic action. These imperfections may be defined in terms of irregular layouts as load transfer to the building foundations becomes more complex. Local stresses, which exceed the strength of the main structural elements might also occur. The effects of these imperfections are further exacerbated by the effects of a soft-storey basement (devoid of transverse walls for functional reasons, such as car parking), which produce a significant reduction in the structural lateral stiffness. Adequate shear transfer across a structure requires uniform thickness of walls, which might not always be the case, thus creating large eccentricities, which are then transferred to the foundations.

Malta's streetscape is defined through varying heights of URM buildings. When evaluating such buildings from a seismic response perspective, different frequencies of vibration are expected (Borg et al., 2008).

### **2.2.4 Earthquake Ground Motion Parameters**

Ground Motion factors may be distinguished depending on the point of origin (source), path and also site effects. Whilst assessing ground motion behaviour during seismic action, the parameters, which prove to be most important would be the maximum amplitude, duration and frequency content. However, it is important to keep in mind that such factors vary depending on their site location and site conditions. This can be observed through varying effects experienced by different locations throughout the same seismic event.

#### **2.2.4.1 Duration**

Duration with respect to earthquake ground motion may be defined as being the period at which the ground begins to experience seismic waves up to the point it returns to its original condition. Shoji et al. (2004) also emphasize that, during the same earthquake event, the duration of the earthquake ground motion varies based on site location.

Throughout the research work carried out by Shoji et al. (2004), design parameters, such as peak ground acceleration, duration and seismic intensity were categorised into two, namely the site or the event. It was concluded that, in both categories, the results of duration vs amplitude vary inversely as follows:

$$0.05 \leq \frac{\int_0^t a^2(t)dt}{\int_0^T a^2(t)dt} \leq 0.95$$

*Equation 2 Duration*

### **2.2.4.2 Peak Ground Acceleration (PGA), Peak Ground Velocity (PGV) and Peak Ground Displacement (PGD)**

One of the most important design parameters used to describe seismic action is the Peak Ground Acceleration (PGA). It is defined as causing the greatest seismic force, which is induced onto a rigid body. This definition takes into consideration forces acting in the x, y, and z directions. The PGA is typically a high frequency motion. At times, it is also possible to use Peak Ground Velocity (PGV) in order to describe seismic action for structures, which happen to have a relatively longer natural period of vibration, such as bridges. In this case, the frequency of ground motion is generally of intermediate intensity.

Peak Ground Displacement (PGD) is not a design parameter, which is regularly used to describe seismic action. However, it is generally governed by a low frequency of ground motion. It is mainly considered appropriate when dealing with structures, which have a prolonged natural period of vibration.

Amplitude parameters are frequently measured through accelerograms. For instance, if one seeks to obtain a measure of the equivalent horizontal force of a particular structure throughout the occurrence of seismic action, it would be required to simply multiply the mass of the structure with the peak ground acceleration (PGA). Amplitude parameters may be misleading for the simple reason that a greater PGA does not necessarily mean that a greater structural damage is sustained by the building. A building may experience a lower PGA, but greater energy, and thus greater structural damage would be expected.

### **2.2.4.3 Frequency Content Elastic Response Spectra**

The intensity of an earthquake event is generally defined with respect to the ground acceleration and its variability across a time (return) period. Obviously, the ground acceleration differs with every earthquake event, which takes place. There are various methods by which this response may be measured. Elghazouli (2017) explains how the Duhamel's integral approach may be used for this purpose, where *'the earthquake record is treated as a sequence of short impulses, and the time-varying responses to each impulse are summed to give the total response'*.

The main aim of plotting acceleration response spectra is to determine the peak (maximum displacement/ acceleration/ velocity) value at which a single degree of freedom (SDOF) structure has responded to one particular earthquake event. In addition, when comparing different acceleration response spectra of different earthquake events, it is possible to notice similarities in the frequency content and their nature. These comparisons provide a better understanding of the behaviour of such events and how they can be considered for earthquakes in the future.

As previously described, there are essentially three types of elastic acceleration response spectra, namely:

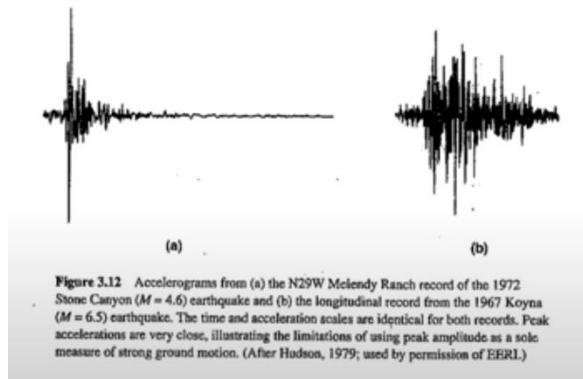


**Figure 2 Accelerogram Comparison**

1. Displacement Response Spectra (PSD): The purpose of a PSD is to obtain the maximum displacement of a SDOF system, whilst being subject to varying natural period of vibration and also damping.
2. Acceleration Response Spectra (PSA): This parameter is dependent on the displacement response spectra. Stratan (2014) defines ERS as ‘*the equivalent static force induced in an elastic structure with a unit mass*’.

$$PSA = \left(\frac{2\pi}{T}\right)^2 \cdot PSD$$

**Equation 3 Acceleration Spectra**

3. Velocity Spectra (PSV): This parameter is dependent on the displacement spectra. Stratan (2014) defines PSV as ‘*related to the maximum strain energy induced in the system*’.

$$PSV = \frac{2\pi}{T} \cdot PSD$$

**Equation 4 Velocity Spectra**

Eurocode 8 categorises two types of elastic response spectra, namely Type 1 which deals with high seismicity areas ( $M_s > 5.5$ ), and Type 2 which deals with moderate seismicity areas ( $M_s \leq 5.5$ ). These categories are further subdivided into segments depending on varying types of soil, as follows:

A: Rock

B: Very dense sand or gravel

C: Dense sand or gravel, or stiff clay

D: Loose-to-medium cohesionless soil, or soft-to-firm cohesive soil

E: Soil profiles with a surface layer of alluvium of thickness 5 to 20m. These elastic response spectra take into consideration 5% as a structural damping ratio.

Ultimately, the aim is to determine the lateral force being applied onto the structure and also the maximum displacement, which it is subjected to. From the above graphs, it is possible to determine  $S_e$ , which is the peak spectral acceleration, and also to approximate values for the natural period of vibration ( $T_n$ ) and the damping ratio  $\zeta$ .

When the structure experiences a damping force of zero, this would mean that the acceleration is at a maximum, and so is the displacement.

$$F = mSe$$

*Equation 5 Damping Force*

### **2.2.5 Factors affecting seismic activity**

The main parameters, which directly influence the behaviour of a building under seismic action include:

- Local site conditions
- Source Factors
- Path Effects
- Soil-Structure Relationship

#### **2.2.5.1 Local Site Conditions**

The soil layers found below a structure directly influence its response to ground motion. One of the effects, which may take place, would be soil amplification. Soil amplification varies for all ground materials whether it is rock, stiff soil, deep cohesionless soil or soft-to-medium clays and sands. Stiff soils tend to perform similar to rock, but with greater amplifications due to ground motion. The softer the ground material, the response spectra tend to stretch in the outward direction, and thus indicating

higher periods of vibration, which, in turn, produce greater amplification. On the other hand, rock and possibly harder soils generate low amplifications. Not only does it affect amplitudes, but also the duration and frequency content, which immediately bring about a change in the magnitude of the earthquake being experienced and also a difference in structural damage sustained by the building.

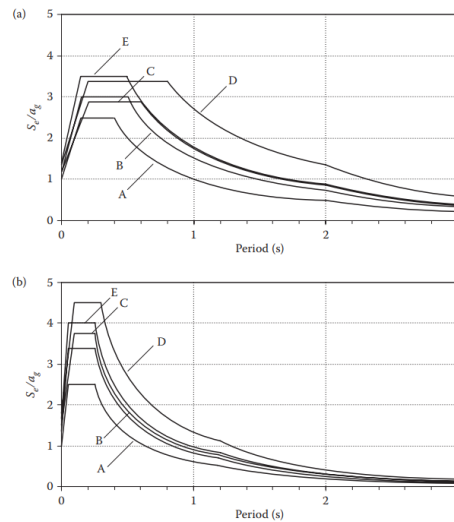


**Figure 3** Acceleration Response Spectra for different local site conditions  
Source: Eurocode 8 (EN 1998)

### 2.2.5.2 Source Factors

Stratan (2014) discusses the tectonic regimes as source factors. Tectonic regimes are essentially subdivided into the following categories:

- Active Regions (Inter-Plate Earthquakes)

The active regions are those earthquakes, which happen at large magnitudes. This would mean that large peak ground accelerations, durations and intensities are experienced.

- Interior of Tectonic Plates (Intra-Plate Earthquakes)

On the other hand, these earthquakes are of a much lower magnitude than those described above. These earthquakes are defined through lower frequency content, duration and intensities.

- Subduction Zones

Subduction zones are areas where two tectonic plate boundaries converge to a point, however, one plate rises above the other. The accumulation of stress occurs as the plates interlock with one another. Once an earthquake occurs, this energy is dissipated resulting in catastrophic structural damage.

Stern (2002) essentially defines these areas as ‘*sediments, oceanic crust, and mantle lithosphere return to and re equilibrate with Earth’s mantle.*’ Any earthquake activity, which occurs within these zones take place at large depths.

Galea (2007) also expresses the impact of subduction zones on seismic hazard and makes reference to the fatal earthquakes, which took place within the Hellenic Arc. Seismic activity taking place within this zone can reach an intensity of up to VII and covers distances, which exceed 1,000km.

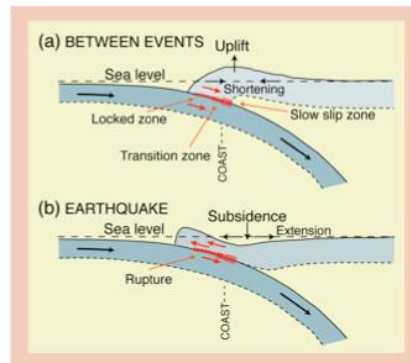


**Figure 4** Subduction Zones  
Source: Hyndman & Wang, 1995

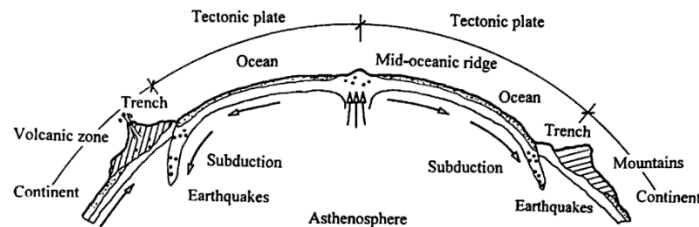


**Figure 5** Mechanisms of motion of tectonic plates at their boundaries  
Source: (Tomazevic, 1999)

### 2.2.5.3 Path Effects

Just like any other wave, due to inhomogeneous terrain, seismic waves are prone to experience reflection, refraction, diffraction and multiple other obstacles. Path effects ultimately bring about a considerable increase in the duration of a seismic event depending on the movement of these seismic waves (Cardenas-Soto & Chavez-Garcia, 2003). The European Seismic Hazard Model aimed at providing the peak ground acceleration, which is expected in certain regions on the European Continent, depending on the return period of a seismic activity (Giardini, Wossner, & Danciu, 2014).

Within Malta itself and areas close by, earthquakes of large intensities have been recorded since 1530. Path effects, which pose a hazard locally, would be the active fault zone of the Sicily Channel Rift Zone and, as mentioned in the previous section, the Hellenic Arc (Galea, 2007). Seismic waves can be used to locate the epicentre, and thus the direction of the earthquake source.

One must not forget the impact of having clusters of buildings built close to one another. In such cases, these structure no longer act separately from each other, but rather tend to act in conjunction with those adjacent to them. The seismic energy accumulated in the ground strata is dissipated through vibrations from interacting structures (Lou et al., 2011).

As discussed earlier, the structural response to seismic action is also dependent on the contact between the building foundations and the soil strata below. Buildings, which rest upon softer forms of terrain, undergo enhanced motion leading to overturning moments. A crucial factor to keep in mind is also the direction of origin of the seismic wave. As tectonic plates slip onto one another, these seismic waves dissipate in concentric elliptical motions. The maximum wave energy is described through the alignment of such motion (Farrugia, 2022).

#### 2.2.5.4 Soil Structure Relationship

Throughout their study, Mylonakis & Gazetas (2000) discuss the influence of seismic action upon the soil environment. Soft soil environments may amplify the fundamental frequency of a seismic wave, leading to rather catastrophic results. As a result of seismic loading, multi-storey buildings experience translational forces. However, in the event that such structures are also built on soft soils, the building also experiences additional rotational forces. In such instances, the waves of the structure and the soil do not vibrate coherently, but in an out-of-phase manner.

Lou et al. (2011) found that, structures undergoing a seismic event, behave differently when constructed over different soil strata, and thus they compared flexible soil to a rigid base. Tamari & Towhati (2003) also carried out a study dealing with soil-structure interaction, the soil being under the process of liquefaction. Liquefaction generally occurs in soils, which are cohesionless, leading structures to collapse or sink.

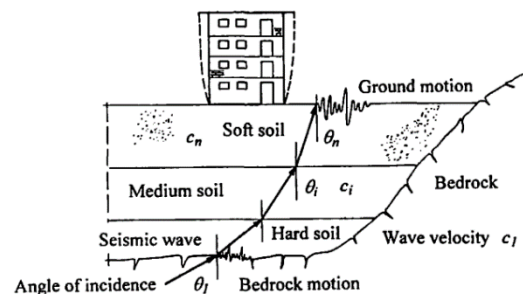


*Figure 6 Propagation of seismic waves from the rock to the surface*

*Source: (Tomazevic, 1999)*

Material	P-waves (m/s)	S-waves (m/s)
Sand	300–900	100–500
Clay	400–2000	100–600
Sandstone	2400–4300	900–2100
Limestone	3500–6500	1800–3800
Granite	4600–7000	2500–4000
Basalt	5400–6400	2900–3200

*Table 2 Wave propagation in various types of soil*

*Source: (Tomazevic, 1999)*



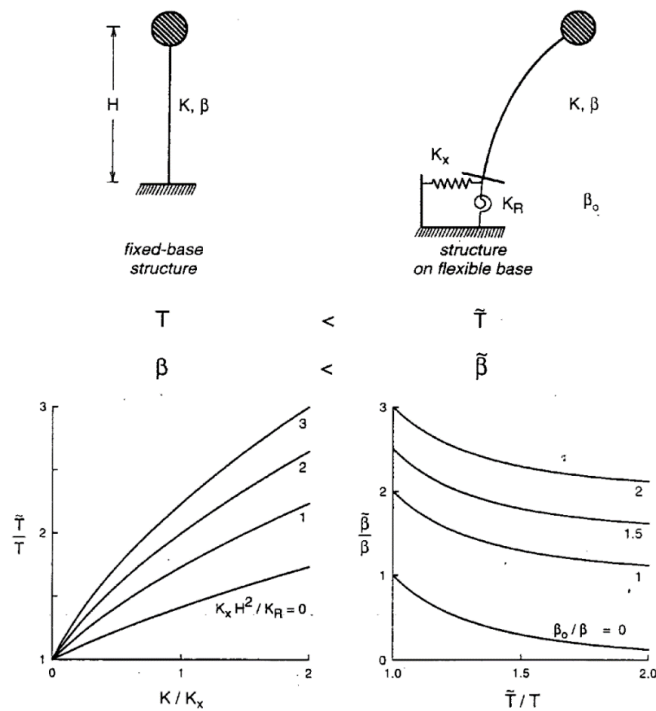


Fig. 1. Effect of soil-structure interaction on fundamental natural period and effective damping of a structure on flexible foundation according to NEHRP-97 provisions.

**Figure 7** Effect of soil-structure interaction  
Source: (Mylonakis & Gazetas, 2000)

### Chapter 3: Failure Modes of Unreinforced Masonry Buildings

#### 3.1 Introduction

Locally, masonry has been a building material of choice due to its abundance in supply. Thus, it is used mainly due to its cost effectiveness, and also workmanship is considered to be easier than that entailed by steel or concrete. However, over the years, it was gradually realized that masonry is subject to collapse due to its sole ability to withstand compressive loads. In addition, one must also take into consideration the interaction between block and mortar. A mortar paste is generally spread over the surfaces of a block so as to connect each block in compression and shear. This also allows the load to be distributed in an even manner within the staggered blocks. In Italy, many retrofit interventions have been implemented within URM buildings due to their seismic vulnerability at the connections (Frumento et al., 2006).

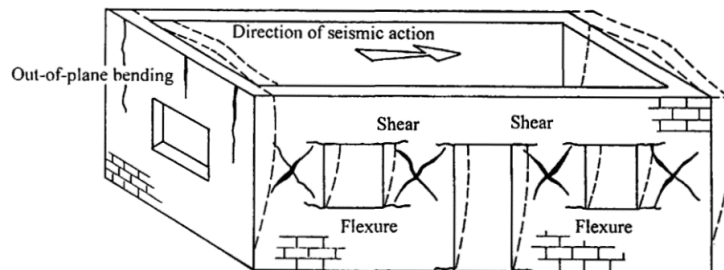


**Figure 8** Deformation of the building and typical damage to structural wall  
Source: (Tomazevic, 1999)

Camilleri (1988) highlights the negative consequences with the widespread use locally of masonry as a building material, since it is weak in tension owing to its lack of material ductility. In areas in a URM building where tension is developed, it may be necessary to use of reinforcement or also post-tensioned masonry.

(Bhowmik & Mohanty, 2008) Numerous research studies have been carried out over the years on URM construction due to the structural collapse of masonry buildings during earthquakes, and this makes it a cause of concern. Bhowmik & Mohanty (2008) identified several failure modes, which could take place due to the additional loads acting on a structure experiencing vibrations due to earthquakes, such as:

- Sliding Shear Failure
- Diagonal Cracks
- Non-Structural Failure
- Failure due to overturning

Bothara & Brzev (2011) outline several deficiencies of URM buildings, namely:

- Lack of structural integrity
- Roof collapse
- Wall delamination
- Out-of-plane collapse
- In-Plane Shear Cracking
- Poor quality in construction
- Foundation issues

**TABLE 1**  
Estimated Compressive Strength of Masonry for 9" blocks (N/mm<sup>2</sup>)

Mortar Designation	Compressive Strength of Unit N/mm <sup>2</sup>			
	Globigerina			Coralline*
	<b>18</b>	<b>20</b>	<b>23</b>	<b>75</b>
(i)	9.5	10.3	11.4	26.3
(ii)	8.2	8.9	9.7	20.8
(iii)	7.6	8.0	8.8	18.0
(iv)	6.8	7.2	7.8	15.2

**TABLE 2**  
Estimated Compressive Strength of Masonry for 6" blocks (N/mm<sup>2</sup>)

Mortar Designation	Compressive Strength of Unit N/mm <sup>2</sup>			
	Globigerina			Coralline*
	<b>18</b>	<b>20</b>	<b>23</b>	<b>75</b>
(i)	12.3	13.3	14.7	34.4
(ii)	10.7	11.5	12.6	27.0
(iii)	9.9	10.4	11.4	23.4
(iv)	8.9	9.3	10.0	19.3

**Table 3** Compressive Strength of Masonry  
Source: (Camilleri, 1988)

### 3.2 Walls

Structural integrity is ultimately dependent on the degree of the connection between walls, wall-to-floor connections and also wall-to-roof connections. As can be seen in Figure 9 (a) the structural walls perform independently from one another due to their loose connection. Walls which happen to be orthogonal to the direction of propagation of the seismic wave experience out-of-plane vibrations. Walls which are parallel to the direction of propagation experience in-plane vibrations. In contrast, in Figure 9 (b), the structure acts monolithically due to diaphragm action when subject to seismic loading.

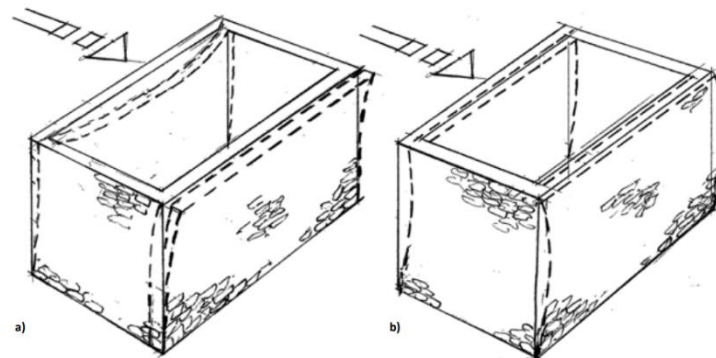


**Figure 9** Masonry building during earthquake shaking a) loosely connected walls without slab at roof level, and b) a building with well-connected walls and a roof slab

Source: (Tomazevic, 1999)

The performance of masonry load-bearing walls when subject to seismic loading is highly dependent on the point of application horizontally. This is because masonry walls are generally designed to be higher in comparison to their thickness. Furthermore, it is important to take into consideration the wall's geometry in terms of particular structural members, such as location piers, lintels, nodes and openings. All these structural elements contribute in determining the stiffness and slenderness of in-plane loading (Lourenco et al., 2011).

Tomazevic (1999) outlines the ideal type of masonry, which is to be made use of depending on the seismicity of the area and also its structural system, as follows:

Design ground acceleration $a_g$	< 0.2 g	0.2–0.3 g	≥ 0.3 g
Unreinforced masonry	10 m	8 m	6 m
Confined masonry	15 m	12 m	8 m
Reinforced masonry	15 m	12 m	8 m

**Table 4** Recommended maximum distance between structural walls

Source: (Tomazevic, 1999)

### 3.2.1 Wall Openings

Tomazevic (1999) recommended that, when designing masonry structures, one must give careful consideration to the position and size of openings within walls. The position of openings contributes to the resistance against seismic loading when applied in-plane. As seismic loading is applied onto a structure, a large portion of the stress distribution tends to concentrate at the openings, and thus resulting to major cracks.

The ideal locations to position openings are as follows:

- In walls, which distribute a lower vertical gravity load
- In both orthogonal directions, equally to allow for a symmetrical plan
- They shall not intervene with any structural beam
- Ensure alignment to both the horizontal and the vertical directions
- Shall not be located at beam supports due to concentrated loading

Wall openings properties, which provide reduced stiffness (Parisi & Augenti, 2012) include:

- Differently-sized openings
- Number of openings at each floor is irregular
- Openings that do not align neither to the horizontal nor the vertical from floor to floor

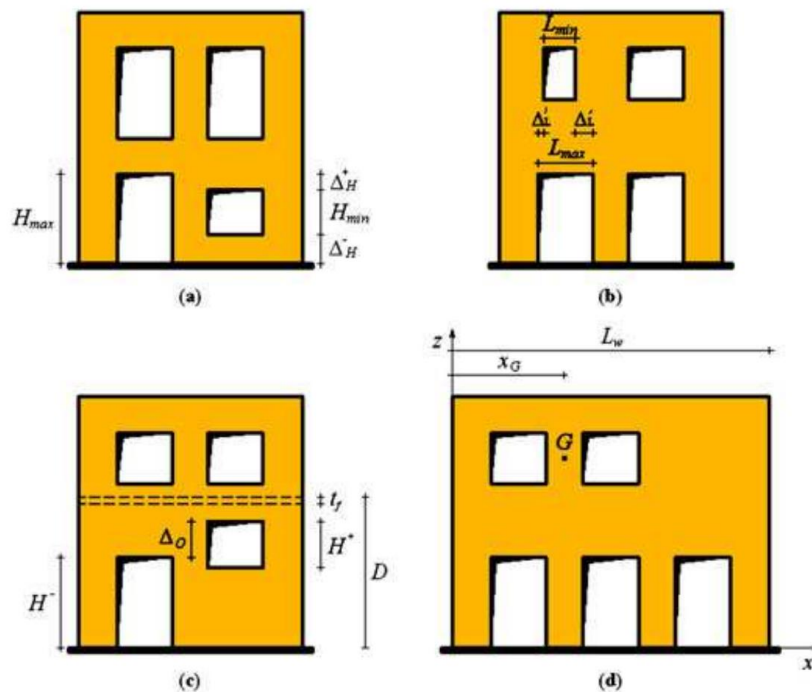


**Figure 10** a) horizontal irregularity, b) vertical irregularity, c) offset irregularity, and d) variable openings number irregularity  
 Source: (Parisi & Augenti, 2012)

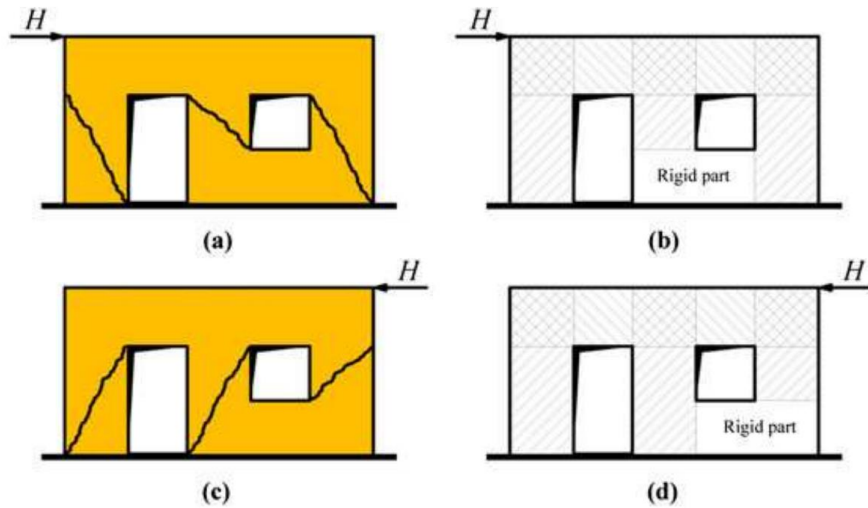


**Figure 11** Diagonal Cracking due to different opening heights for (a,b) rightward and (c,d) leftward orientation of seismic action  
 Source: (Parisi & Augenti, 2012)

### 3.2.2 In-Plane Loading

Under the effects of seismic loading, in-plane structural damage tends to be less prevalent than that which occurs out-of-plane. Many times, contributing factors, which lead to in-plane failure would be the insufficient mortar strength and the structural inefficiency in the construction of the walls.

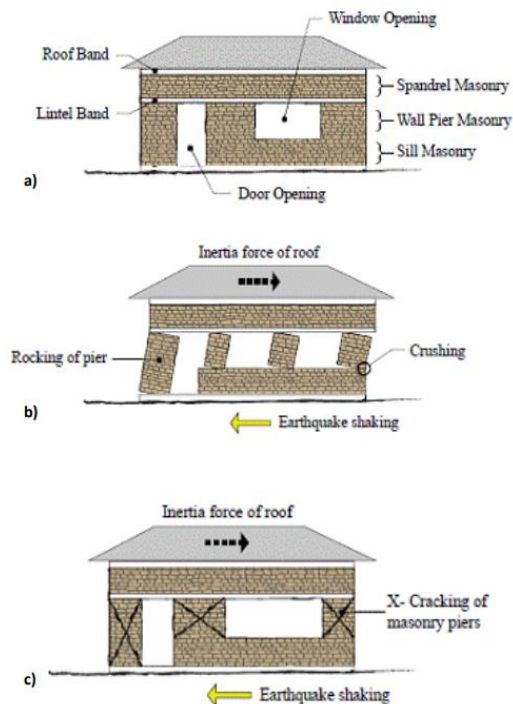


**Figure 12** In-plane damage of stone masonry walls: a) typical wall with openings b) rocking failure, and c) diagonal shear cracking (adapted from Murty 2005)  
 Source: (Bothara & Brzev, 2011)

As seismic waves are applied in-plane to the structure, there could be two types of failures, namely flexural failure or shear failure. Flexural behaviour may essentially be categorized into two types, namely rocking and crushing. Rocking can be seen in Figure 13 (b), where the masonry piers between openings tend to rotate about a toe in a direction opposite to that of the seismic wave. Crushing occurs in areas where large concentrations of load are found, and thus lead to sub-vertical cracks.

On the other hand, shear failure may be categorized into two types, namely sliding and diagonal cracking. Figure 13 (c) shows the possibility of having diagonal cracking. Diagonal cracking generally occurs when the masonry's tensile resistance is not sufficient to withstand the tensile stress being applied. Diagonal cracking usually propagates from the centre point of the pier. Normally, the walls, which are the most vulnerable to this sort of failure, would be those at the bottom-most floor due to the accumulation of loads from upper floors being directed towards it.

In sliding shear failure, sliding occurs parallel to a horizontal bed joint plane due to insufficient shear resistance of the mortar joints (Calderini et al., 2008) (Bothara & Brzev, 2011)

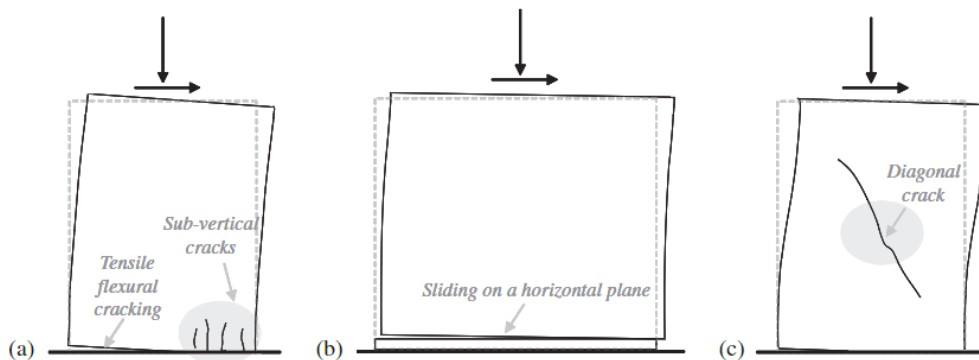


**Figure 13** Typical failure modes of masonry piers a) rocking, b) sliding shear failure, and c) diagonal cracking  
 Source: (Calderini et al., 2008)

### 3.2.3 Out-of-Plane Loading

The most prominent issue of masonry structures under the effect of earthquake actions would be that of out-of-plane loading. Out-of-plane loading gives rise to both tension and compression at opposing faces of masonry walls. The scale at which displacement occurs is dependent on the ratio between both the in-plane gravity load and bending moment.

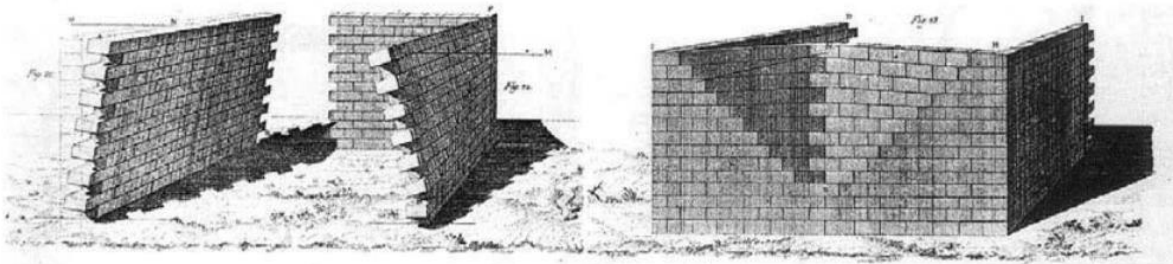


**Figure 14** Collapse mechanisms due to out-of-plane action  
 Source: (Ferreira et al., 2015)

One of the main contributing factors to this form of seismic vulnerability would be its low strength-to-mass ratio. Therefore, the structure is insufficient in terms of its strength and stiffness. Out-of-plane loading may also bring about overturning. Out-of-plane collapse requires a much lesser force to produce damage in comparison to that required to produce in-plane damage.

The previous section discussed how in-plane failure generally occurs at the lower levels of a structure. In contrast, out-of-plane failure is more likely to directly influence the top-most parts of the structure. This is because, as the building height is further increased, the vertical gravity load is at a minimum, and thus it is much less resistant to seismic acceleration than the bottom storeys of an URM structure.

Critical features, which directly influence out-of-plane failure, include:

- Wall slenderness must be stable enough
- Connections between walls and horizontal structures must ensure monolithic behaviour rather than structural elements vibrating independently
- Rigid diaphragms
- Brick-and-mortar joints must be adequate

(Ferreira et al., 2015)

### 3.3 Diaphragms

The last major factor which contributes to an existing URM structure withstanding seismic loading would be the effectiveness of diaphragms with respect to their in-plane stiffness. If the diaphragm is not adequately connected to the masonry walls, then lateral loads imposed through seismic action are not suitably distributed to the foundations. Slabs are horizontal elements, which allow the structure to act monolithically (Piazza et al., 2008).

Essentially, the floor slab acts as a simply supported beam whose span to depth ratio is relatively lower in comparison to that of a beam. In addition, it experiences both bending and shear forces in the horizontal direction (Diaphragms, 2022).

Diaphragms may be categorized into three types namely:

- *Fully Rigid*

Fully-rigid structures behave monolithically, and thus this would mean that any loads acting onto the slab are efficiently directed to its supporting piers or masonry walls. Some of the forces acting on such an element due to seismic action would be inertia, torsion, and shear. Due to their sufficient connections to supports, damage is highly improbable. Fully-rigid diaphragms can ‘*translate and rotate but cannot deform*’ (Adams, 2020).

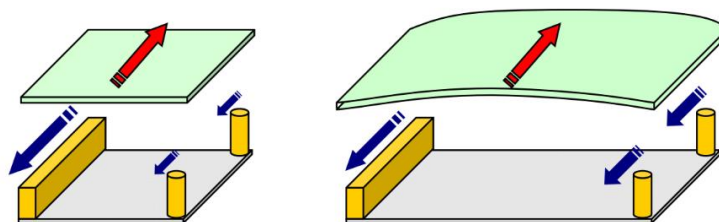


**Figure 15** Rigid diaphragm action  
Source: (Murty et al., 2012)

- *Flexible*

When taking into consideration flexible diaphragms, their stiffness is practically insignificant. Therefore, the diaphragm, in this case, would not be serving its purpose to transfer horizontal loads to its supports. Unlike fully rigid diaphragms, flexible slabs are capable of deforming and may undergo greater damage (Adams, 2020).

- *Semi-Rigid*

A semi-rigid diaphragm may be described as a slab, which retains properties pertaining to both rigid and flexible diaphragms. A semi-rigid diaphragm exhibits some stiffness, however it is still capable of enduring translation, rotation, and some deformation. The extent to which deformation occurs affects the distribution of loads to its supports. Hence, the slab may suffer some damage due to its partial deformation (Adams, 2020).

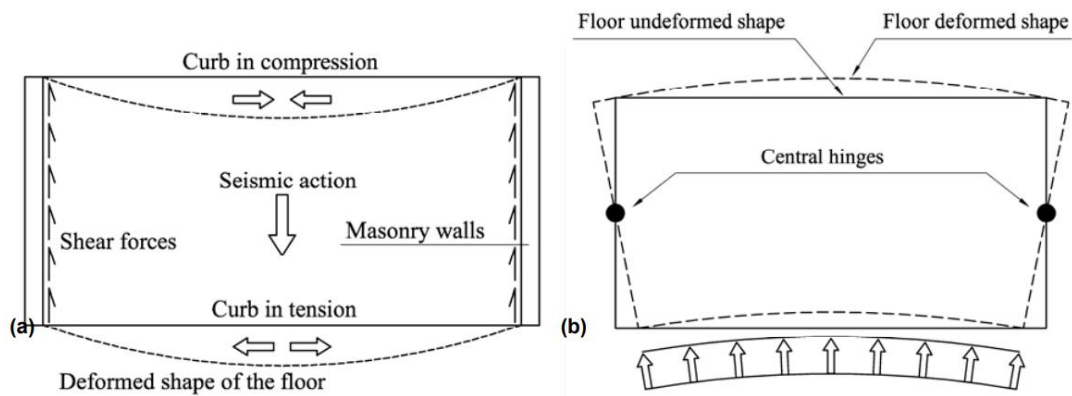


**Figure 16** Load distribution across diaphragms  
Source: (Piazza et al., 2008)

The above diagram is extracted from a report written by Piazza et al. (2008), which a) depicts the load distribution and b) shows the ideal load distribution in controlled environments.

One must also take into consideration that seismic action may be acting on multiple adjacent structures. One of the main causes of structural damage could be caused by pounding of adjacent buildings against each other. The structural characteristics of one building to another are usually different and, thus, seismic action may lead to oscillations, which are out-of-phase. Due to the hammering action, rigid diaphragms transmit concentrated lateral loads onto adjacent buildings.

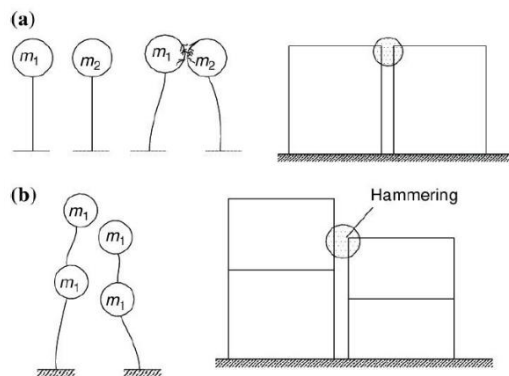


**Figure 17** Pounding action on a) same-storey levels, b) different storey levels  
Source: (Brinca, 2020)



### 3.4 Foundations

Bothara & Brzev (2011) outline that, throughout a seismic event in 2005 in Pakistan, buildings which had an appropriately sized foundations for their requirements, endured much less structural damage in comparison to the buildings, which made use of inadequately sized foundations. However, they also highlighted the importance of the soil – structure relationship.

One ought to consider the possibility of strengthening existing foundations, however it is a rather laborious and expensive task. There are essentially two ways in which this strengthening may be done, namely either by underpinning or otherwise through the construction of a reinforced concrete supporting beam.

In order to ensure an enhanced earthquake performance, one might also consider the use of piles, especially in sites defined through loose sand, uncompacted soil, or soft clay. In such cases, the piles need to be designed deep enough to reach the most stable form of ground.

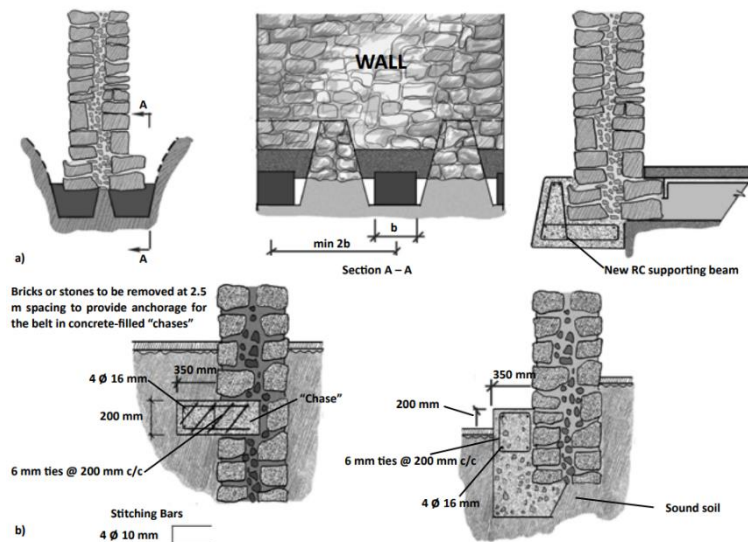


**Figure 18** Strengthening existing foundation a) underpinning the foundation, and b) external RC belt  
Source: (Bothara & Brzev, 2011)

## Chapter 4: Retrofitting Techniques

### 4.1 Introduction

As previously discussed, the main issue with the use of URM construction would be its inability to withstand imposed lateral loads due to seismic action. The previous chapter briefly outlined some of the factors, which bring about poor seismic performance in a building. This chapter aims to deal with the available options, which may be implemented in order to improve the earthquake performance of most of the local URM construction types instead of complete demolition.

In order to outline the ideal retrofitting strategy for a particular case, one has to take into consideration the following constraints (Bothara & Brzev, 2011):

- Socio-economic
- Structural system
- Construction materials
- Quality of construction
- Building condition
- Site condition

### 4.2 Ties & Tie Rods

The use of steel ties has been commonly used as a solution for seismic retrofitting. Usually, their thickness varies between 16mm-20mm and they are mounted in parallel beneath horizontal elements, such as floors or roofs. Confinement is provided at the rods' ends using anchor plates. The main aim behind the implementation of such a retrofitting technique is to enhance the connection between walls and roofs and to prevent these elements from vibrating independently. Such ties are also highly effective when they are connected to flexible diaphragms as they provide an increase in their in-plane stiffness, thus lowering any bending moments generated (Bothara & Brzev, 2011).

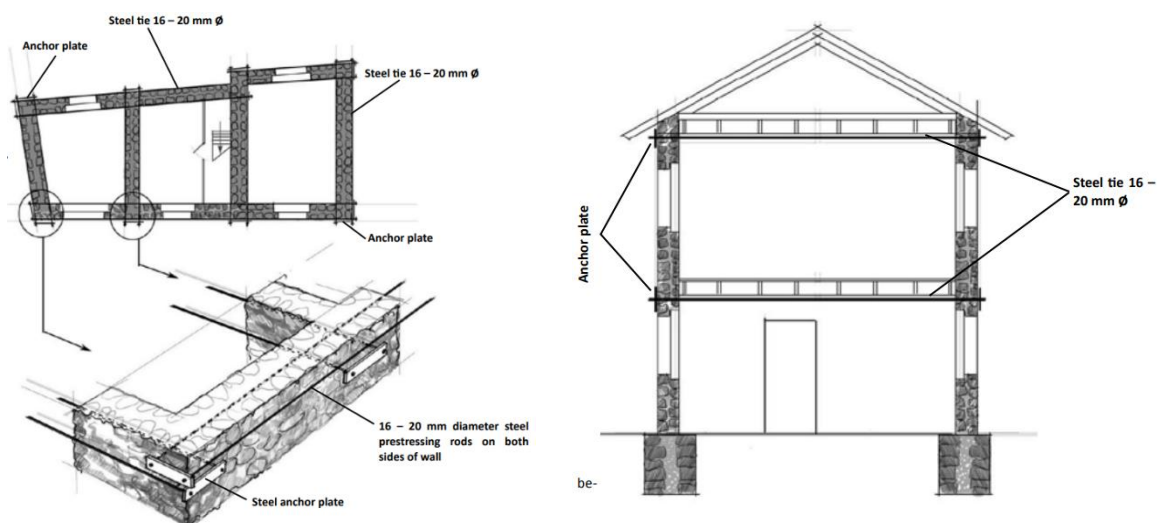


**Figure 19** Plan view showing use of steel ties connected through anchor plates  
Source: Source: (Bothara & Brzev, 2011) adapted from (Tomazevic, 1999)

### 4.3 Steel Frames & Trusses

Global case studies have proven that steel frames and trusses are a suitable form of seismic retrofit. For instance, Abeling et al. (2018) made use of steel trusses oriented in the vertical direction in order to reinforce the building to withstand in-plane loading. Utilising a steel frame, also aids the building in increasing its structural rigidity.

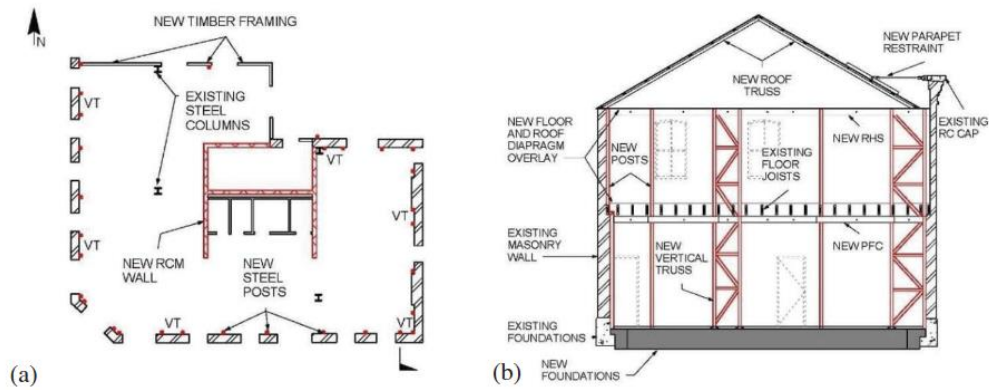


**Figure 20** Retrofitting of Moorhouse Avenue using Vertical Trusses  
Source: (Abeling, Dizhur, & Ingham, 2018)

In addition, the seismic analyses conducted by Ismail (2019) concluded the following:

- Due to the additional stiffness provided to such structures, they were able to reduce the fundamental period of vibration of a structure.
- A significant decrease in inter-story drift was observed.
- The shear resistance experienced at the base of a structure was enhanced, and thus reduced the possibility of moments taking place, which could lead to overturning.

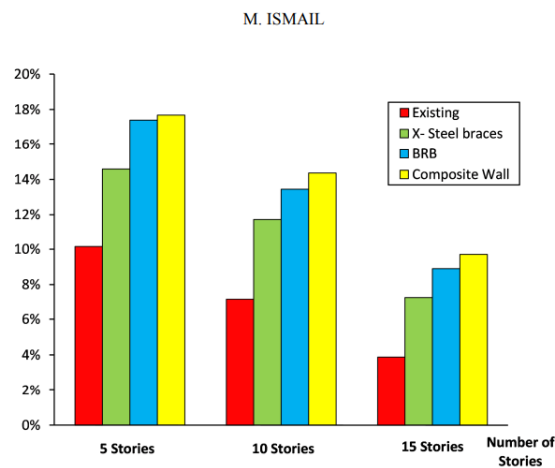


**Figure 21** Base shear-to-weight ratio for varying storey levels in comparison to existing  
Source: (Ismail, 2019)

Ismail (2019) showed that such retrofit techniques are capable of improving their base shear resistance due to improved in-plane stiffness.

#### 4.4 Seismic Bands (Ring Beams)

Seismic bands are essentially seen as the most promising form of retrofitting technique used in URM buildings. They are generally applied in locations, such as roofs, floors, or lintel levels. Their efficacy is entirely dependent on their material and the quality of workmanship. The main aim of such an installation would be to enhance the connections between horizontal elements to walls and other vertical structural elements, thus ensuring monolithic behaviour.

In cases where there are large openings, the effective wall height, which resists out of plane action, is significantly reduced. Therefore, employing seismic bands, reduces the stresses experienced in bending in the event of an earthquake.

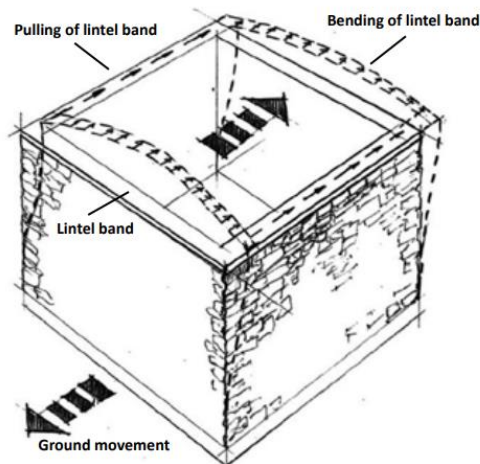


*Figure 22 Application of seismic bands*  
*Source: (Bothara & Brzev, 2011) adapted from*  
*(Murty, 2005)*

As shown in Figure 22, a seismic band undergoes both compression and tension. The seismic band, which lies orthogonal to the seismic wave, undergoes bending, whilst the seismic band, which lies parallel to the seismic wave, undergoes tension. These seismic bands may either be constructed using timber or reinforced concrete. However, the latter has proved to be more durable (Bothara & Brzev, 2011).

#### 4.4 Base Isolation

When utilizing base isolators, the main aim is to set apart the motion imposed on the building due to seismic action from the ground motion itself. Therefore, this allows the building to restore its natural period of vibration. Through the use of this form of retrofit, the structural damage suffered by buildings is greatly diminished, both structurally and architecturally. However, one must keep in mind that such a technique should be thought of early in the seismic design stage, since it is rather difficult to make use of this technique on existing buildings due to difficult installation issues. There are primarily two types of available base isolators, namely sliders, which are either composed of Teflon or stainless steel, or otherwise it is possible to make use of elastomeric bearings, which are either of Neoprene or natural rubber (Guh & Altoontash, 2006).

## 4.5 Jacketing

Jacketing is ultimately defined by Bothara & Brzev (2011) as being the treatment of a masonry surface either by using shotcrete, micro-concrete or also reinforced mortar. Once the surface of a wall is treated using either of these processes, it is kept in place through the installation of wall anchors. If the installation is carried out appropriately, the resistance of the structure to both in-plane and out-of-plane loading is substantially enhanced.

For such a measure to enhance the wall seismic behaviour, proper adhesion between the freshly applied jacketing and the existing wall surface is to be ensured. This retrofitting technique increases the weight of the walls, and thus overturning moments are further reduced. Ideally, it is also applied to both inner and outer surfaces of the wall, however this at times may not always be feasible.

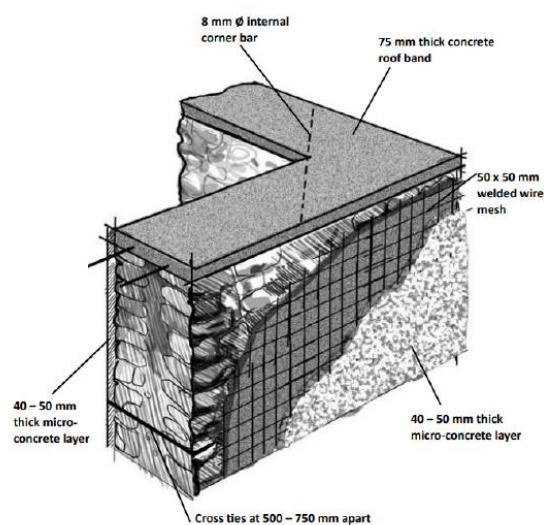


*Figure 23 Jacketing layered process*  
*Source: (Bothara & Brzev, 2011)*

## 4.6 Wall-to-floor/roof connections

As previously discussed, one of the main issues experienced by the URM buildings in the event of seismic action is that the connection tying walls to roofs and floors is not sufficient to allow them to behave simultaneously.

One may consider opting for the installation of steel straps. The connection between external walls and diaphragms is ultimately dependent on their orientation to one another. Beams, which are constructed parallel to the external wall, may make use of V-shaped straps, whilst beams, which are constructed perpendicular to the external wall, may simply make use of a vertical strap. These steel straps are connected by anchor bolts. By applying straps, the diaphragm's ability to endure tension is enhanced.

In addition, one may decide on the benefit from diagonal bracing systems to further stiffen existing diaphragm elements. However, one must also question the cost-effectiveness of such measures as it may be much more economically feasible to possibly reconstruct a floor slab, which fits the required criteria.

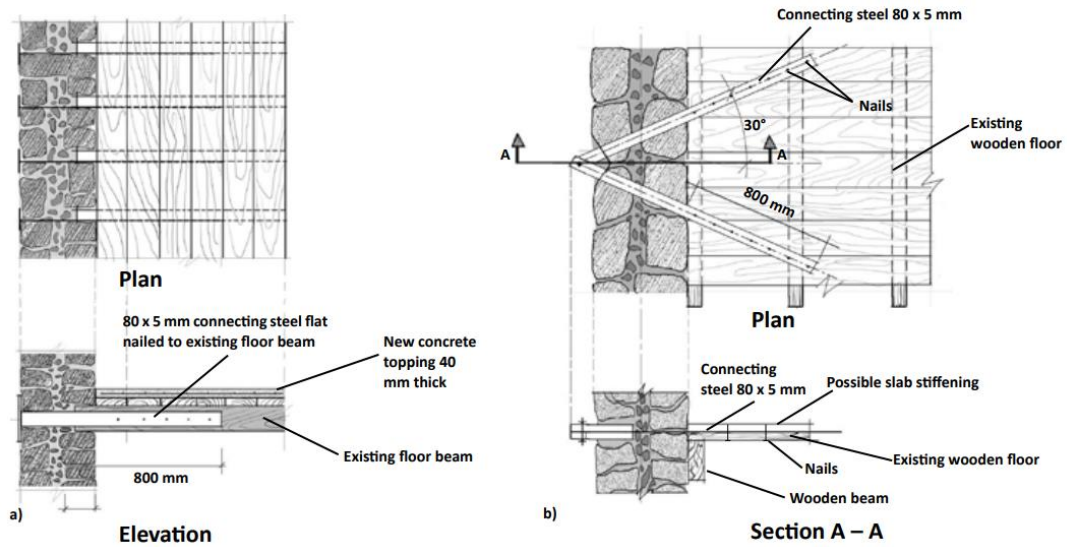


**Figure 24** Steel straps for wall-to-floor anchorage: a) floor beams perpendicular to wall and b) floor beams parallel to wall

Source: (Bothara & Brzev, 2011) adapted from (UNIDO, 1983)

#### 4.7 Grout Epoxy Injections

This retrofitting method is a very popular one. Grout epoxy injections may either be cement-based or also polymer-based. For URM buildings, cement-based grouts are preferred because of familiarity with the material. In addition, the process of application is rather straightforward. (Elsayed & Ghanem, 2017), The application process is briefly described below:

- Holes are drilled using a drilling machine
- Holes are cleaned from the debris
- Plastic tubes are inserted into the drilled holes
- Water is injected into the holes to assess their efficiency
- Any holes, which are deemed inefficient, are closed, whilst the others are prepared for grouting
- The grout mix is thoroughly filtered for coarse material
- Grout is then injected through the use of a rubber syringe



(a) Drilling Injection Holes      (b) Injecting Grout      (c) Grouted Specimens

**Figure 25** Grout Procedure  
Source: (Elsayed & Ghanem, 2017)

The main aim of this retrofit solution is to strengthen a masonry wall against out-of-plane action. The grout is generally applied to the voids or through the drilling process as explained above. However, Tomazevic (1999) discourages the use of epoxy grout in cases where cracks or voids in masonry walls happen to be larger than 10mm.

#### 4.8 FRP/GFRP Systems

The use of Fiber Reinforced Polymer seems to be a reaction to the laborious procedure used in jacketing. FRP is an alternative to the steel mesh reinforcement, and, when combined with plaster mortars, it replaces the traditionally used cement-mortar mix. Throughout the study carried out by Triller et al. (2017), glass fiber reinforced polymer (GFRP) was utilized to test its efficacy when applied to masonry. It was determined that GFRP was a hopeful solution, especially in aiding the masonry walls through increased shear resistance and increased rigidity. However, one of the drawbacks observed was the possibility of delamination between the masonry and the GFRP. Proper adhesion of both systems is to be ensured.

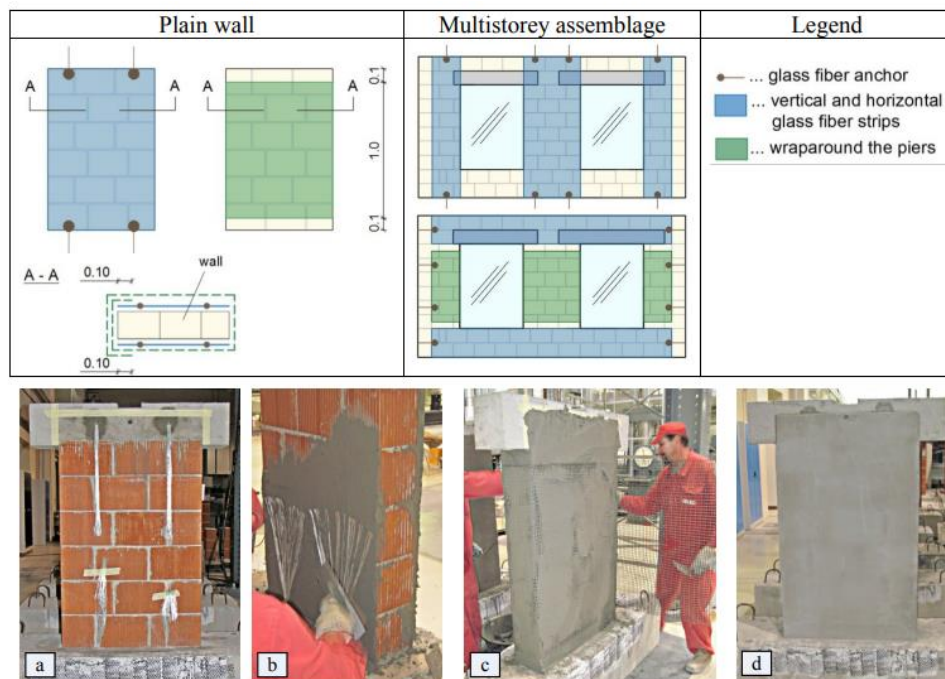


Figure 3. **a:** Placing of glass fiber anchors on the wall specimen; **b:** Spreading the fibers of anchors; **c:** layer of mortar over the vertical strip and wraparound of the wall; **d:** Wall specimen in the strengthened state.

**Figure 26** Strengthening of walls through GFRP  
Source: (Triller et al., 2017)

## 4.9 Post-tensioning Tendons

URM structures prove to be vulnerable to large tensile stresses, and buildings of a certain vertical height are prone to experience out-of-plane flexural failure. To improve the URM building's tensile strength, one can make use of vertical post-tensioned tendons. The quality of these post-tensioned tendons relies on the post-tensioning force used, the confinement of these tendons (whether they are left unbonded, or bonded to the cavities with URM walls), the types and spacing of tendons, and finally the restraint conditions (Ismail et al., 2011)

One could also make use of post-tensioning to improve the bending capacity of masonry walls.

## 4.10 Ring Beams

The benefit of making use of ring beams is similar to that described for seismic bands. They aid the connection between wall-to-floor and wall-to-roof by allowing the distribution of horizontal forces and they increase building resistance to overturning moments. Generally, such ring beams are installed at the top-most floors of a building due to the lower gravity loads experienced.

There are mainly two variations, which may be used for this purpose, namely reinforced concrete or otherwise steel ring beams. Many times, steel ring beams are the preferred solution for the simple reason that they may be altered to suit any wall irregularities. In addition, due to their low self-weight, they impose minimal changes on the existing structure and its performance to seismic action.

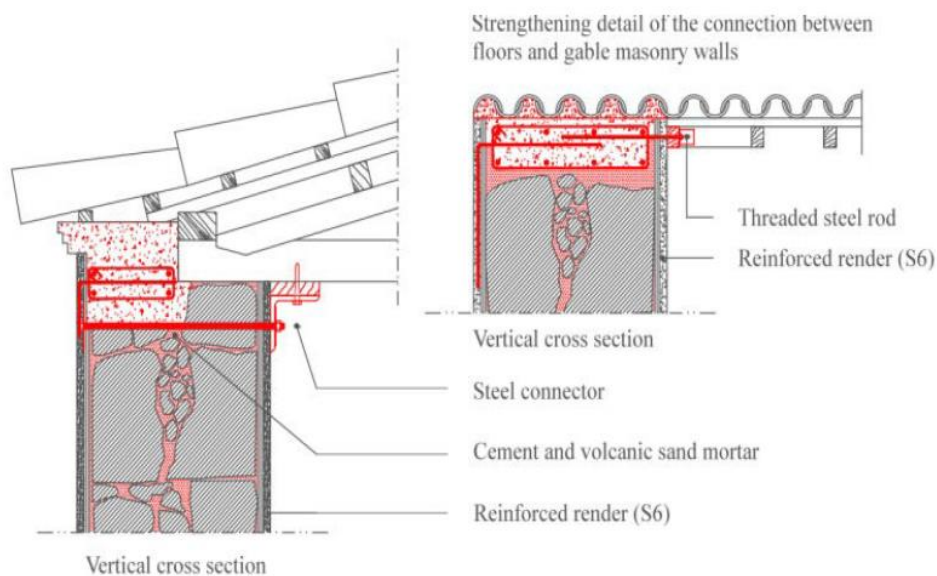


**Figure 27** Use of RC ring beams  
Source: (Brincat, 2020) adapted from (Ferreira et. al., 2015)



## Chapter 5: Seismic Vulnerability of Local URM Building Aggregates

### 5.1 Introduction

As seen locally and abroad, buildings generally form part of an entire compound defined by multiple building aggregates whose behavior affects the adjoining building through their interaction with one another. URM building aggregates also largely define the local urban context within the Maltese Islands. Building aggregates may have varying properties, such as the height of the individual buildings (single units) which make up the aggregate, the storey heights, the number of floors, the period during which the buildings were erected and their structural typology. Thus, URM building aggregates may be very complex to analyse seismically due to the several uncertainties associate with the dispersion of the horizontal seismic loading across structural elements of the URM buildings.

It is important to note that locally, URM building aggregates often have shared party walls between its constituent single unit buildings, and thus loads coming from two adjacent structures are distributed across the center line of the shared party wall. The Italian O.P.C.M. 3431/05 (2005), M.D. 14/01/08 (2008) and M.C. 02/02/09 n. 617 (2009) Standard, clearly states that a building aggregate is formed by a group of structural units, which are inhomogeneous and whose connection to one another is relatively efficient. A structural unit, SU, is an entire aggregate also including its parts *“having a unitary and homogenous behavior towards static and dynamic loads”* (Formisano, 2016).

Structural engineers seek to analyze the response of multiple structural single units, which make up a URM building aggregate, when subjected to seismic loading. This allows the prediction of the URM building aggregate response to such loading. URM building aggregates is expected to have increased seismic performance compared to a URM single unit for the simple reason that horizontal loading is counteracted by group behavior. This structural behaviour has also been observed for URM building aggregates built using low quality masonry. Another important point is that URM building aggregates are not modelled as a group of independent and individual URM single units side-by-side, as it would not reflect the interaction which occurs between the multiple structural single units during a seismic event. A possible modelling solution would be either to model the entirety of the URM building aggregate or to model one individual URM single unit with side restraints that portray the effect of adjacent single units (Formisano, 2016) (Borg, 2021).

## 5.2 Building Configuration of Local URM Building Aggregates and their Seismic Response

### 5.2.1 Local Building Typologies and Characteristics

The Maltese urban landscape is essentially characterized by the construction of blocks of apartments having their lowest floor being used as a basement garage. This building typology has recently outnumbered the construction of existing farmhouses and terraced houses due to the increasing demand for housing. One of the main construction materials used locally in existing URM buildings is Globigerina Limestone blocks, which constitutes a large part of the local geological formation, essentially covering more than half of Malta's surface area (Bartolo, 2011).

Another main construction material used extensively in recent years is hollow concrete blockwork (HCB). In fact, Globigerina Limestone masonry has nowadays been largely replaced by HCB for internal walls and the rear external walls, except sometimes on the outer leaf of the double leaf masonry cavity wall on the street façade, which is constructed in Globigerina Limestone blocks for architectural purposes (Buhagiar & Tonna, 2012).



**Figure 28** (left) Two skins of 230mm soft stone with a 50mm cavity, total 510mm and (right) Two skins of 160mm soft stone, typically with no cavity, total 360mm  
Source: (Buhagiar & Tonna, 2012)

Bonello (2018) considered the seismic behaviour of URM building aggregates composed of multiple URM single units. Beyond a certain number of URM single units within the URM building aggregate, it was observed that there was no additional benefit for the seismic performance of the aggregate and so, it would be ideal to incorporate seismic gaps at certain intervals within the aggregate. Such seismic gaps would need to be provided with the necessary width in order to avoid the risk of pounding in the event of an earthquake.

As previously mentioned, many local URM building aggregates make use of a shared party wall, which eventually mean that, during an earthquake event, floor slabs from both parties would be directing their horizontal loads onto the slender party wall. If an independent party wall is used for every single, there would be a significant decrease in the axial stress within the party wall. However, such a scenario would not correspond to a URM building aggregate, since each single unit could be oscillating independently out-of-phase from the other adjacent single units. Furthermore, Bonello (2018) confirmed that the seismic resistance that could be achieved by a URM building aggregate constructed on rock using Globigerina Limestone is up to 150% of the seismic resistance of a corresponding URM single unit.

Camilleri (2003) outlines the importance of risk minimisation measures, which should be implemented within the Maltese Islands in order to reduce seismic risk. Camilleri (2003) recommended that URM buildings should make use of reinforced masonry walls made of HCB, which is infilled with concrete and vertical steel bar reinforcement in order to connect the reinforced concrete floors slabs to the vertical wall structural system.

## Chapter 6: Research Methodology

### 6.1 Lateral Stiffness of Masonry Walls

This dissertation is a continuation of the research work carried out by Borg (2021), who investigated the seismic resistance of an existing residential URM building aggregate constructed using Globigerina Limestone with M2 mortar strength and composed of single units, each with a plan aspect ratio 1:4 (corresponding to the maximum ratio prescribed EC8). Borg (2021) considered several different unretrofitted URM building aggregates, each having a soft storey basement, in order to determine safe number of floors in the aggregate, beyond which it would fail under seismic loading. A peak ground acceleration of 0.10g with a return period of 475 years (corresponding to the design earthquake for the Maltese Islands) was considered throughout this research study. This dissertation will adopt the same design parameters considered by Borg (2021) in order to be able to compare the results of unretrofitted and retrofitted URM building aggregates. Moreover, as in Borg (2021), Ground Types A (Rock subsoil), B (Stiff Clay) and C (Weak Clay) were also considered.

In this dissertation, the URM building aggregates have been assumed to be retrofitted within the soft storey basement by means of the installation of moment-resisting portal frames constructed either using structural steelwork or reinforced concrete. In order to facilitate the installation of these plane frames within the basement, it has also been assumed that the foundations would be pinned, even though the corresponding sway resistance would be one-fourth of that for fixed base foundations. Using 3DMacro, several non-linear static pushover analyses were carried out in order to determine the safe height of a URM single unit and also of other URM building aggregates subjected to seismic loading.

The first step throughout this research study was to obtain the lateral sway stiffness of the transverse masonry shear walls at Ground Floor, which were missing within the basement level. This lateral stiffness was then to be replicated within the soft storey using moment-resisting plane frames situated directly beneath the transverse masonry shear walls within the Ground Floor. This lateral sway stiffness (Bhowmik & Mohanty, 2008) was computed as suggested by Bhowmik & Mohanty (2008) and Alexander (2010), using Microsoft Excel spreadsheets for computational simplicity.

As stated earlier, throughout this research study, the moment-resisting frames were assumed to be pinned and not fixed at the base foundations. Thus, the sway stiffness of each of the two columns making up the single bay plane portal frame would be:

$$K_s = \frac{3 E I}{L^3}$$

*Equation 6 Sway Stiffness of Pinned-Base Columns*

On the other hand, the sway stiffness of each of the two columns, which are fixed at the base would be:

$$K_s = \frac{12 E I}{L^3}$$

*Equation 7 Sway Stiffness of Fixed-Base Columns*

Where:

E: Young's Modulus of Elasticity

I: Moment of Inertia

L: Length of column

1. Fixed-Fixed Column

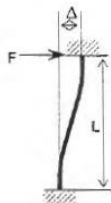


Figure 1: Fixed-fixed Sway Column

The Total Deflection is comprised of a Bending component and a shear component.

$$\Delta = \Delta_b + \Delta_s = \frac{FL^3}{12EI} + \frac{FL}{GA_s} \quad (1)$$

2. Pinned-fixed Column

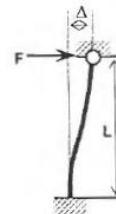


Figure 3: Pinned-fixed Sway Column

The Total Deflection is comprised of a Bending component and a shear component.

$$\Delta = \Delta_b + \Delta_s = \frac{FL^3}{3EI} + \frac{FL}{GA_s} \quad (6)$$

Figure 29 left) Fixed-fixed Sway Column, (right) Pinned-fixed Sway Column  
Source: (Alexander, 2010)

In addition, as suggested by Arnold (2001), a building was assumed to be irregular if there is a difference in sway stiffness between one level and another of more than 30%. Thus,  $K_s$ , the sway stiffness of the portal frames introduced in the basement cannot be less than 70% of  $K_m$ , the sway stiffness of the overlying transverse masonry shear wall at Ground Floor. In this regard, the original intention of this research study was to consider plane frames in the soft storey basement with both a reduced sway stiffness (70% of  $K_m$ ) and a full sway stiffness (100% of  $K_m$ ) in order to investigate the relative structural efficiency of both scenarios. However, as will be discussed later, the sway stiffnesses of the structural steelwork column section sizes available on the market were far smaller than the above required sway stiffnesses. For this reason, it was decided to use instead sway stiffnesses of 35% of  $K_m$  and 50% of  $K_m$  in the parametric seismic analyses carried out. The following procedure was used to determine the input data for the 3D Macro software:

**Step 1:** Identify general information

Properties:

- Density of Concrete: 24 kN/m<sup>3</sup>
- Density of Masonry Wall: 20 kN/m<sup>3</sup>
- Density of Screed/Finish: 18 kN/m<sup>3</sup>

Building Dimensions:

- Length: 24.83m
- Width: 6.03m
- Height: 15.35m (initial building height before it is increased for additional floors)

Building Ratios:

- Height-to-width: 2.546 (initial building ratio before it is increased for additional floors)
- Length-to-width: 4.118

**Step 2:** Determine the total dead load and live load accumulated at each level

Dead Load								
Level	Member	Loading	1/2 wall above	Unfactored Loading				
				Thickness (m)	Length (m)	Span (m)	Density (kN/m <sup>3</sup> )	Loading (kN)
5	350mm Slab	Dead	0	0.35	8.19	6.03	24	414.83988
	225mm Slab	Dead	0	0.225	14.66	6.03	24	477.35892
	230mm Wall	Dead	0.5	0.23	79.72	3	20	550.068
	180mm Wall	Dead	0.5	0.18	14.8395	3	20	80.1333
	150mm Screed	Dead	0	0.15	22.85	6.03	18	372.02085
	25mm Tile	Dead	0	0.025	22.85	6.03	18	62.003475
	<b>Total Dead Load at Level 5</b>							<b>0</b>
4	350mm Slab	Dead	0	0.35	8.19	6.03	24	414.83988
	225mm Slab	Dead	0	0.225	14.66	6.03	24	477.35892
	230mm Wall	Dead	0.5	0.23	79.72	3	20	550.068
	180mm Wall	Dead	0.5	0.18	14.8395	3	20	80.1333
	150mm Screed	Dead	0	0.15	22.85	6.03	18	372.02085
	25mm Tile	Dead	0	0.025	22.85	6.03	18	62.003475
	<b>Total Dead Load at Level 4</b>							<b>1956.424425</b>
3	350mm Slab	Dead	0	0.35	8.19	6.03	24	414.83988
	225mm Slab	Dead	0	0.225	14.66	6.03	24	477.35892
	230mm Wall	Dead	0.5	0.23	79.72	3	20	550.068
	180mm Wall	Dead	0.5	0.18	14.8395	3	20	80.1333
	150mm Screed	Dead	0	0.15	22.85	6.03	18	372.02085
	25mm Tile	Dead	0	0.025	22.85	6.03	18	62.003475
	<b>Total Dead Load at Level 3</b>							<b>1956.424425</b>
2	350mm Slab	Dead	0	0.35	8.19	6.03	24	414.83988
	225mm Slab	Dead	0	0.225	14.66	6.03	24	477.35892
	230mm Wall	Dead	0.5	0.23	79.72	3	20	550.068
	180mm Wall	Dead	0.5	0.18	14.8395	3	20	80.1333
	150mm Screed	Dead	0	0.15	22.85	6.03	18	372.02085
	25mm Tile	Dead	0	0.025	22.85	6.03	18	62.003475
	<b>Total Dead Load at Level 2</b>							<b>1956.424425</b>
1	350mm Slab	Dead	0	0.35	8.19	6.03	24	414.83988
	225mm Slab	Dead	0	0.225	14.66	6.03	24	477.35892
	230mm Wall	Dead	0.5	0.23	79.72	3	20	550.068
	180mm Wall	Dead	0.5	0.18	14.8395	3	20	80.1333
	150mm Screed	Dead	0	0.15	22.85	6.03	18	372.02085
	25mm Tile	Dead	0.5	0.025	22.85	6.03	18	62.003475
	<b>Total Dead Load at Level 1</b>							<b>1956.424425</b>

*Table 5 Accumulation of Dead Load  
Source: (Author, 2023)*

0	350mm Slab	Dead	0	0.35	14.29	6.03	24	226.92096
	225mm Slab	Dead	0	0.225	4.48	4.26	24	103.05792
	230mm Wall	Dead	0.5	0.23	70.5464	3	20	973.54032
	180mm Wall	Dead	0.5	0.18	0	3	20	0
	150mm Screed	Dead	0	0.15	18.77	6.03	18	305.59437
	25mm Tile	Dead	0	0.025	18.77	6.03	18	50.932395
<b>Total Dead Load at Level 0</b>							<b>1660.045965</b>	
<b>Total Dead Load Accumulated</b>							<b>9485.743665</b>	

Live Load						
Level	Function	Loading	Imposed Loading (kN/m <sup>2</sup> )	Length (m)	Span (m)	Loading (kN)
4	Roof	Live	0.4	22.85	6.03	55.1142
3	Residential	Live	2	22.85	6.03	275.571
2	Residential	Live	2	22.85	6.03	275.571
1	Residential	Live	2	22.85	6.03	275.571
0	Residential	Live	2	18.77	6.03	226.3662
<b>Total Live Load Accumulated</b>						<b>1108.1934</b>

**Table 6** Final Dead Load & Live Load values  
Source: (Author, 2023)

### Step 3: Determine the Seismic Weight of the structure

For this part of the procedure, reference was made to EN1991-1-1:2002 Table 4.2 in order to determine  $\varphi$  (dynamic magnification factor),  $\psi_{2,I}$  (factor for combination value of a variable action (imposed load)), and, hence,  $\psi_{E,I}$ , the reduction factor for variable action. For this purpose, the Equivalent Lateral Force (ELF) Method was used. The seismic weight is the sum of the full Dead Load acting at each floor centre and a reduced Imposed Load. These forces are then accumulated at each floor, making up the seismic weight of the structure. Noting that seismic weight is equal to the seismic mass multiplied by the acceleration due to gravity,  $g$  ( $9.81\text{m/s}^2$ ):

$$\text{Seismic Mass} = \Sigma G_{k,j} + \Sigma \psi_{E,I} \times Q_{k,j}$$

**Equation 8** Seismic Mass

Where:

$G_{k,j}$ : Dead Load

$\psi$ : Live Load reduction factor

$Q_{k,j}$ : Live Load

$$\psi_{E,I} = \varphi \times \psi_{2,I}$$

**Equation 9** Factor for combination value of a variable action

The following values were adopted:

$$\Phi = 1.0$$

$$\Psi_{2,I} = 0.3$$

$$\Psi_{E,I} = 0.3, \text{ as } 1.0 \times 0.3 = 0.3$$

Level	G	Q	$\Psi_{E,I}$	$\Sigma G_{k,j} + \Sigma(\Psi_{E,I})^*(Q_{k,j})$
	(kN)	(kN)		(kN)
5	0	0	0.3	0
4	1956.424425	55.1142	0.3	1972.958685
3	1956.424425	275.571	0.3	2039.095725
2	1956.424425	275.571	0.3	2039.095725
1	1956.424425	275.571	0.3	2039.095725
0	1660.045965	226.3662	0.3	1727.955825
$\Sigma$	9485.743665	1108.1934	0.3	9818.201685

**Table 7** Result values for seismic weight  
Source: (Author, 2023)

**Table A1.1 - Recommended values of  $\psi$  factors for buildings**

Action	$\psi_0$	$\psi_1$	$\psi_2$
Imposed loads in buildings, category (see EN 1991-1-1)			
Category A : domestic, residential areas	0,7	0,5	0,3
Category B : office areas	0,7	0,5	0,3
Category C : congregation areas	0,7	0,7	0,6
Category D : shopping areas	0,7	0,7	0,6
Category E : storage areas	1,0	0,9	0,8
Category F : traffic area, vehicle weight $\leq 30$ kN	0,7	0,7	0,6
Category G : traffic area, $30$ kN < vehicle weight $\leq 160$ kN	0,7	0,5	0,3
Category H : roofs	0	0	0
Snow loads on buildings (see EN 1991-1-3)*			
Finland, Iceland, Norway, Sweden	0,70	0,50	0,20
Remainder of CEN Member States, for sites located at altitude $H > 1000$ m a.s.l.	0,70	0,50	0,20
Remainder of CEN Member States, for sites located at altitude $H \leq 1000$ m a.s.l.	0,50	0,20	0
Wind loads on buildings (see EN 1991-1-4)	0,6	0,2	0
Temperature (non-fire) in buildings (see EN 1991-1-5)	0,6	0,5	0
NOTE The $\psi$ values may be set by the National annex.			
* For countries not mentioned below, see relevant local conditions.			

**Table 8** EN1990:2002 Annex A1, Table A1.1



#### Step 4: Base Shear Force and Force Distribution

Before obtaining a value for the base shear force, it is necessary to determine the fundamental period of vibration, T, of the building using EC8:

$$T = C_t \times H^{\frac{3}{4}}$$

*Equation 10 Fundamental Period of Vibration*

Where, T is the periodic time, and H is the height of the building. In this case, C<sub>t</sub> is 0.05, as obtained from EN1998-1: Cl. 4.3.3.2.2 (3) under the category of all other structures.

In order to determine the base shear force, F<sub>B</sub>, the building was classified as Class II ( EN1998-1: Cl. 4.2.5 Table 4.3) and the type of soil considered was Ground Type A (rock) ( EN1998-1: Cl. 3.1.2 Table 3.1). It is also necessary to identifying the time period parameters associated with the design acceleration response spectrum, S<sub>d</sub>(T<sub>1</sub>). In this case, a Type 2 elastic acceleration response spectrum was adopted, corresponding to the genera seismicity of the Maltese Islands.

$$F_b = S_d(T) \cdot m \cdot \lambda$$

*Equation 11 Base Shear Force*

and,

$$F_b = \frac{\lambda w S_d (T_1)}{g}$$

*Equation 12 Base Shear Force in terms of seismic weight of the building*

where:

λ is the correction factor, the value of which is equal to 0.85 if T<sub>1</sub> ≤ 2T<sub>C</sub>

w is the cumulative seismic weight

S<sub>d</sub>(T<sub>1</sub>) is the design acceleration response spectrum for the fundamental (first mode) time period, T<sub>1</sub>

g is the acceleration due to gravity taken as 9.81 m/s<sup>2</sup>

$$F_i = F_b \times \frac{z_i \times m_i}{\sum z_j \times m_j}$$

*Equation 13 Horizontal Distribution of Base Shear Force*

where:

F<sub>b</sub> is the base shear force, which is calculated from Equation 13.

Z<sub>i</sub> is the vertical distance of the mass relative to the location of application of the base shear force

M<sub>i</sub> is the mass at each seismic level calculated in Step 3

F<sub>i</sub> the horizontal force at the seismic level being taken into consideration

### Step 5: Determination of Wall Rigidities

In this part of the analysis, it is necessary to distinguish whether each transverse masonry shear wall may be considered to be a cantilever wall or a fixed pier. In locations where solid continuous walls are located, the wall may be deemed to be acting as a cantilever wall whose fixity solely lies at the bottom. In locations where transverse walls have openings present, the wall is then further subdivided into areas categorised as strips and piers. The strips, alternatively referred to as spandrel beams, obtain their fixity at the top (to the spandrel beam) and at the bottom (to the foundation). Both the strips and piers are then defined according to their height-to-width ratio as demonstrated in Figure 30.

It is worth noting the importance of the sway deflection at this stage. In accordance with Taly (2010), a wall containing openings may be referred to as a perforated wall. Perforated walls drastically reduce the sway stiffness of the wall in comparison to that of a solid wall. Thus, the resulting sway rigidity of the wall is much lower, even though their overall dimensions may be the same. The solid wall, which ultimately possesses a much greater stiffness, would thus attract a greater portion of the lateral load acting on the structure.

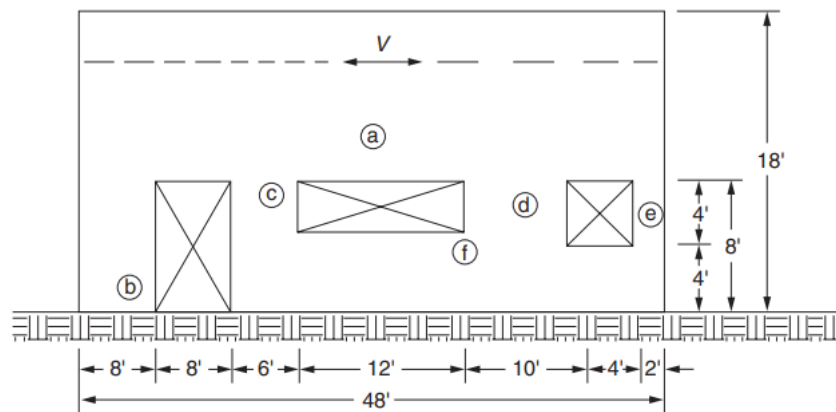


**Figure 30** Shear Wall with openings  
Source: (Taly, 2010)

For perforated walls, a wall is initially considered solid, thus acting as a cantilever. Then, the sway deflection experienced in the strip is determined, and this value is then subtracted from the deflection of the solid cantilever wall. The final step involves adding the sway deflections of all piers within the wall. This procedure is summarised in Equation 14. The sway rigidity of the wall is then a result of the reciprocal of its deflection as shown in Equation 15.

$$\Delta_{TOTAL\ WALL} = \Delta_{SOLID\ (C)} - \Delta_{STRIP\ (C)} + \Delta_{PIERS\ (F)}$$

**Equation 14** Total Deflection of the Wall

$$\frac{1}{R_W} = \frac{1}{R_{SOLID\ (C)}} - \frac{1}{R_{STRIP\ (C)}} + \frac{1}{R_{PIERS\ (F)}}$$

**Equation 15** Rigidity of the wall

$$R_C = \frac{E_m t}{4 (h/d)^3 + 3(h/d)}$$

**Equation 16** Rigidity of a cantilever wall

$$R_F = \frac{E_m t}{(h/d)^3 + 3(h/d)}$$

**Equation 17** Rigidity of a fixed pier

### Rigidity of Masonry Walls

$$\Delta_{total} = \Delta_{solid [c]} - \Delta_{strip [c]} + \Delta_{pier [f]}$$

$$R = \frac{1}{\Delta_{total}} \qquad \Delta_{total} = \frac{1}{R}$$

$$\text{Rigidity of cantilever wall } R_c = \frac{E_m \times t}{4(h/d)^3 + 3(h/d)}$$

$$\text{Rigidity of fixed pier } R_f = \frac{E_m \times t}{(h/d)^3 + 3(h/d)}$$

Type	Section	Part	Connection	Height	Width	Rigidity	Defn/ Et
Wall A	Solid		Cantilever	3	6.03	3.522687563	0.283874168
	Strip		Cantilever	0.83	6.03	96.27740365	0.010386653
	Pier	R1	Fixed	2.1	1.09	0.077333493	12.93100772
		R2	Fixed	2.1	1.09	0.077333493	12.93100772
				<b>Total R</b>		<b>0.03826213</b>	<b>26.13550296</b>
Wall B	Solid		Cantilever	3	2.46	3.796378585	0.263408924
	Strip		Cantilever				
	Pier		Fixed				
				<b>Total R</b>		<b>0.263408924</b>	<b>0.263408924</b>
Wall C	Solid		Cantilever	3	6.03	3.522687563	0.283874168
	Strip		Cantilever	0.83	2.46	7.521146882	0.132958446
	Pier	R1	Fixed	2.1	0.81	0.039676268	25.20398313
		R2	Fixed	2.1	0.58	0.017144685	58.32711468
				<b>Total R</b>		<b>0.011949999</b>	<b>83.68201354</b>
Wall D	Solid		Cantilever	3	2	4.574074074	0.218623482
	Strip		Cantilever				
	Pier		Fixed				
				<b>Total R</b>		<b>0.218623482</b>	<b>0.218623482</b>
Wall E	Solid		Cantilever	3	4.8347	2.907911531	0.343889417
	Strip		Cantilever				
	Pier		Fixed				
				<b>Total R</b>		<b>0.343889417</b>	<b>0.343889417</b>
Wall F	Solid		Cantilever	3	6.03	3.522687563	0.283874168
	Strip		Cantilever	0.83	4.8347	49.92496645	0.020030059
	Pier	R1	Fixed	2.1	1.2174	0.097013854	10.30780617
		R2	Fixed	1	1.2174	0.331289172	3.018510973
R3		Fixed	1	0.6	0.103846154	9.62962963	
				<b>Total R</b>		<b>0.04306671</b>	<b>23.21979088</b>

*Table 9 Division of each wall segment into solid, strip and pier  
Source: (Author, 2023)*

Wall G	Solid	Cantilever		3	3.0647	3.203192254	0.312188567
	Strip	Cantilever					
	Pier	Fixed					
				<b>Total R</b>	<b>0.312188567</b>	<b>3.203192254</b>	
Wall H	Solid	Cantilever		3	4.8347	2.907911531	0.343889417
	Strip	Cantilever					
	Pier	Fixed					
				<b>Total R</b>	<b>0.343889417</b>	<b>2.907911531</b>	
Wall I	Solid	Cantilever		3	6.03	3.522687563	0.283874168
	Strip	Cantilever		0.83	4.8347	49.92496645	0.020030059
	Pier	R1	Fixed	2.1	1.2174	0.097013854	10.30780617
		R2	Fixed	1	1.2174	0.331289172	3.018510973
		R3	Fixed	1	0.6	0.103846154	9.62962963
				<b>Total R</b>	<b>0.04306671</b>	<b>23.21979088</b>	

*Table 10 Continuation of Table 9  
Source: (Author, 2023)*

Relative Stiffness of Wall					
Level	Type	Rigidity	Thickness	Total Rigidity of Walls	Relative Stiffness
1 till 4	Wall A	0.038	0.23	0.00880029	0.023642747
1 till 4	Wall B	0.263	0.23	0.060584053	0.162764347
1 till 4	Wall C	0.012	0.23	0.0027485	0.007384085
1 till 4	Wall D	0.219	0.23	0.050283401	0.135090746
1 till 4	Wall E	0.344	0.23	0.079094566	0.212494456
1 till 4	Wall F	0.043	0.23	0.009905343	0.02661157
1 till 4	Wall G	0.312	0.23	0.07180337	0.192906023
1 till 4	Wall H	0.344	0.23	0.079094566	0.212494456
1 till 4	Wall I	0.043	0.23	0.009905343	0.02661157
<b>Total</b>				<b>0.372219432</b>	

*Table 11 Rigidity of each wall  
Source: (Author, 2023)*

## 6.2 Retrofitting Plane Frames in the Soft Storey Basement

This section deals with finding the required structural steelwork and reinforced concrete column sections, which have the equivalent sway stiffness of the overlying transverse masonry shear walls. In order to obtain this sway stiffness, one must multiply the value wall rigidity, obtained in the previous section, with the thickness of the wall and the Modulus of Elasticity of masonry. As described in the previous section, pinned-fixed (pinned at the base and rigid at the beam/column eaves connection) columns were employed, and thus the sway stiffness of this column is as described in Equation 18. The main reason as to why pinned-base columns were selected would be so as to avoid the creation of moments within the foundation, which would require larger foundations adjacent to the third party walls. However, in this case, larger section sizes (than would have been required for fixed bases) are to be implemented to generate the rigidity, which is required.

$$I_{column} = \frac{L^3}{3 E_{steel} \times \text{no. of columns}} \times K_{wall}$$

*Equation 18 Moment of Inertia for a pinned-fixed column*

$$I_{column} = \frac{L^3}{12 E_{steel} \times \text{no. of columns}} \times K_{wall}$$

*Equation 19 Moment of Inertia of fixed-pinned column*

L: Height of basement

E<sub>steel</sub>: Modulus of Elasticity of steel

K<sub>wall</sub>: Sway Stiffness of masonry wall

I<sub>column</sub>: Moment of Inertia of a column

$$K_{wall} = R \times E_{masonry} \times t$$

*Equation 20 Stiffness of masonry wall*

R: Wall rigidity

E<sub>masonry</sub>: Modulus of Elasticity of masonry

t: Wall Thickness

K<sub>wall</sub>: Sway Stiffness of masonry wall

Once the sway stiffness of the column section was obtained using the above procedure, this value was multiplied by 2 in order to obtain the required sway stiffness for each plane frame and then multiplied by 0.7 to obtain 70% of  $K_m$  (or by 1.0 to obtain 100% of  $K_m$ ). However, in the case of the structural steelwork plan frames, it was realised that the required column sway stiffnesses could not be catered for using the largest available section sizes on the market. In the case of the reinforced concrete plane frames, the required column sway stiffnesses would have necessitated the use of excessively large column sections. For these reasons, it was decided instead to provide plane frames with 35% of  $K_m$  and 50% of  $K_m$ . The corresponding resulting column stiffnesses are shown in Table 12. It should be noted that the values, which are marked in yellow, required additional steel flange plates, since the largest available section sizes available on the market could not provide the required column sway stiffness.

As the seismic analyses were conducted, numerous hurdles were encountered, which led to the consideration of other options. Consequently, opting to examine the behaviour of both structural steelwork and reinforced concrete plane frames seemed to be a viable solution, along with varying levels of rigidity. In addition to the 35% of  $K_m$  sway stiffness structural steelwork plane frames, this research study also considered 50% of  $K_m$  sway stiffness structural steelwork plane frames, 35% of  $K_m$  sway stiffness reinforced concrete plane frames, and also 50% of  $K_m$  sway stiffness reinforced concrete plane frames.

Section sizes used at each transverse wall for **35%  $K_m$  sway stiffness structural steelwork plane frame**:

**Wall A:** HD 400 x 382

**Wall B:** HD 400 x 1299 + 20mm thick flange plates

**Wall C:** HD 360 x 147

**Wall D:** HD 400 x 1299 + 5mm thick flange plates

**Wall E:** HD 400 x 1299 + 50mm thick flange plates

**Wall F:** HD 400 x 421

**Wall G:** HD 400 x 1299 + 35mm thick flange plates

**Wall H:** HD 400 x 1299 + 10mm thick flange plates

**Wall I:** HD 400 x 421

Section sizes used at each transverse wall for **50%  $K_m$  sway stiffness structural steelwork plane frame**:

**Wall A:** HD 400 x 900

**Wall B:** HD 400 x 1299 + 180mm thick flange plates

**Wall C:** HD 360 x 347

**Wall D:** HD 400 x 1299 + 140mm thick flange plates

**Wall E:** HD 400 x 1299 + 200mm thick flange plates

**Wall F:** HD 400 x 900

**Wall G:** HD 400 x 1299 + 170mm thick flange plates

**Wall H:** HD 400 x 1299 + 200mm thick flange plates

**Wall I:** HD 400 x 900

Section sizes used at each transverse wall for **35%  $K_m$  sway stiffness reinforced concrete plane frame**:

**Wall A:** 400 x 700

**Wall B:** 500 x 1200

**Wall C:** 300 x 500

**Wall D:** 600 x 1050

**Wall E:** 500 x 1300

**Wall F:** 400 x 700

**Wall G:** 550 x 1200

**Wall H:** 550 x 1100

**Wall I:** 400 x 700

Section sizes used at each transverse wall for **50%  $K_m$  sway stiffness reinforced concrete plane frame**:

**Wall A:** 500 x 900

**Wall B:** 700 x 1500

**Wall C:** 400 x 650

**Wall D:** 700 x 1400

**Wall E:** 900 x 1500

**Wall F:** 600 x 900

**Wall G:** 850 x 1500



Wall H: 900 x 1500

Wall I: 600 x 900

**Finding the required Steel Column Sections which have the equivalent Sway Stiffness of the Stone Masonry Walls**

**Stiffness of Walls = Stiffness of Columns**  
**Stiffness of Column =      No. of Columns x       $\frac{3EI}{L^3}$**

**Modulus of Elasticity      N/mm<sup>2</sup>**  
 Masonry E<sub>stone</sub>      21000  
 Steel E<sub>s</sub>      210000

**Height of Floor =      3000      mm**

Type	K <sub>wall</sub>				K <sub>col</sub>		
	R	E <sub>stone</sub> N/mm <sup>2</sup>	t mm	K <sub>wall</sub> N/mm	No. of Columns	E <sub>s</sub> N/mm <sup>2</sup>	L <sup>3</sup> mm <sup>3</sup>
Wall A	0.038	21000	230	184806.086	2	210000	27000000000
Wall B	0.263	21000	230	1272265.11	2	210000	27000000000
Wall C	0.012	21000	230	57718.4964	2	210000	27000000000
Wall D	0.219	21000	230	1055951.42	2	210000	27000000000
Wall E	0.344	21000	230	1660985.88	2	210000	27000000000
Wall F	0.043	21000	230	208012.209	2	210000	27000000000
Wall G	0.312	21000	230	1507870.78	2	210000	27000000000
Wall H	0.344	21000	230	1660985.88	2	210000	27000000000
Wall I	0.043	21000	230	208012.209	2	210000	27000000000
<b>Σ K<sub>wall</sub></b>				<b>7816608.067</b>			

The sway stiffness of a pinned-base column is given by:

$$K = \frac{3EI}{L^3}$$

Type	$I = \frac{L^3}{3 \times E \times \text{No. of Col.}} \times K_{\text{wall}}$		
I of section required to have same K of wall mm <sup>4</sup>		35% of K <sub>m</sub> Required	Steel Column Stiffness Provided
Wall A	3960130408	1386045642.81	1410000000
Wall B	27262823681.22	9541988288.43	7550000000
Wall C	1236824923.60	432888723.26	4630000000
Wall D	22627530364.37	7919635627.53	7550000000
Wall E	35592554627.03	12457394119.46	7550000000
Wall F	4457404484.08	1560091569.43	1600000000
Wall G	32311516698.17	11309030844.36	7550000000
Wall H	35592554627.03	8304929412.97	7550000000
Wall I	4457404484.08	1560091569.43	1600000000

*Table 12 Required structural steelwork column sections for plane frame with equivalent sway stiffness of the stone masonry walls*

*Source: (Author, 2023)*

## 6.3 Non-Linear Static Pushover Analysis

### 6.3.1 General Introduction

Throughout this part of the research process, Gruppo Sismica kindly provided a full license to utilise the 3DMacro macro-element software program. The software provides an accurate representation of how the URM building is expected to deform and fail in a progressive manner when subjected to seismic loads.

The static inelastic analysis is an approach, which may be adopted for new and existing buildings, and which quantifies the strength and capacity of the structure to withstand earthquakes. The capacity pushover curve, which is achieved by such an analysis is also considered to be a more practical and realistic assessment of the structural behaviour during a seismic event (Shehu, 2021).

The crucial parameters of behaviour as described by Alguhane et al. (2016) and Krawinkler & Seneviratna (1998) are:

- Inter-story drift
- Global drift
- Inelastic element deformations depending on the yield value
- Element deformations
- Connection forces between elements

The crucial difference between Pushover Analysis and the Conventional Seismic Analysis as described by Leslie (2012) is that both analyses estimate a value for lateral seismic load, which is calculated based upon the fundamental period of time. However, in Conventional Seismic Analysis, this lateral load is considered to be constant and applied uniformly all throughout the analysis, whereas in the Pushover Analysis, the lateral load is continuously re-calculated as the analysis progresses.

Another fundamental distinction between both types of analyses lies in the fact that the Conventional Seismic Analysis employs an elastic model, whilst Pushover Analysis utilises a non-linear model where all the hinges are considered to be non-linear. At such hinge positions, significant failures are anticipated through cracking and yielding as the structure starts to approach its ultimate strength.

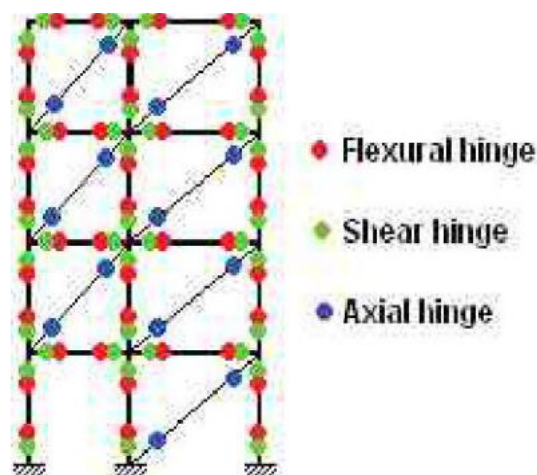


*Figure 31 Typical locations of hinges within a structural model  
Source: (Leslie, 2012)*

Krawinkler & Seneviratna (1998) state that the pushover analysis is not based on fail-safe theoretical models. An assumption, which is usually made when using the pushover analysis is that the structural response may be directly correlated to a single degree of freedom (SDOF) system. Thus, the way in which the structure responds is ultimately dependent on a singular node, which is continuous all throughout the analysis. These assumptions were outlined by Leslie (2012).

However, it is important to note that such analyses allow the prediction of the response of a structure rather than the precise determination of its failure, and thus safety factors will always be required due to the uncertainties in the seismic analysis. Additionally, the pushover analysis may also allow the determination of which structural members are most likely to experience failure mechanisms, so that appropriate strengthening measures of these members may possibly be carried out in the case of existing buildings.

### 6.3.2 3DMacro

Formisano & Chieffo (2018,) studied the efficiency and accuracy of several available seismic analysis software packages, one of which was 3DMacro by Gruppo Sismica, which was made use of in this research study. Figure 38 (left) shows a typical deformed state of a panel situated at the edge of a masonry wall. 3D Macro automatically converts these macro-elements into quadrilateral elements, which are interconnected with one another through springs. In this manner, this modelling approach correctly tackles possible failure mechanisms, which may be critical, such as shear taking place diagonally and sliding shear. In addition, 3D Macro also allows the analysis to be carried out in the X- and Y-directions, as well as in eccentric directions.

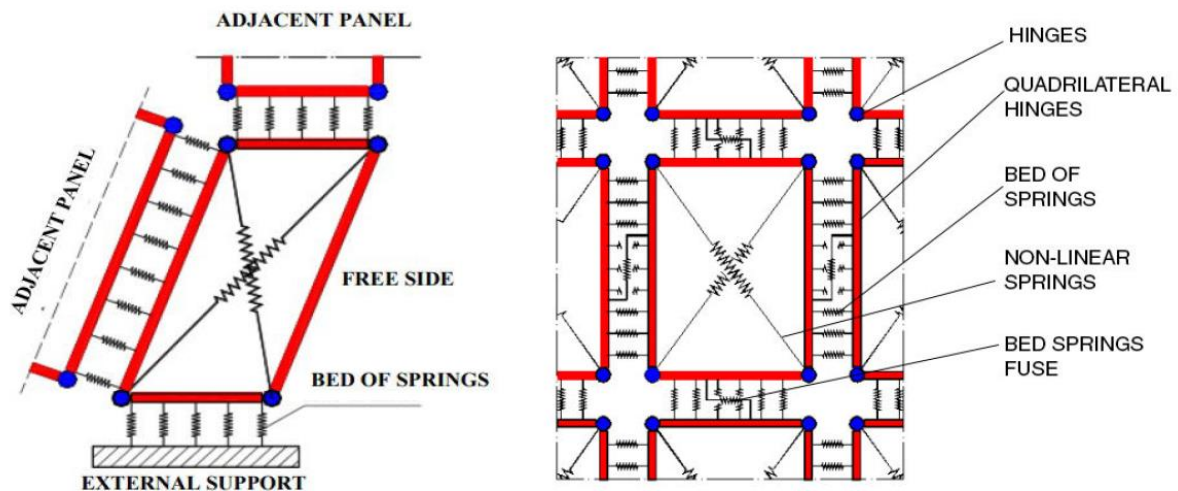


**Figure 32** (left) Modelling of a typical edge panel in its deformed state, (right) Wall modelled using a mesh of interconnected macro-element quadrilaterals  
 Source: (Brincat, 2020) adapted from  
 Left: (Formisano & Chieffo, 2018)  
 Right: 3DMacro Manuale Teorico

In this way, a complex masonry structure may then be simplified into multiple quadrilaterals Figure 32 (right). Every quadrilateral, or rather panel, may perform in conjunction with another panel due to a ‘discrete distribution of non-linear springs’ as described by Panto et al. (2016). Each quadrilateral is composed of four rigid edges having a diagonal link, which replicates the behaviour of shear, whilst the springs at the interface model axial and flexural deformations. Figure 33 shows the orientation of springs at each interface, having a row of springs acting orthogonal to the interface, whilst another row acting parallel to the interface. The level of accuracy, which may be achieved throughout the macro-element seismic analysis is dependent on the number of springs used at the element interface.

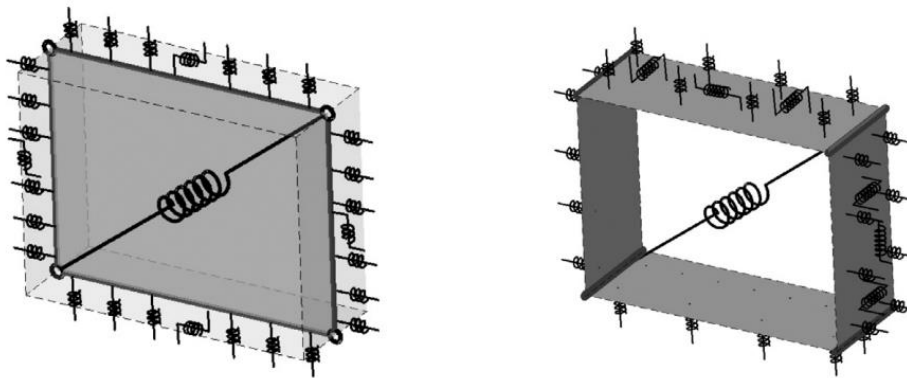


*Figure 33 Equivalent mechanical representation of the macro-element (left) The plane macro-element (right) The spatial macro-element  
Source: Panto et al. (2016)*

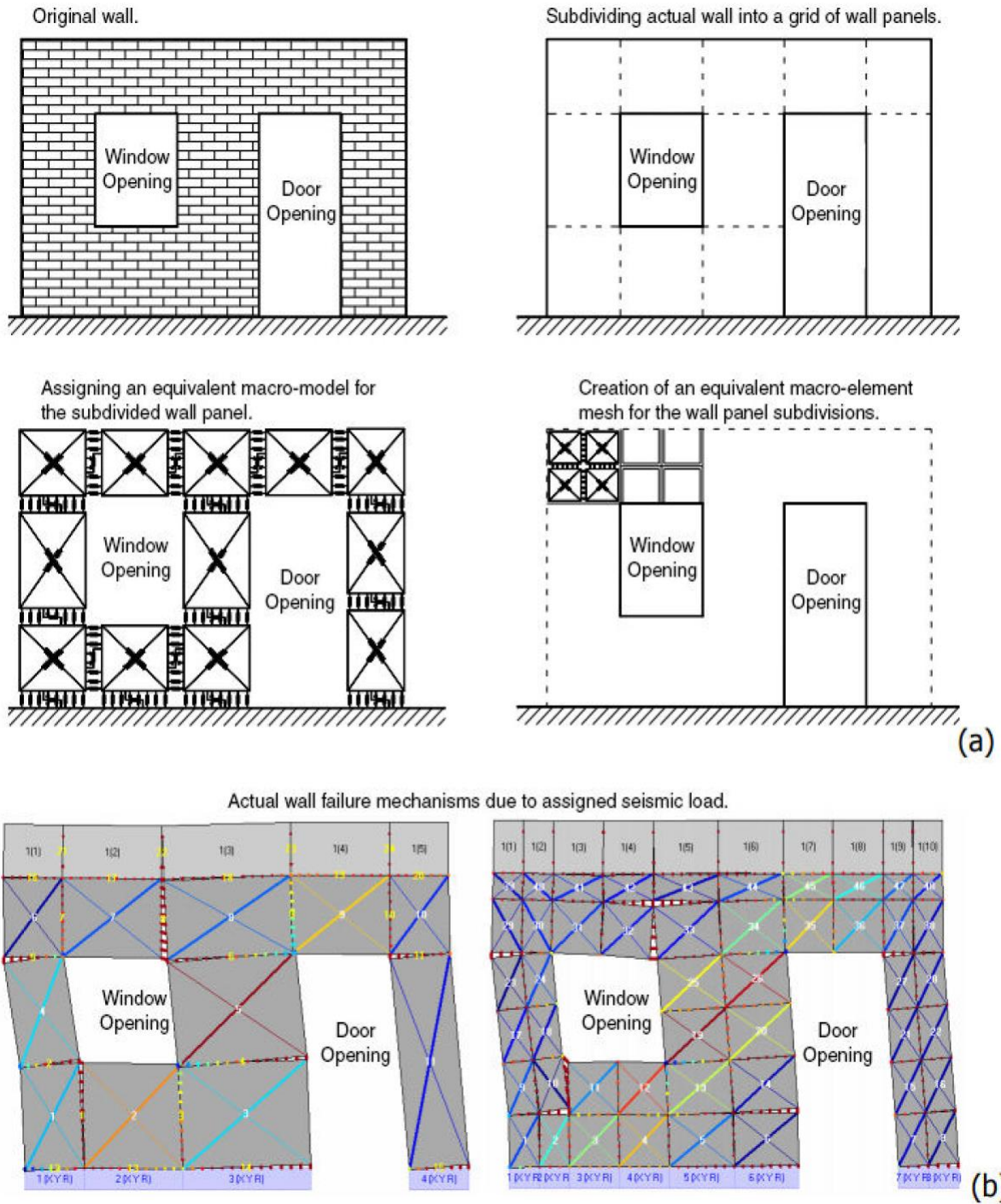
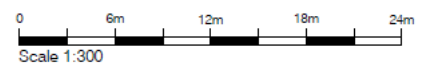
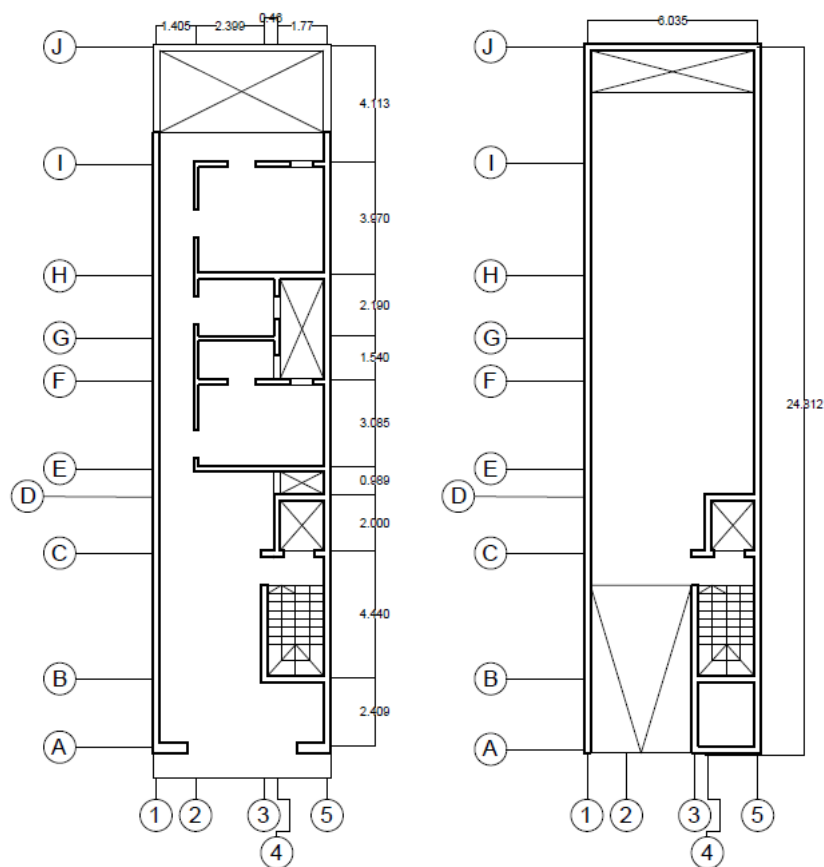


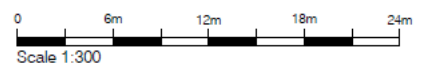
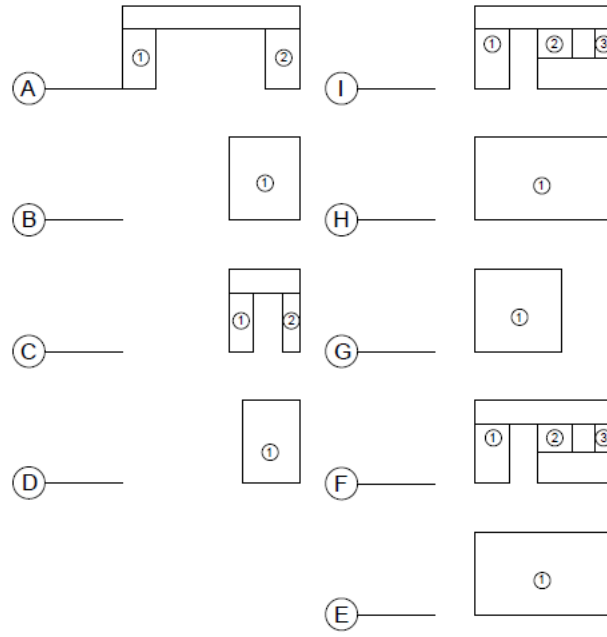
**Figure 34** (a) Simplification of numerical model using 3D Macro (b) Resulting collapse mechanism  
 Source: 3D Macro Manuale Teorico

## 6.4 Building Plans, General Layouts and Building Aggregate Combinations

### 6.4.1 Introduction






This dissertation examines the identical plan typologies explored in both Borg (2017) and Borg (2021). The residential URM building, shown in the figure below, portrays a single unit (SU) plan having an aspect ratio of 1:4, in accordance with the maximum ratio stipulated in EC8. Each URM building considered contains a soft storey basement. In addition, the URM building aggregates considered are composed of combinations of these URM single unit buildings situated side-by-side forming a row of adjacent SUs, each SU with the plan layout below (Appendix B).

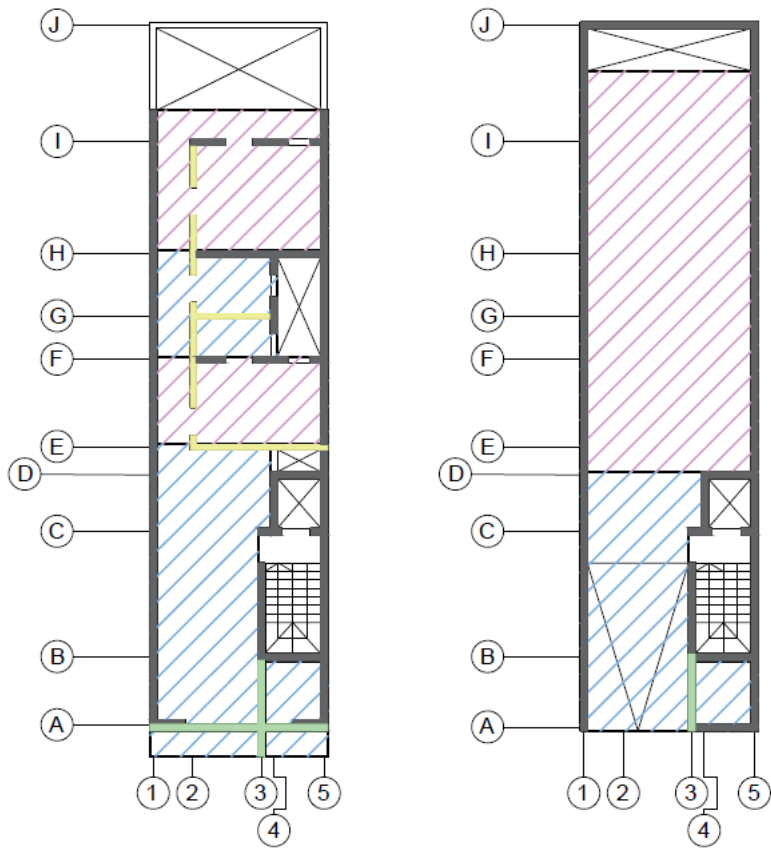






**Figure 35** Typical layout plan (left) basement level (right) all upper floors  
 Source: (Author, 2023)

-  225mm thick Cast-in-situ Concrete Slab
-  350mm thick Cast-in-situ Concrete Slab
-  230mm thick Globigerina Limestone Masonry Wall
-  180mm thick Globigerina Limestone Masonry Wall
-  Down stand beam





#### **6.4.2 Plan Definition**

As previously mentioned, this research follows up on the work carried out by Borg (2021). Therefore, the SU properties adopted by Borg (2021) have also been used in this research study. Moreover, it should be noted that the SU considered is an already existing residential building. In addition, local Globigerina Limestone blocks with M2 mortar strength were considered.

Plan size of the SU plot:

Width: 6.03m

Length: 24.83m

Internal and external masonry wall thicknesses:

Façade & third party walls: 230mm

Internal walls: 180mm

## 6.5 Method of Seismic Analysis

### 6.5.1 Definition of Material Properties

The mechanical properties of masonry blocks and mortar were adopted from previous research carried out by Borg (2021), Brincat (2020), Cachia (1985) and Buhagiar (2019).

Mechanical Properties of Masonry Blocks and Mortar			
Symbol	Description	Value (N/mm <sup>2</sup> )	Reference
$E_b$	Young's Modulus of Elasticity of Limestone Block	21,000	Brincat (2020)
$E_m$	Young's Modulus of Elasticity of Mortar	8,000	Brincat (2020)
$G_b$	Shear Modulus of Elasticity of Block	8,400	Brincat (2020)
$G_m$	Shear Modulus of Elasticity of Mortar	3,076.9	Brincat (2020)
	Compressive Strength of Block	17.5	Xuereb (1991)
	Compressive Strength of Mortar	2 <sup>134</sup>	Brincat (2020)
	Tensile Strength of Block	3	Cachia (1985)
	Tensile Strength of Masonry	0	Brincat (2020)
$f_{mk}$	Characteristic Strength of Masonry	4.108	Buhagiar (2019)

*Table 13 Mechanical Properties of Masonry Blocks and Mortar  
Source: Borg (2021) adapted from Brincat (2020)*

Equation 21 has been used to obtain the smeared physical properties of the building materials used within the seismic analyses. This equation considers the relative proportions of masonry block and mortar areas individually in comparison to the entire area of the masonry wall.

$$X_t = \frac{[X_b \times A_b] + [X_m \times A_m]}{[A_b + A_m]}$$

*Equation 21 Smeared property equation  
Source: Borg (2021) adapted from Brincat (2020)*

where:

$X_b$ : Material property of masonry block

$A_b$ : Area of one singular masonry block taken at elevation

$X_m$ : Material property of mortar block

$A_m$ : Area filled with mortar taken at elevation

$X_t$ : Final smeared material property value (used in 3DMacro)

<b>Smearred Properties of Masonry</b>			
<b>Symbol</b>	<b>Description</b>	<b>Value (N/mm<sup>2</sup>)</b>	<b>Reference</b>
<b>E<sub>bm</sub></b>	Young's Modulus of Elasticity	20337.12	Brincat (2020)
<b>G<sub>bm</sub></b>	Shear Modulus of Elasticity	8128.52	Brincat (2020)
<b>f<sub>kbm</sub></b>	Compressive Strength	20.03	Brincat (2020)
<b>f<sub>tbm</sub></b>	Tensile Strength	2.85	Brincat (2020)
<b>τ<sub>bm</sub></b>	Shear Strength	0.603	Brincat (2020)

*Table 14 Smearred Properties of Masonry  
Source: Borg (2021) in Brincat (2020)*

## 6.5.2 Definition of Geometrical Properties

### 6.5.2.1 Site Topography

Initially, the research was based on a ground stratum classified as Ground Type A corresponding to strong rock. The site topography is also assumed to be flat for ease of computation. With regards to the elastic acceleration response spectra, the site topography is also defined as Type 1. Eventually, the parametric seismic analyses were repeated for Ground Types B and C.

### 6.5.2.2 Structural Walls

As stated in the research carried out by Borg (2021), the material utilised for the structural walls was Globigerina Limestone blocks with thicknesses of 230mm and 150mm. The basement level was constructed entirely using 230mm thick walls, whilst for the upper floors, some of the internal walls were 150mm thick. It is important to note that for the lift shaft, ventilation shafts and stairwell, a 230mm thick wall has been utilised all throughout.

### 6.5.2.3 Floor Diaphragms

Sizing of floor diaphragms have remained coherent to that carried out by Borg (2021) and all concrete elements were assumed to have a C20/25 grade. In addition, staircases were modelled as voids for reasons of ensuring proper comparison of results.

### 6.5.2.4 Loads

The following loads were extracted from the research work done by Borg (2021):

Imposed Loads (Category A)

- Floors,  $q_k = 2.0 \text{ kN/m}^2$  (unfactored)
- Balconies,  $q_k = 2.5 \text{ kN/m}^2$  (unfactored)

Dead Loads

- Screed layer (150mm thick) =  $0.15 \times 18 \text{ kN/m}^3 = 2.70 \text{ kN/m}^2$
- Tile layer (25 mm) =  $0.025 \times 18 \text{ kN/m}^3 = 0.45 \text{ kN/m}^2$

### 6.5.3 Numerical Model Build Up

Prior to commencing the numerical model generation on 3D Macro, a set of design parameters dealing with location of the site, life of the structure and, hence, determining its importance factor, soil type, structural damping, limit states and ground acceleration response spectra were initially established. Details of these design parameters are provided in Appendix A.

The next step of the procedure was to determine the number of seismic levels, which were to be designed within that numerical model. Each seismic level was taken to be 3m in height for simplicity. Subsequently, the material properties for all masonry, concrete and steel elements were defined in order to design the section sizes for walls, beams, slabs and foundations. Once this part of the process was completed, the numerical model was generated according to the typical plan layout shown in Section 6.4.1. The final part of this procedure includes specifying the load cases, which are to be conducted for the pushover analysis.

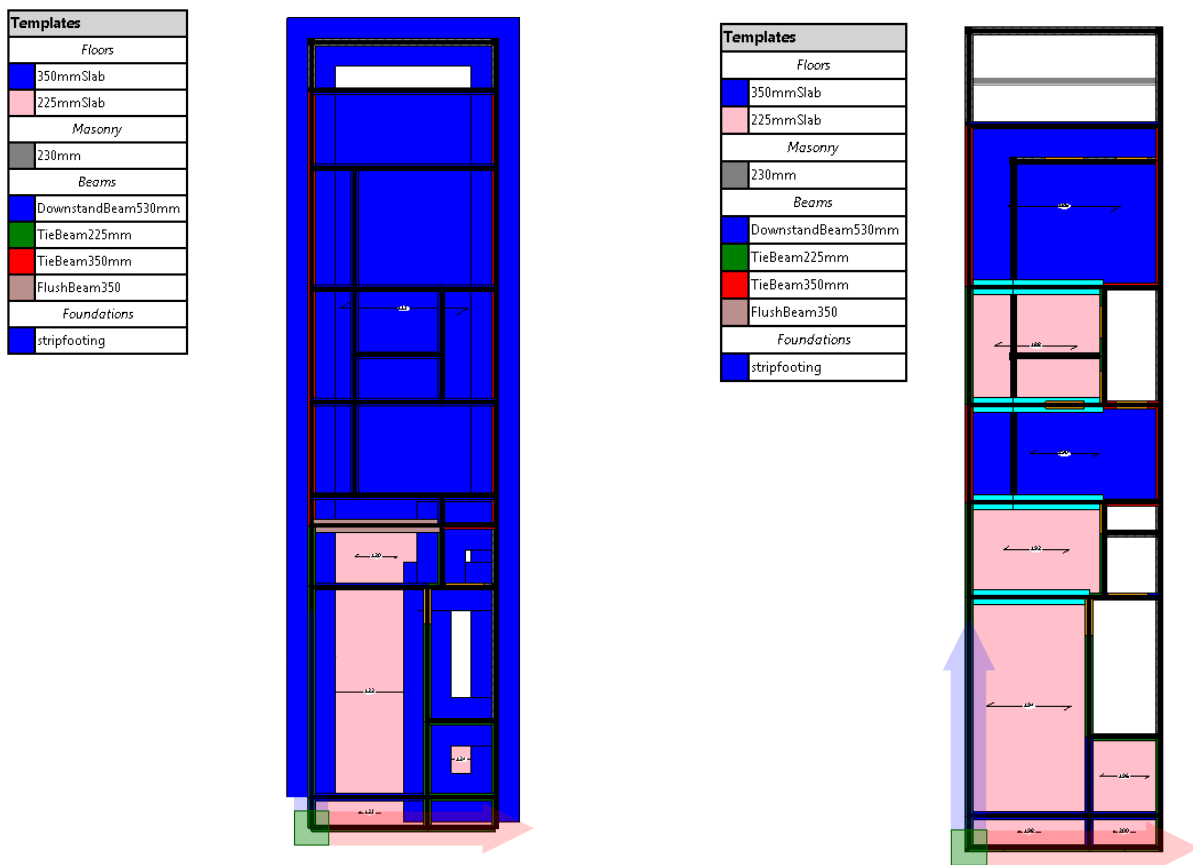


Figure 36 Typical layout plan (left) basement level (right) all upper floors  
Source: (Author, 2023)

## 6.5.4 Seismic Analysis

During the numerical modelling procedure on 3D Macro, the ‘Ministerial Decree of 17 January 2018 Technical standards for Construction (NTC 2018)’ guidelines have been utilised. In this recent update, the Italian Guidelines outline the recommended process to strengthen an existing building and, hence, to determine the seismic risk classification based on a safety index parameter. This process ultimately allows the determination of effective retrofitting measures and an assessment the corresponding seismic vulnerability of the retrofitted URM building. This recent update was prompted due to the recognition that a considerable percentage of building stock in Italy are vulnerable to seismic events, which is very similar to the local situation. As a result of the last three seismic events, Italy suffered several fatalities, significant structural damage and consequent substantial economic burdens. Therefore, there is a nationwide imperative to retrofit existing buildings in order to withstand natural disasters caused by such seismic phenomena.

It is important to consider that this research study has considered the safety index parameter for both the ‘Life Protection Limit State’ (SLV) and the ‘Collapse Prevention Limit State’ (SLC). These limit states are comprehensively outlined in NTC 2018 Cl. 3.2.1. The ‘Life Protection Limit State’ is equivalent to the ‘Significant Damage’ (SD) limit state described in EC8: Part 3. Similarly, the ‘Collapse Prevention Limit State’ (SLC) is equivalent to the ‘No Collapse Requirement’ (NC) in EC8: Part 1.

### 3.2.1. STATI LIMITE E RELATIVE PROBABILITÀ DI SUPERAMENTO

Nei confronti delle azioni sismiche, sia gli Stati limite di esercizio (SLE) che gli Stati limite ultimi (SLU) sono individuati riferendosi alle prestazioni della costruzione nel suo complesso, includendo gli elementi strutturali, quelli non strutturali e gli impianti.

Gli Stati limite di esercizio (SLE) comprendono:

- **Stato Limite di Operatività (SLO):** a seguito del terremoto la costruzione nel suo complesso, includendo gli elementi strutturali, quelli non strutturali e le apparecchiature rilevanti in relazione alla sua funzione, non deve subire danni ed interruzioni d'uso significativi;
- **Stato Limite di Danno (SLD):** a seguito del terremoto la costruzione nel suo complesso, includendo gli elementi strutturali, quelli non strutturali e le apparecchiature rilevanti alla sua funzione, subisce danni tali da non mettere a rischio gli utenti e da non compromettere significativamente la capacità di resistenza e di rigidità nei confronti delle azioni verticali ed orizzontali, mantenendosi immediatamente utilizzabile pur nell'interruzione d'uso di parte delle apparecchiature.

Gli Stati limite ultimi (SLU) comprendono:

- **Stato Limite di salvaguardia della Vita (SLV):** a seguito del terremoto la costruzione subisce rotture e crolli dei componenti non strutturali ed impiantistici e significativi danni dei componenti strutturali cui si associa una perdita significativa di rigidità nei confronti delle azioni orizzontali; la costruzione conserva invece una parte della resistenza e rigidità per azioni verticali e un margine di sicurezza nei confronti del collasso per azioni sismiche orizzontali;
- **Stato Limite di prevenzione del Collasso (SLC):** a seguito del terremoto la costruzione subisce gravi rotture e crolli dei componenti non strutturali ed impiantistici e danni molto gravi dei componenti strutturali; la costruzione conserva ancora un margine di sicurezza per azioni verticali ed un esiguo margine di sicurezza nei confronti del collasso per azioni orizzontali.

Le probabilità di superamento nel periodo di riferimento  $P_{V_g}$  cui riferirsi per individuare l'azione sismica agente in ciascuno degli stati limite considerati, sono riportate nella Tab. 3.2.I.

*Figure 37 Extract from NTC 2018 Cl. 3.2.1*

Furthermore, seismic loads have been considered to act in different horizontal orientations, including eccentric directions. The load cases, which were considered within the seismic analyses are the following,

Main Axis:

1. Pushover + X Acc
2. Pushover – X Acc
3. Pushover + Y Acc
4. Pushover – Y Acc

Main Axis and Eccentricities:

1. Pushover + X Acc + e
2. Pushover – X Acc + e
3. Pushover + Y Acc + e
4. Pushover – Y Acc + e

Combined Orthogonal Seismic Loading:

1. Pushover  $E_x + 0.3E_y$  Acc
2. Pushover  $0.3E_x + E_y$  Acc
3. Pushover  $-0.3E_x + E_y$  Acc
4. Pushover  $-E_x + 0.3E_y$  Acc

### 6.5.5 Limitations

One limitation, which somewhat initially stifled the seismic analysis process was that the numerical models generated in the study by Borg (2021) were not generating the required pushover curves using the latest version of 3D Macro. Consequently, new models needed to be generated leading to possible discrepancies between both sets of models and their corresponding results.

The steel section sizes used for retrofitting were not verified for local buckling, as only the sway stiffness of the steel section was taken into consideration. Some of the findings suggest that failure primarily occurred within the section rather than the masonry elements. Moreover, 3D Macro does not include any pre-defined standard steel sections, and so they are to be defined within the frame elements from scratch by the user.

Furthermore, when standard steel section sizes were insufficient in providing the required sway stiffnesses, flange plates were added to the outer surfaces of the flanges of the column section in order to achieve the required column sway stiffness. These flange plates necessitated a slight increase in width of approximately 25mm at each end beyond the column flange edge so as to allow room for inserting fillet welds. Unfortunately, 3D Macro does not allow for the inclusion of flange plates at the steel section flanges, and thus it was decided to increase the column flange thickness by the thickness of the flange plate as if it were one single thicker column flange.

As stated earlier, the column section sizes used for retrofitting are quite considerable in size, and thus there may be concern that they may pose an obstruction to the intended functionality of the basement as a car park. However, in a practical situation, the existing ground slab could possibly be dismantled and lowered to accommodate the required headroom after the installation of the plane frame beam. Therefore, the headroom requirement in the basement was essentially not deemed to be of concern in this research study.

When starting off the process of retrofitting, the portal frames were to be constructed at a certain distance away from the party wall, with the horizontal beam located below the existing slabs. However, problems were encountered with this arrangement in 3D Macro. Therefore, this configuration was altered in such a way that the columns were positioned along the centerline of the party wall. Also, due to modelling problems in 3D Macro, the horizontal beam inserted below the slab had to be removed, and instead the column heads were rigidly connected to the underside of the thick floor slab over the basement. This problem suggests that the numerical model was experiencing slipping between the top surface of the beam and the underside of the floor slab over the basement due to insufficient connection between them. Additionally, the software does not allow the placement of a foundation which is not centered along the masonry party wall. Therefore, separate pad footings were employed in order to provide adequate foundation bases for all the columns.

## Chapter 7: Discussion of Results

### 7.1 Introduction

Prior to examining the results obtained for each retrofitting technique, it is necessary to explain the impact of having an unsymmetrical plan on the seismic analysis. As expected, the most critical earthquake direction was in the transverse X-direction, since the building is subjected to minor axis bending on plan. The data presented in Figure 38 illustrates that the lowest values for  $\alpha$  (safety factor) is consistently found within the following load cases (marked in blue in Figure 38):

- Pushover – X Acc
- Pushover – X Acc + e
- Pushover – Ex + 0.3Ey Acc

It also important to keep in mind throughout this discussion that the X-direction refers to the transverse direction, whilst the Y-direction corresponds to the longitudinal. When taking into consideration the Y-direction, the resistance of the masonry building in this orientation would ultimately not be affected by any form of retrofitting. This is because in such a case, resistance to seismic loading is solely being generated by the party walls and any longitudinal masonry shear walls at basement level, while the transverse masonry shear walls or the plane frames at basement level do not enhance the longitudinal seismic resistance of the URM building. This is primarily due to the fact that the masonry walls are only capable of providing resistance to seismic loading when the earthquake is acting in the same plane as the shear wall.

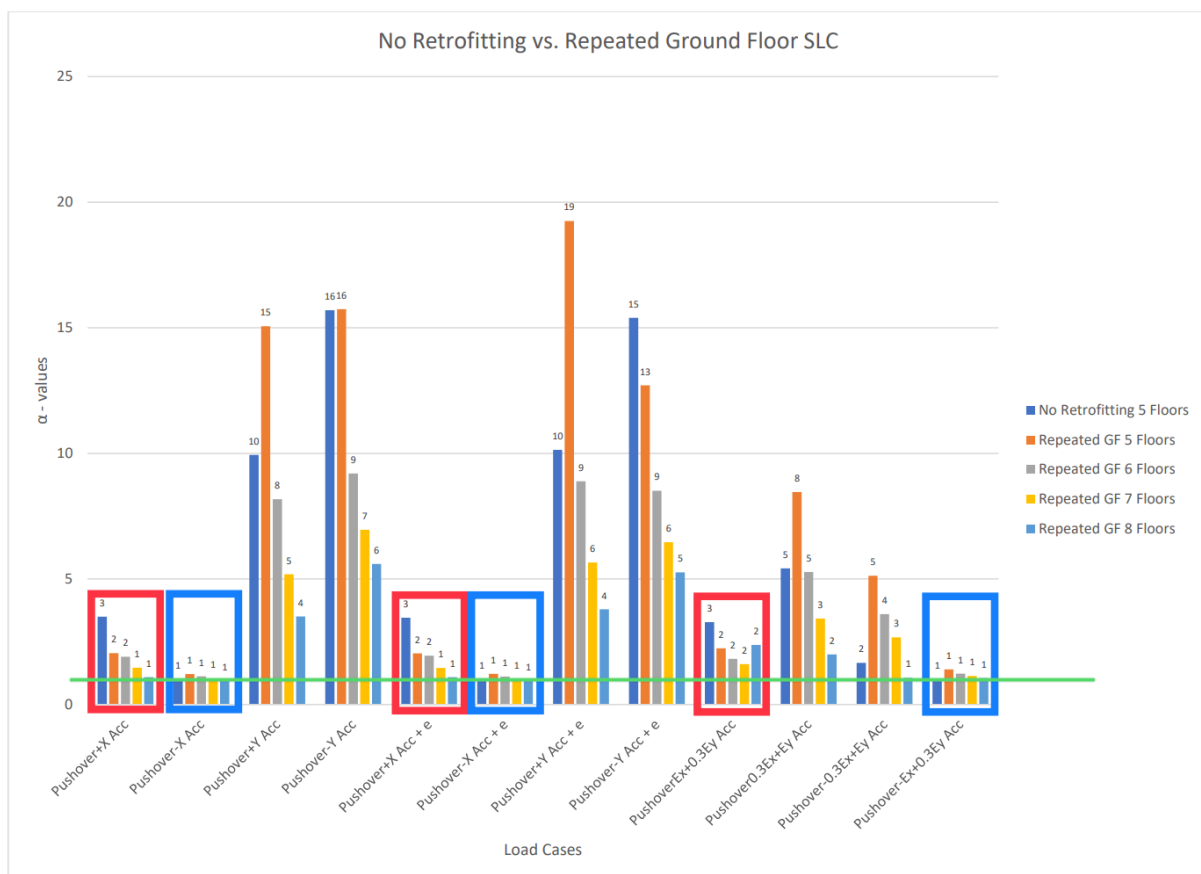


Figure 38 Comparison between No Retrofitting vs Repeated GF in SLC



Similarly, when there is an earthquake acting in the X-direction, the third party masonry walls would not contribute to the transverse seismic resistance, since it is the transverse masonry shear walls and any plane frames, which resist the earthquake.

Furthermore, it is also important to consider the differences, which arise between transverse earthquakes in the Positive X-direction and the Negative X-direction. It may also be noted from Figure 38, that the safety factors for the Negative X-direction are much lower in comparison to those for the Positive X-direction. Also, when comparing within any positive X-direction (red boxes), the safety factor for the unretrofitted building is always greater than that of the retrofitted. For instance, this can be observed in the following load cases for the building without any retrofitting:

- Pushover + X Acc,  $\alpha = 3$  (rounded up to the nearest integer)
- Pushover – X Acc,  $\alpha = 1$

This occurs because the plan geometry used in this dissertation is not symmetrical along the longitudinal centre line of the plot, and thus if the building sways to the right, its resistance is different to that when it sways to the left. Furthermore, the lift shaft and stair core are acting in compression when the earthquake is in the Positive X-direction (hence, adding further seismic resistance to the URM building), while they are acting in tension when the earthquake is in the Negative X-direction.

Furthermore, these  $\alpha$ -values were extracted from distinct numerical models. The process of selecting these values involved the consideration of all load cases for multiple directions of earthquake action. For each retrofitted URM building, the minimum value of  $\alpha$  was selected, and thus it could be determined whether the structure could sustain the corresponding number of floors during an earthquake event. If the value for  $\alpha$  was below 1, the building was considered to fail. A typical example of this is shown in Appendix D.

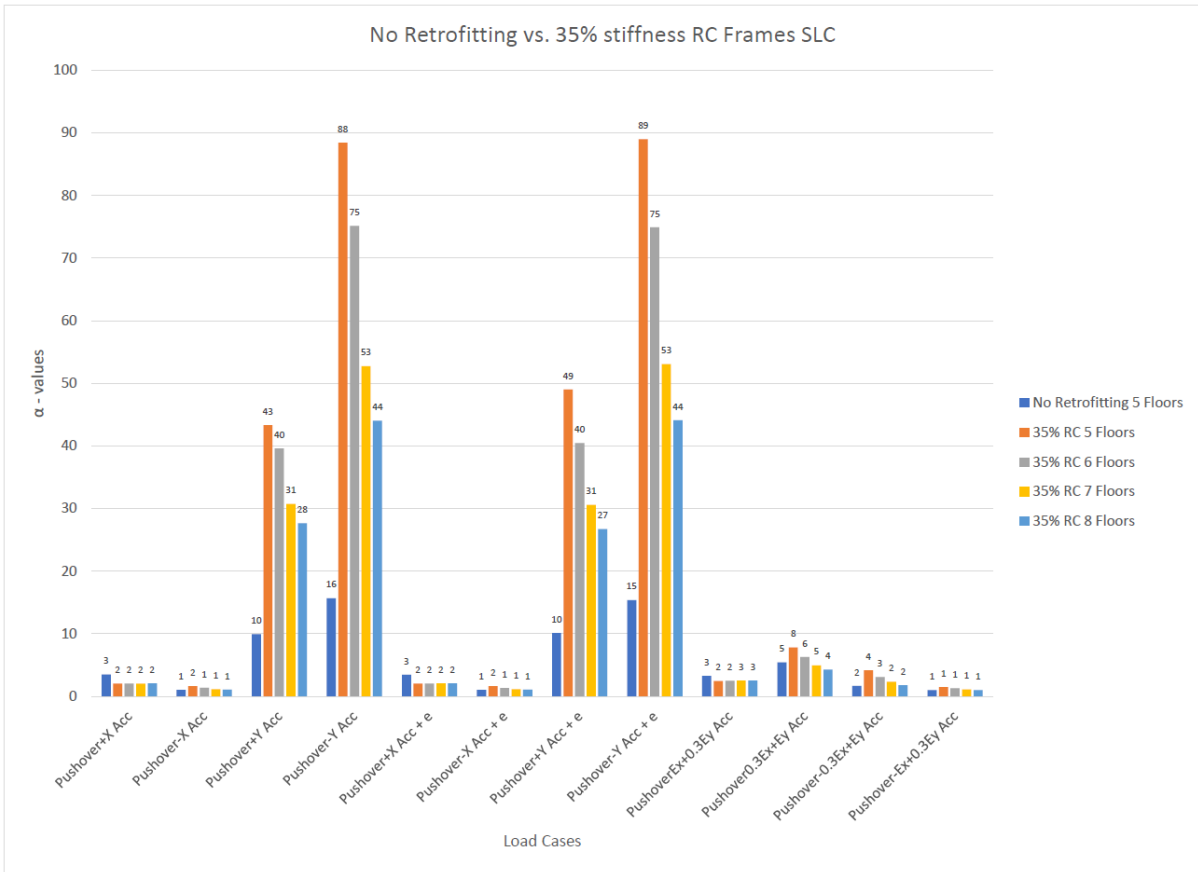


**Figure 39** Comparison between No Retrofitting vs 35% of  $K_m$  sway stiffness in RC in SLC

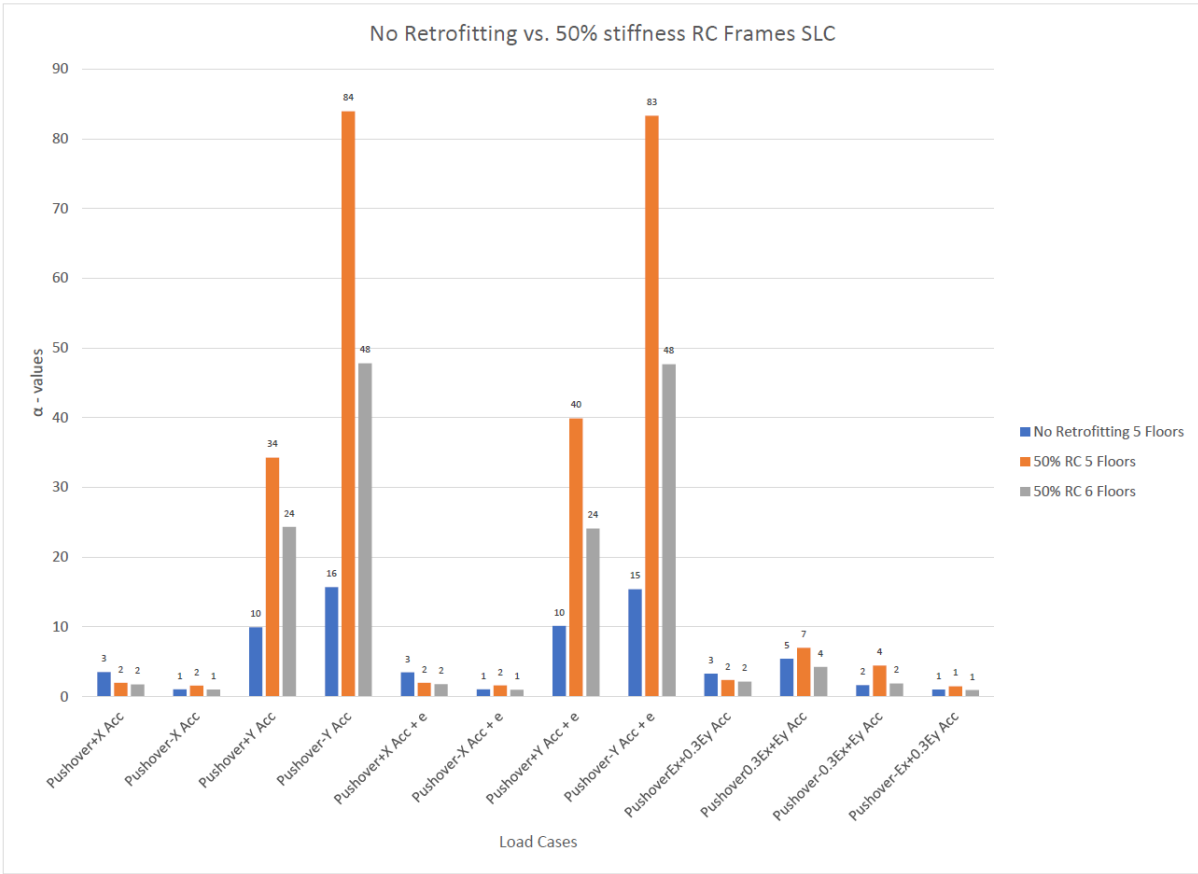


**Figure 40** Comparison between No Retrofitting vs 50% of  $K_m$  sway stiffness in RC in SLC

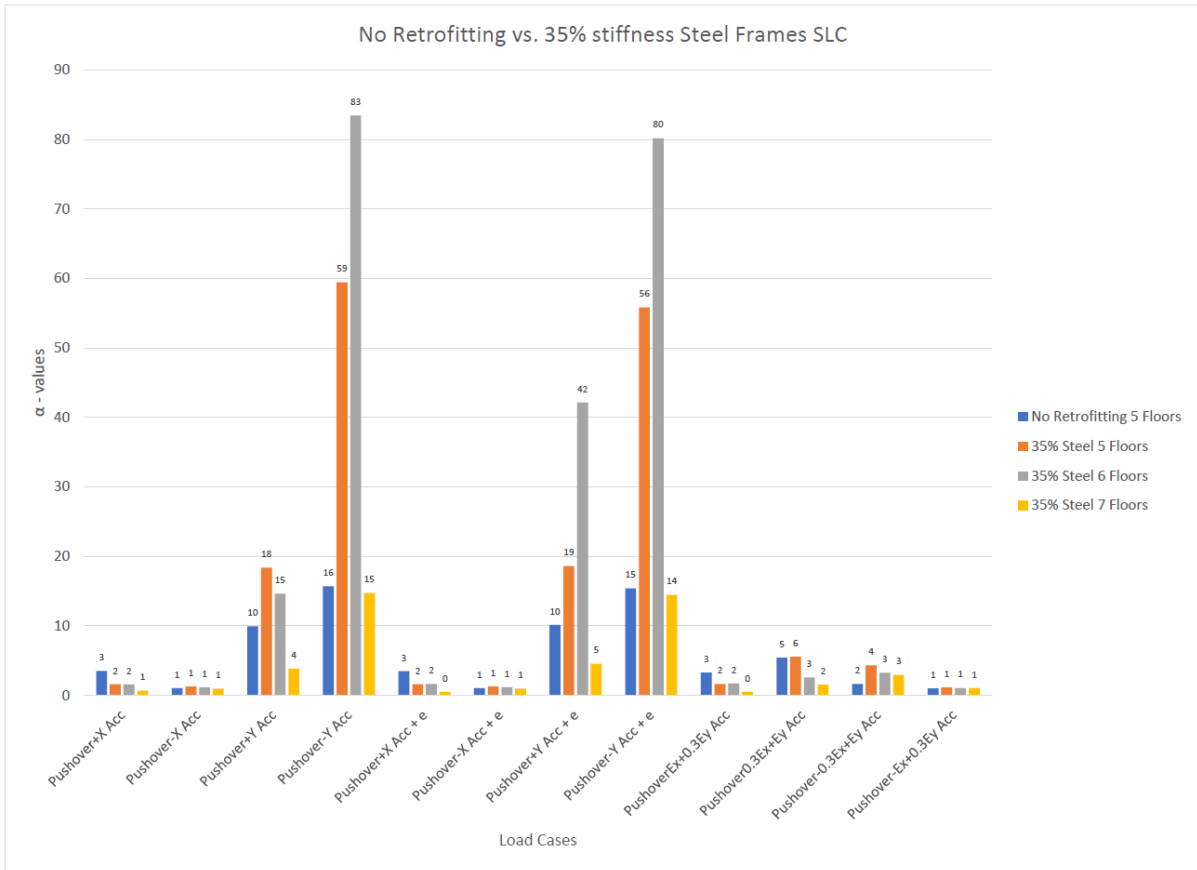


**Figure 41** Comparison between No Retrofitting vs 35% of  $K_m$  sway stiffness in Steel in SLC

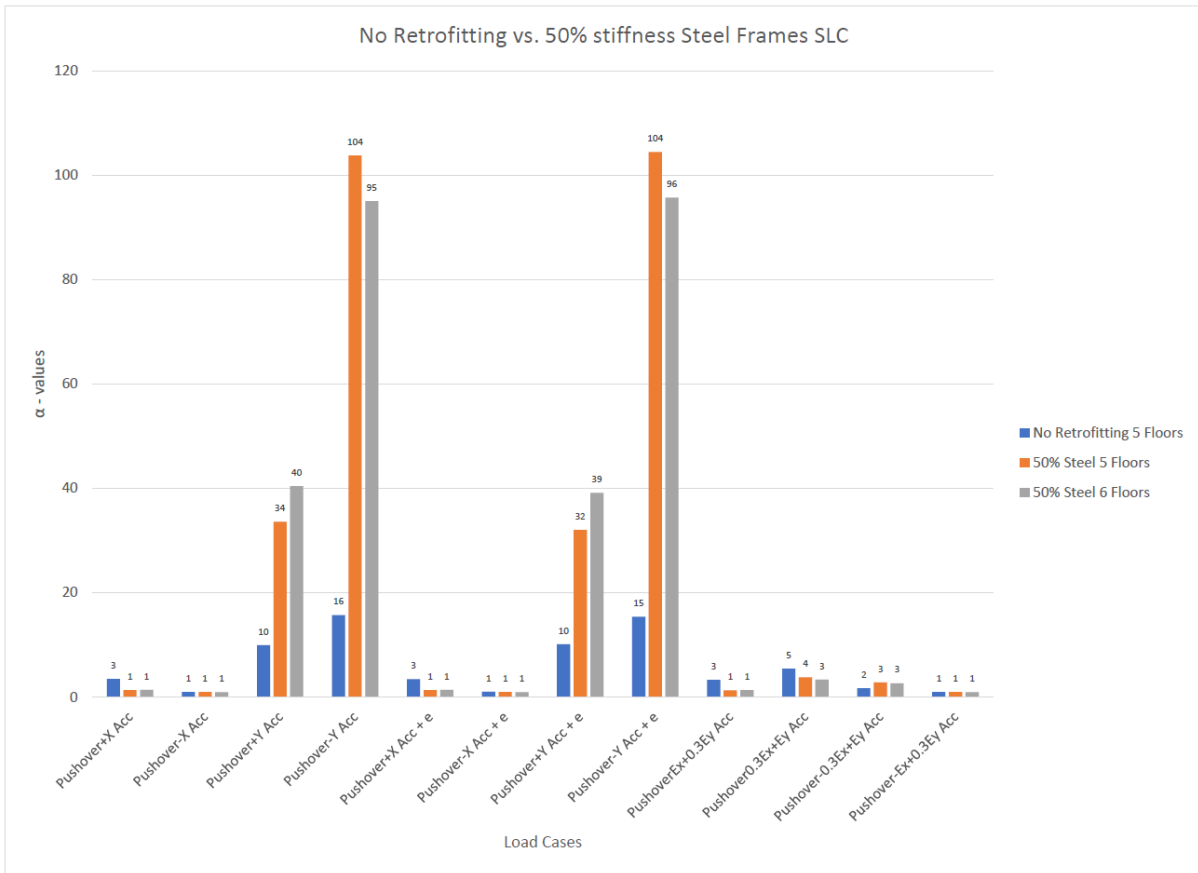


**Figure 42** Comparison between No Retrofitting vs 50% of  $K_m$  sway stiffness in Steel in SLC

## 7.2 One Unit

When examining the single unit building **without retrofitting** across all ground types, it may be observed that:

A = 4 Floors,  $\alpha = 1.188$

B = 2 Floors,  $\alpha = 2.479$

C = 2 Floors,  $\alpha = 1.258$

For the **Ground Floor (GF) Repeated** at basement:

A = 7 Floors,  $\alpha = 1.01$

B = 4 Floors,  $\alpha = 0.997^1$

C = 3 Floors,  $\alpha = 1.38$

For the **35% of  $K_m$  Sway Stiffness Reinforced Concrete Plane Frames**:

A = 7 Floors,  $\alpha = 1.047$

B = 4 Floors,  $\alpha = 1.202$

C = 3 Floors,  $\alpha = 2.074$

For the **50% of  $K_m$  Sway Stiffness Reinforced Concrete Plane Frames**:

A = 5 Floors,  $\alpha = 1.483$

B = 4 Floors,  $\alpha = 1.158$

C = 2 Floors,  $\alpha = 1.592$

For the **35% of  $K_m$  Sway Stiffness Structural Steelwork Plane Frames**:

A = 6 Floors,  $\alpha = 1.066$

B = 3 Floors,  $\alpha = 1.022$

C = 3 Floors,  $\alpha = 1.521$

For the **50% of  $K_m$  Sway Stiffness Structural Steelwork Plane Frames**:

A = 5 Floors,  $\alpha = 0.995$

B = 2 Floors,  $\alpha = 2.449$

C = 2 Floors,  $\alpha = 1.706$

As one considers the number of floors between the Repeated GF and the 35% of  $K_m$  sway stiffness in RC, it may be observed that both URM buildings would sustain the same number of floors. However, the alpha-values suggest that the URM building with the Ground Floor Repeated at basement is closer to reaching the safety limit than the retrofitted URM building with 35% of  $K_m$  sway stiffness in RC, thereby concluding that it indeed is beneficial to employ such retrofitting techniques. Furthermore, it is

---

<sup>1</sup> In instances where the alpha-values reached 0.99, they were assumed to be rounded off to 1.00, indicating that the URM building just survived.

vital to acknowledge the limitation of using such a coarse yardstick for assessing seismic resistance, which restricts the assessment to an integer number of floors due to functionality reasons.

When comparing the results obtained between retrofitted URM buildings with 35% of  $K_m$  and 50% of  $K_m$  sway stiffnesses in RC, a notable decrease in seismic performance may be observed for the URM building retrofitted with higher sway stiffness, except for Ground Type B. It appears that, having frames which are excessively stiff, can induce failure just above the basement, particularly within the Ground Floor, as may be observed in Appendix C.2. In addition, the retrofitted numerical models do not include the internal walls within the basement as shown in the plan layout in Section 6.4.1, and thus the predictions of seismic resistance are conservative. The above observation is also noted when comparing the seismic performance of retrofitted URM buildings with 35% of  $K_m$  and 50% of  $K_m$  stiffnesses in structural steelwork.

It was also observed that, comparing the retrofitted URM building with 35% of  $K_m$  sway stiffness in RC and the retrofitted URM building with 35% of  $K_m$  in structural steelwork, the latter building could carry one floor less than the former building. This observation is possibly due to the steel columns experiencing premature failure, since both buildings should sustain the same number of floors if the sway stiffnesses of the RC and structural steelwork plane frames in the basement are identical.

Retrofitting Techniques	Number of Floors	$\alpha$ - value	Load Case
	Ground Type A		
No Retrofitting	4	1.187706	Pushover-X Acc
Repeated Ground Floor	7	1.009821	Pushover-X Acc + e
35% Stiffness RC Frames	7	1.047473	Pushover-X Acc + e
50% Stiffness RC Frames	5	1.482829	Pushover-Ex+0.3Ey Acc
35% Stiffness Steel Frames	6	1.065607	Pushover-Ex+0.3Ey Acc
50% Stiffness Steel Frames	5	0.995336	Pushover-X Acc

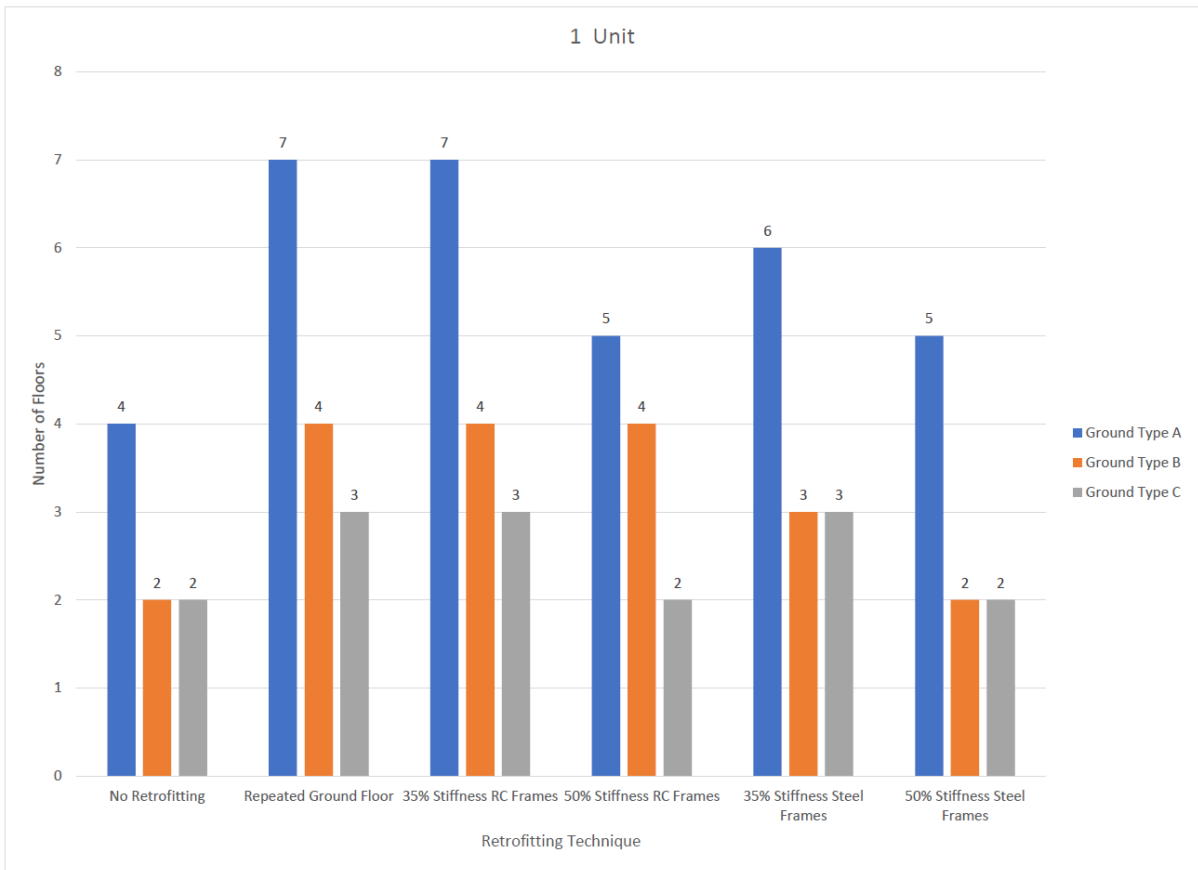
  

Retrofitting Techniques	Number of Floors	$\alpha$ - value	Load Case
	Ground Type B		
No Retrofitting	2	2.478821	Pushover-Ex+0.3Ey Acc
Repeated Ground Floor	4	0.997332	Pushover-X Acc + e
35% Stiffness RC Frames	4	1.201738	Pushover-Ex+0.3Ey Acc
50% Stiffness RC Frames	4	1.158222	Pushover-Ex+0.3Ey Acc
35% Stiffness Steel Frames	3	1.021605	Pushover-Ex+0.3Ey Acc
50% Stiffness Steel Frames	2	2.449191	Pushover+X Acc + e

Retrofitting Techniques	Number of Floors	$\alpha$ - value	Load Case
	Ground Type C		
No Retrofitting	2	1.257602	Pushover-Ex+0.3Ey Acc
Repeated Ground Floor	3	1.380481	Pushover-X Acc
35% Stiffness RC Frames	3	2.073621	Pushover+X Acc + e
50% Stiffness RC Frames	2	1.592157	Pushover+X Acc
35% Stiffness Steel Frames	3	1.521066	Pushover-Ex+0.3Ey Acc
50% Stiffness Steel Frames	2	1.70604	Pushover+X Acc + e

*Table 15 Results for One Unit, Ground Type A, B and C respectively*



**Figure 43** Results indicating number of floors sustained by each retrofitting technique in a One Unit building



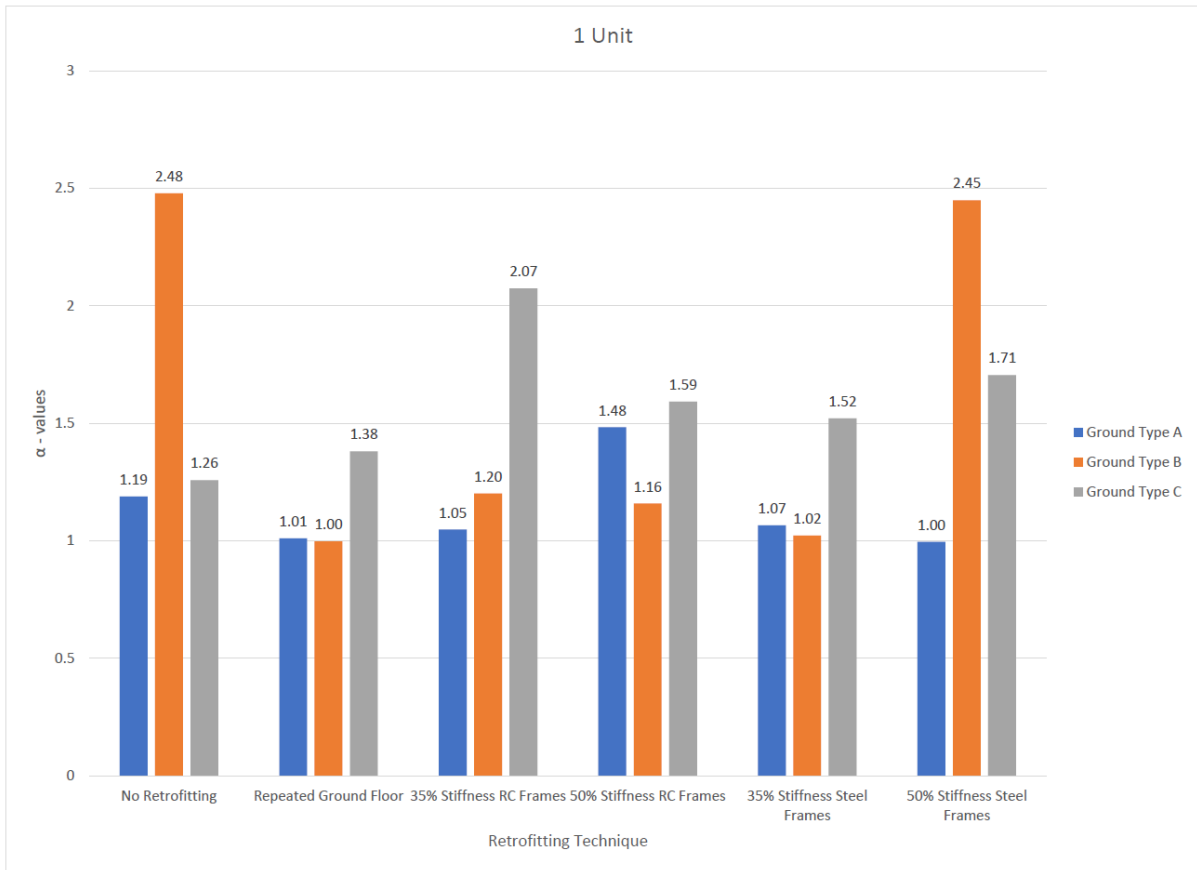


**Figure 44** Results indicating alpha values of each retrofitting technique in a One Unit building

### 7.3 Two-Unit Aggregate

When examining the two-unit aggregate **without retrofitting** across all ground types, it may be observed that:

A = 6 Floors,  $\alpha = 1.014$

B = 5 Floors,  $\alpha = 0.998$

C = 3 Floors,  $\alpha = 1.194$

For the **Ground Floor (GF) Repeated** at basement:

A = 8 Floors,  $\alpha = 1.437$

B = 7 Floors,  $\alpha = 1.196$

C = 6 Floors,  $\alpha = 1.245$

For the **35% of  $K_m$  Sway Stiffness Reinforced Concrete Plane Frames**:

A = 8 Floors,  $\alpha = 1.002$

B = 5 Floors,  $\alpha = 0.998$

C = 3 Floors,  $\alpha = 1.194$

For the **50% of  $K_m$  Sway Stiffness Reinforced Concrete Plane Frames**:

A = 6 Floors,  $\alpha = 1.014$

B = 5 Floors,  $\alpha = 0.998$

C = 3 Floors,  $\alpha = 1.194$

For the **35% of  $K_m$  Sway Stiffness Structural Steelwork Plane Frames**:

A = 8 Floors,  $\alpha = 1.135$

B = 5 Floors,  $\alpha = 0.998$

C = 3 Floors,  $\alpha = 1.194$

For the **50% of  $K_m$  Sway Stiffness Structural Steelwork Plane Frames**:

A = 7 Floors,  $\alpha = 1.019$

B = 5 Floors,  $\alpha = 0.998$

C = 3 Floors,  $\alpha = 1.194$

An initial observation for the two-unit aggregate revealed that there is a notable reduction in performance between the URM building aggregate with a Repeated GF at basement and the retrofitted URM building with 35% of  $K_m$  sway stiffness in RC. This observation is likely due to the internal masonry walls at basement level that were not modelled in 3D Macro, whereas their inclusion may have likely improved results. The weaker the subsoil, the more amplified are these effects due to a substantial increase in ground amplifications. This observation, however, does not apply for the retrofitted URM building with 35% of  $K_m$  sway stiffness in RC for Ground Type A.

The difference in seismic resistance between the retrofitted URM building aggregates with 35% of  $K_m$  and 50% of  $K_m$  sway stiffnesses in RC, is only observed for Ground Type A. Thus, when increasing the sway stiffness of the RC plane frames, the effect of not modelling the internal walls at basement level is only experienced for a rock subsoil. In addition, for the retrofitted URM building aggregate with 50% of  $K_m$  sway stiffness in RC, failure appears to commence within the ground floor rather than within the soft storey.

A distinction may be observed between the results obtained for the single unit retrofitted URM building and those for the two unit retrofitted URM building aggregates with 35% of  $K_m$  sway stiffness in RC and 35% of  $K_m$  sway stiffness in structural steelwork. In this case, both these URM building aggregates exhibit similar seismic performance, indicating that premature failure in the steel columns no longer appears to be an issue for these aggregates.

Once again, it is evident that the difference in seismic behaviour between retrofitted URM building aggregates with 35% of  $K_m$  and 50% of  $K_m$  sway stiffnesses in RC is only observed for a rock subsoil. The same observation also applies when for retrofitted URM building aggregates with structural steelwork plane frames with 35% of  $K_m$  and 50% of  $K_m$  sway stiffnesses. These observations demonstrate that both structural materials exhibit similar performance, also noting that Ground Type A allows a greater seismic capacity to sustain more floors within the aggregates. Additionally, the retrofitted URM building aggregate with 50% of  $K_m$  sway stiffness in structural steelwork could sustain one more floor than the corresponding retrofitted URM building aggregate with RC plane frames with 50% of  $K_m$  sway stiffness.

The alpha-values (safety factors) are highlighted in yellow in the subsequent tables (including those for the 3-unit and 4-unit URM building aggregates). The results of the seismic analyses showed that the corresponding alpha-values for retrofitting were less than the alpha-values for no retrofitting due to convergence problems. These alpha-values are unlikely to be correct. Since additional verification is required, the alpha-values for these cases were conservatively taken as the alpha-value corresponding to no retrofitting, which should be the minimum alpha-value from all the seismic analyses.

Retrofitting Techniques	Number of Floors	$\alpha$ - value	Load Case
	Ground Type A		
No Retrofitting	6	1.014414	Pushover-Ex+0.3Ey Acc
Repeated Ground Floor	8	1.43698	Pushover+X Acc
35% Stiffness RC Frames	8	1.001608	Pushover-Ex+0.3Ey Acc
50% Stiffness RC Frames	6	1.014414	Pushover-Ex+0.3Ey Acc
35% Stiffness Steel Frames	8	1.1351	Pushover-X Acc
50% Stiffness Steel Frames	7	1.019213	Pushover-X Acc + e

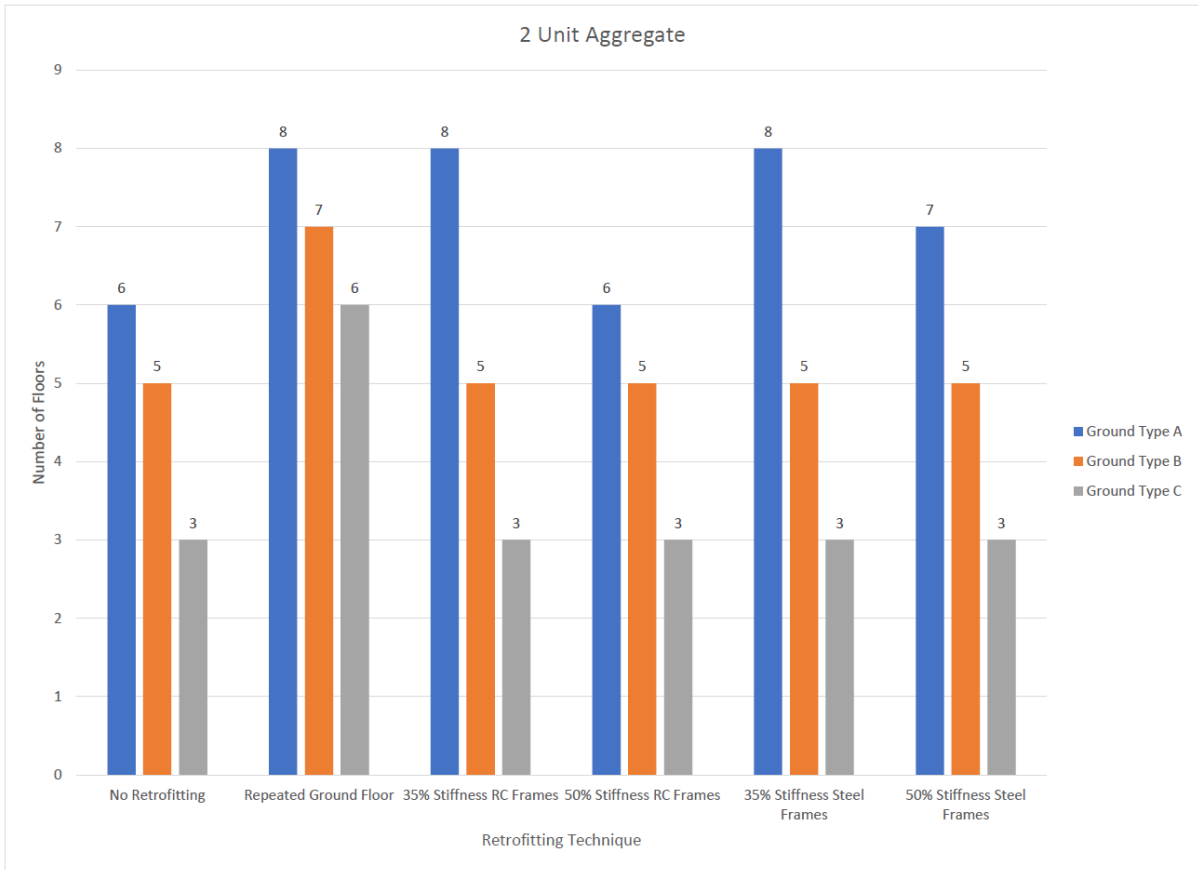
  

Retrofitting Techniques	Number of Floors	$\alpha$ - value	Load Case
	Ground Type B		
No Retrofitting	5	0.998188	Pushover-Ex+0.3Ey Acc
Repeated Ground Floor	7	1.195885	Pushover+X Acc
35% Stiffness RC Frames	5	0.998188	Pushover-Ex+0.3Ey Acc
50% Stiffness RC Frames	5	0.998188	Pushover-Ex+0.3Ey Acc
35% Stiffness Steel Frames	5	0.998188	Pushover-Ex+0.3Ey Acc
50% Stiffness Steel Frames	5	0.998188	Pushover-Ex+0.3Ey Acc

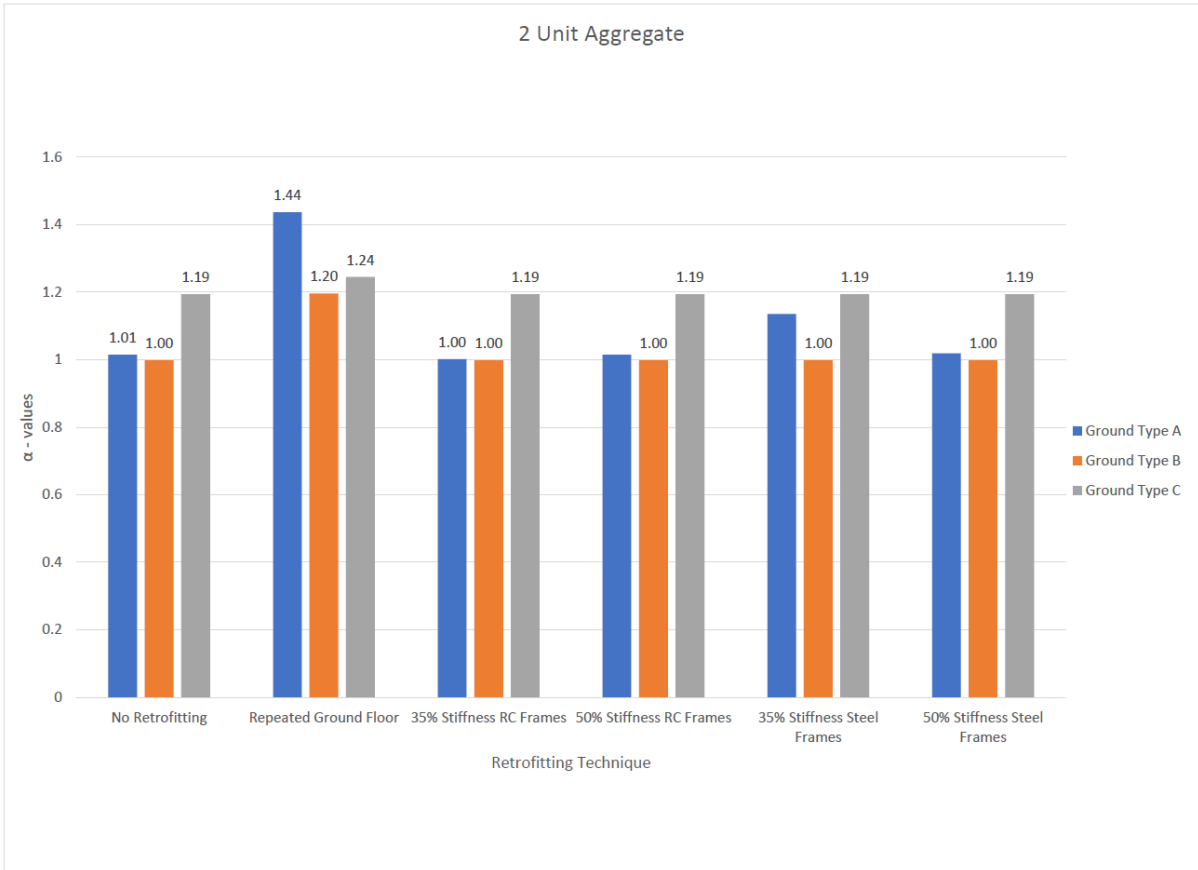
  

Retrofitting Techniques	Number of Floors	$\alpha$ - value	Load Case
	Ground Type C		
No Retrofitting	3	1.193617	Pushover-X Acc
Repeated Ground Floor	6	1.244786	Pushover+X Acc + e
35% Stiffness RC Frames	3	1.193617	Pushover-X Acc
50% Stiffness RC Frames	3	1.193617	Pushover-X Acc
35% Stiffness Steel Frames	3	1.193617	Pushover-X Acc
50% Stiffness Steel Frames	3	1.193617	Pushover-X Acc

*Table 16 Results for Two Unit, Ground Types A, B and C respectively*



**Figure 46** Results indicating number of floors sustained by each retrofitting technique in a Two-Unit aggregate



**Figure 47** Results indicating alpha values of each retrofitting technique in a Two-Unit aggregate

## 7.4 Three-Unit Aggregate

When examining the three-unit aggregate **without retrofitting** across all ground types, it may be observed that:

A = 6 Floors,  $\alpha = 1.283$

B = 5 Floors,  $\alpha = 1.083$

C = 2 Floors,  $\alpha = 1.627$

For the **Ground Floor (GF) Repeated** at basement:

A = 8 Floors,  $\alpha = 1.031$

B = 5 Floors,  $\alpha = 1.083$

C = 3 Floors,  $\alpha = 1.627$

For the **35% of  $K_m$  Sway Stiffness Reinforced Concrete Plane Frames**:

A = 8 Floors,  $\alpha = 1.075$

B = 5 Floors,  $\alpha = 1.083$

C = 2 Floors,  $\alpha = 1.627$

For the **50% of  $K_m$  Sway Stiffness Reinforced Concrete Plane Frames**:

A = 8 Floors,  $\alpha = 1.047$

B = 5 Floors,  $\alpha = 1.083$

C = 2 Floors,  $\alpha = 1.627$

For the **35% of  $K_m$  Sway Stiffness Structural Steelwork Plane Frames**:

A = 8 Floors,  $\alpha = 1.151$

B = 5 Floors,  $\alpha = 1.083$

C = 2 Floors,  $\alpha = 1.627$

For the **50% of  $K_m$  Sway Stiffness Structural Steelwork Frames**:

A = 7 Floors,  $\alpha = 1.12$

B = 5 Floors,  $\alpha = 1.083$

C = 2 Floors,  $\alpha = 1.627$

An initial observation for the three-unit URM building aggregate reveals no enhancement in either of the retrofitting techniques for Ground Type B, rendering the retrofitting frames ineffective. With regards to Ground Type C, enhancement is solely observed for the Repeated GF, where an additional floor was attained.

Comparing the results for the 35% of  $K_m$  sway stiffnesses in both RC and structural steelwork, their corresponding seismic performances seems to be identical in terms of the number of floors which may

be sustained during an earthquake event. However, it should be noted that 35% of  $K_m$  sway stiffness in structural steelwork provides a greater safety factor than for RC, thus increasing its resistance against structural collapse.

Furthermore, when comparing the results for the 35% of  $K_m$  and 50% of  $K_m$  sway stiffness in RC, the same number of floors may be sustained. However, the stiffer RC plane frames provide a lower safety factor, indicating that stiffer frames appear to be less beneficial. This observation is even more evident for the 35% of  $K_m$  and 50% of  $K_m$  sway stiffness in structural steelwork, since the latter can sustain one floor less than the former when the retrofitted URM building aggregates are founded on rock.

Retrofitting Techniques	Number of Floors	$\alpha$ - value	Load Case
	Ground Type A		
No Retrofitting	6	1.282733	Pushover-0.3Ex+Ey Acc
Repeated Ground Floor	8	1.031184	Pushover-X Acc + e
35% Stiffness RC Frames	8	1.07498	Pushover-Ex+0.3Ey Acc
50% Stiffness RC Frames	8	1.046002	Pushover-Ex+0.3Ey Acc
35% Stiffness Steel Frames	8	1.150705	Pushover-X Acc
50% Stiffness Steel Frames	7	1.199783	Pushover-X Acc + e

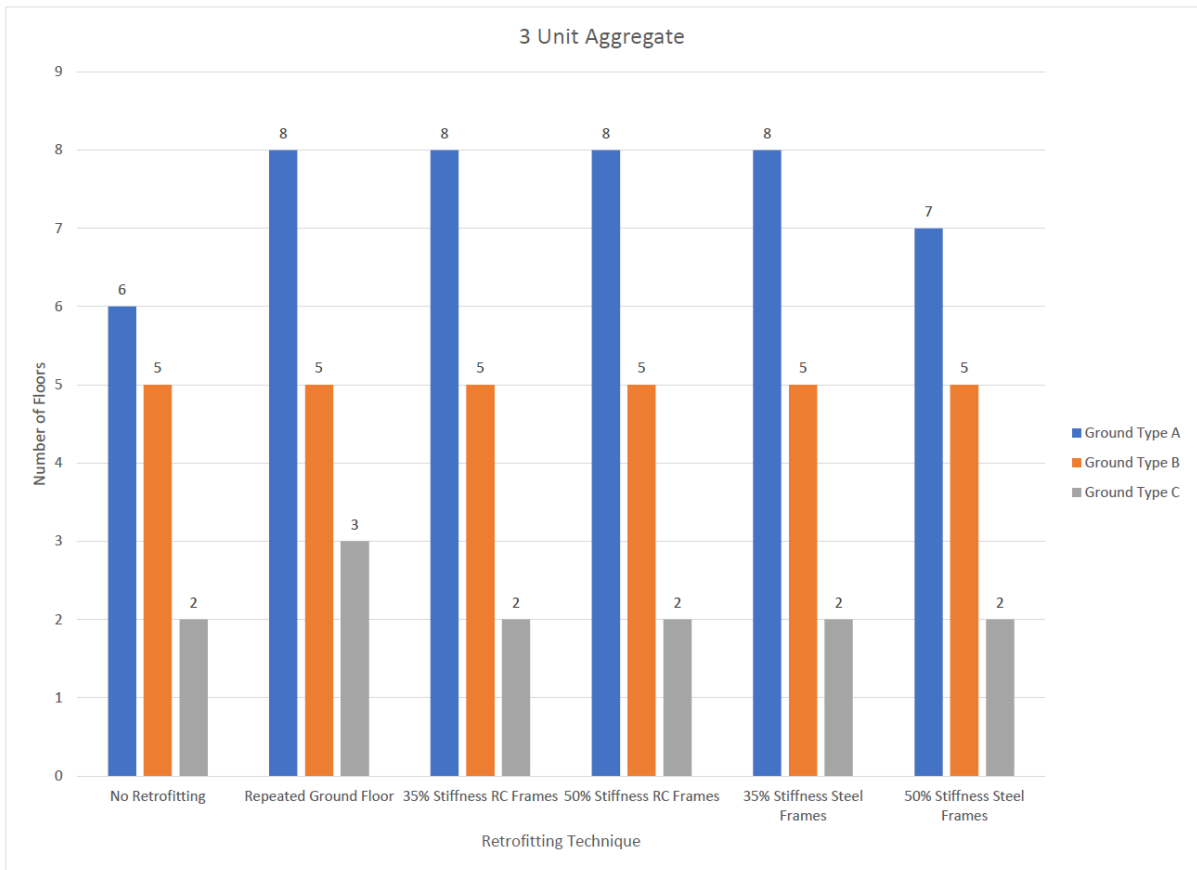
Retrofitting Techniques	Number of Floors	$\alpha$ - value	Load Case
	Ground Type B		
No Retrofitting	5	1.082858	Pushover-Ex+0.3Ey Acc
Repeated Ground Floor	5	1.082858	Pushover-Ex+0.3Ey Acc
35% Stiffness RC Frames	5	1.082858	Pushover-Ex+0.3Ey Acc
50% Stiffness RC Frames	5	1.082858	Pushover-Ex+0.3Ey Acc
35% Stiffness Steel Frames	5	1.082858	Pushover-Ex+0.3Ey Acc
50% Stiffness Steel Frames	5	1.082858	Pushover-Ex+0.3Ey Acc

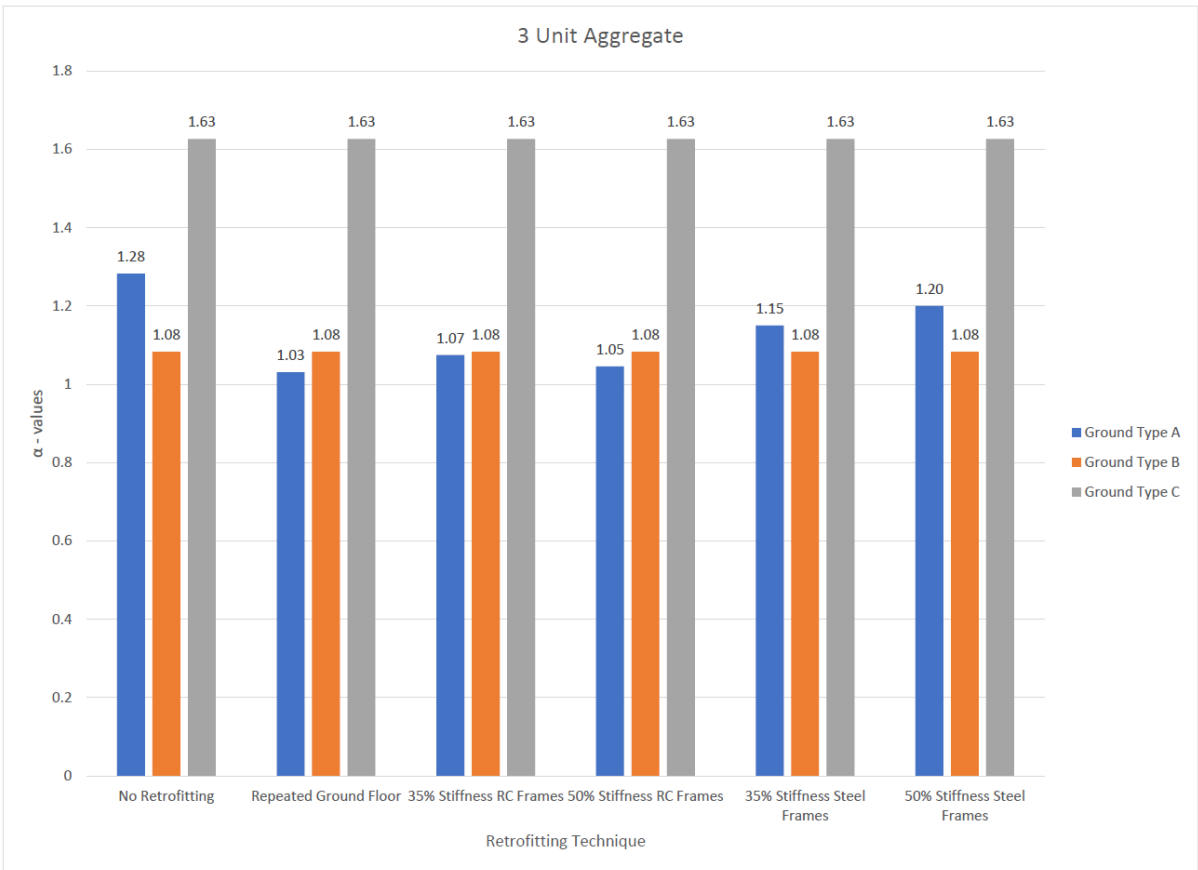
Retrofitting Techniques	Number of Floors	$\alpha$ - value	Load Case
	Ground Type C		
No Retrofitting	2	1.626691	Pushover-X Acc + e
Repeated Ground Floor	3	1.626691	Pushover-X Acc + e
35% Stiffness RC Frames	2	1.626691	Pushover-X Acc + e
50% Stiffness RC Frames	2	1.626691	Pushover-X Acc + e
35% Stiffness Steel Frames	2	1.626691	Pushover-X Acc + e
50% Stiffness Steel Frames	2	1.626691	Pushover-X Acc + e

Table 17 Results for Three-Unit aggregates, Ground Type A, B and C respectively





**Figure 48** Results indicating number of floors sustained by each retrofitting technique in a Three-Unit aggregate



**Figure 49** Results indicating alpha values of each retrofitting technique in a Three-Unit aggregate

## 7.5 Four Unit Aggregate

When examining the four-unit aggregate **without retrofitting** across all ground types, it may be observed that:

A = 6 Floors,  $\alpha = 1.275$

B = 4 Floors,  $\alpha = 1.097$

C = 2 Floors,  $\alpha = 1.704$

For the **Ground Floor (GF) Repeated** at basement:

A = 8 Floors,  $\alpha = 1.033$

B = 4 Floors,  $\alpha = 1.097$

C = 3 Floors,  $\alpha = 1.704$

For the **35% of  $K_m$  Sway Stiffness Reinforced Concrete Plane Frames**:

A = 7 Floors,  $\alpha = 1.054$

B = 4 Floors,  $\alpha = 1.097$

C = 2 Floors,  $\alpha = 1.704$

For the **50% of  $K_m$  Sway Stiffness Reinforced Concrete Plane Frames**:

A = 6 Floors,  $\alpha = 1.276$

B = 4 Floors,  $\alpha = 1.097$

C = 2 Floors,  $\alpha = 1.704$

For the **35% of  $K_m$  Sway Stiffness in Structural Steelwork Plane Steel Frames**:

A = 8 Floors,  $\alpha = 1.057$

B = 4 Floors,  $\alpha = 1.097$

C = 2 Floors,  $\alpha = 1.704$

For the **50% of  $K_m$  Sway Stiffness in Structural Steelwork Plane Frames**:

A = 6 Floors,  $\alpha = 1.276$

B = 4 Floors,  $\alpha = 1.097$

C = 2 Floors,  $\alpha = 1.704$

One of the initial findings suggests that performance for the four-unit URM building aggregate is comparable to that of the three-unit aggregate. For the Repeated GF at basement level, both the three-unit and the four-unit retrofitted URM building aggregates experience an improvement of 2 storeys for Ground Type A compared to the corresponding unretrofitted URM building aggregates, while there is no enhancement for Ground Type B and an additional storey for Ground Type C.

When observing all retrofitting techniques, the findings suggest that, for Ground Types B and C, there is generally no of enhancement. The plane frames seem to be too weak in side sway stiffness to make

any difference in seismic resistance, whilst the safety factors remain unchanged. This pattern is consistent across all URM building aggregates.

Another interesting comparison is that for four-unit retrofitted URM building aggregates with 35% of  $K_m$  sway stiffnesses in both RC and structural steelwork. In this case, the aggregate with structural steelwork plane frames can sustain an additional floor in comparison to the aggregate with RC plane frames for Ground Type A. Thus, unlike the URM single unit building, premature failure of the steel columns does not appear to be an issue. Hence, in the case of retrofitted URM building aggregates, the results show that structural steelwork plane frames offer a better enhancement in seismic resistance than RC plane frames.

In conclusion, it may be noted that, apart from the case when the URM building aggregates are founded in rock, none of the retrofitting techniques provided any benefit in enhancing the structural seismic resistance. With regards to Ground Type C, the only improvement, which was observed was in the Repeated GF at basement level. On the other hand, for Ground Type A, no improvement was noted for retrofitted URM building aggregates with 50% of  $K_m$  sway stiffness in both RC and structural steelwork. This result contrasts with the corresponding improvement noted in the seismic resistance, as discussed above, when the sway stiffnesses of the RC and structural steelwork plane frames were reduced to 35% of  $K_m$ , which is somewhat a surprising result.

Retrofitting Techniques	Number of Floors	$\alpha$ - value	Load Case
			Ground Type A
No Retrofitting	6	1.275747	Pushover-0.3Ex+Ey Acc
Repeated Ground Floor	8	1.033461	Pushover-X Acc
35% Stiffness RC Frames	7	1.054346	Pushover-X Acc + e
50% Stiffness RC Frames	6	1.275747	Pushover-0.3Ex+Ey Acc
35% Stiffness Steel Frames	8	1.056702	Pushover-X Acc
50% Stiffness Steel Frames	6	1.275747	Pushover-0.3Ex+Ey Acc

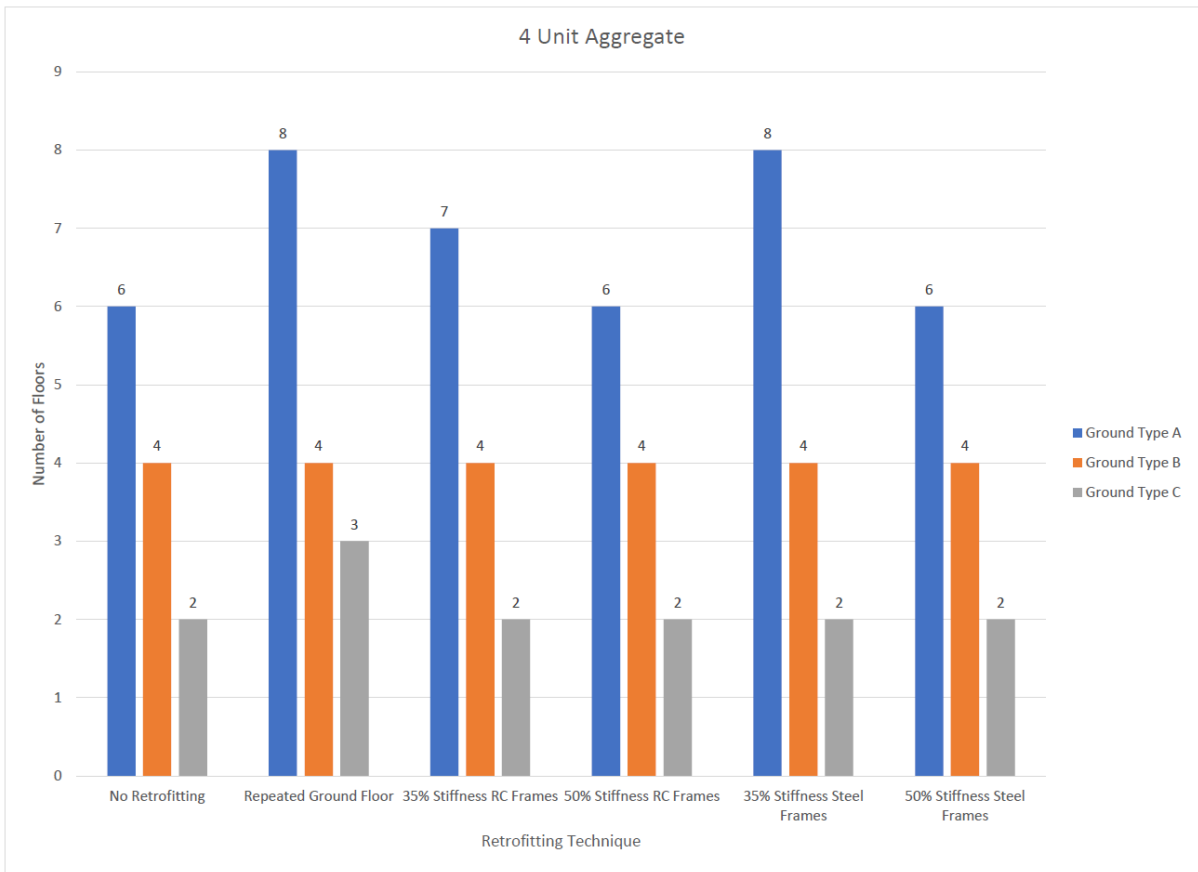
  

Retrofitting Techniques	Number of Floors	$\alpha$ - value	Load Case
			Ground Type B
No Retrofitting	4	1.09654	Pushover-Ex+0.3Ey Acc
Repeated Ground Floor	4	1.09654	Pushover-Ex+0.3Ey Acc
35% Stiffness RC Frames	4	1.09654	Pushover-Ex+0.3Ey Acc
50% Stiffness RC Frames	4	1.09654	Pushover-Ex+0.3Ey Acc
35% Stiffness Steel Frames	4	1.09654	Pushover-Ex+0.3Ey Acc
50% Stiffness Steel Frames	4	1.09654	Pushover-Ex+0.3Ey Acc

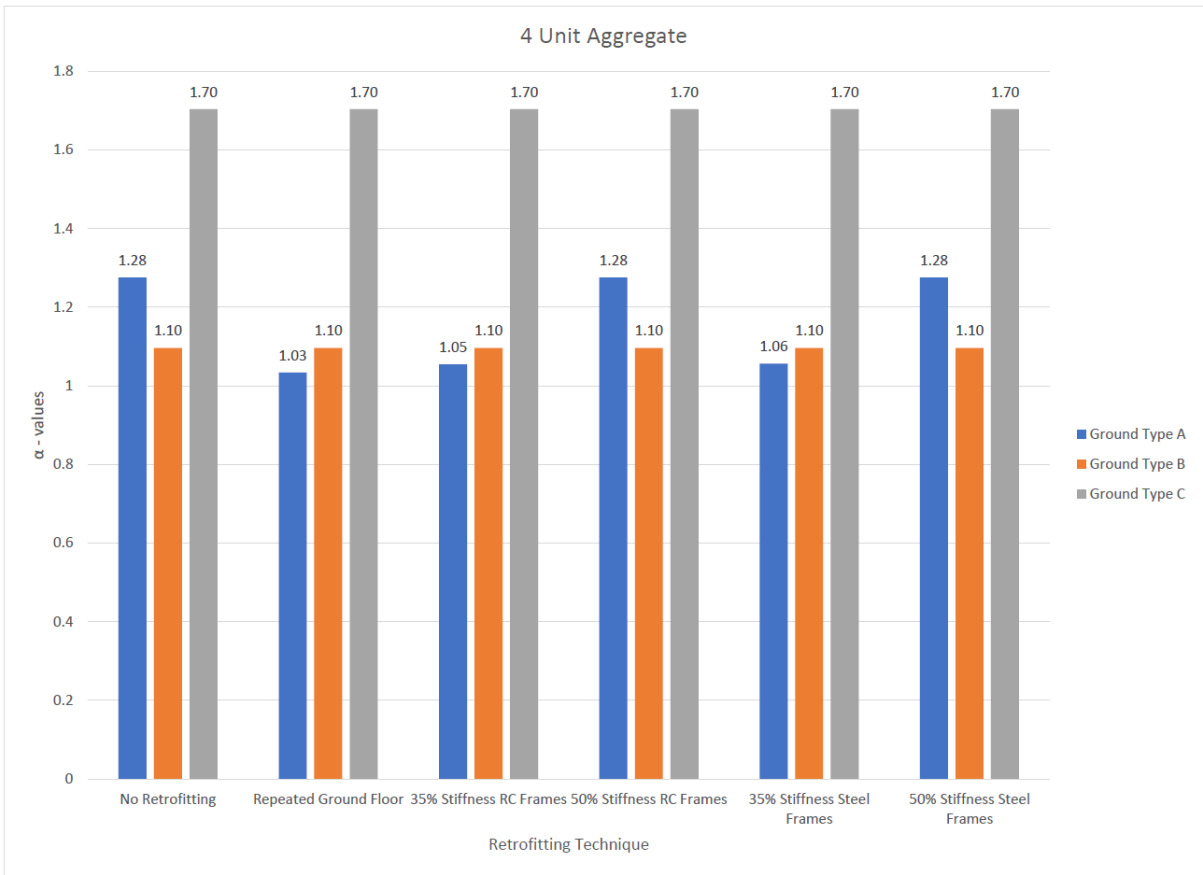
  

Retrofitting Techniques	Number of Floors	$\alpha$ - value	Load Case
			Ground Type C
No Retrofitting	2	1.703894	Pushover-X Acc
Repeated Ground Floor	3	1.703894	Pushover-X Acc
35% Stiffness RC Frames	2	1.703894	Pushover-X Acc
50% Stiffness RC Frames	2	1.703894	Pushover-X Acc
35% Stiffness Steel Frames	2	1.703894	Pushover-X Acc
50% Stiffness Steel Frames	2	1.703894	Pushover-X Acc

Table 18 Results for Four-Unit aggregate, Ground Types A, B and C respectively



**Figure 50** Results indicating number of floors sustained by each retrofitting technique in a Four-Unit aggregate



*Figure 51 Results indicating alpha values of each retrofitting technique in a Four-Unit aggregate*

## 7.6 Comparing across Ground Type A

As the number of single units is increased within the URM building aggregates, the plan aspect ratio of the aggregate is reduced compared to that of a single unit. As a result, the sway stiffness experiences an increase. However, one must also keep in mind that the seismic mass is also increasing as more single units are added to the aggregate. If the rate of increase in sway stiffness per additional unit in the aggregate is less than the rate of increase of the seismic mass per additional unit in the aggregate, the benefit of additional stiffness would be swamped by the drawback of additional seismic mass (and, hence, additional horizontal seismic inertial forces during an earthquake event) and, therefore, the outcome would not necessarily be advantageous. Indeed, adding more single units to the aggregate could even become detrimental to the URM building aggregate seismic resistance.

Building Type	Aspect Ratio
1 Unit	1:4
2 Unit	1:2
3 Unit	1:1.5
4 Unit	1:1

When taking the above into consideration, this observation becomes evident in the case of retrofitted URM building aggregates with 35% of  $K_m$  sway stiffness in RC as well as the 50% of  $K_m$  sway stiffness in steel. There appears to be a trend where, a two-unit retrofitted URM building aggregate could sustain 1 to 2 floors more than a URM single unit building. Adding another single unit shows that the three-unit retrofitted URM building aggregate does not lead to any more floors that can be sustained by the aggregate. Furthermore, adding another single unit shows that the four-unit retrofitted URM building aggregate, in fact, can generally sustain one floor less than the three-unit retrofitted URM building aggregate, demonstrating that the ideal retrofitted URM building aggregate is one that has seismic gaps at every third single unit. This is, of course, quite difficult to achieve in practice unless the whole URM building aggregate forms part of an entire development project. In the case of retrofitted URM building aggregates with 50% of  $K_m$  sway stiffness in both RC and steel, it appears that failure occurs at the Ground Floor instead of the basement, indicating that stiffer plane frames do not necessarily provide better seismic performance for URM building aggregates.

When comparing the retrofitted URM building aggregates with 35% and 50% of  $K_m$  sway stiffnesses in RC, a reduction in the number of floors sustained of 2 floors was observed for a single-unit building and a two-unit aggregate, and a reduction 1 floor for a four-unit aggregate. On the other hand, for the 3-unit aggregate, there is no reduction in the floors sustained. This latter result seems to be somewhat unexpected, and warrants further investigation as it does not follow the trend of the other aggregates.

Another important observation lies in the comparison between the retrofitted URM building aggregates with 35% of  $K_m$  sway stiffnesses in both RC and Steel frames. The single one-unit building with steel frames can support one less floor than with RC frames, which suggests premature failure in the steel frames columns. Conversely, for the retrofitted URM building aggregates with 50% sway stiffness in RC frames, there is a reduction of two floors that can be sustained by a four-unit aggregate compared to a three-unit aggregate. However, there was no reduction in the number of floors that can be sustained for two-unit and three-unit retrofitted URM building aggregates with 35% sway stiffness in steel frames.

Once again, this suggests that structural steelwork plane frames offer a better enhancement than RC plane frames in the seismic resistance of retrofitted URM building aggregates.

Ground Type A			
Units	Retrofitting Technique	Number of Floors	$\alpha$ - values
1 Unit	No Retrofitting	4	1.187705874
2 Unit	No Retrofitting	6	1.01441431
3 Unit	No Retrofitting	6	1.28273344
4 Unit	No Retrofitting	6	1.275747061

*Table 19 Results for Ground Type A, No Retrofitting*

Ground Type A			
Units	Retrofitting Technique	Number of Floors	$\alpha$ - values
1 Unit	Repeated Ground Floor	7	1.009820938
2 Unit	Repeated Ground Floor	8	1.436980128
3 Unit	Repeated Ground Floor	8	1.03118372
4 Unit	Repeated Ground Floor	8	1.03118372

*Table 20 Results for Ground Type A, Repeated Ground Floor*

Ground Type A			
Units	Retrofitting Technique	Number of Floors	$\alpha$ - values
1 Unit	35% Stiffness RC Frames	7	1.047473192
2 Unit	35% Stiffness RC Frames	8	1.001608372
3 Unit	35% Stiffness RC Frames	8	1.074980259
4 Unit	35% Stiffness RC Frames	7	1.054346204

*Table 21 Results for Ground Type A, 35% of  $K_m$  sway stiffness in RC Frames*



Ground Type A			
Units	Retrofitting Technique	Number of Floors	$\alpha$ - values
1 Unit	50% Stiffness RC Frames	5	1.482828975
2 Unit	50% Stiffness RC Frames	6	1.01441431
3 Unit	50% Stiffness RC Frames	8	1.04600215
4 Unit	50% Stiffness RC Frames	6	1.275747061

*Table 22 Results for Ground Type A, 50% of  $K_m$  sway stiffness in RC Frames*

Ground Type A			
Units	Retrofitting Technique	Number of Floors	$\alpha$ - values
1 Unit	35% Stiffness Steel Frames	6	1.065606833
2 Unit	35% Stiffness Steel Frames	8	1.135099888
3 Unit	35% Stiffness Steel Frames	8	1.150705457
4 Unit	35% Stiffness Steel Frames	8	1.05670166

*Table 23 Results for Ground Type A, 35% of  $K_m$  sway stiffness in Steel Frames*

Ground Type A			
Units	Retrofitting Technique	Number of Floors	$\alpha$ - values
1 Unit	50% Stiffness Steel Frames	5	0.995335758
2 Unit	50% Stiffness Steel Frames	7	1.019212723
3 Unit	50% Stiffness Steel Frames	7	1.199783206
4 Unit	50% Stiffness Steel Frames	6	1.275747061

*Table 24 Results for Ground Type A, 50% of  $K_m$  sway stiffness in Steel Frames*

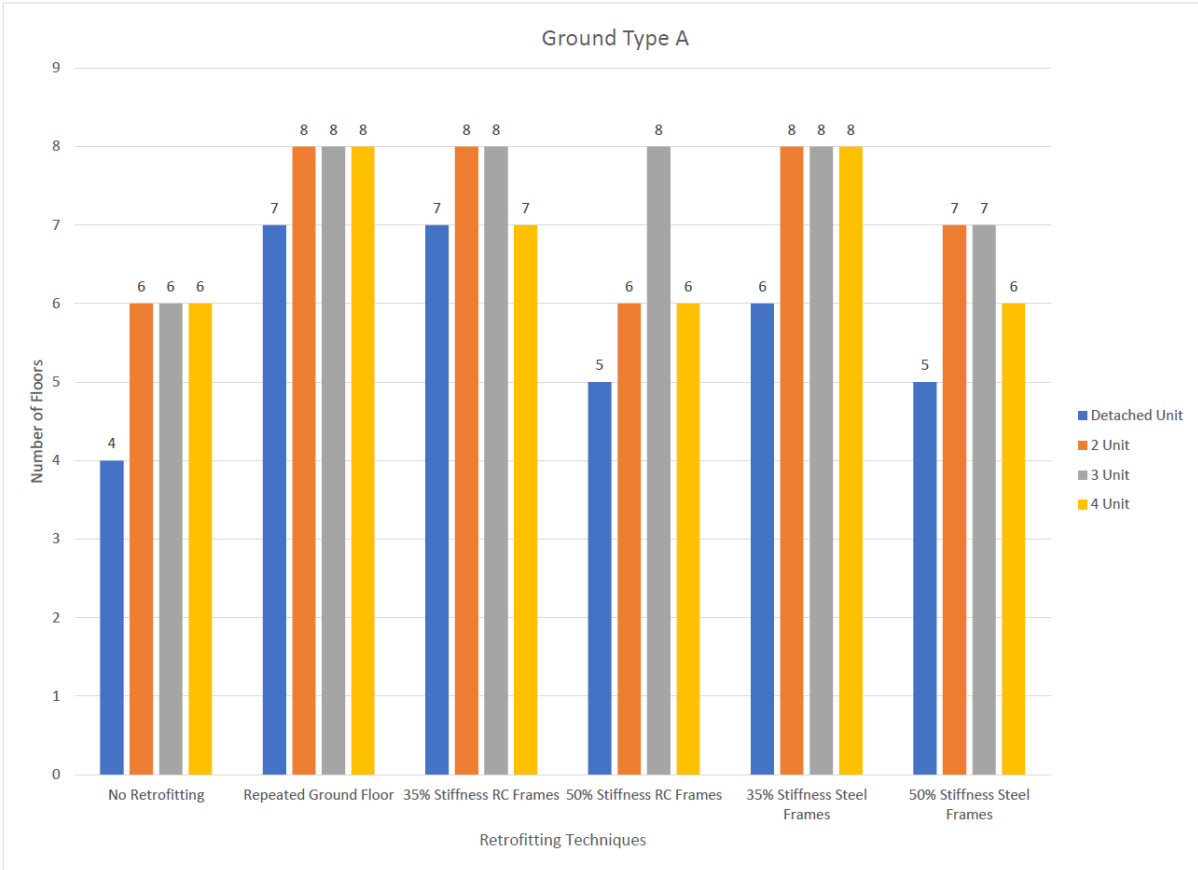


**Figure 52** Results indicating number of floors sustained by each retrofitting technique across the 1 unit building and all building aggregates for Ground Type A

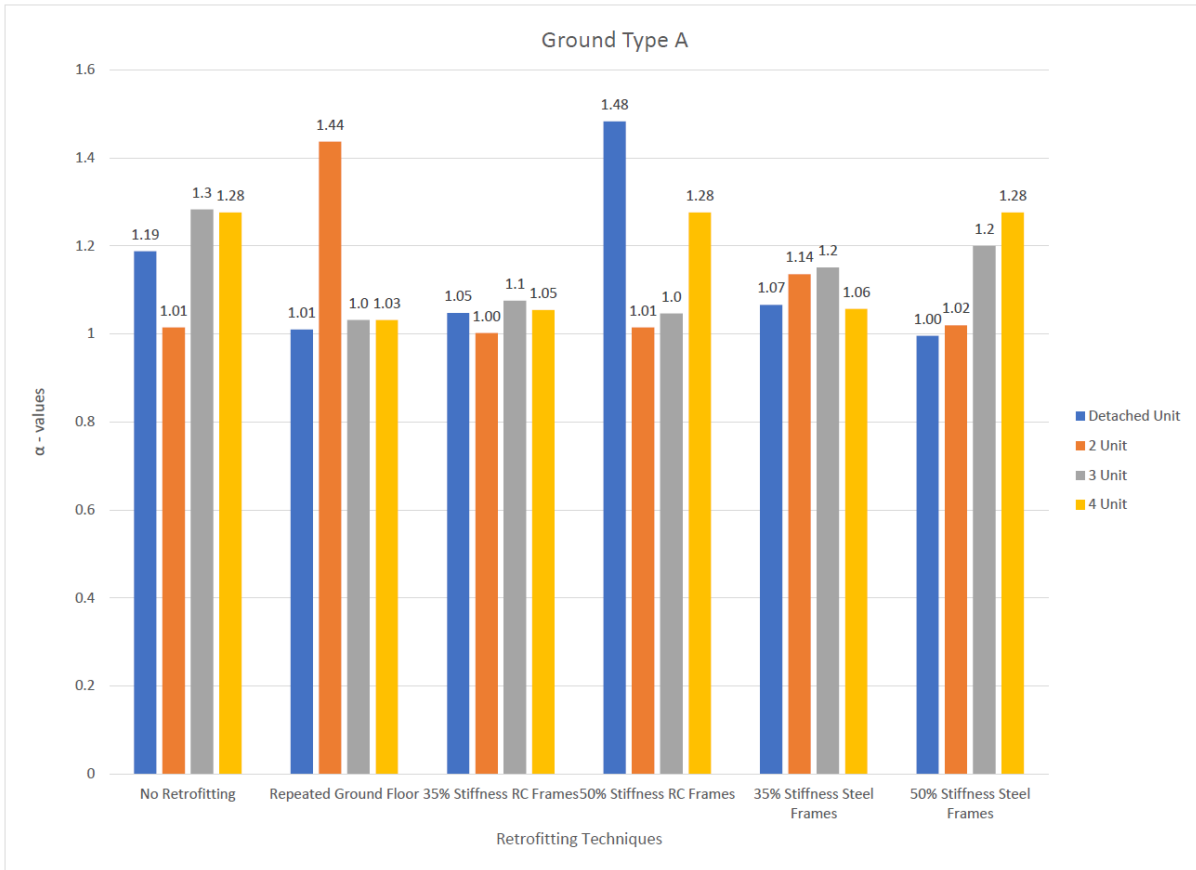


**Figure 53** Results indicating the safety factor in terms of alpha by each retrofitting technique across the 1 unit building and all building aggregates for Ground Type A

## 7.7 Comparing across Ground Type B

When analysing the results for no retrofitting within Ground Type B, the adverse effect of having a greater rate of increase in seismic mass in comparison to the rate of increase in sway stiffness as the number of single units with the URM building aggregate units is increasing becomes apparent once again. The seismic mass is what determines the base shear of the foundations of the buildings. This base shear, in turn, influences the horizontal seismic inertial forces at each floor. The higher the seismic mass, the higher is the base shear and the higher are the horizontal seismic forces acting at each floor.

The results show that both the two-unit and three-unit unretrofitted URM building aggregates can sustain two additional floors compared to the URM single unit building, whilst the four-unit unretrofitted URM building aggregate can sustain only one additional floor compared to the URM single unit building. Therefore, in the case of the four-unit unretrofitted URM building aggregate, the increase in seismic mass is cancelling out the increase in sway stiffness and is becoming detrimental to the overall seismic resistance of the aggregate.

Comparing the results for the unretrofitted URM building aggregates with those for the URM building aggregates with a Repeated Ground Floor at basement level, it may be noted that the latter aggregates can sustain two more floors than the former in the case of the single-unit building and the two-unit aggregate, while there is no improvement in seismic resistance for the three-unit and four-unit aggregates. Moreover, when considering the results for the URM building aggregates with a Repeated Ground Floor at basement level, it is clear that the two-unit and three-unit aggregates can sustain three floors and one floor more than the single-unit building respectively, while there is no enhancement in seismic resistance in the case of the four-unit aggregate.

In the case of the retrofitted URM building aggregates with 35% of  $K_m$  and 50% of  $k_m$  sway stiffness in RC Frames, their corresponding seismic resistance is identical in terms of the number of floors that can be sustained during an earthquake event. However, the safety factor for the retrofitted single-unit building indicates that with 35% of  $K_m$  sway stiffness in RC frames is higher than that corresponding to 50% of  $K_m$  sway stiffness in RC frames. This implies that the RC frames with lower sway stiffness provide the retrofitted single-unit building with a greater margin of safety compared to the stiffer RC frames, making the building less vulnerable to seismic load. In contrast to the results obtained for the retrofitted URM building aggregates with Repeated Ground Floor at basement level, the retrofitted URM building aggregates with 35% of  $K_m$  and 50% of  $K_m$  sway stiffness in RC frames were both able to sustain the same number of floors in the case of the two-unit and three-unit aggregates, which observation follows the same trend as that observed in the case of Ground Type A.

Considering the results obtained for the retrofitted URM building aggregates with 35% of  $K_m$  and 50% of  $K_m$  sway stiffness in steel frames, the trend in seismic performance was identical to that discussed above for the retrofitted aggregates with RC frames, except that the single-unit building with the stiffer steel frames could sustain one floor less than the steel frames with lower stiffness due to premature failure in the steel columns.

Ground Type B			
Units	Retrofitting Technique	Number of Floors	$\alpha$ - values
1 Unit	No Retrofitting	2	2.478820801
2 Unit	No Retrofitting	5	0.998187959
3 Unit	No Retrofitting	5	1.082858205
4 Unit	No Retrofitting	4	1.096540213

*Table 25 Results for Ground Type B, No Retrofitting*

Ground Type B			
Units	Retrofitting Technique	Number of Floors	$\alpha$ - values
1 Unit	Repeated Ground Floor	4	0.997332394
2 Unit	Repeated Ground Floor	7	1.19588542
3 Unit	Repeated Ground Floor	5	1.082858205
4 Unit	Repeated Ground Floor	4	1.096540213

*Table 26 Results for Ground Type B, Repeated Ground Floor*

Ground Type B			
Units	Retrofitting Technique	Number of Floors	$\alpha$ - values
1 Unit	35% Stiffness RC Frames	4	1.201737523
2 Unit	35% Stiffness RC Frames	5	0.998187959
3 Unit	35% Stiffness RC Frames	5	1.082858205
4 Unit	35% Stiffness RC Frames	4	1.096540213

*Table 27 Results for Ground Type B, 35% of  $K_m$  sway stiffness in RC Frames*

<b>Ground Type B</b>			
<b>Units</b>	<b>Retrofitting Technique</b>	<b>Number of Floors</b>	<b><math>\alpha</math> - values</b>
<b>1 Unit</b>	<b>50% Stiffness RC Frames</b>	<b>4</b>	<b>1.158222437</b>
<b>2 Unit</b>	<b>50% Stiffness RC Frames</b>	<b>5</b>	<b>0.998187959</b>
<b>3 Unit</b>	<b>50% Stiffness RC Frames</b>	<b>5</b>	<b>1.082858205</b>
<b>4 Unit</b>	<b>50% Stiffness RC Frames</b>	<b>4</b>	<b>1.096540213</b>

*Table 28 Results for Ground Type B, 50% of  $K_m$  sway stiffness in RC Frames*

<b>Ground Type B</b>			
<b>Units</b>	<b>Retrofitting Technique</b>	<b>Number of Floors</b>	<b><math>\alpha</math> - values</b>
<b>1 Unit</b>	<b>35% Stiffness Steel Frames</b>	<b>3</b>	<b>1.021605372</b>
<b>2 Unit</b>	<b>35% Stiffness Steel Frames</b>	<b>5</b>	<b>0.998187959</b>
<b>3 Unit</b>	<b>35% Stiffness Steel Frames</b>	<b>5</b>	<b>1.082858205</b>
<b>4 Unit</b>	<b>35% Stiffness Steel Frames</b>	<b>4</b>	<b>1.096540213</b>

*Table 29 Results for Ground Type B, 35% of  $K_m$  sway stiffness in Steel Frames*

<b>Ground Type B</b>			
<b>Units</b>	<b>Retrofitting Technique</b>	<b>Number of Floors</b>	<b><math>\alpha</math> - values</b>
<b>1 Unit</b>	<b>50% Stiffness Steel Frames</b>	<b>2</b>	<b>2.449191332</b>
<b>2 Unit</b>	<b>50% Stiffness Steel Frames</b>	<b>5</b>	<b>0.998187959</b>
<b>3 Unit</b>	<b>50% Stiffness Steel Frames</b>	<b>5</b>	<b>1.082858205</b>
<b>4 Unit</b>	<b>50% Stiffness Steel Frames</b>	<b>4</b>	<b>1.096540213</b>

*Table 30 Results for Ground Type B, 50% of  $K_m$  sway stiffness in Steel Frames*

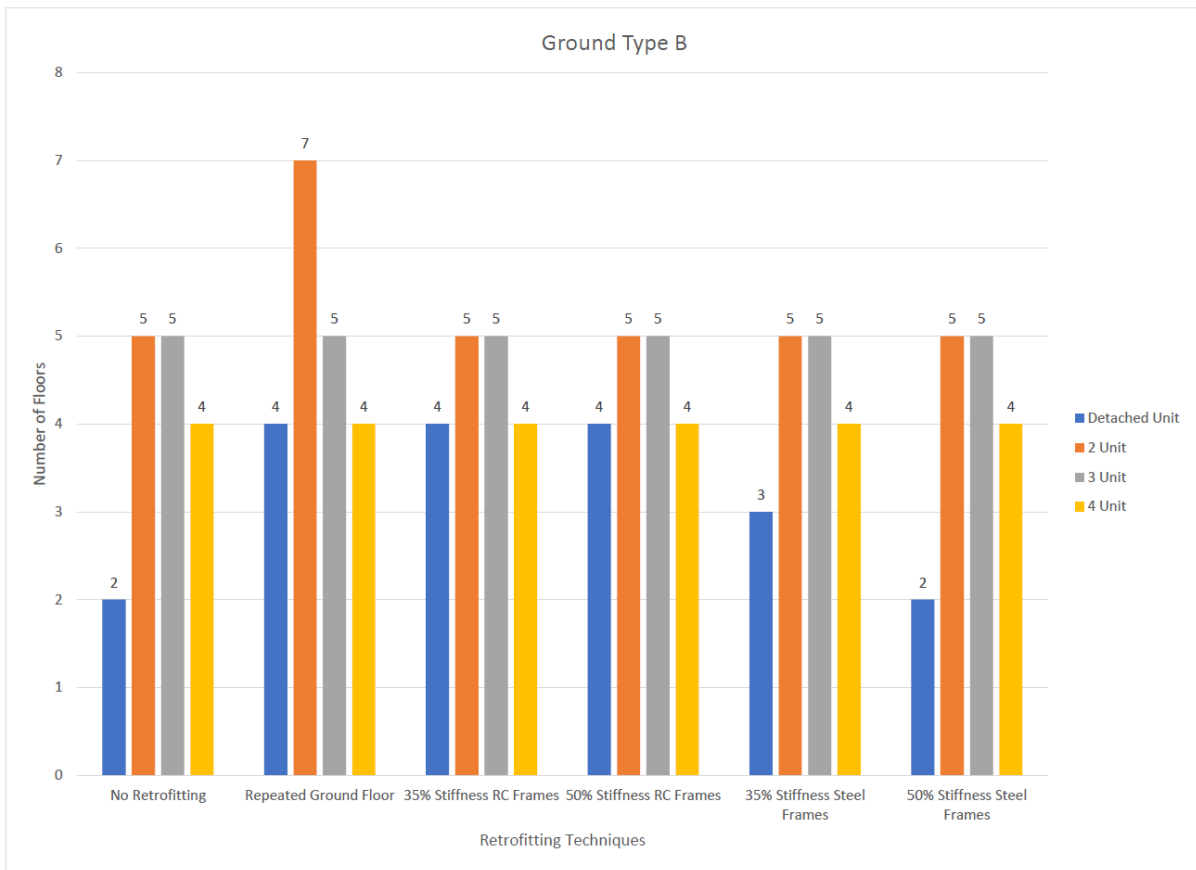


**Figure 54** Results indicating number of floors sustained by each retrofitting technique across the 1 unit building and all building aggregates for Ground Type B

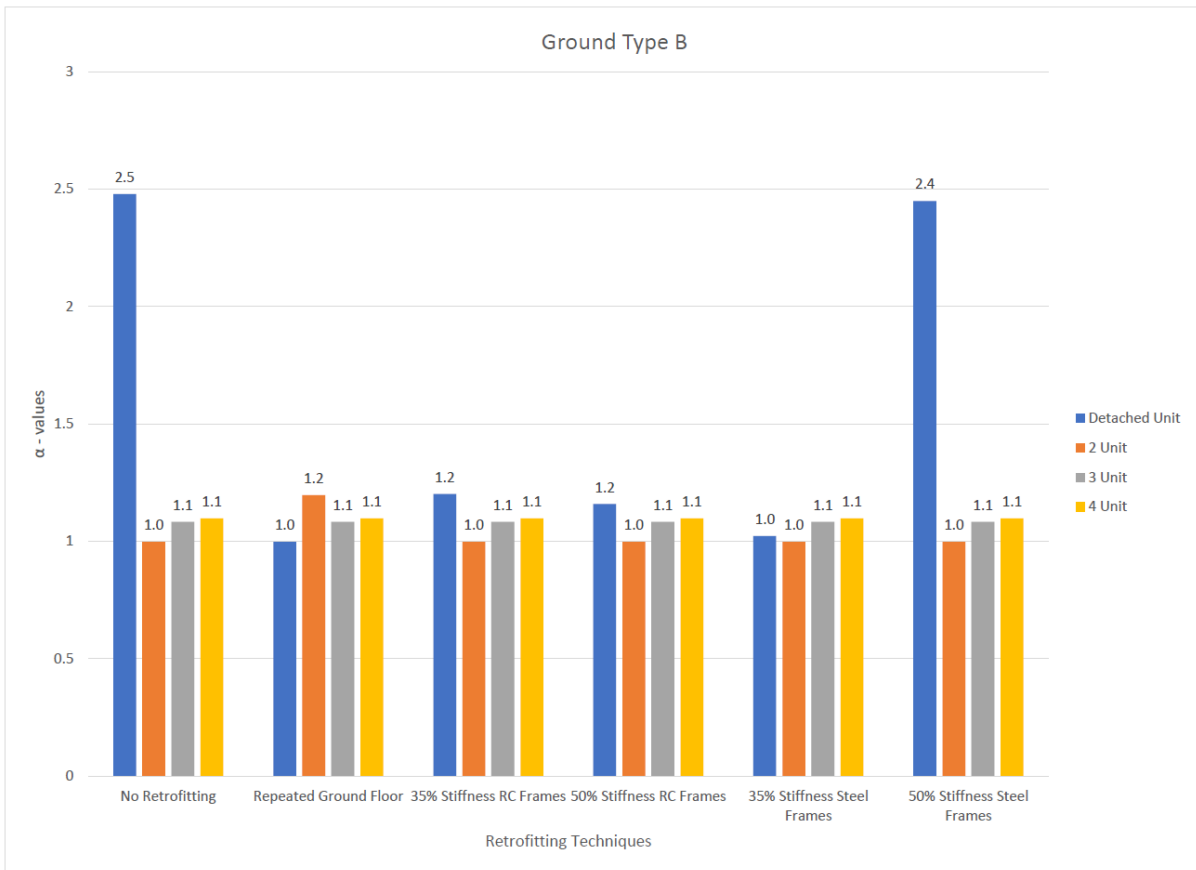


**Figure 55** Results indicating the safety factor in terms of alpha by each retrofitting technique across the 1 unit building and all building aggregates for Ground Type B



## 7.8 Comparing across Ground Type C

Comparing the results of Ground Type C between the URM building aggregates with a Repeated Ground Floor at basement level and the unretrofitted URM building aggregates, certain improvements may be observed. An additional floor is observed for the single-unit building, and for the three-unit and four-unit aggregates. However, a significant improvement of three floors may be observed for the two-unit aggregate.

Comparing the results of Ground Type C between the retrofitted and unretrofitted URM single-unit building, it was noted that the retrofitted buildings with 35% of  $K_m$  sway stiffness in both RC and steel frames could sustain one floor more than the unretrofitted buildings, while there was no improvement in the case of the retrofitted buildings with 50% of  $K_m$  sway stiffness in both RC and steel frames. Considering the seismic performance of the retrofitted URM building aggregates with 35% of  $K_m$  sway stiffnesses in RC frames, it was observed that the only enhancement observed was in the single-unit building, where the retrofitted building can sustain one floor more than the unretrofitted building. With respect to the two-unit, three-unit and four-unit URM building aggregates, it may be observed that there are no improvements of retrofitting these aggregates. The same trend was noted for aggregates with 35% of  $K_m$  sway stiffness in steel frames, 50% of  $K_m$  sway stiffness in RC frames and 50% of  $K_m$  sway stiffness in steel frames.

In the case of Ground Type C, characterised by weak clay, the effectiveness of any strengthening procedure carried out in a URM building or a URM building aggregate generally becomes immaterial as the weakness of the subsoil dictates the seismic performance. The weakness of the subsoil gives rise to seismic amplifications, which render the retrofitting measures futile. However, in Ground Type B, characterised by stiff clay, several improvements in seismic resistance were still observed, despite the subsoil conditions generating higher seismic amplifications than Ground Type A.

Ground Type C			
Units	Retrofitting Technique	Number of Floors	$\alpha$ - values
1 Unit	No Retrofitting	2	1.257601857
2 Unit	No Retrofitting	3	1.193616509
3 Unit	No Retrofitting	2	1.626691341
4 Unit	No Retrofitting	2	1.7038939

*Table 31 Results for Ground Type C, No Retrofitting*

Ground Type C			
Units	Retrofitting Technique	Number of Floors	$\alpha$ - values
1 Unit	Repeated Ground Floor	3	1.380481005
2 Unit	Repeated Ground Floor	6	1.244786263
3 Unit	Repeated Ground Floor	3	1.626691341
4 Unit	Repeated Ground Floor	3	1.7038939

*Table 32 Results for Ground Type C, Repeated Ground Floor*

Ground Type C			
Units	Retrofitting Technique	Number of Floors	$\alpha$ - values
1 Unit	35% Stiffness RC Frames	3	2.073621273
2 Unit	35% Stiffness RC Frames	3	1.193616509
3 Unit	35% Stiffness RC Frames	2	1.626691341
4 Unit	35% Stiffness RC Frames	2	1.7038939

*Table 33 Results for Ground Type C, 35% of  $K_m$  sway stiffness in RC Frames*

Ground Type C			
Units	Retrofitting Technique	Number of Floors	$\alpha$ - values
1 Unit	50% Stiffness RC Frames	2	1.592157125
2 Unit	50% Stiffness RC Frames	3	1.193616509
3 Unit	50% Stiffness RC Frames	2	1.626691341
4 Unit	50% Stiffness RC Frames	2	1.7038939

*Table 34 Results for Ground Type C, 50% of  $K_m$  sway stiffness in RC Frames*

Ground Type C			
Units	Retrofitting Technique	Number of Floors	$\alpha$ - values
1 Unit	35% Stiffness Steel Frames	3	1.521066308
2 Unit	35% Stiffness Steel Frames	3	1.193616509
3 Unit	35% Stiffness Steel Frames	2	1.626691341
4 Unit	35% Stiffness Steel Frames	2	1.7038939

*Table 35 Results for Ground Type C, 35% of  $K_m$  sway stiffness in Steel Frames*

Ground Type C			
Units	Retrofitting Technique	Number of Floors	$\alpha$ - values
1 Unit	50% Stiffness Steel Frames	2	1.706040144
2 Unit	50% Stiffness Steel Frames	3	1.193616509
3 Unit	50% Stiffness Steel Frames	2	1.626691341
4 Unit	50% Stiffness Steel Frames	2	1.7038939

*Table 36 Results for Ground Type C, 50% of  $K_m$  sway stiffness in Steel Frames*

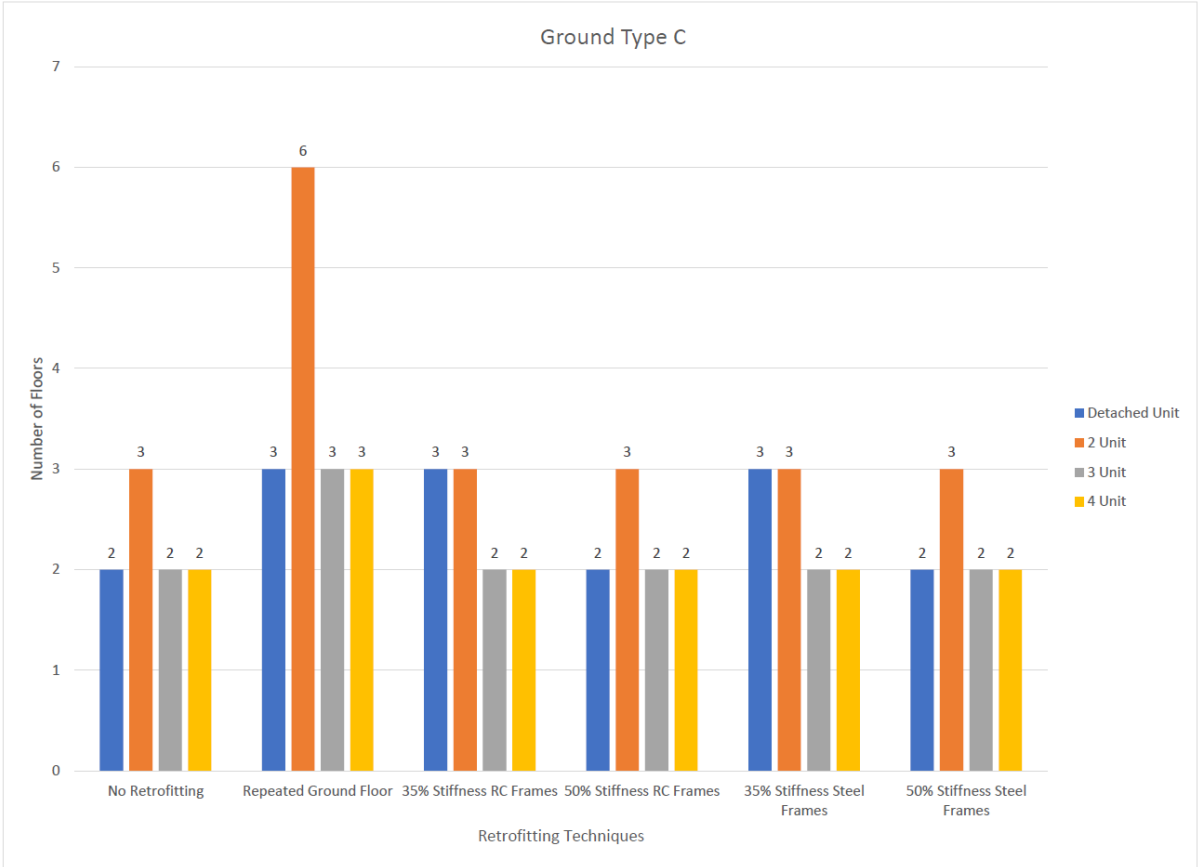


**Figure 56** Results indicating number of floors sustained by each retrofitting technique across the 1 unit building and all building aggregates for Ground Type C

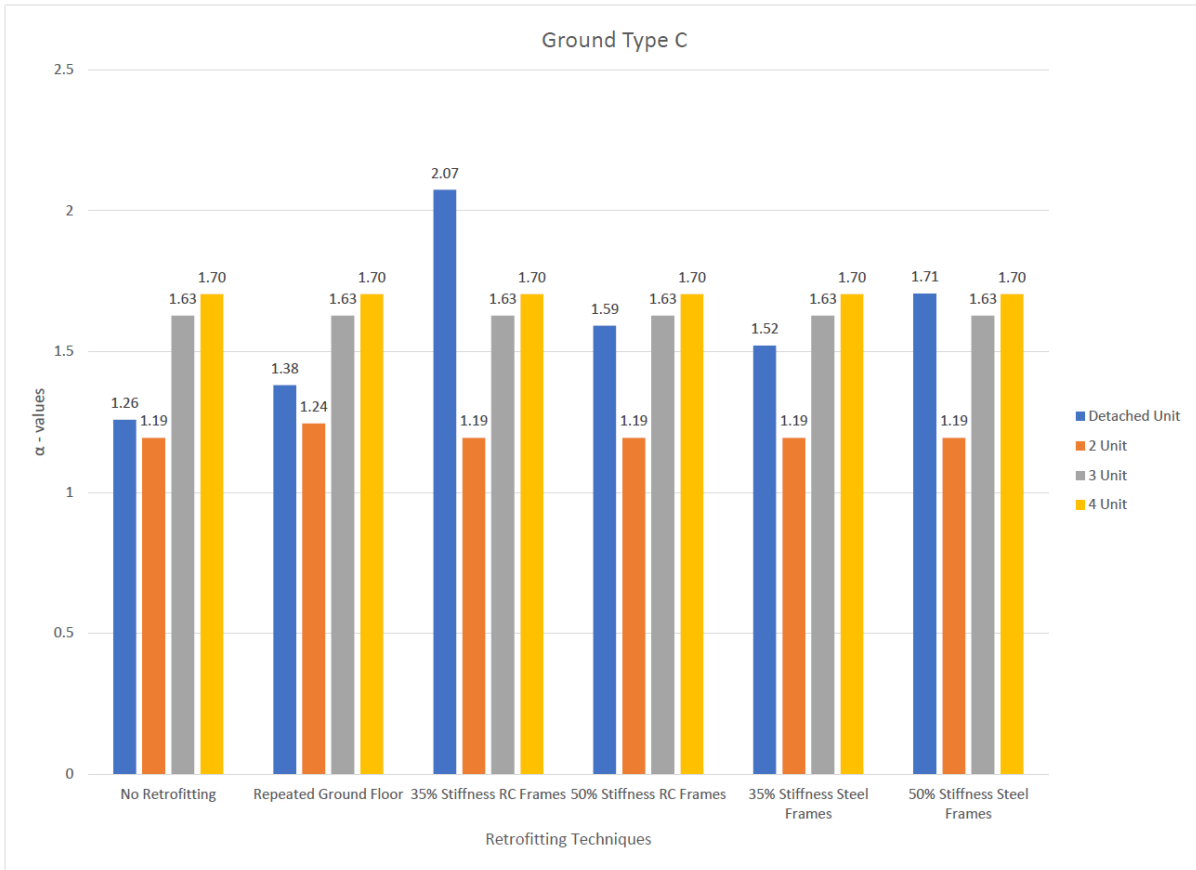


**Figure 57** Results indicating the safety factor in terms of alpha by each retrofitting technique across the 1 unit building and all building aggregates for Ground Type C

## Chapter 8: Conclusions and Recommendations for Future Research Work

### 8.1 Conclusions

The primary objective of this research study was to determine the benefits, or otherwise, of improving seismic resistance by introducing retrofitting interventions within the basement soft storey of unreinforced masonry (URM) single-unit buildings and URM building aggregates. These retrofitting interventions consisted of the installation of pinned base, single storey, single bay rectangular portal plane frames constructed using reinforced concrete (RC) or structural steelwork and placed directly below the transverse masonry shear walls in the Ground Floor, which were missing within the soft storey basement. Two scenarios were considered, namely plane frames with a sway stiffness equal to 35% and 50% of the sway stiffness of the overlying transverse masonry shear walls,  $K_m$ . Due to the large size of column sections required for this purpose, it was not possible to consider plane frames with larger sway stiffnesses. This parametric study was carried out using numerical macro-element non-linear static pushover seismic analyses conducted using the 3D Macro computational software. The salient conclusions of this dissertation are briefly discussed below:

One of the initial observations considered within this research study was the effect of utilising an asymmetrical plan with respect to the centre line of the longitudinal axis of the URM single-units that make up the URM building aggregates. In general, differences in seismic performance are evident for earthquakes in the transverse X-direction or the longitudinal Y-direction of the building. However, due to this plan geometry, differences were also observed for earthquakes in the positive and negative X-directions with reference to the safety factors (alpha-values) obtained from the seismic analyses. Parts of the plan layout include a stairwell and a lift shaft on the positive X-side of the plan. When the earthquake acts in the positive X-direction, the masonry walls pertaining to the stairwell and lift shaft are acting in compression, providing the building with additional seismic resistance. Conversely, when the earthquake acts in the negative X-direction, these walls are acting in tension providing no benefit to the seismic resistance of the building. Of course, since a building is expected to oscillate in both the positive and negative X-directions during an earthquake event, the worst case scenario of an earthquake acting in the negative X-direction becomes the critical case.

As the seismic analysis results for each URM building and URM building aggregate were considered to obtain the corresponding seismic resistance in terms of the integer number of floors that can be sustained during an earthquake event, the limitation of using such a coarse measurement was acknowledged. This yardstick of comparison necessarily restricts the seismic resistance evaluation to an integer number of floors due to functionality purposes. However, a more refined judgement can also be carried out with reference to the safety factors (alpha-values) obtained for each seismic analysis.

In several cases, it was generally observed that there was a notable decrease in seismic resistance of retrofitted URM buildings and URM building aggregates when the sway stiffness of the RC or steel plane frames was increased from the 35% of  $K_m$  to 50% of  $K_m$ . This observation indicates that, providing excessively stiff frames within the soft storey basement may result in failure within the Ground Floor rather than within the basement level. However, it should be noted that the results of the seismic analyses may be considered to be conservative, since the few internal masonry walls within the basement level were not modelled within the numerical models of the URM buildings and URM building aggregates.

It was also noted that for the URM single unit building, the retrofitted building with 35% of  $K_m$  sway stiffness in steel frames failed before the retrofitted building with 35% of  $K_m$  sway stiffness in RC frames. This observation appears to be due to the premature failure of the steel columns within the plane frame. However, this observation was not noted in the case of any of the retrofitted URM building aggregates. Furthermore, in most cases it was noted that the retrofitted URM building aggregates using either RC or structural steelwork produced similar seismic resistance in terms of the number of floors that can be sustained during an earthquake event. However, differences in seismic resistance were noted when comparing the safety factors (alpha-values) obtained from the seismic analyses, in fact, indicating that generally the structural steelwork plane frames provided a higher seismic resistance than the RC plane frames.

As the number of building units in a building aggregate increase there is a tendency that the rate of increase in seismic mass (and, hence, horizontal seismic inertial forces) is greater than the rate of increase in sway stiffness thereby cancelling the beneficial effect of having more units within a URM building aggregate. In fact, this trend was observed for all retrofitted URM building aggregates founded on Ground Type B (stiff clay) and Ground Type C (weak clay) subsoil strata. The weaker the subsoil, the more amplified are these seismic effects.

As the single unit buildings within a URM building aggregate increase, the aggregate plan aspect ratio is reduced. This would essentially imply that the sway stiffness of the structure is greater. However, as the sway stiffness increases, so does the seismic mass. In many cases as comparisons across the different ground types were carried out, it was noticed that from the single-unit building to the two-unit building aggregate, the number of floors that can be sustained during an earthquake event increases by one to three floors. Increasing the two-unit aggregate to a three-unit aggregate does not lead to any further increase in the number of floors that can be sustained, while increasing the aggregate size further to a four-unit aggregate, in fact, leads to a reduction of one floor in the number of floors that can be sustained compared to the three-unit aggregate.

The results obtained clearly implies that, beyond the three-unit URM building aggregate, the increase in seismic mass per additional single-unit building within the aggregate is detrimental to the seismic resistance of the aggregate, which experiences larger horizontal forces at each floor. In this respect, the ideal retrofitted URM building aggregate is one that has seismic gaps at every third single unit. This is, of course, quite difficult to achieve in practice unless the whole URM building aggregate forms part of an entire development project.

Furthermore, most enhancement from seismic retrofitting seems to occur for URM buildings and URM building aggregates founded on Ground Type A (rock). For Ground Type C (weak clay), almost all retrofitting measures used within the URM buildings and URM building aggregates were rendered futile and ineffective due to seismic amplifications caused by the weak subsoil. In the case of Ground Type B (stiff clay), the retrofitting measures were partially effective due to the reduced influence of seismic amplifications.

## 8.2 Recommendations for Further Research Work

There are multiple routes in which this study may be furthered. In the following, a number of possible recommendations for future research work are suggested:

- One possibility would be to carry out a parametric seismic analysis across varying plan aspect ratios. Due to time constraints, throughout this research study, only a plan aspect ratio of 1:4 was considered.
- This dissertation was mainly concerned with the seismic resistance of retrofitted existing URM buildings and URM building aggregates constructed using Globigerina Limestone blocks and M2 mortar strength. Given the widespread use of hollow concrete blockwork (HCB) nowadays within the local construction industry, it would be interesting to repeat the research carried out, but using HCB and M5 mortar strength, which is the minimum mortar strength prescribed by Eurocode 8 (EN 1998) for the seismic design of unreinforced masonry (URM) construction.
- In this research study, the portal plane frames were assumed to be pinned base, since pinned foundations are cheaper and easier to design and construct, in practice, compared to fixed foundations. However, as stated earlier, the sway stiffnesses selected for the plane frames (35% of  $K_m$  and 50% of  $K_m$ ) could not be increased because the structural steelwork column sizes corresponding to these sway stiffnesses were just about the largest columns available on the market. However, given that the sway stiffness of fixed base columns is four times greater than that of pinned base columns, there are clearly benefits in considering the seismic resistance of retrofitted URM buildings and URM building aggregates using fixed base columns. Such a research initiative would allow the investigation of the effect of using plane frames with higher sway stiffnesses than those used in this research study, still using column section sizes available on the market. Nevertheless, the challenges of achieving fixed base conditions on site, especially within an existing soft storey basement (possibly, using deep micro-piled foundations) cannot be under-estimated.
- As suggested by Borg (2021), it could also be worthwhile to assess the impact on seismic resistance of not having a shared third party wall between the URM single-unit buildings making up the URM building aggregates.
- Finally, it is also worth considering the effect on the seismic resistance of URM buildings aggregates composed of URM single-unit buildings whose floor slabs are not aligned at the same level. This building configuration may be especially dangerous as individual floor slabs tend to exert lateral seismic forces to the mid-height of the third party walls.



## Bibliography

1. Abeling, S., Dizhur, D., & Ingham, J. (2018). An evaluation of successfully seismically retrofitted URM buildings in New Zealand and their relevance to Australia.
2. Adams, A. (2020, July 8). *Learn with SE U*. Retrieved from Learn with SE U: <https://learnwithseu.com/flexible-vs-semi-rigid-vs-rigid-diaphragms/>
3. Alexander, D. (2010). *Seismic Analysis Course Notes*.
4. Alguhane, T. M., Khalil, A. H., Fayed, N. M., & Ismail, A. M. (2016). Pushover Analysis of Reinforced Concrete Buildings Using Full Jacket Technics: A Case Study on an Existing Old Building in Madinah.
5. Anagnostopoulos, S. (1988). Pounding of building in series during earthquake.
6. Arnold, C. (2001). *The Seismic Design Handbook, Chapter 6 Architectural Considerations*.
7. B. Lourenco, P., Mendes, N., F. Ramos, L., & V. Oliveira, D. (2011). Analysis of Masonry Structures without Box Behaviour.
8. Bartolo, G. (2011). Development of an Environmental Profile for Globigerina Limestone Blocks and Locally-Manufactured Hollow Concrete Blocks through the use of Life Cycle Analysis.
9. Bhowmik, A., & Mohanty, S. (2008). Analysis and Design of Earthquake Resistant Masonry Buildings.
10. Bianco, L. (2017). Sustainable Architectural Design of the Central Mediterranean.
11. Bommer, J., & Alarcon, J. (2006). The Prediction and Use of Peak Ground Velocity. 1-31.
12. Bonello, E. (2018). A Parametric Study of Effect of Plan Typology on the Seismic Sway Resistance of Local Unreinforced Masonry Buildings within an Urban Building Aggregate.
13. Borg, D. (2017). A Parametric Study of the Effect of Geometric Proportions on the Permissible Height of Local Masonry Buildings Fitted with Anti-Seismic Sway-Resisting Frames at Basement Level.
14. Borg, D. (2021). The Seismic Resistance of Unreinforced Masonry (URM) Building Aggregates of High Building Unit Plan Slenderness with Soft Storey Basements on Rock Subsoil.
15. Borg, R. (2010). Seismicity & Earthquake Engineering - L'Aquila Earthquake of April 2009.
16. Borg, R., Borg, R., & Borg Axisa, G. (2008). The Seismic Risk of Buildings in Malta.
17. Bothara, J., & Brzev, S. (2011). A TUTORIAL: Improving Seismic Performance of Stone Masonry Buildings.
18. Brincat, A. (2020). Seismic Vulnerability Assessment and Retrofitting of Local Historical Unreinforced Masonry Buildings.

19. Buhagiar, L. (2019). Seismic Vulnerability Assessment of the Inquisitor's Palace at Vittoriosa in Malta.
20. Buhagiar, V., & Tonna, G. (2012). Beyond National Minimum Standards: A Comparison of the Traditional HCB and the AB Thermablock.
21. Cachia, J. (1985). The Mechanical and Physical Properties of the Globigerina Limestone as used in Local Masonry Construction.
22. Calderini, C., Cattari, S., & Lagomarsino, S. (2008). In-plane strength of unreinforced masonry piers.
23. Camilleri, D. (1988). Globigerina Limestone As a Structural Material. *The Architect*.
24. Camilleri, D. H. (2003). Malta's risk minimisation to earthquake, volcanic and tsunami damage.
25. Camilleri, D. H. (2019). Seismic Vulnerability of Masonry Constructions in Malta.
26. Cardenas-Soto, M., & J. Chavez-Garcia, F. (2003). Regional Path Effects on Seismic Wave Propagation in Central Mexico.
27. Chieffo, N., Formisano, A., & Vaiano, G. (2021). Seismic Vulnerability Assessment and Strengthening Interventions of Structural Units of a Typical Clustered Masonry Building in the Campania Region of Italy.
28. Cosenza, E., Del Vecchio, C., Di Ludovico, M., Dolce, M., Moroni, C., Prota, A., & Renzi, E. (2018). The Italian guidelines for seismic risk classification of constructions: technical principles and validation.
29. Curtin, W., Shaw, G., Beck, J., & Bray, W. (2006). *Structural Masonry Designer's Manual*. John Wiley & Sons, Incorporated.
30. D'Alpaos, C., & Bragolusi, P. (2020). The Market Price Premium for Buildings Seismic Retrofitting.
31. D'Amico, S., & Galea, P. (2013). Earthquake Ground-Motion Simulations for the Maltese Archipelago.
32. D'Amico, S., Akinci, A., Malagnini, L., & Galea, P. (2012). Prediction of High-Frequency Ground Motion Parameters Based on Weak Motion Data.
33. Dauda, J., Lourenco, P., & Luorio, O. (2020). Out-of-plane testing of masonry walls retrofitted with oriented strand board timber panels.
34. De Felice, G., & Giannini, R. (2000). Out-of-Plane Seismic Resistance of Masonry Walls.
35. Di Carlo, F., Coccia, S., & Imperatore, S. (2020). Masonry Walls Retrofitted with Vertical FRP Rebars.
36. *Diaphragms*. (2022, May 11). Retrieved from Northern Architecture: <https://www.northernarchitecture.us/seismic-forces/diaphragms.html>

37. Dizhur, D., Ingham, J., Moon, L., Griffith, M., Schultz, A., Senaldi, I., . . . Lourenco, P. (2011). Performance of Masonry Buildings and Churches in the 22nd February 2011 Christchurch Earthquake.
38. Elsayed, T., & Ghanem, G. (2017). Retrofitting multiwythe historic stone masonry walls in egypt using grout injection technique.
39. Farrugia, D., Paolucci, E., D'Amico, S., & Galea, P. (2015). Site Characterisation and Response Study in Rabat, Malta.
40. Farrugia, K. (2022). Seismic Vulnerability Comparative Assessment and Retrofitting of Local Historical Belfries.
41. Ferreira, T. M., Costa, A., & Costa, A. (2015). Analysis of the Out-Of-Plane Seismic Behavior of Unreinforced Masonry: A Literature Review.
42. Formisano, A. (2016). Local and global scale seismic analyses of historical masonry compounds in San Pio delle Camere (L'Aquila, Italy).
43. Formisano, A., & Chieffo, N. (2018). Non-linear static analyses on an Italian masonry housing building through different calculation software packages.
44. Formisano, A., Di Lorenzo, G., Babilio, E., & Landolfo, R. (2017). Capacity Design Criteria of 3D Steel Lattice Beams for Applications into Cultural Heritage Constructions and Archaeological Sites.
45. Formisano, A., Marzo, A., Marghella, G., & Indirli, M. (2013). Damage mechanisms and retrofitting interventions on masonry buildings damaged by last Italian earthquake.
46. Frumento, S., Giovinazzi, S., Logamarsino, S., & Podesita, S. (2006). Seismic Retrofitting of Unreinforced Masonry Buildings in Italy.
47. Galdes, A. (2013). Vulnerability of Local Masonry Buildings to Seismic Loading.
48. Galea, J. (2013). Assessment of the Seismic Performance and Retrofitting Strengthening Techniques of Local Heritage Buildings.
49. Galea, P. (2007). Seismic History of the Maltese Islands and considerations on seismic risk.
50. Gauci, M. (2022). The effects of externally applied reinforcement methodologies on Globigerina Limestone Masonry Walls.
51. Giardini, D., Wossner, J., & Danciu, L. (2014). Mapping Europe's Seismic Hazard. 261-262.
52. Guh, T., & Altoontash, A. (2006). Seismic Retrofit of Historic Building Structures.
53. Ismail, M. (2019). Seismic Retrofit of Steel Frame Structures.
54. Ismail, N., Lazzarini, D., Laursen, P., & Ingham, J. (2011). Seismic performance of face loaded reinforced masonry walls retrofitted using post-tensioning.
55. J. Stern, R. (2002). *Reviews of Geophysics*.
56. Krawinkler, H., & Seneviratna, G. (1998). Pros and cons of a pushover analysis of seismic performance evaluation.

57. Lang, K. (2002). *Seismic Vulnerability of Existing Buildings*. Retrieved from <https://www.research-collection.ethz.ch/bitstream/handle/20.500.11850/146255/eth-25201-01.pdf>
58. Leslie, R. (2012). The Pushover Analysis in its Simplicity.
59. Lou, M., Wang, H., Chen, X., & Zhai, Y. (2011). Structure - soil - structure interaction: Literature review.
60. Magenes, G., & Calvi, G. M. (1997). In-plane seismic response of brick masonry walls.
61. Mangion, A. (2015). Seismic Vulnerability of Masonry Heritage Buildings in Malta.
62. Marafini, F. (2020). Seismic Performance of Masonry Buildings Enlarged with Additional Stories in Barcelona Urban Centre.
63. Marmara', R. (2016). Seismic Design of Existing Load-Bearing Unreinforced Masonry Buildings Overlying Open Plan Basements Retrofitted with Reinforced Concrete Plane Frames.
64. Morandi, P. (2006). Second order effects in out-of-plane strength of URM walls subjected to bending and compression.
65. Murty, C., Goswami, R., Vijayanarayanan, A., & Mehta, V. (2012). Some Concepts in Earthquake Behaviour of Buildings.
66. Mylonakis, G., & Gazetas, G. (2000). Seismic Soil-Structure Interaction: Beneficial or Detrimental?
67. Panto, B., Cannizzaro, F., Caddemi, S., & Calio, I. (2016). 3D macro-element modelling approach for seismic assessment of historical masonry churches.
68. Parisi, F., & Augenti, N. (2012). Seismic capacity of irregular unreinforced masonry walls with openings.
69. Pavia, A., Scozzese, F., Petrucci, E., & Zona, A. (2021). Seismic Upgrading of a Historical Masonry Bell Tower through an Internal Dissipative Steel Structure.
70. Piazza, M., Baldessari, C., & Tomasi, R. (2008). The role of in-plane floor stiffness in the seismic behaviour of traditional buildings.
71. Pujades, L., Barbat, A., Gonzalez-Drigo, R., Avila, J., & Lagomarsino, S. (2010). Seismic performance of a block of buildings representative of the typical construction in the Eixample district in Barcelona (Spain).
72. Rota, M., Penna, A., & Magenes, G. (2013). A framework for the seismic assessment of existing masonry buildings for different sources of uncertainty.
73. Sapiano, P. (2019). Seismic Vulnerability of the Contemporary Loadbearing Masonry Building Typology.
74. Sciarretta, F. (2020). Seismic Retrofitting of Traditional Masonry with Pultruded FRP Profiles.

75. Segreto, M., Marghella, G., Marzo, A., & Carpani, B. (2012). *Messa in sicurezza post-sism della parrocchia della visitazione di maria santissima a reno finalese (MO)*.
76. Shehu, R. (2021). *Implementation of Pushover Analysis for Seismic Assessment of Masonry Towers: Issues and Practical Recommendations*.
77. Shoji, Y., Tanii, K., & Kamiyama, M. (2004). *The Duration and Amplitude Characteristics of Earthquake Ground Motions with Emphasis on Local Site Effects*.
78. Stratan, A. (2014). *2C09 Design for seismic and climate changes, Lecture 10: Characterisation of seismic motion*. Politehnica University of Timisoara.
79. Stratan, A. (2014). *Lecture 10: Characterisation of Seismic Motion*.
80. Taly, N. (2010). *Design of Reinforced Masonry Structures Second Edition*.
81. Tamari, Y., & Towhata, I. (2003). *Seismic soil-structure interaction of cross sections of flexible underground structures subjected to soil liquefaction*. 69-87.
82. Tarque, N., Crowley, H., Pinho, R., & Varum, H. (2015). *Displacement-Based Fragility Curves for Seismic Assessment of Adobe Buildings in Cusco, Peru*.
83. Terracciano, G., Di Lorenzo, G., Formisano, A., & Landolfo, R. (2014). *Cold-formed thin-walled steel structures as vertical addition and energetic retrofitting systems of existing masonry buildings*.
84. Tomazevic, M. (1999). *Earthquake-Resistant Design of Masonry Buildings*. World Scientific.
85. Tong, M. (2016). *Seismic Design of New Load-Bearing Unreinforced Masonry Buildings Overlying Open Plan Basements Employing Structural Steelwork Plane Frames*.
86. Triller, P., Tomazevic, M., & Gams, M. (2017). *Seismic Response of URM Walls Strengthened with FRP Reinforced Coating*.
87. Vella, K. (2018). *Structural Reliability Analysis of Local Contemporary Unreinforced Masonry Buildings Subject to Seismic Loading*.
88. Wald, D., Quitariano, V., Heaton, T., & Kanamori, H. (1999). *Relationships between Peak Ground Acceleration, Peak Ground Velocity, and Modified Mercalli Intensity in California*.
89. Wang, Z. (2006). *Understanding Seismic Hazard and Risk Assessments: An Example in the New Madrid Seismic Zone of the Central United States*.
90. Xuereb, D. (1991). *Elastic Constants of Globigerina Limestone*.
91. Y.Elghazouli, A. (2017). *Seismic Design of Buildings to Eurocode 8, Second Edition*.
92. Zhenming, W. (2009). *Seismic Hazard vs. Seismic Risk*. 673-674.

# Appendix A: Design Parameters for 3DMacro Numerical Modelling

## Appendix A.1 3DMacro General Settings & Geometric Settings

Current code
Ministerial Decree of 17 January 2018 Technical standards for constructions (NTC2018) Related codes ...

**General data**
↓

Data model

Name	2_unit_aggregate_3_Floors_05.06_70_Steel	The model name is automatically set as the TDM file name
Author	sarah.chetcuti.17@um.edu.mt	
Company		
Comment		

Building data

<input type="radio"/> New building <input checked="" type="radio"/> Existing building	Default level of knowledge
<input type="radio"/> Masonry <input checked="" type="radio"/> Mixed structure masonry-reinforced concrete <input type="radio"/> Reinforced concrete	Muratura ordinaria
Body of the building: <input checked="" type="radio"/> Detached <input type="radio"/> Aggregated	

Location	⇒
Life of the structure\importance factor	⇒
Soil	⇒
Damping	⇒
Limit states	⇒
Spectra	⇒

✕ Cancel and Close ✓ Accept and close

Current code
Ministerial Decree of 17 January 2018 Technical standards for constructions (NTC2018) Related codes ...

**Location**
↓

Construction site

<div style="border: 1px solid #ccc; padding: 2px; display: flex; align-items: center;"> <div style="width: 30px; height: 30px; background-color: #ccc; margin-right: 5px;"></div> <div> <b>Vita (TP)</b>                      Sicilia                      37° 51' 59" N; 12° 48' 59" E                 </div> </div>	<input type="button" value="Edit..."/>
---	--

Seismicity of the site

<b>Ground acceleration</b> for the expected earthquake with a probability of 10% in 50 years	<input style="width: 80%;" type="text" value="0.09999 g"/>
<input checked="" type="checkbox"/> Multiplier	<input style="width: 80%;" type="text" value="1.0602"/>


More information on the location of the building (not used for the purposes of seismic zonation)

Place:

Address:

Life of the structure\importance factor	⇒
Soil	⇒
Damping	⇒
Limit states	⇒
Spectra	⇒

✕ Cancel and Close ✓ Accept and close

Current code: Ministerial Decree of 17 January 2018 Technical standards for constructions (NTC2018) Related codes ... 

General data ⇒

Location ⇒

**Life of the structure\importance factor** ⇅

Construction type: Ordinary structures Table 2.4.I - Nominal Life VN for different types of structures - Structures with normal performance levels.

Class of service: II Par. 2.4.2 - Classes of service - Buildings whose use provides normal crowdings, no dangerous content for the environment and without essential public and social functions. Industries with non-hazardous activities for the environment. Bridges, infrastructure, road networks that is not part of Class of service III or Class of service IV, rail networks, whose interruption does not cause emergency situations. Dams whose collapse does not cause

Nominal life of the structure,  $V_n$ :  years The nominal life of the structure must be at least 50 years

Reference period,  $V_r$ :  years

Coefficient of use,  $C_u$ :


Soil ⇒

Damping ⇒

Limit states ⇒

Spectra ⇒

X Cancel and Close ✓ Accept and close

Current code: Ministerial Decree of 17 January 2018 Technical standards for constructions (NTC2018) Related codes ... 

General data ⇒

Location ⇒

Life of the structure\importance factor ⇒

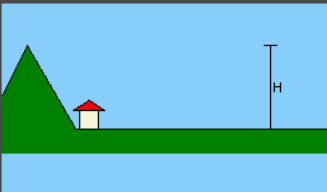
**Soil** ⇅

Category of soil: A Tab. 3.2.II - Subsoil categories that allow the adoption of the simplified approach - Cluster emerging rocks or very stiff soil characterized by values of  $V_{s,30}$  greater than 800 m/s, possibly including the surface in a layer of alteration, with a maximum thickness of 3 m.

Topographic condition: T1 Table 3.2.IV - Flat surface, slopes and isolated peaks with an average inclination  $i \leq 15^\circ$  or height or  $< 30$  m.

Slope height  $H > 30$  m:  m

Level of the building with respect to the base of the slope  $Q_e$  =  m

 Coefficient of topographic amplification  $S_t$  =

Damping ⇒

Limit states ⇒

Spectra ⇒

X Cancel and Close ✓ Accept and close

Current code: Ministerial Decree of 17 January 2018 Technical standards for constructions (NTC2018) Related codes ...

General data ↔

Location ↔

Life of the structure\importance factor ↔

Soil ↔

**Damping** ↕

Modal damping  $\xi$  =

Coefficient  $\eta$   $\sqrt{10/(5 + \xi)} \geq 0,55$

Limit states ↔

Spectra ↔

✕ Cancel and Close ✓ Accept and close

Current code: Ministerial Decree of 17 January 2018 Technical standards for constructions (NTC2018) Related codes ...

General data ↔

Location ↔

Life of the structure\importance factor ↔

Soil ↔

Damping ↔

**Limit states** ↕

Limit state	P [%]*	T <sub>r</sub>	ag	F <sub>0</sub>	T <sup>*</sup>	η	S	T <sub>B</sub>	T <sub>C</sub>	T <sub>D</sub>	Notes
SLO	81	30	0.0277	2.393	0.19	1	1	0.0634	0.19	1.71	
SLD	63	50	0.0369	2.418	0.212	1	1	0.0708	0.212	1.75	
SLV	10	474	0.1	2.474	0.31	1	1	0.103	0.31	2	
SLC	5	974	0.133	2.518	0.323	1	1	0.108	0.323	2.13	Ultimate State

(\*): Probability of occurrence of the earthquake corresponding to the considered limit state in a time equal to the life of the structure

Select a limit state to edit its properties

🔒 Lock limit states

➕ Add

Spectra ↔

✕ Cancel and Close ✓ Accept and close





## Appendix A.2 Material Definition

### Defining Masonry:

The screenshot shows the 'Masonry materials' software interface. The 'Selected material' is 'GlobigerinaLimestone' with the comment 'Masonry material'. The 'Masonry typology' is set to 'Regular masonry of soft stone blocks (tuff, limestone, etc)'. The 'Knowledge level' is 'LC-3' and the 'Confidence Factor' is '1'. The 'Mechanical properties (design values)' are listed in a table:

Property	Value
Young's modulus, $E$	20337.1 N / mm <sup>2</sup>
Shear modulus, $G$	8126.5 N / mm <sup>2</sup>
Compressive strength, $f_m$	2003 N / cm <sup>2</sup>
Shear strength, $\tau_a$	60.3 N / cm <sup>2</sup>
Specific weight, $w$	18 kN / m <sup>3</sup>
Yielding Criterion	Mohr Coulomb

The 'Yielding Criterion' is set to 'Mohr Coulomb'. The 'Unit Measurements' are set to 'According to the code'. The 'Current code' is 'Ministerial Decree of 17 January 2018 Technical standards for constructions (NTC2018)'. The interface also includes a 'Masonry picture' section with a sample image and a 'Choose a custom image...' button.

The 'Set to default' window allows users to set the design values of the mechanical properties of the material directly. It includes a diagram of a masonry wall under a horizontal force  $F$  and a vertical load  $q$ . The 'Behavior' is set to 'Nonlinear'. The 'Unit Measurements' are set to 'According to the code'. The 'Density,  $w$ ' is set to '18 kN / m<sup>3</sup>'. The 'Mechanical properties (design values)' are listed in a table:

Property	Value
Young's modulus, $E$	20337.1 N / mm <sup>2</sup>
Compressive strength, $f_m$	2003 N / cm <sup>2</sup>
Tensile strength, $f_{tm}$	285 N / cm <sup>2</sup>
Limit rotation*	0.6%
Tensile ductility	Infinite
Compressive ductility	Infinite

\*The set limit rotation value will be used to determine the activation of the limit state in which the corresponding criterion has been included.

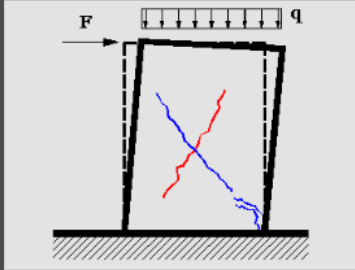
Set to default Close

This window allows you to set the directly the design values of the mechanical properties of the material without taking into account automatically the corrective factors, the confidence factor (for existing masonry) or partial safety factors (for new masonry).

Unit Measurements  
According to the code

Density, w 18 kN / m<sup>3</sup>

Rocking mechanism



Diagonal shear cracking mechanism

Sliding shear mechanism

Behavior  Linear  Nonlinear

Shear modulus, G 8128.5 N / mm<sup>2</sup>

Yielding criterion  Mohr-Coulomb  Turnsek-Cacovic

Shear Strength, tau0 60.3 N / cm<sup>2</sup>

Friction ratio 0.3

Ultimate shear strain 0.4%

Coefficient b 1.5

Damage

Kinematic a -1

Cyclic alpha -1 gamma -1

Unload

Initial beta 0

### Defining Steel for Reinforcement and Retrofitting Steel Sections

Materials for frame

List of objects Selected object properties

Name LooseBars Comment Steel material Color

New steel

Existing steel

Steel for reinforcement bars

Working steel

Unit Measurements  
According to the code

Type of steel B 450 C Knowledge level LC-3 Partial safety fact  $\gamma = 1.15$


From code rec Set to 1

Mechanical parameters	Design value
Young's modulus, E	<span style="border: 1px solid gray; padding: 2px;">210000</span> N / mm <sup>2</sup>
Poisson's ratio, nu	<span style="border: 1px solid gray; padding: 2px;">0.2</span>
Yielding strength, f <sub>y</sub>	<span style="border: 1px solid gray; padding: 2px;">45000</span> N / cm <sup>2</sup>
Ultimate strain, epsilon <sub>u</sub>	<span style="border: 1px solid gray; padding: 2px;">0.04</span>
Specific weight, w	<span style="border: 1px solid gray; padding: 2px;">78.5</span> kN / m <sup>3</sup>

Current code: Ministerial Decree of 17 January 2018 Technical standards for constructions (NTC2018)

Materials for frame

List of objects << Selected object properties

Name  Comment   Color

New steel
  Existing steel
  Steel for reinforcement bars
  Working steel

Unit Measurements  ▾


Type of steel  Knowledge level  Partial safety fact  $\gamma = 1.05$

Mechanical parameters	Design value
Young's modulus, $E$	<input type="text" value="21000"/> N / mm <sup>2</sup>
Poisson's ratio, $\nu$	<input type="text" value="0.2"/>
Yielding strength, $f_y$	<input type="text" value="26190.5"/> N / cm <sup>2</sup>
Ultimate strain, $\epsilon_u$	<input type="text" value="0.04"/>
Specific weight, $w$	<input type="text" value="78.5"/> kN / m <sup>3</sup>

Current code: Ministerial Decree of 17 January 2018 Technical standards for constructions (NTC2018)

Materials for frame

List of objects << Selected object properties

Name  Comment   Color

New concrete
  Existing concrete

Unit Measurements  ▾

Concrete type  Knowledge level  Partial safety factor for  $f_c$  **1.5**

Rc mean value from specimens  N / mm<sup>2</sup>

Mechanical parameters	Design value
Young's modulus, $E$	<input type="text" value="27386"/> N / mm <sup>2</sup>
Poisson's ratio, $\nu$	<input type="text" value="0.2"/>
Compressive strength, $f_c$	<input type="text" value="17.6375"/> N / mm <sup>2</sup>
Tensile strength, $f_{ct}$	<input type="text" value="1.58574"/> N / mm <sup>2</sup>
Transition strain, $\epsilon_{c0}$	<input type="text" value="0.002"/>
Ultimate compressive strain, $\epsilon_u$	<input type="text" value="0.0035"/>
Density, $w$	<input type="text" value="25"/> kN / m <sup>3</sup>

Current code: Ministerial Decree of 17 January 2018 Technical standards for constructions (NTC2018)

## Appendix A.3 Section Design

### Masonry Panels:

The screenshot shows the 'Element templates' window for 'Masonry panels'. The 'Selected element template' panel is configured as follows:

- Name:** 230mm
- Comment:** Masonry panel type
- Material:** GlobigerinaLimestone
- Masonry typology:** Regular masonry of soft stone blocks (tuff, limestone, etc.)
- Thickness:** Wall thickness is 0.23 m

At the bottom, the current code is identified as: Ministerial Decree of 17 January 2018 Technical standards for constructions (NTC2018).

### Reinforced Concrete Sections:

The screenshot shows the 'Element templates' window for 'Reinforced Concrete Sections'. The 'Selected element template' panel is configured as follows:

- Name:** DownstandBeam530mm
- Comment:** 2D beam type
- Section:** DownstandBeam530mm
- Shape:** Solid rectangular
- Size:** 23 cm x 53 cm
- Materials:** Main:C20C25; Bar reinforcement:LooseBars
- Reinforcing bar:**
  - Lower bar reinforcement: 3Ø25
  - Upper bar reinforcement: 3Ø20
  - Left bar reinforcement: 1Ø25
  - Right bar reinforcement: 1Ø25
- Behavior:** 2D Beam. Description: 2D beam interacting with the masonry. The plasticity is concentrated in the hinges that do not take into account the influence of axial force on the plastic moment. Suitable for modeling beams that act only in the plane of the wall where they belong.
- Plastic hinge length:**
  - Automatic plastic length:  $L_p = 0.5$  m,  $L_p/H = 1$
  - Fixed plastic length
  - Fixed plastic length according to the height of the section:  $\gamma_E = 1.5$
- Placing plastic hinges:**
  - Frame ends
  - Middle and ends of the frame
  - Along the whole frame

At the bottom, the current code is identified as: Ministerial Decree of 17 January 2018 Technical standards for constructions (NTC2018).

Element templates

Selected element template

Name: **TieBeam350mm** Comment: **3D beam type** Color

**Span section** | End section

Section: **TieBeam350mm** Edit section ...  
Duplicate and edit ...

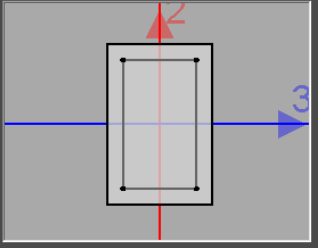
Shape: **Solid rectangular**

Size: **23 cm x 35 cm**

Materials: **Main:C20C25; Bar reinforcement:LooseBars**

Reinforcing bar:
 

- Lower bar reinforcement: 2012
- Upper bar reinforcement: 2012
- Stirrup: Ø10/15 cm Number of branches:2 horizontal,2 vertical.



Behavior: **3D Beam**

3D beam interacting with the masonry. The plasticity is concentrated in the hinges that do not take into account the influence of axial force on the plastic moment. Suitable for modeling beams that work also out of the plane of the wall where they belong.

Plastic hinge length:
 

- Automatic plastic length  $L_p =$   m  $L_p/H =$
- Fixed plastic length
- Fixed plastic length according to the height of the section  $\gamma_E =$

Placing plastic hinges:
 

- Frame ends
- Middle and ends of the frame
- Along the whole frame

Current code: Ministerial Decree of 17 January 2018 Technical standards for constructions (NTC2018)

Element templates

Selected element template

Name: **TieBeam225mm** Comment: **Beam type** Color

**Span section** | End section

Section: **TieBeam225mm** Edit section ...  
Duplicate and edit ...

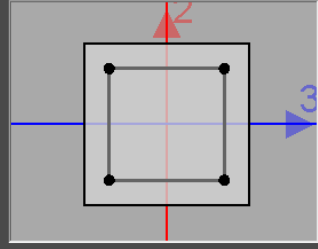
Shape: **Solid rectangular**

Size: **23 cm x 22.5 cm**

Materials: **Main:C20C25; Bar reinforcement:LooseBars**

Reinforcing bar:
 

- Lower bar reinforcement: 2016
- Upper bar reinforcement: 2016
- Stirrup: Ø10/15 cm Number of branches:2 horizontal,2 vertical.



Behavior: **2D Beam**

2D beam interacting with the masonry. The plasticity is concentrated in the hinges that do not take into account the influence of axial force on the plastic moment. Suitable for modeling beams that act only in the plane of the wall where they belong.

Plastic hinge length:
 

- Automatic plastic length  $L_p =$   m  $L_p/H =$
- Fixed plastic length
- Fixed plastic length according to the height of the section  $\gamma_E =$

Placing plastic hinges:
 

- Frame ends
- Middle and ends of the frame
- Along the whole frame


Current code: Ministerial Decree of 17 January 2018 Technical standards for constructions (NTC2018)

Element templates

Selected element template

Name **FlushBeam350** Comment **Beam type** Color

**Span section** **End section**

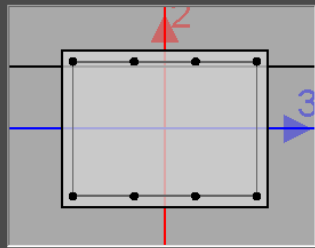
Section  FlushBeam350 Edit section ...  
Duplicate and edit ...

Shape **Solid rectangular**

Size **46 cm x 35 cm**

Materials **Main:C20C25; Bar reinforcementLooseBars**

Reinforcing bar  
 - Lower bar reinforcement: 4020  
 - Upper bar reinforcement: 4020  
 - Stirrup: Ø10/15 cm Number of branches:2 horizontal,2 vertical.



Behavior  
**2D Beam** 2D beam interacting with the masonry. The plasticity is concentrated in the hinges that do not take into account the influence of axial force on the plastic moment. Suitable for modeling beams that act only in the plane of the wall where they belong.

Plastic hinge length  
 Automatic plastic length  $L_p =$   m  $L_p/H =$    
 Fixed plastic length  $\gamma_E =$    
 Fixed plastic length according to the height of the section

Placing plastic hinges  
 Frame ends  Middle and ends of the frame  Along the whole frame


Current code: Ministerial Decree of 17 January 2018 Technical standards for constructions (NTC2018)

Element templates

Selected element template

Name **LintelBeam230** Comment **Beam type** Color

**Span section** **End section**

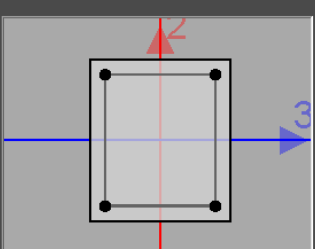
Section  LintelBeam230 Edit section ...  
Duplicate and edit ...

Shape **Solid rectangular**

Size **23 cm x 26.5 cm**

Materials **Main:C20C25; Bar reinforcementLooseBars**

Reinforcing bar  
 - Lower bar reinforcement: 2020  
 - Upper bar reinforcement: 2020  
 - Stirrup: Ø10/15 cm Number of branches:2 horizontal,2 vertical.



Behavior  
**2D Beam** 2D beam interacting with the masonry. The plasticity is concentrated in the hinges that do not take into account the influence of axial force on the plastic moment. Suitable for modeling beams that act only in the plane of the wall where they belong.

Plastic hinge length  
 Automatic plastic length  $L_p =$   m  $L_p/H =$    
 Fixed plastic length  $\gamma_E =$    
 Fixed plastic length according to the height of the section

Placing plastic hinges  
 Frame ends  Middle and ends of the frame  Along the whole frame

Current code: Ministerial Decree of 17 January 2018 Technical standards for constructions (NTC2018)

Element templates

Selected element template

Name **LintelBeam180** Comment **Beam type** Color

Span section | End section

Section **LintelBeam180** Edit section ... Duplicate and edit ...

Shape **Solid rectangular**

Size **18 cm x 26.5 cm**

Materials **Main:C20C25; Bar reinforcementLooseBars**

Reinforcing bar  
 - Lower bar reinforcement: 2020  
 - Upper bar reinforcement: 2020  
 - Stirrup: Ø10/15 cm Number of branches: 2 horizontal, 2 vertical.

Behavior  
 2D Beam 2D beam interacting with the masonry. The plasticity is concentrated in the hinges that do not take into account the influence of axial force on the plastic moment. Suitable for modeling beams that act only in the plane of the wall where they belong.

Plastic hinge length  
 Automatic plastic length  $L_p = 0.5$  m  $L_p/H = 1$   
 Fixed plastic length  $\gamma_E = 1.5$   
 Fixed plastic length according to the height of the section

Placing plastic hinges  
 Frame ends  Middle and ends of the frame  Along the whole frame

Current code: Ministerial Decree of 17 January 2018 Technical standards for constructions (NTC2018)

Element templates

Selected element template

Name **350mmSlab** Comment **Floor type** Color

Floors slab

Section **350mmSlab**

Floor type  
 Rigid floor  
 Deformable floor  
 Floor infinitely deformable in its plane

Own weight  
 Automatically calculated according to the section  
 Assigned **8750** N / m<sup>2</sup>

Current code: Ministerial Decree of 17 January 2018 Technical standards for constructions (NTC2018)



Element templates

Element templates

Floors slab

Filter

Element	Color
350mmSlab	Blue
225mmSlab	Pink

Selected element template

Name: 225mmSlab    Comment: Type of Floor    Color

Section

225mmSlab

Floor type

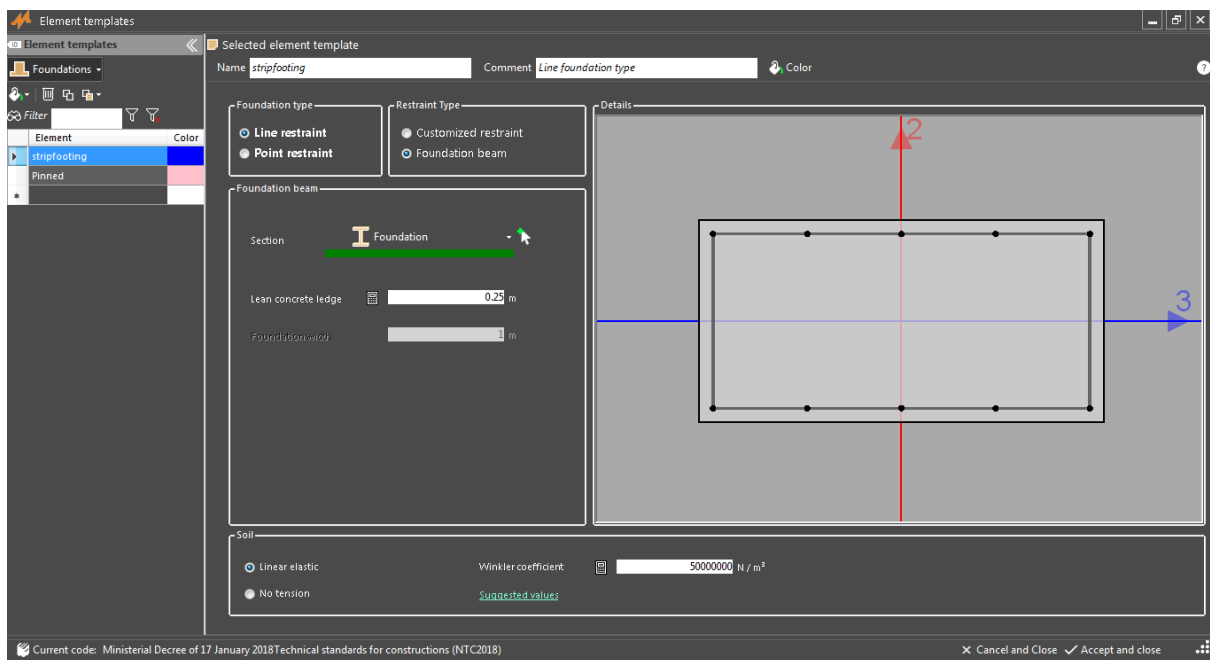
- Rigid floor
- Deformable floor
- Floor infinitely deformable in its plane

Own weight

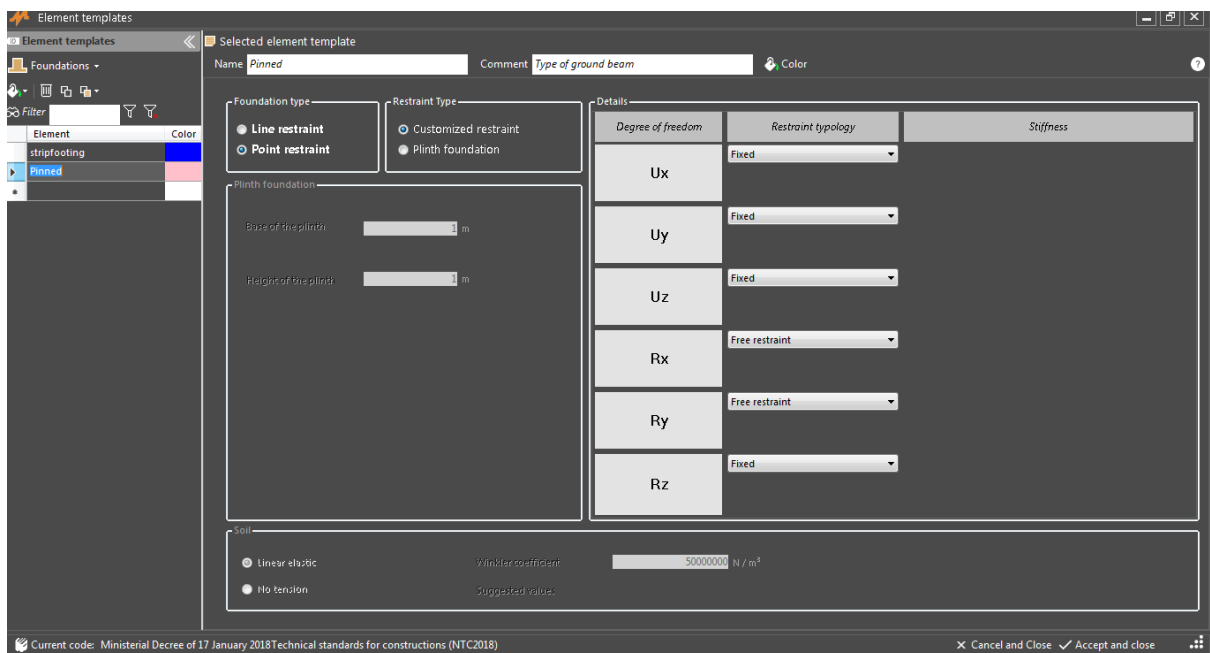
- Automatically calculated according to the section
- Assigned  N / m<sup>2</sup>

Current code: Ministerial Decree of 17 January 2018 Technical standards for constructions (NTC2018)

## Strip Footing Section:

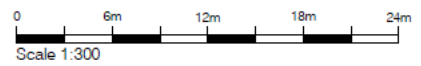
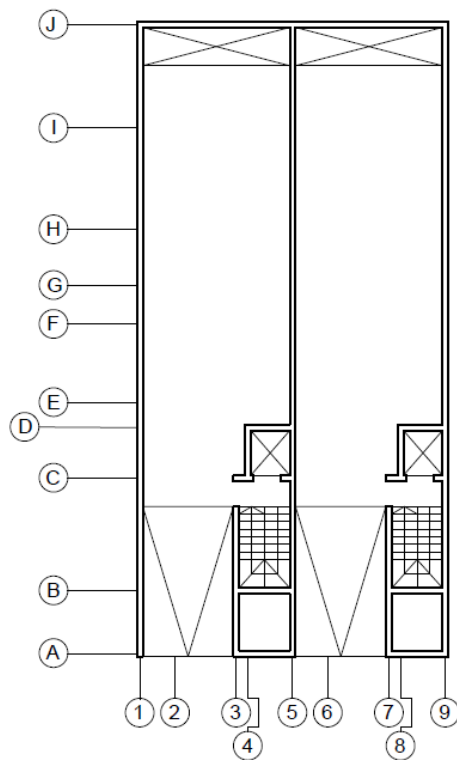
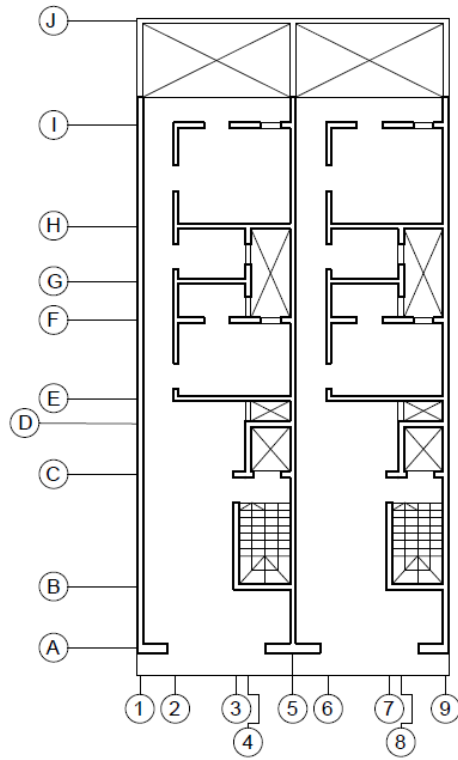


## Pinned Base Restraints:

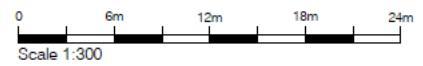
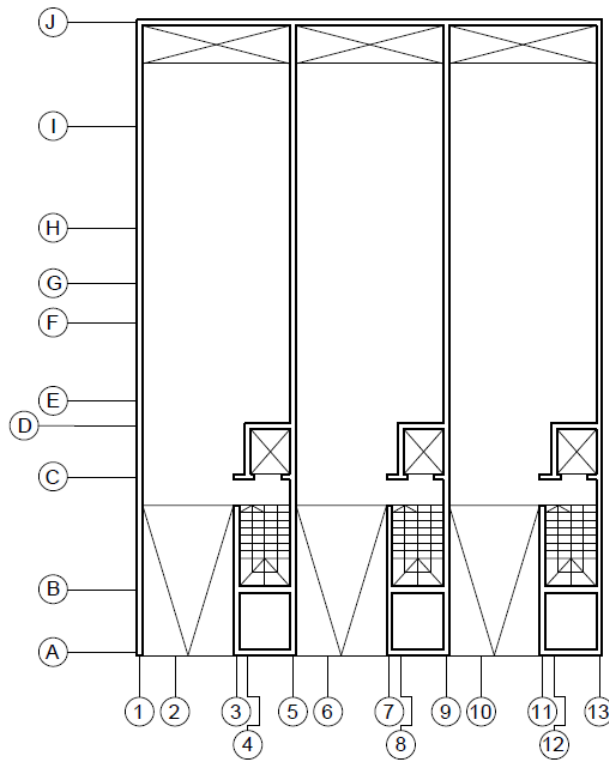
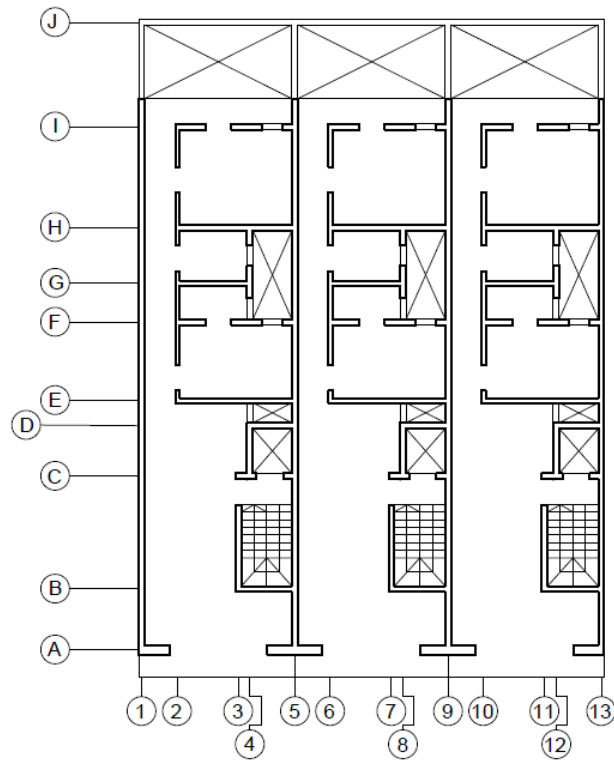


## Appendix B: Plans and Drawings of All Building Aggregates

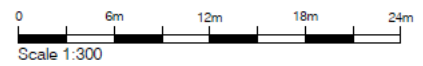
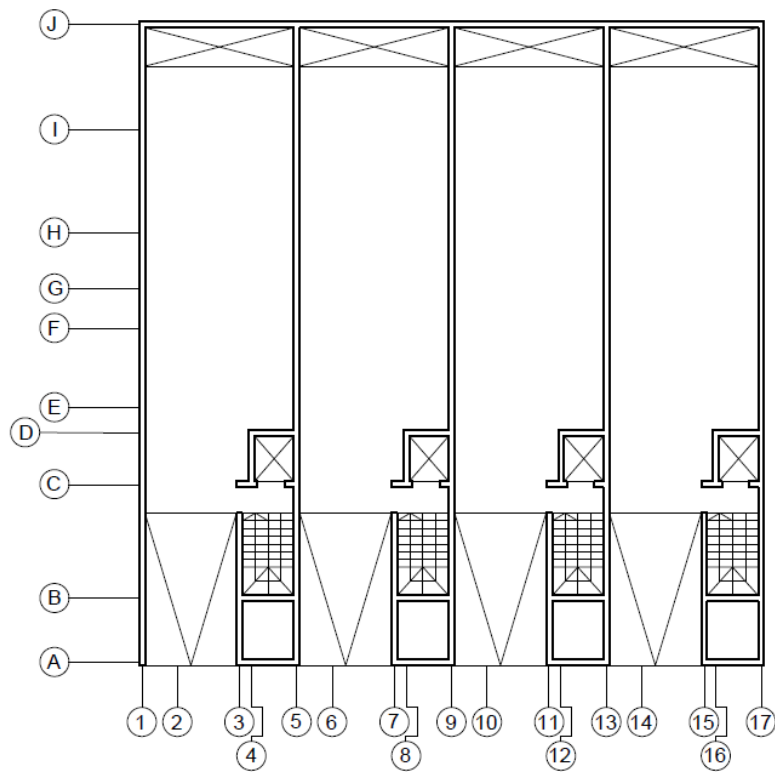
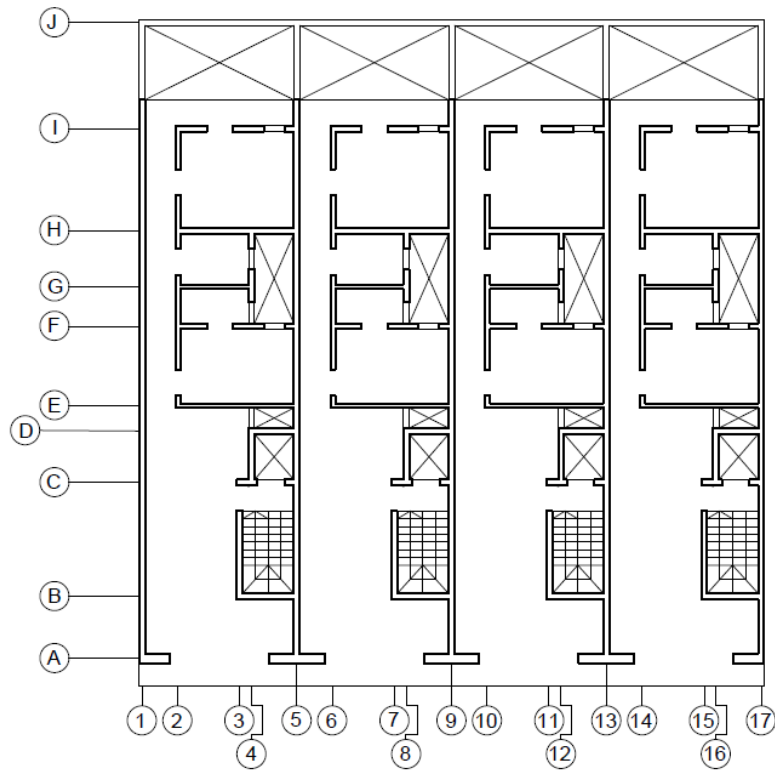
### Appendix B.1 Two-Unit Aggregate



## Appendix B.2 Three-Unit Aggregate



### Appendix B.3 Four-Unit Aggregate

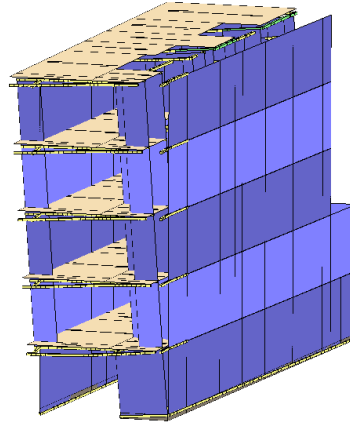


## Appendix C: Screenshots Showing Failure Mechanism at Failing Load Case

### Appendix C.1 Single Unit, Ground Type A

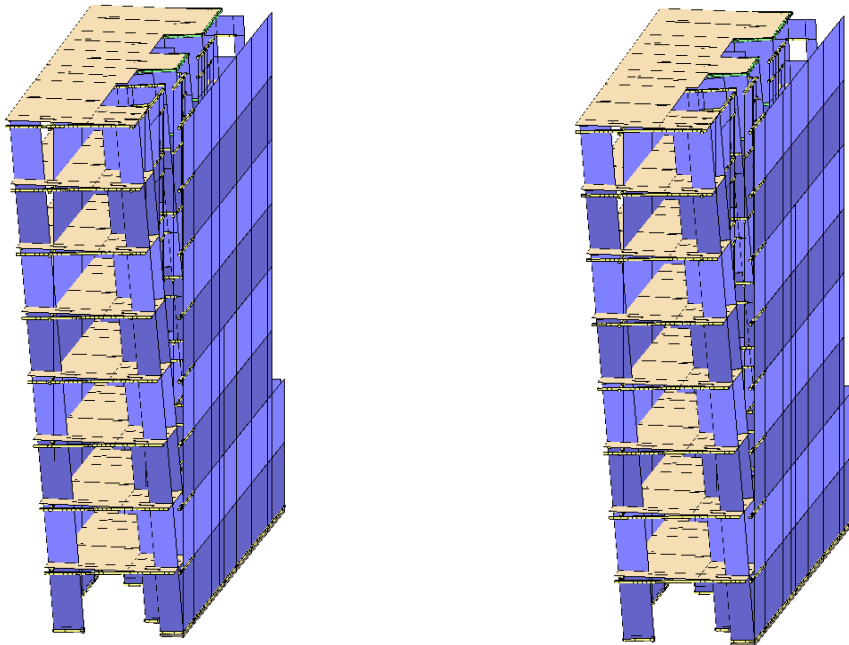
No Retrofitting

Load Case: Pushover Ex + 03Ey Acc



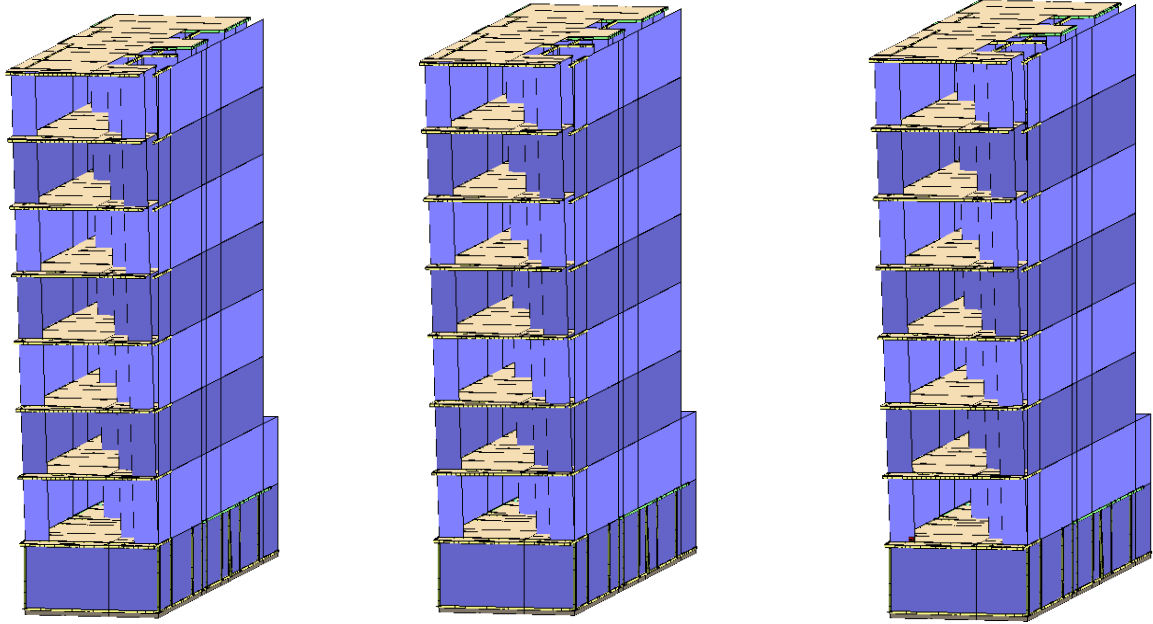
### Repeated Ground Floor

Load Case: (left) Pushover – X Acc, (right) Pushover – X Acc + e



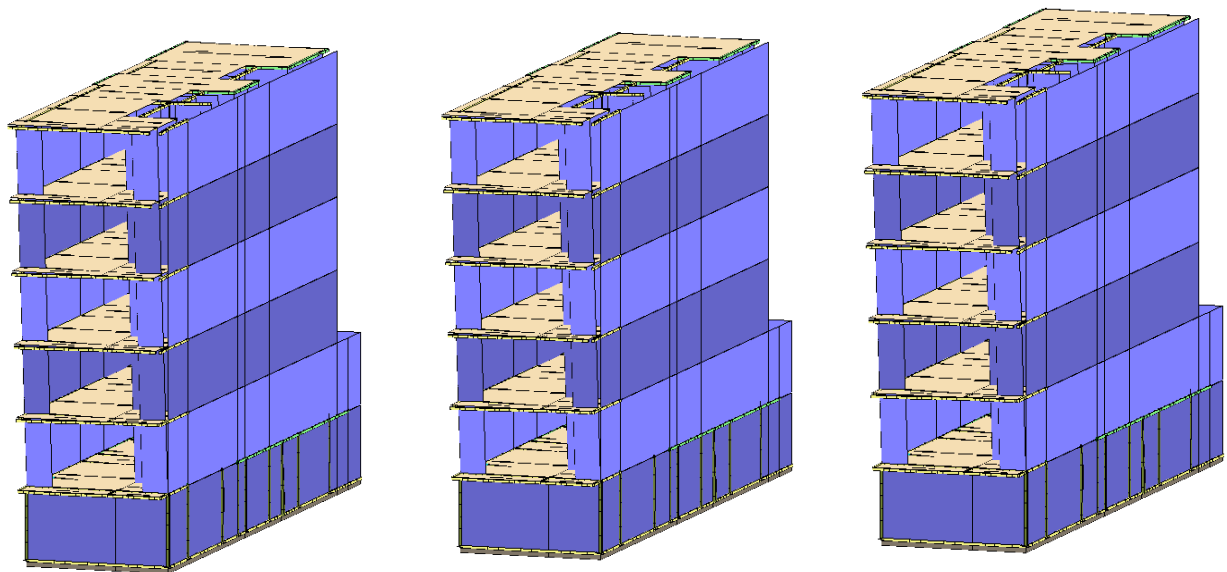
**35% of  $K_m$  Sway Stiffness in RC Frames**

Load Case: (left) Pushover – X Acc, (middle) Pushover – X Acc + e, (right) Pushover -Ex + 0.3 Ey Acc



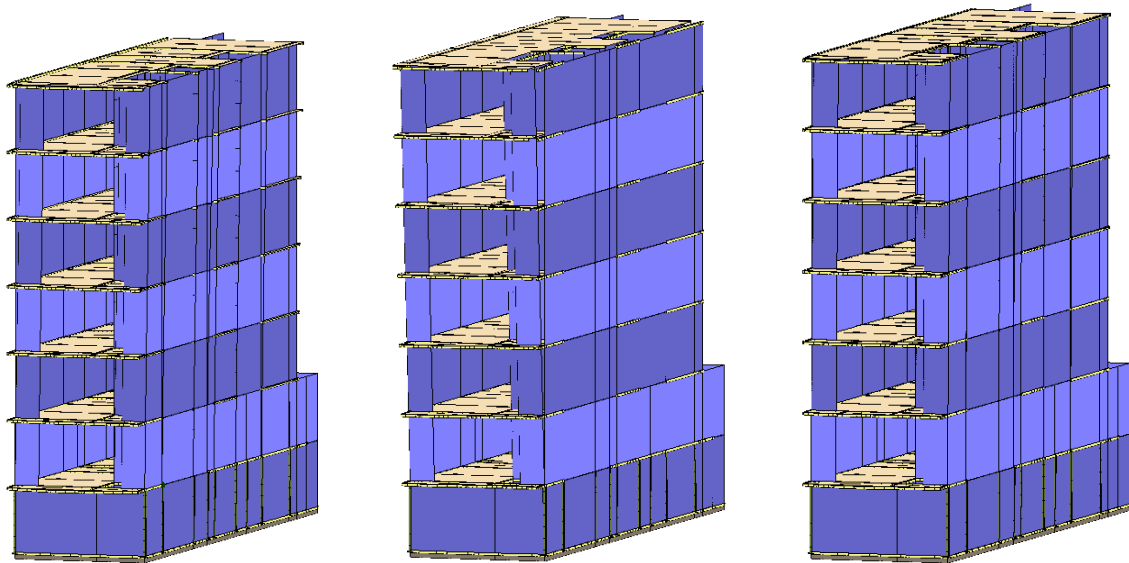
**50% of  $K_m$  Sway Stiffness in RC Frames**

Load Case: (left) Pushover – X Acc, (middle) Pushover – X Acc + e, (right) Pushover – Ex + 0.3Ey Acc

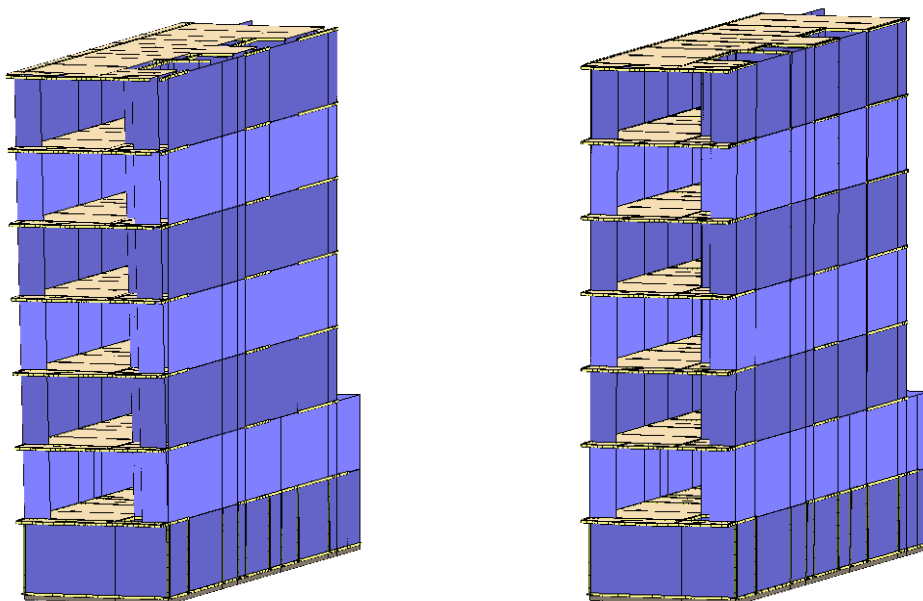


**35% of  $K_m$  Sway Stiffness in Steel Frames**

Load Case: (left) Pushover +X Acc, (middle) Pushover - X Acc, (right) Pushover +X Acc+ e



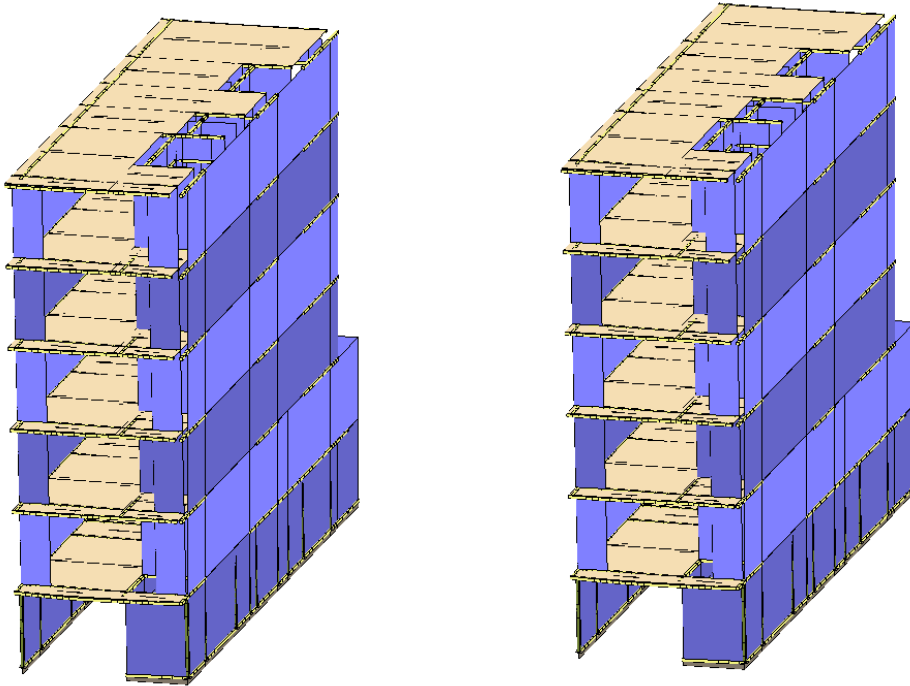
Load Case: (left) Pushover - X Acc + e, (right) Pushover  $E_x + 0.3E_y$  Acc





**50% of  $K_m$  Sway Stiffness in Steel Frames**

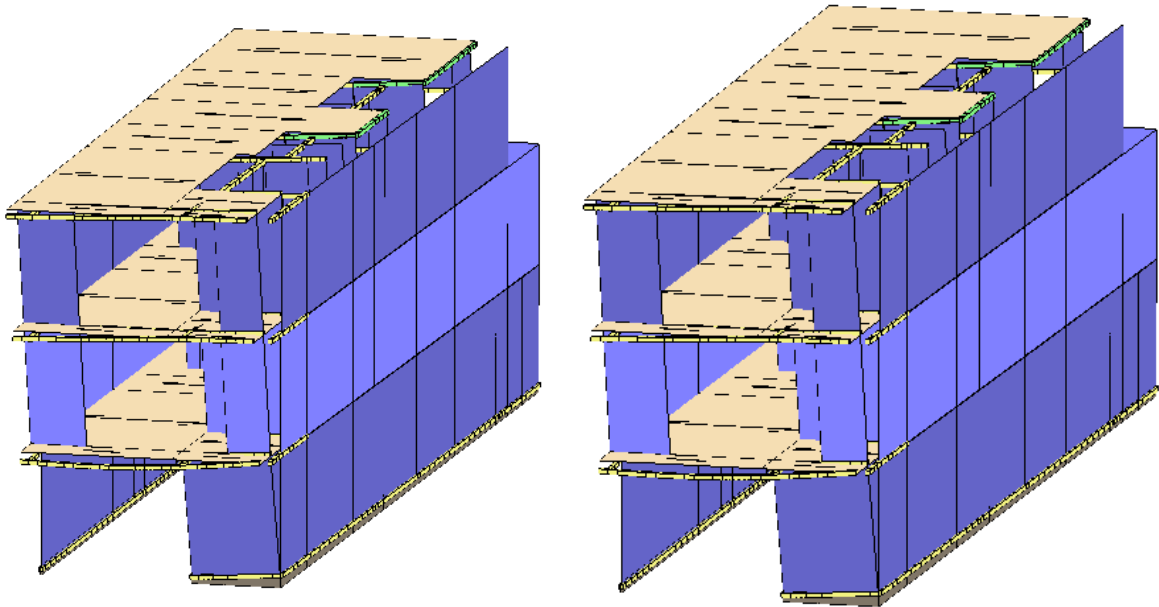
Load Case: (left) Pushover – X Acc, (right) Pushover –  $E_x + 0.3E_y$  Acc



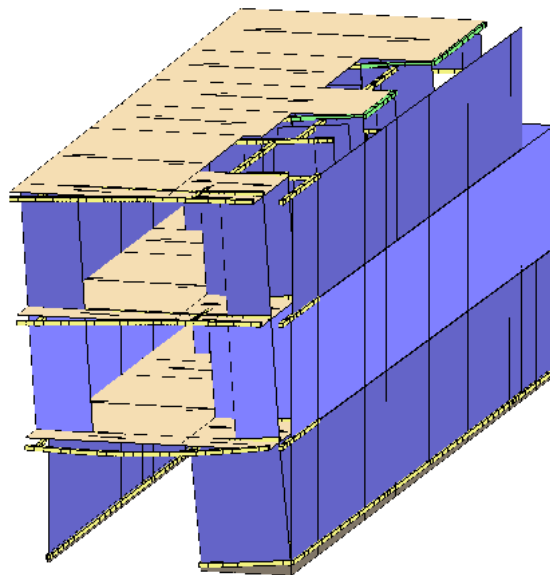
## Appendix C.2 Single Unit, Ground Type B

### No Retrofitting

Load Case: (left) Pushover – X Acc, (right) Pushover – X Acc + e

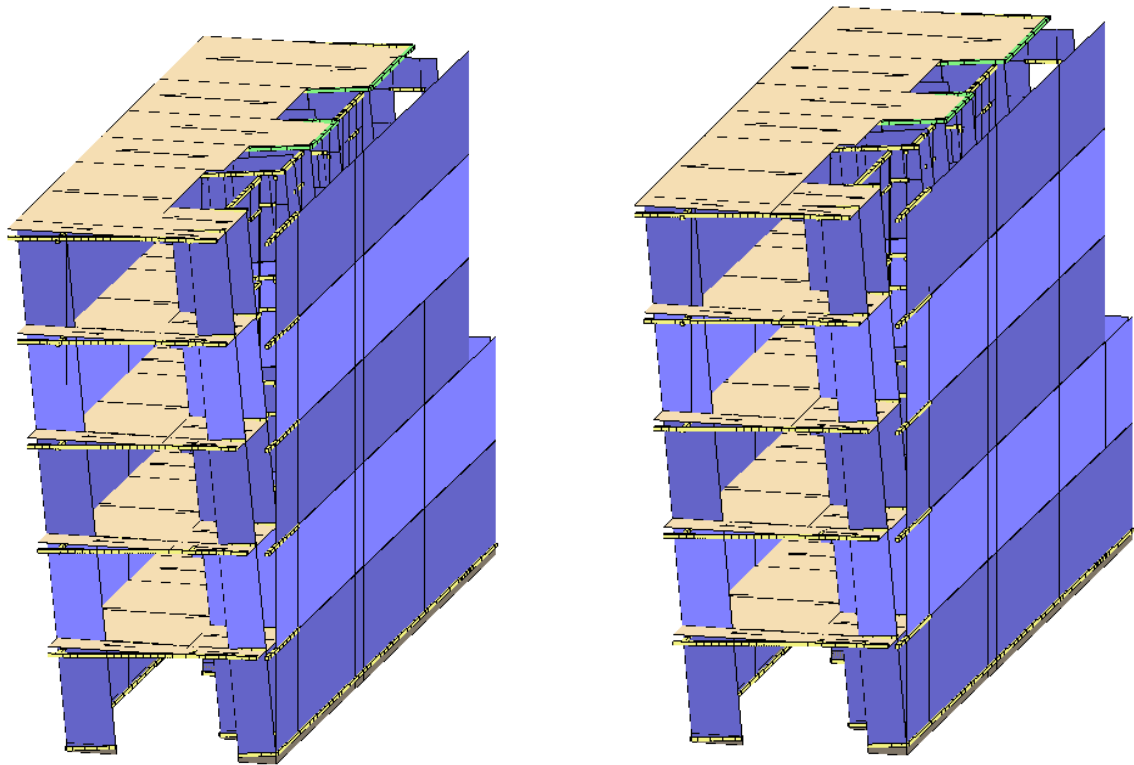


Load Case: Pushover -Ex + 0.3Ey Acc

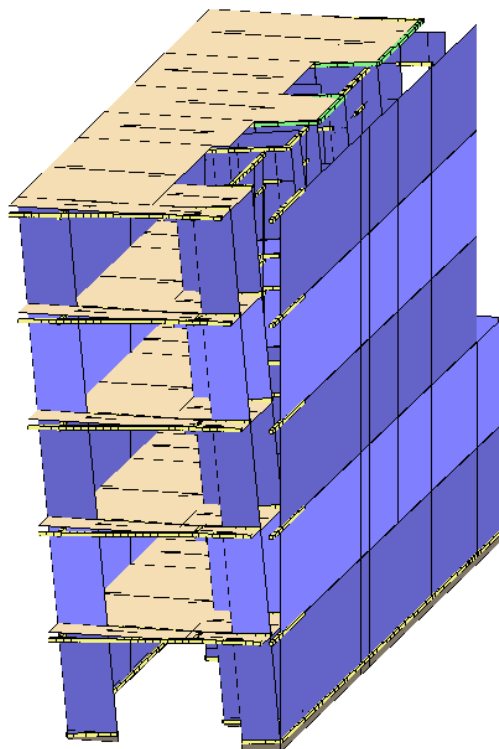


**Repeated Ground Floor**

Load Case: (left) Pushover – X Acc, (right) Pushover - X Acc+ e

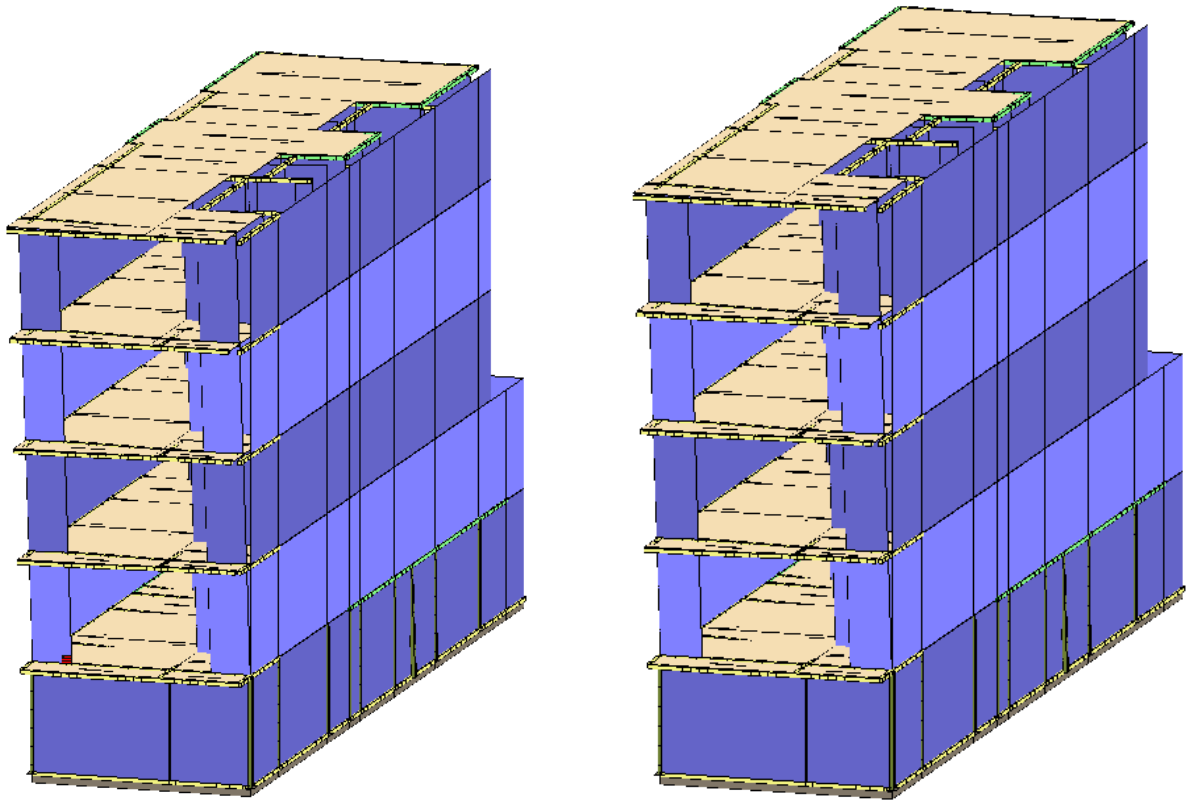


Load Case: Pushover -Ex + 0.3Ey Acc

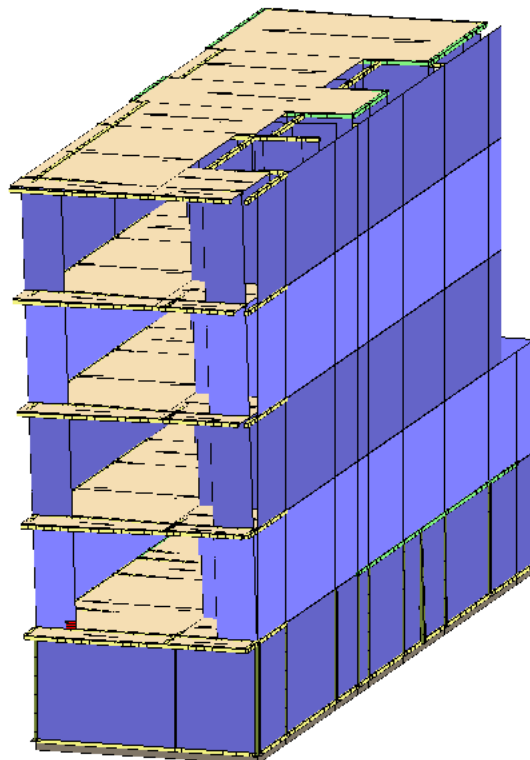


**35% of  $K_m$  Sway Stiffness in RC Frames**

Load Case: (left) Pushover – X Acc, (right) Pushover – X Acc + e

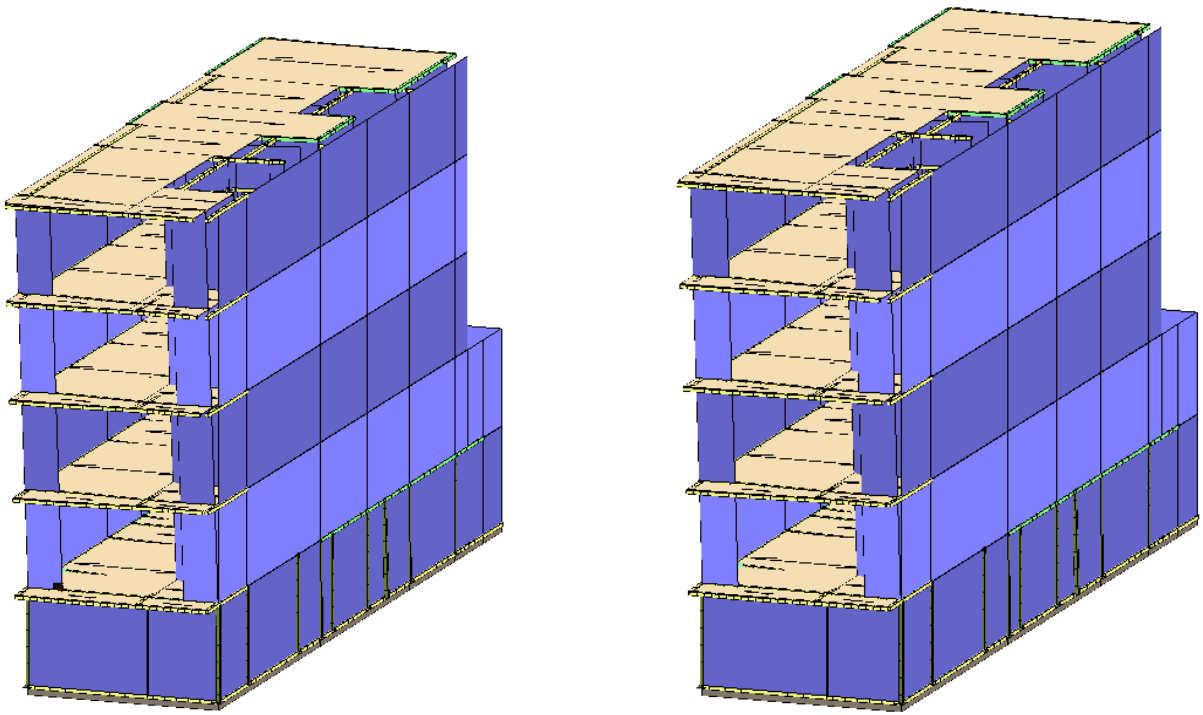


Load Case: Pushover -Ex + 0.3Ey Acc

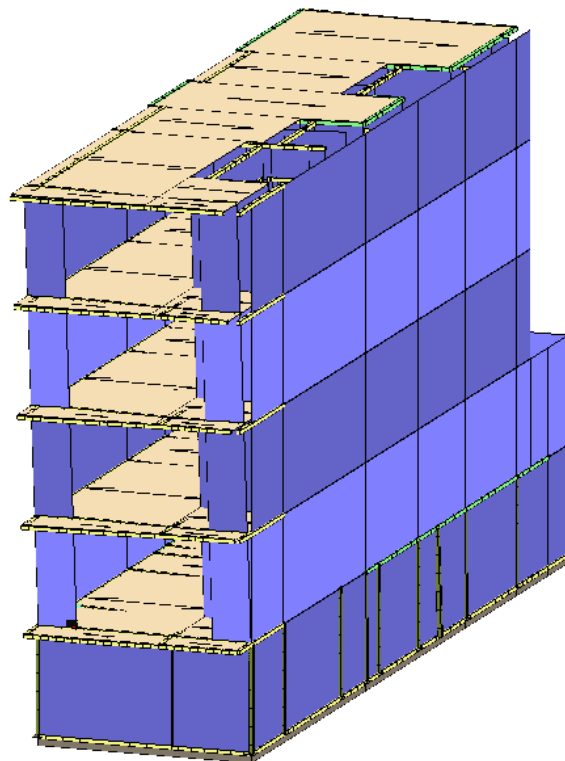


**50% of  $K_m$  Sway Stiffness in RC Frames**

Load Case: (left) Pushover – X Acc, (right) Pushover – X Acc + e

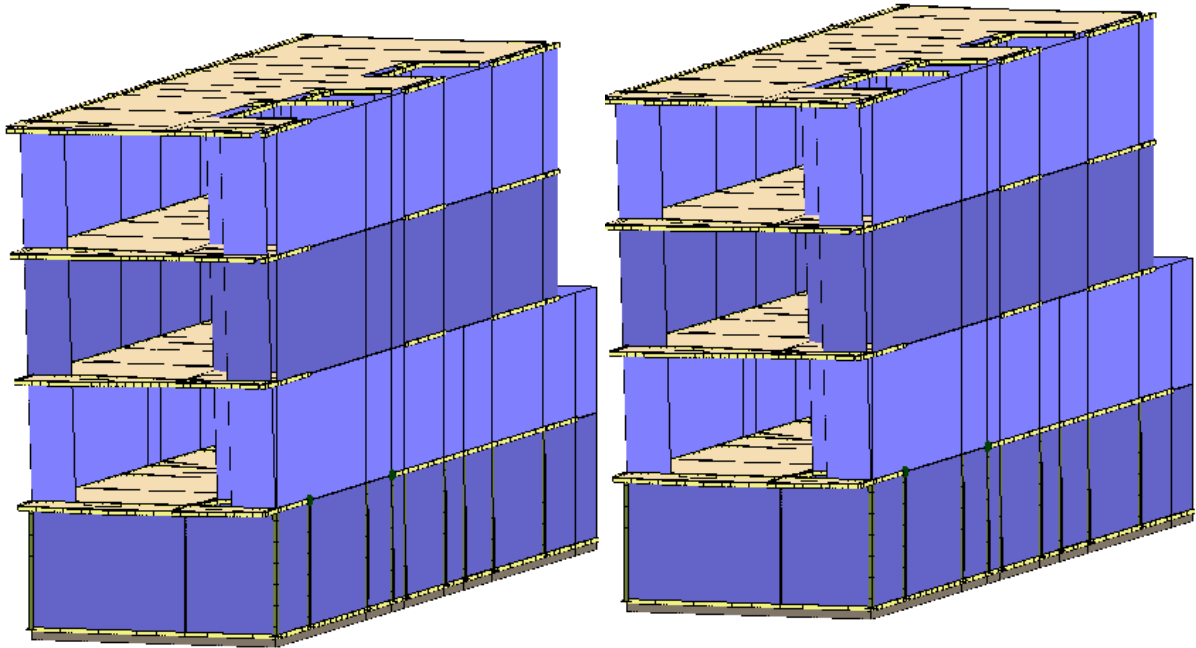


Load Case: Pushover -Ex + 0.3Ey Acc

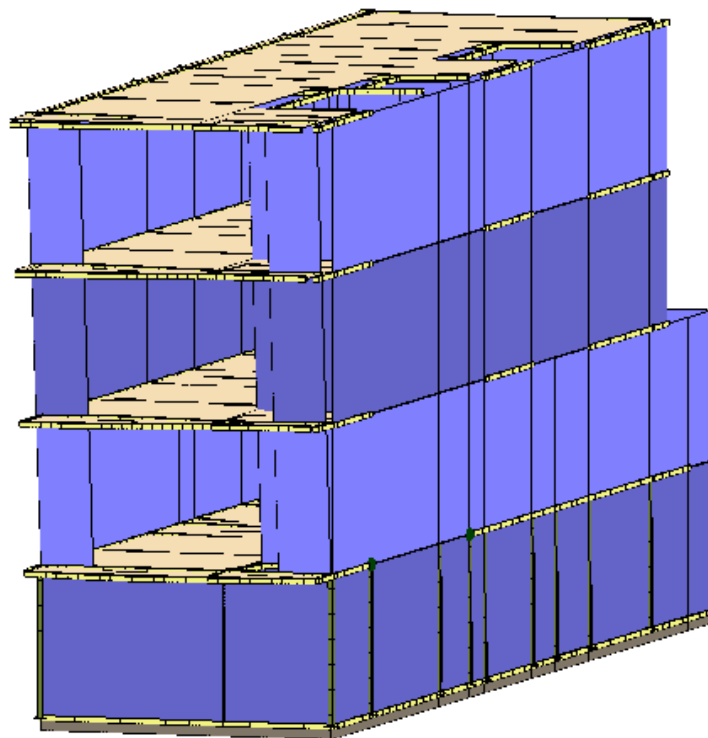


**35% of  $K_m$  Sway Stiffness in Steel Frames**

Load Case: (left) Pushover - X Acc, (right) Pushover -Ex + 0.3Ey Acc

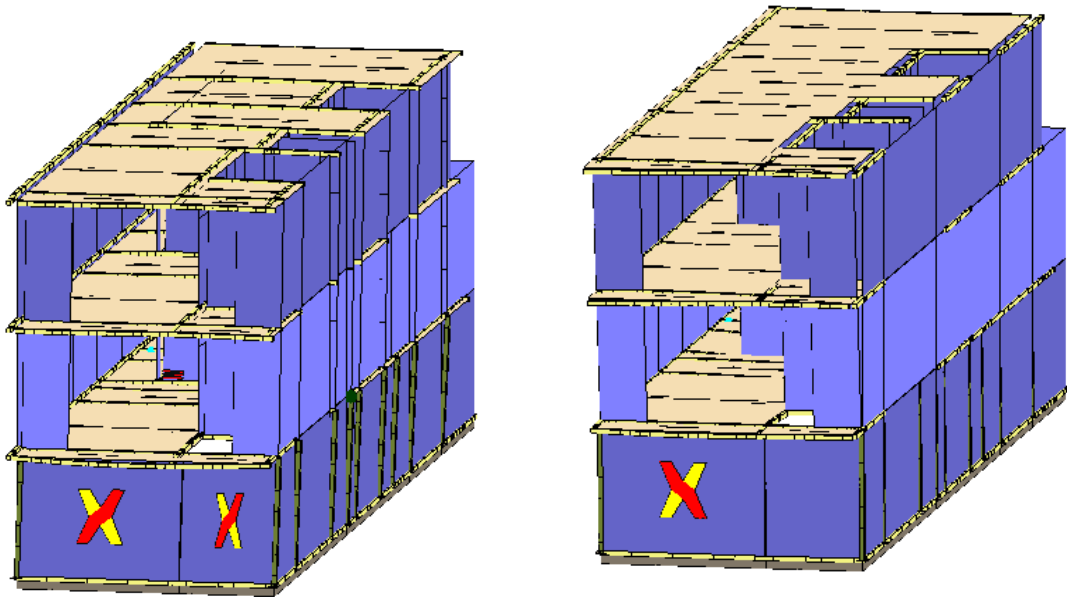


Load Case: Pushover -Ex +0.3Ey Acc

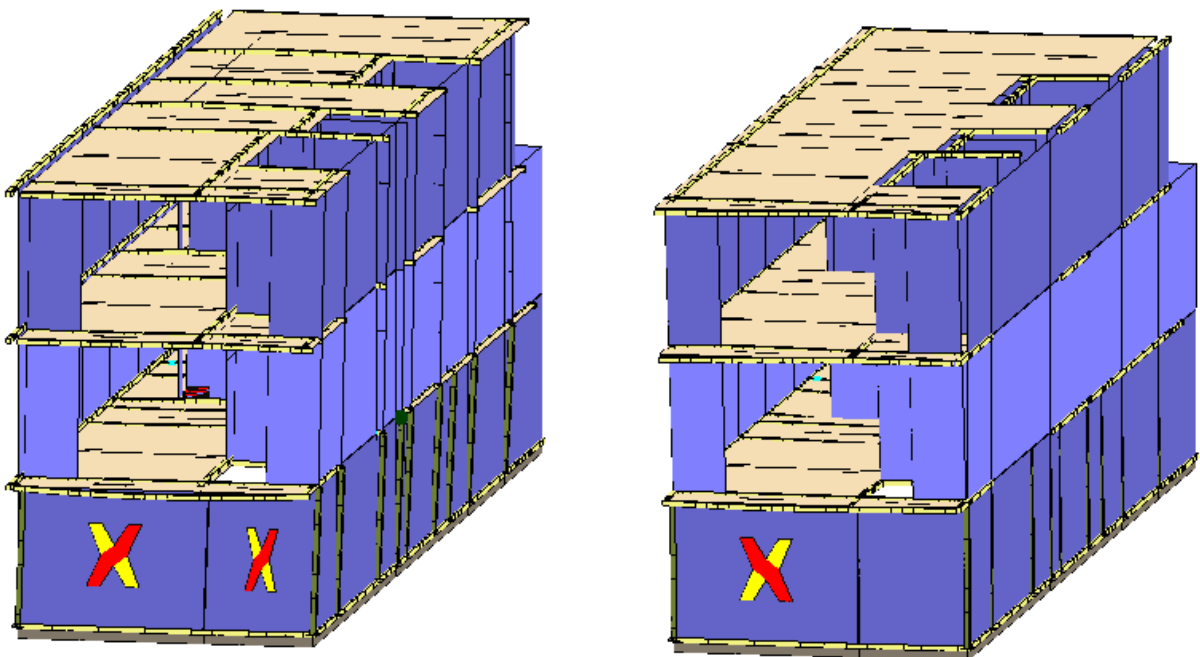


**50% of  $K_m$  Sway Stiffness in Steel Frames**

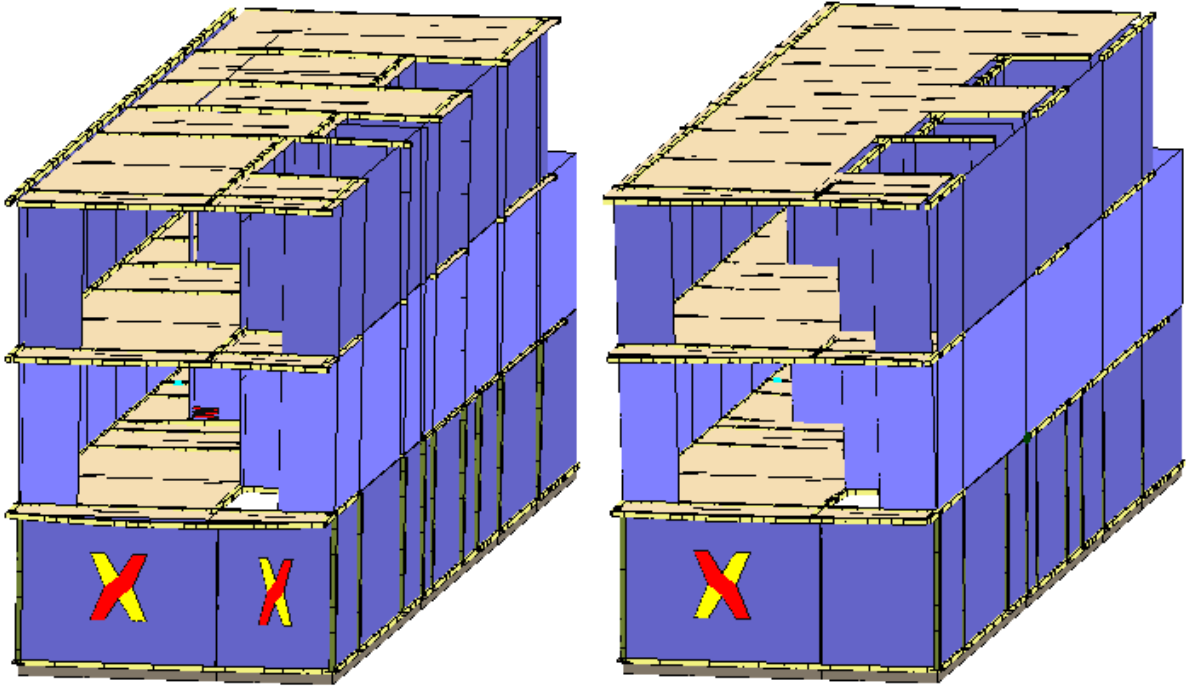
Load Case: (left) Pushover + X Acc, (right) Pushover - X Acc



Load Case: (left) Pushover + X Acc + e, (right) Pushover + X Acc + e



Load Case: (left) Pushover  $E_x + 0.3E_y$  Acc, (right) Pushover  $-E_x + 0.3E_y$  Acc

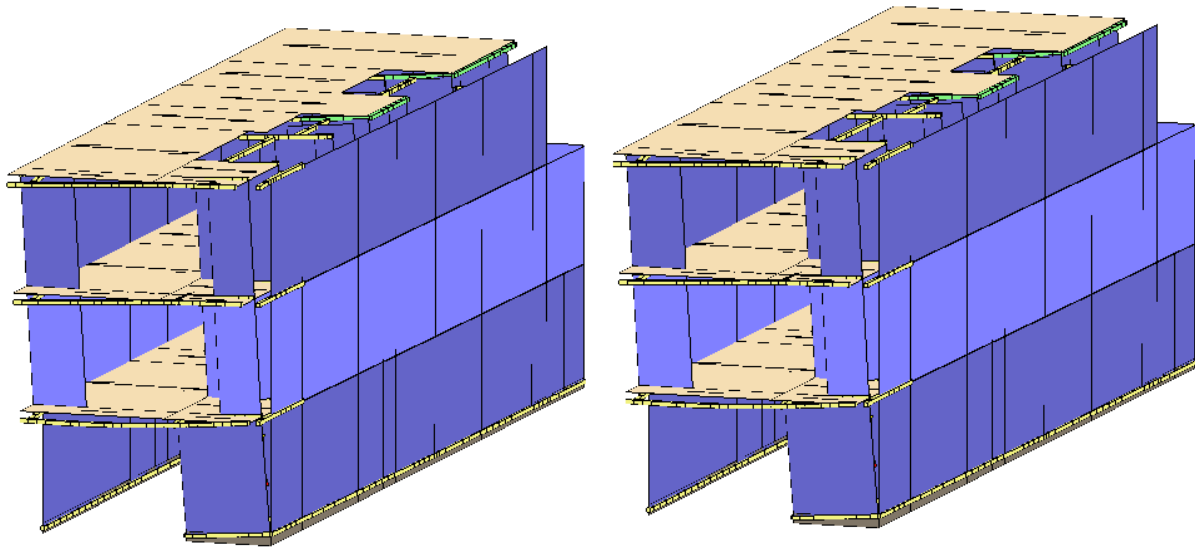




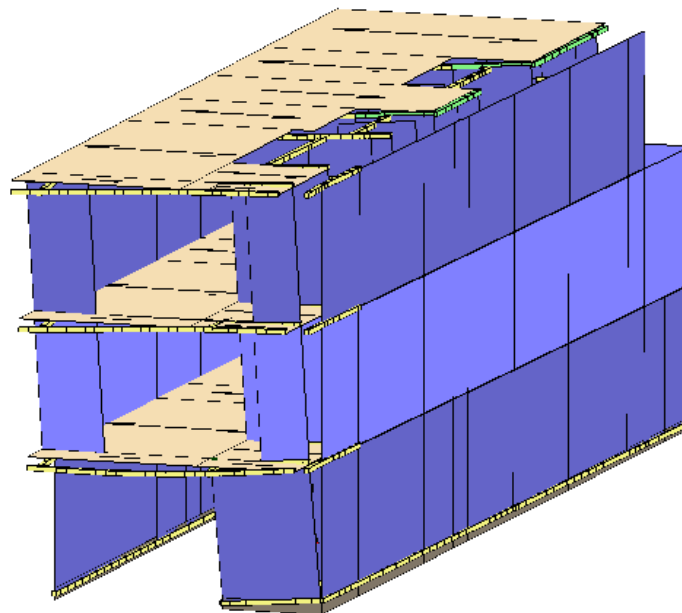
### Appendix C.3 Single Unit, Ground Type C

#### No Retrofitting

Load Case: (left) Pushover – X Acc, (right) Pushover – X Acc + e

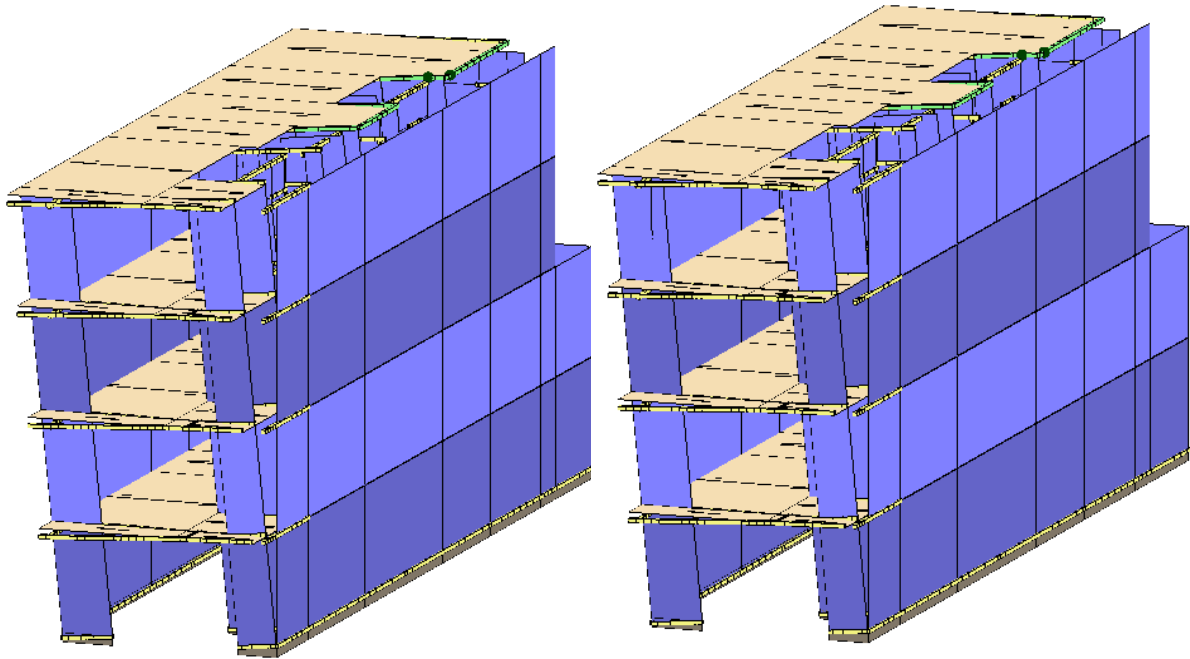


Load Case: Pushover –  $E_x + 0.3 E_y$  Acc

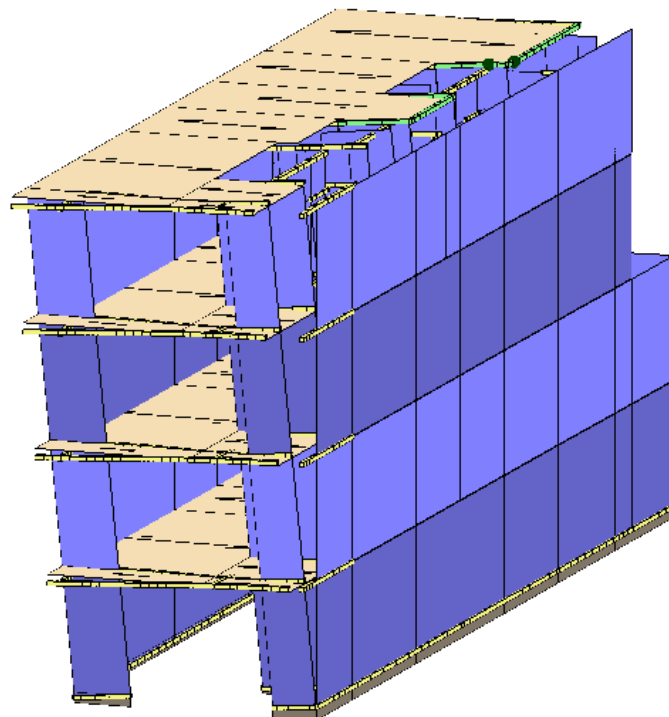


**Repeated Ground Floor**

Load Case: (left) Pushover – X Acc, (right) Pushover – X Acc + e

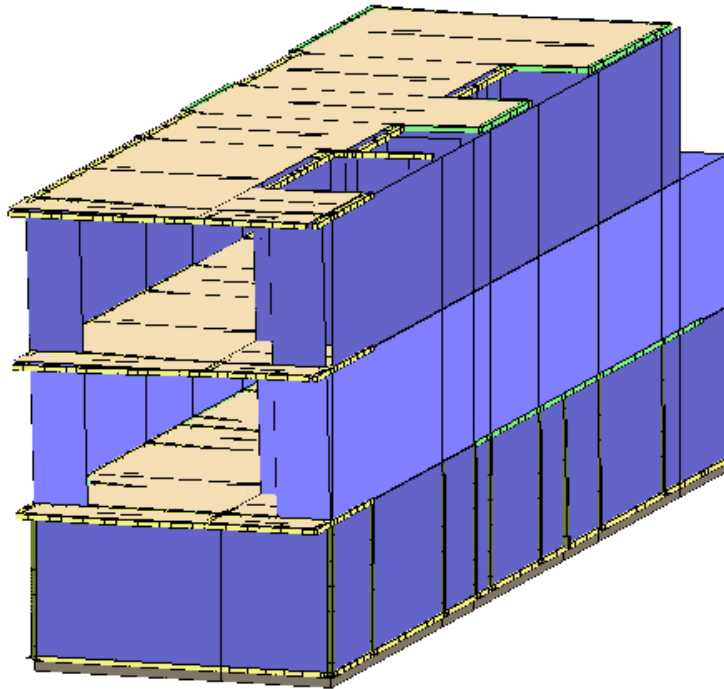


Load Case: Pushover -Ex + 0.3Ey Acc



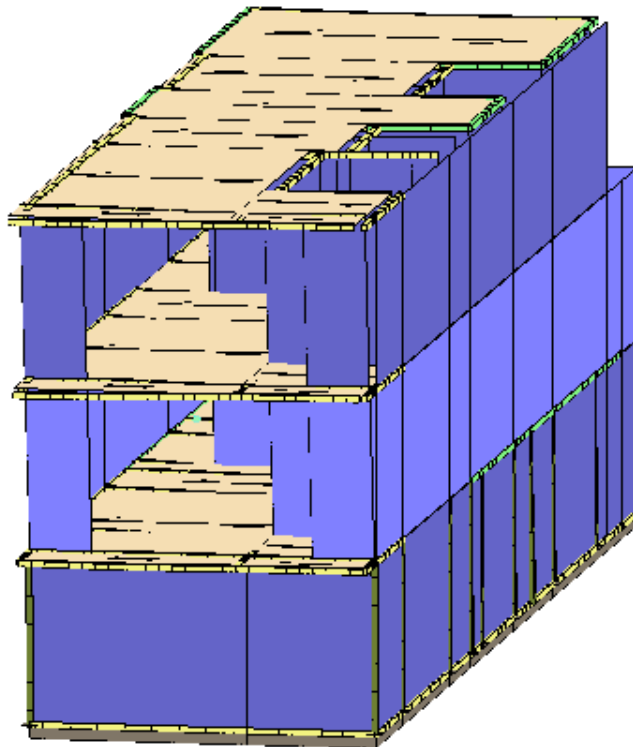
**35% of  $K_m$  Sway Stiffness in RC Frames**

Load Case: Pushover –  $E_x + 0.3E_y$  Acc



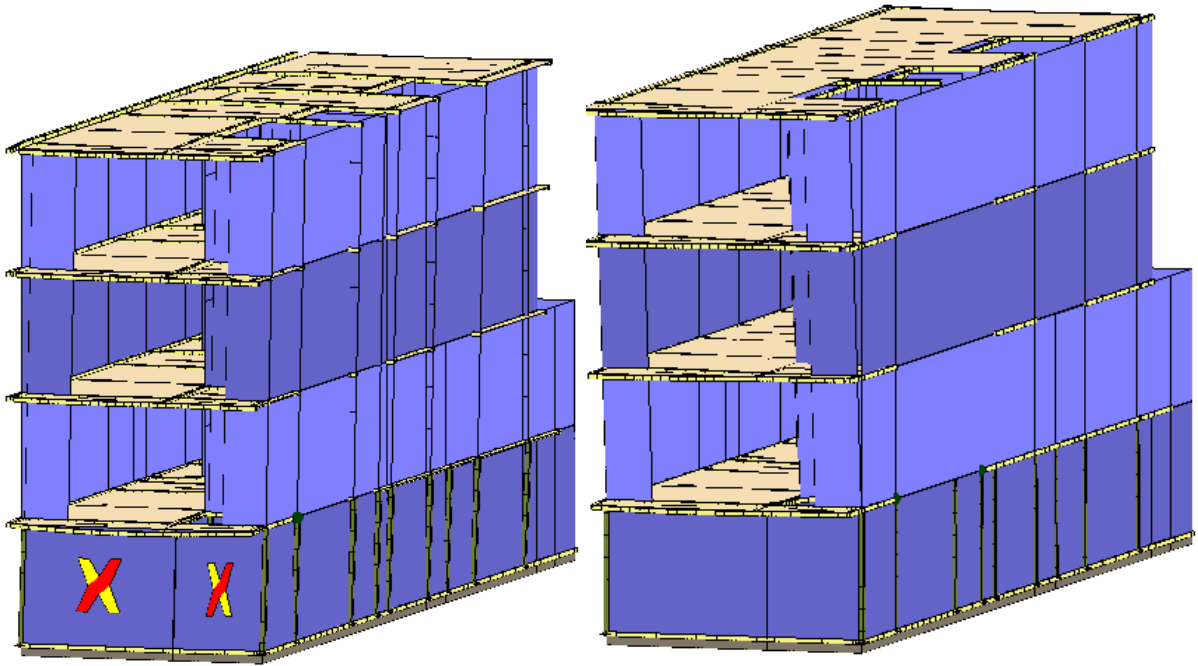
**50% of  $K_m$  Sway Stiffness in RC Frames**

Load Case: Pushover -  $E_x + 0.3E_y$  Acc

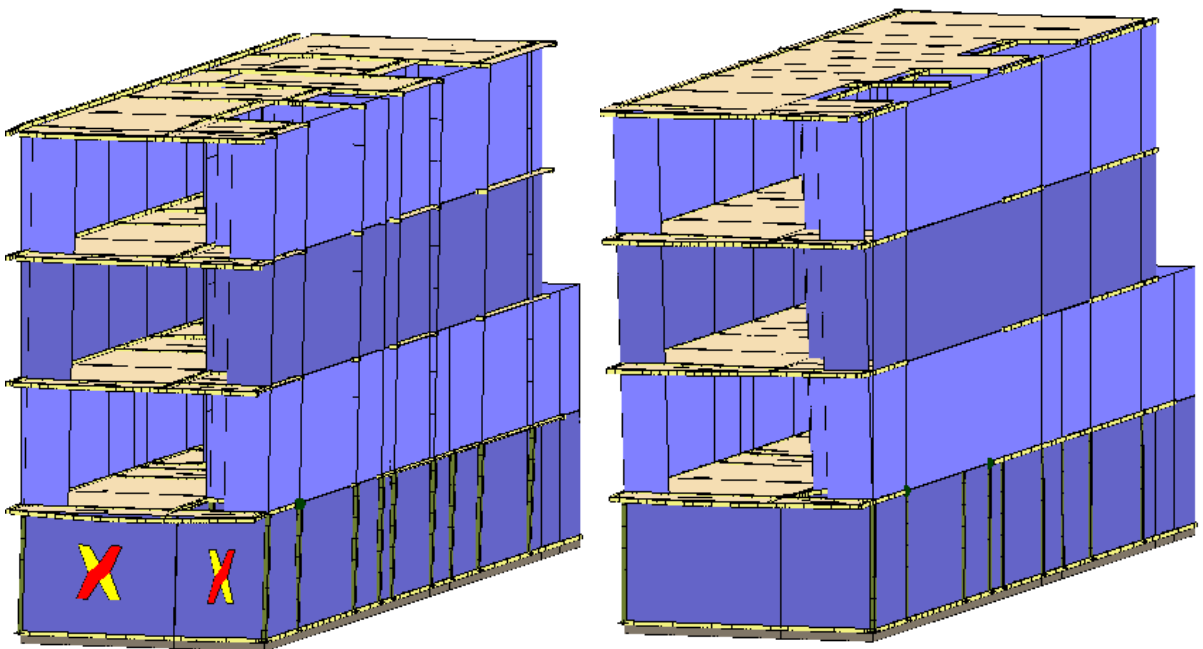


**35% of  $K_m$  Sway Stiffness in Steel Frames**

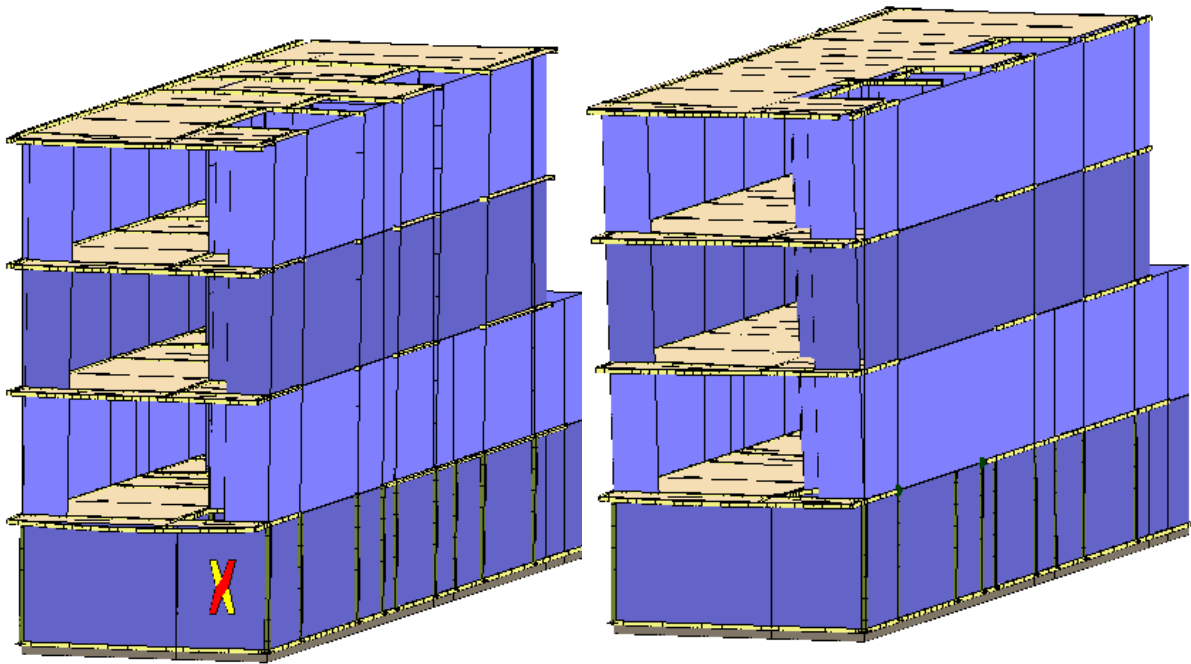
Load Case: (left) Pushover + X Acc, (right) Pushover - X Acc



Load Case: (left) Pushover + X Acc + e, (right) Pushover - X Acc + e

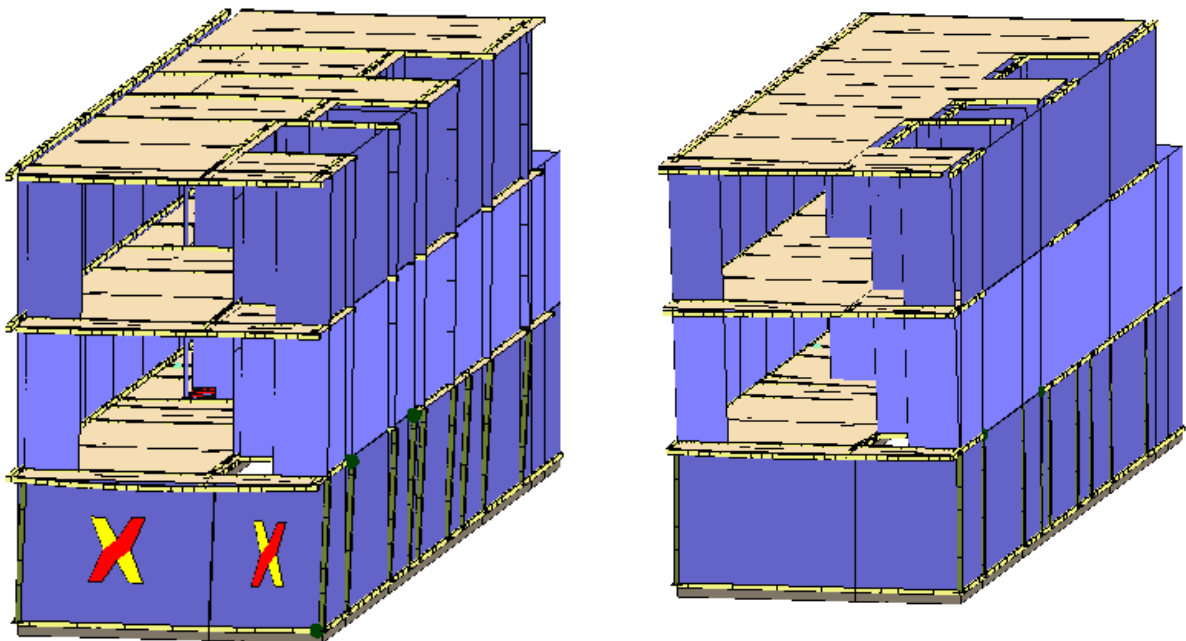


Load Case: (left) Pushover  $E_x + 0.3E_y$  Acc, (right) Pushover  $-E_x + 0.3 E_y$  Acc

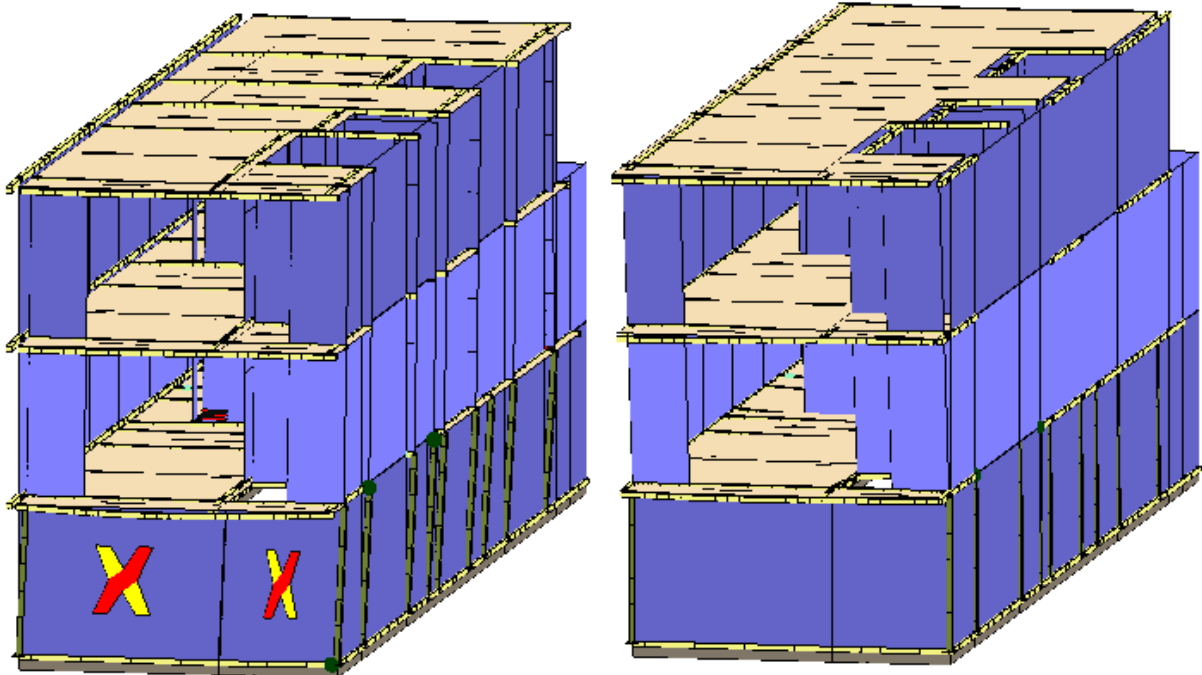


**50% of  $K_m$  Sway Stiffness in Steel Frames**

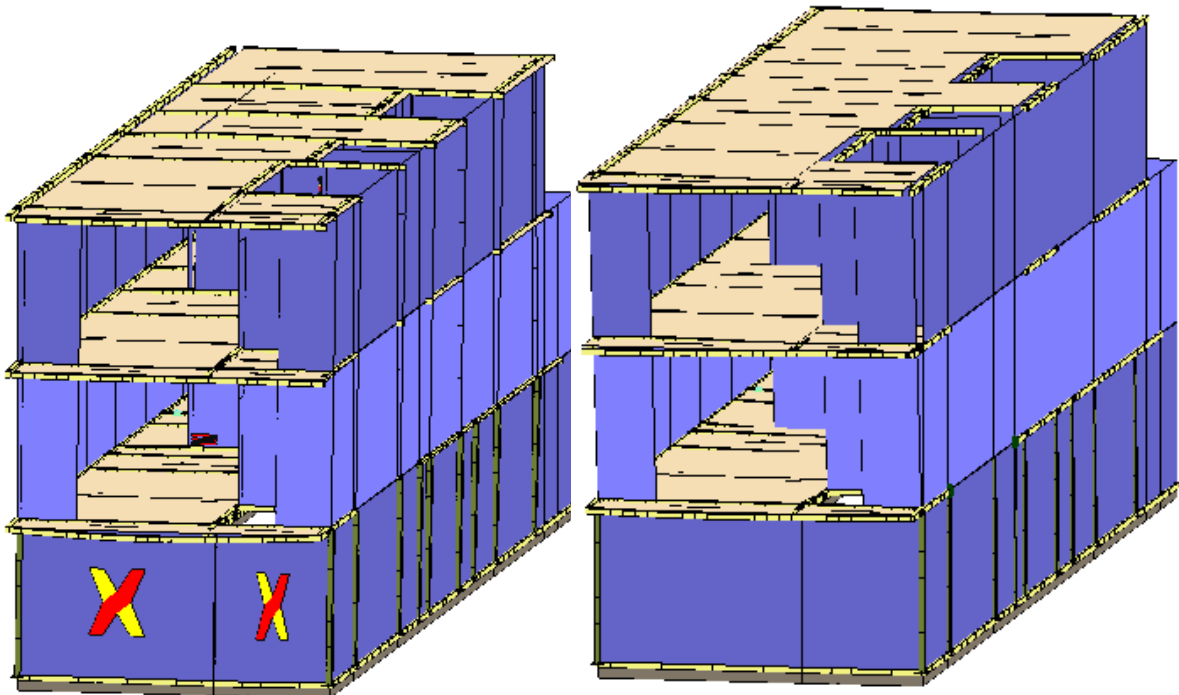
Load Case: (left) Pushover  $+ X$  Acc, (right) Pushover  $- X$  Acc



Load Case: (left) Pushover + X Acc + e, (right) Pushover - X Acc + e



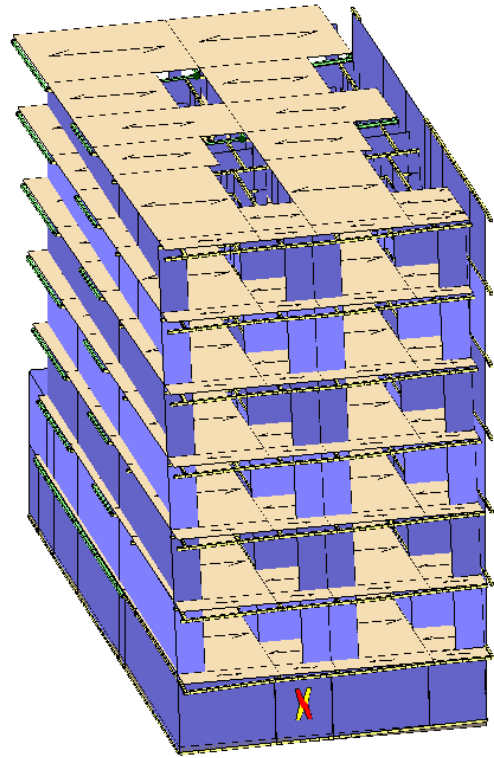
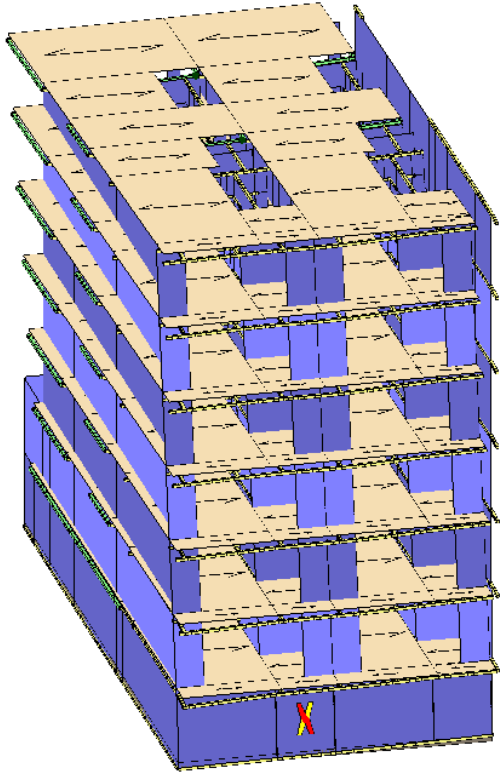
Load Case: (left) Pushover  $E_x + 0.3E_y$  Acc, (right) Pushover -  $E_x + 0.3E_y$  Acc



## Appendix C.4 Two-Unit Aggregate, Type A

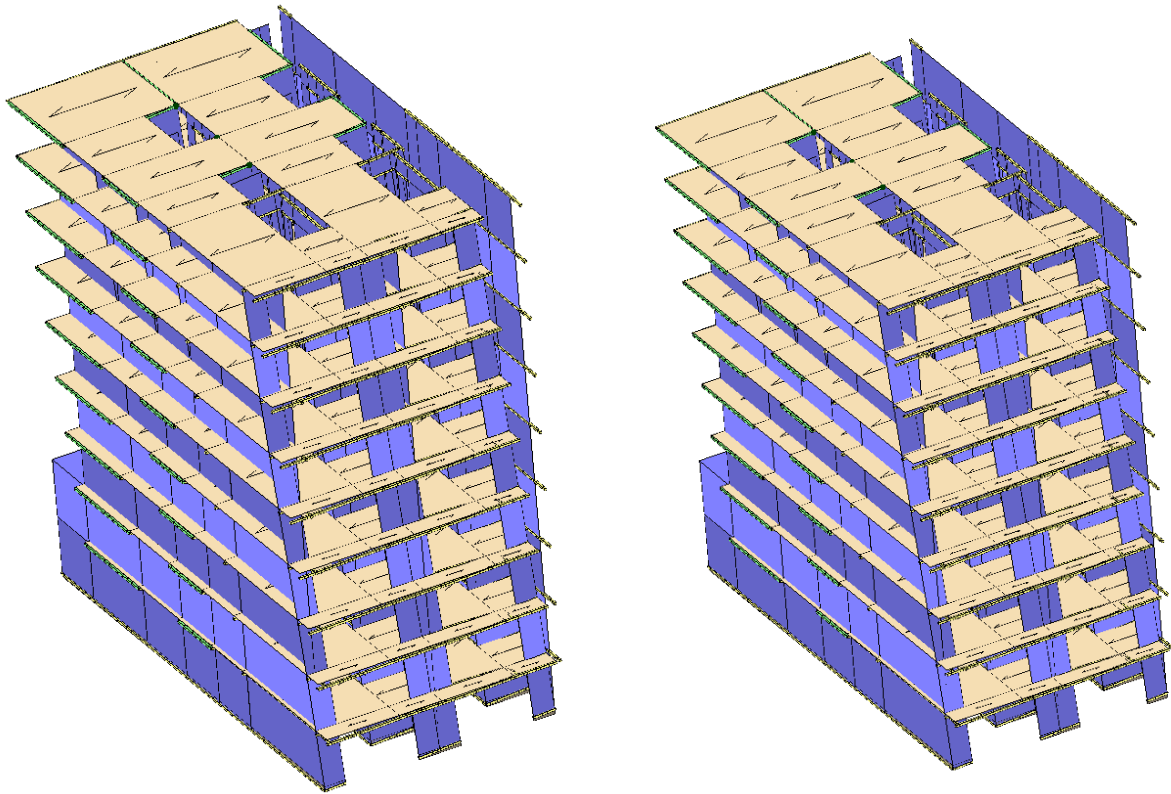
### No Retrofitting

Load Case: (left) Pushover – X Acc, (right) Pushover – X Acc + e



**Repeated Ground Floor**

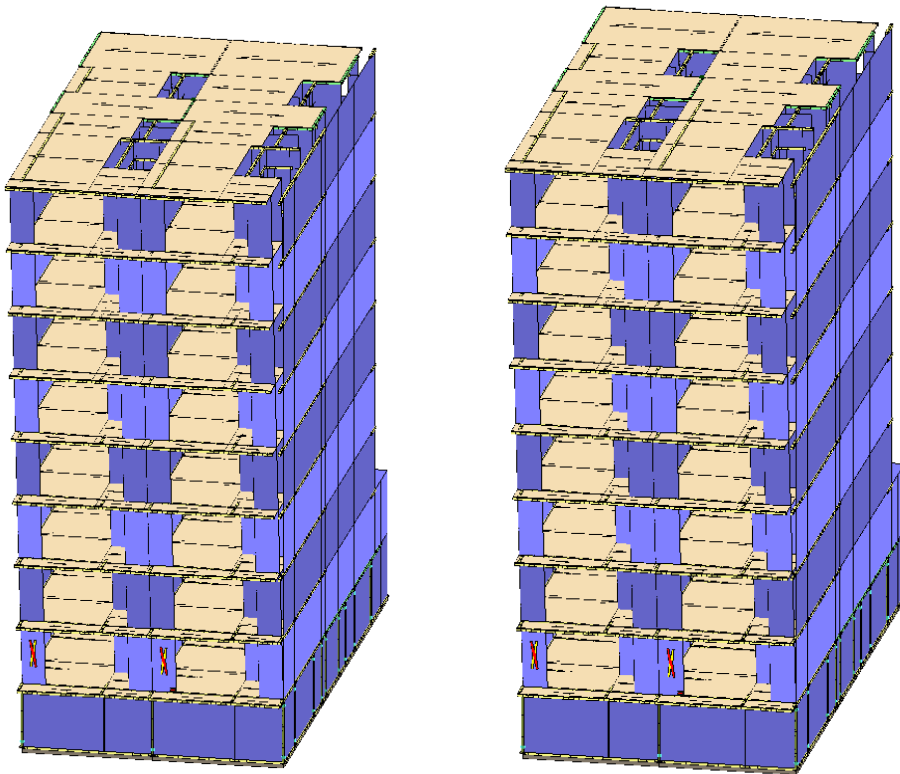
Load Case: (left) Pushover – X Acc, (right) Pushover + X Acc + e



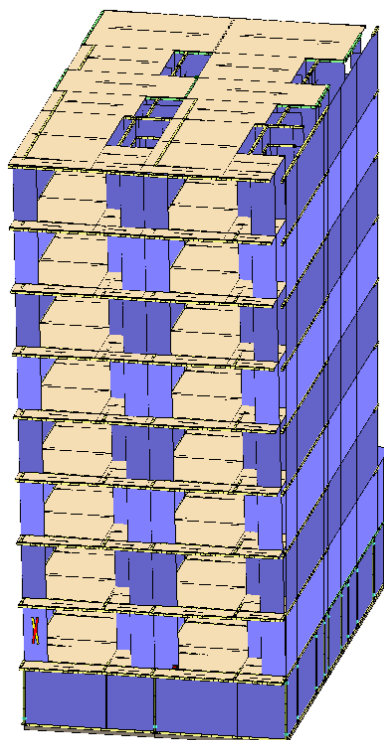


**35% of  $K_m$  Sway Stiffness in RC Frames**

Load Case: (left) Pushover – X Acc, (right) Pushover + X Acc + e

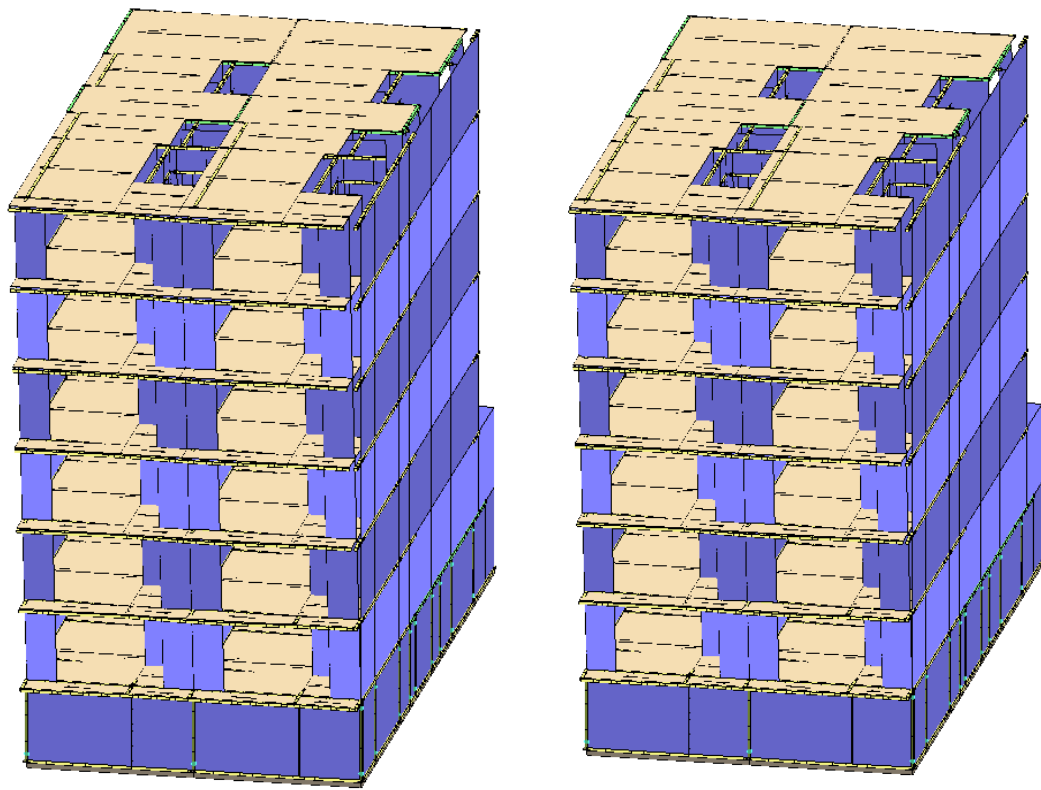


Load Case: Pushover –  $E_x + 0.3E_y$  Acc

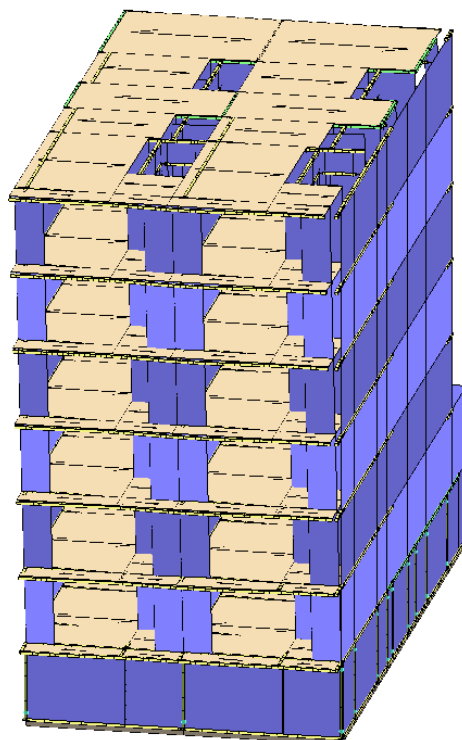


**50% of  $K_m$  Sway Stiffness in RC Frames**

Load Case: (left) Pushover – X Acc, (right) Pushover – X Acc + e

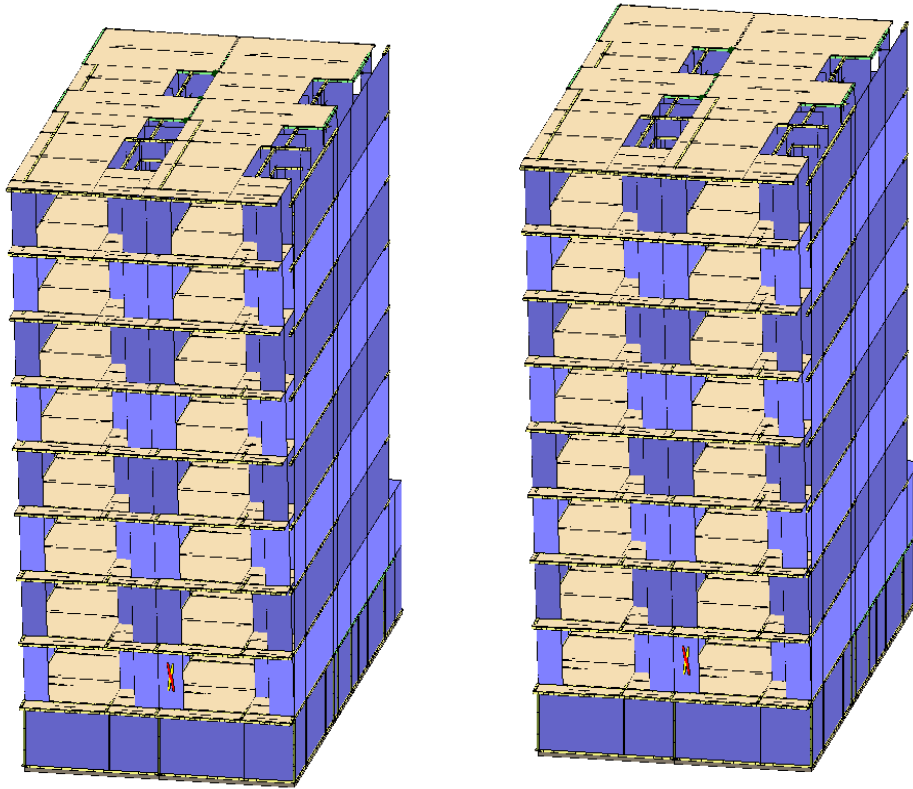


Load Case: Pushover -Ex + 0.3Ey Acc



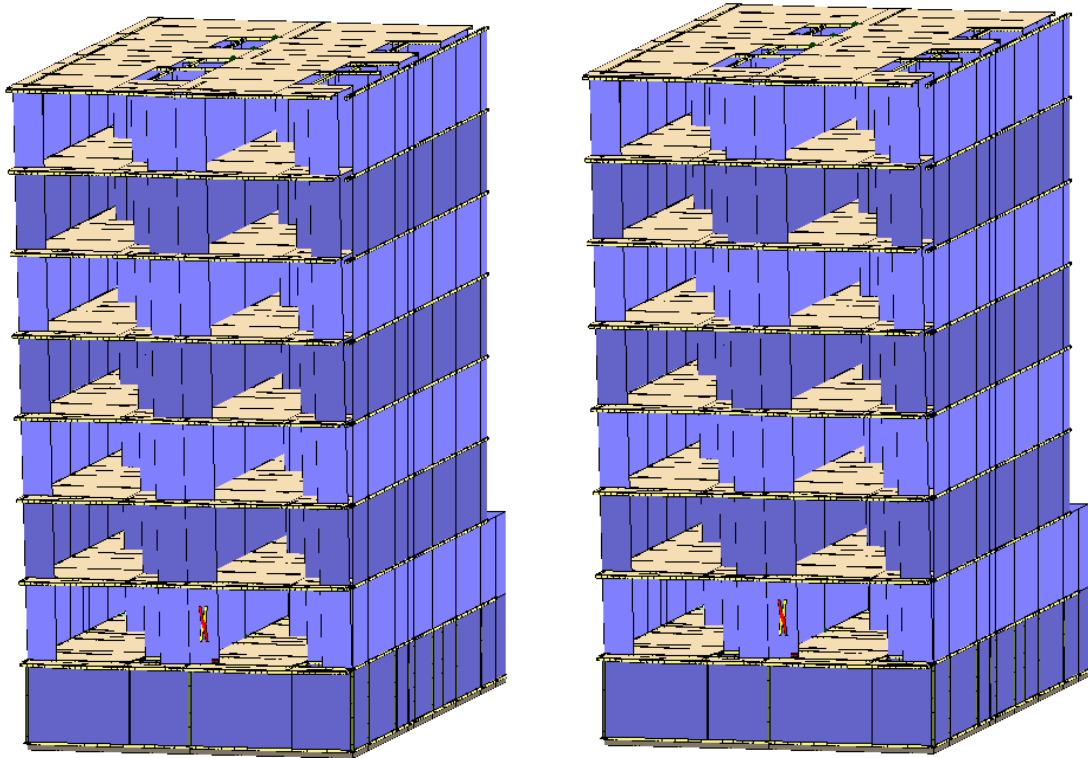
**35% of  $K_m$  Sway Stiffness in Steel Frames**

Load Case: (left) Pushover – X Acc, (right) Pushover – X Acc + e



**50% of  $K_m$  Sway Stiffness in Steel Frames**

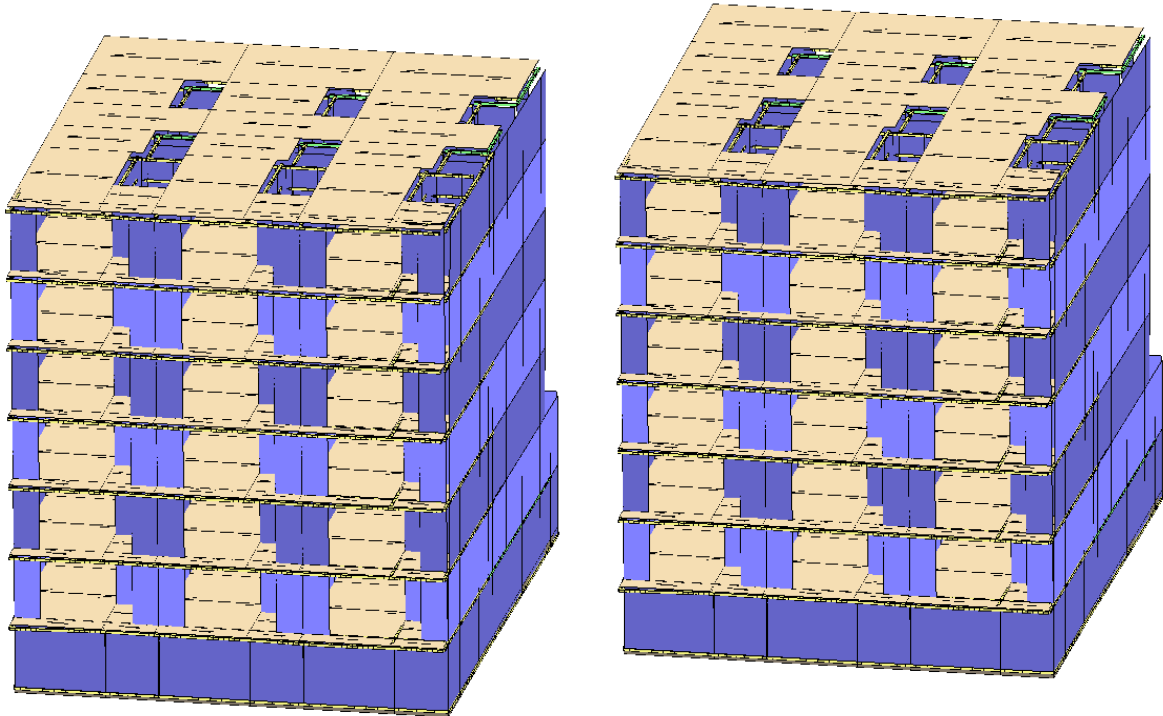
Load Case: (left) Pushover – X Acc, (right) Pushover – X Acc + e



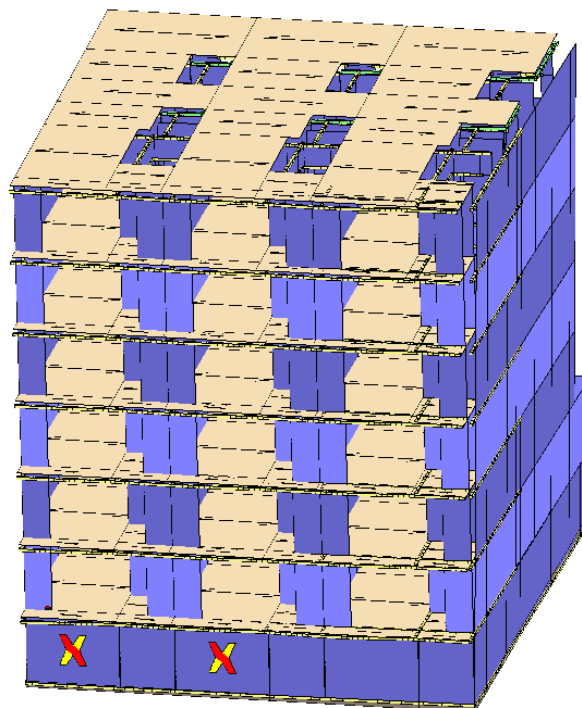
## Appendix C.5 Three-Unit Aggregate, Type A

### No Retrofitting

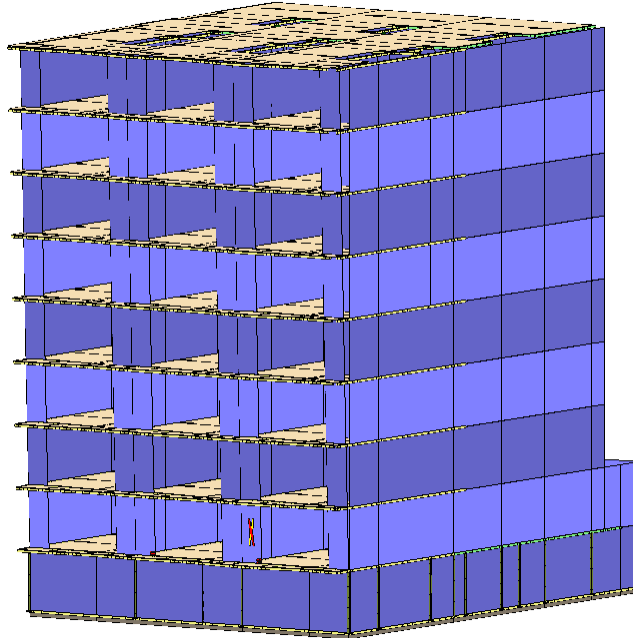
Load Case: (left) Pushover + Y Acc, (right) Pushover + Y Acc + e



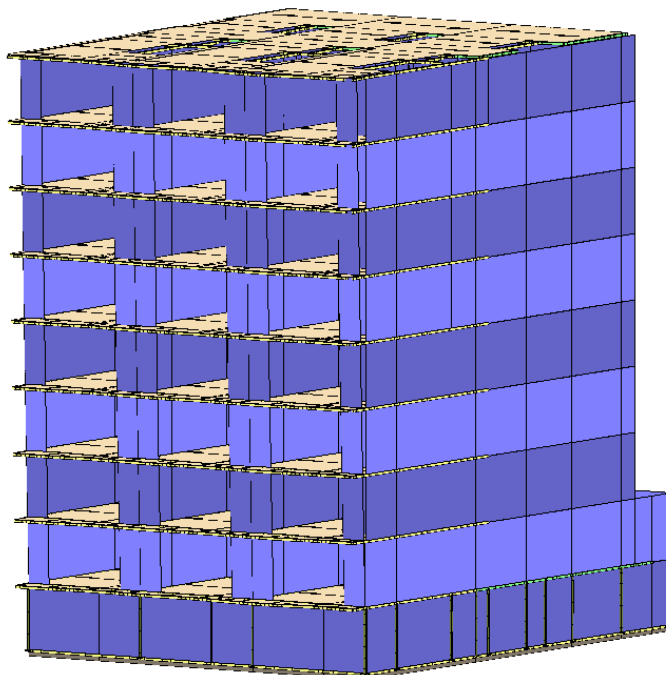
Load Case: Pushover -0.3Ex + Ey Acc



**35% of  $K_m$  Sway Stiffness in RC Frames**  
Load Case: Pushover – X Acc

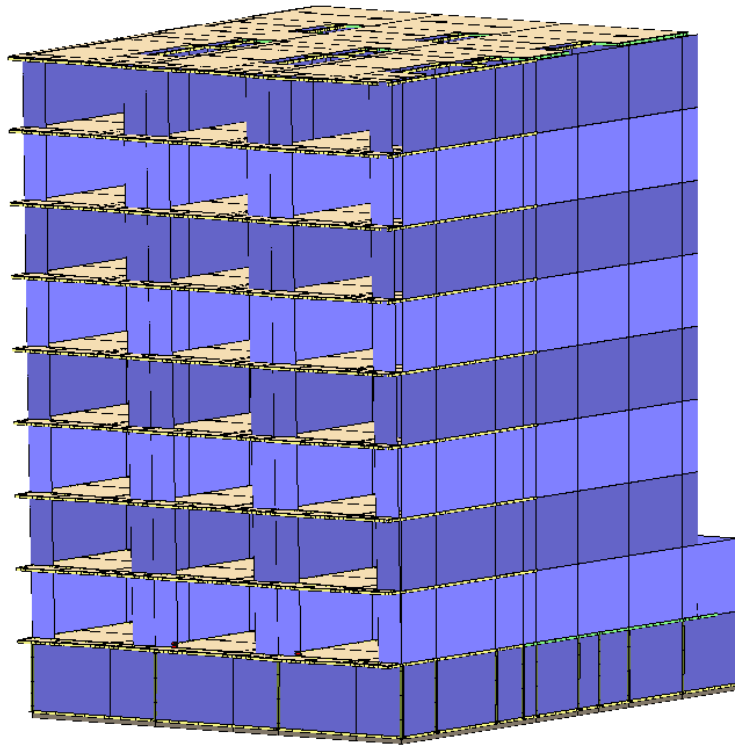


Load Case: Pushover –  $E_x + 0.3E_y$  Acc

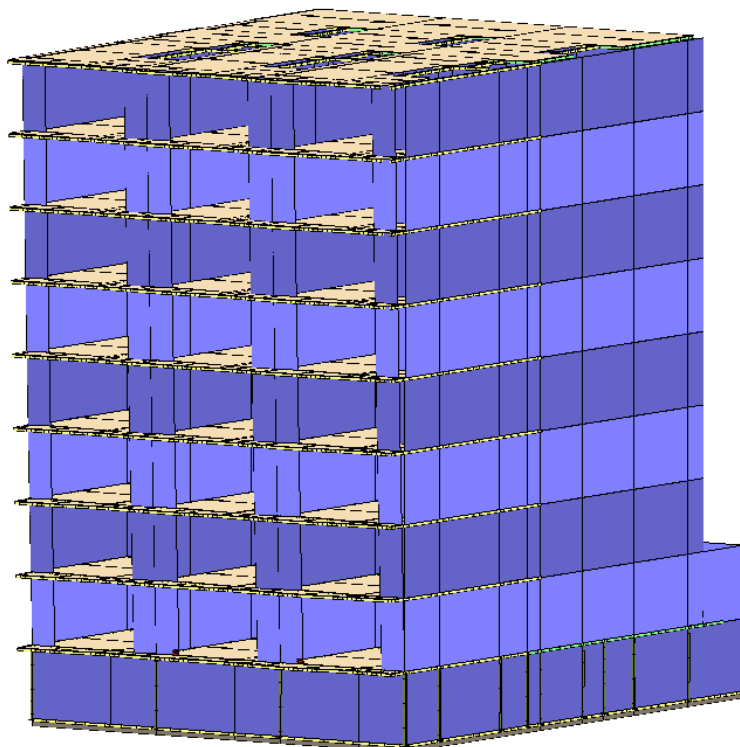


**50% of  $K_m$  Sway Stiffness in RC Frames**

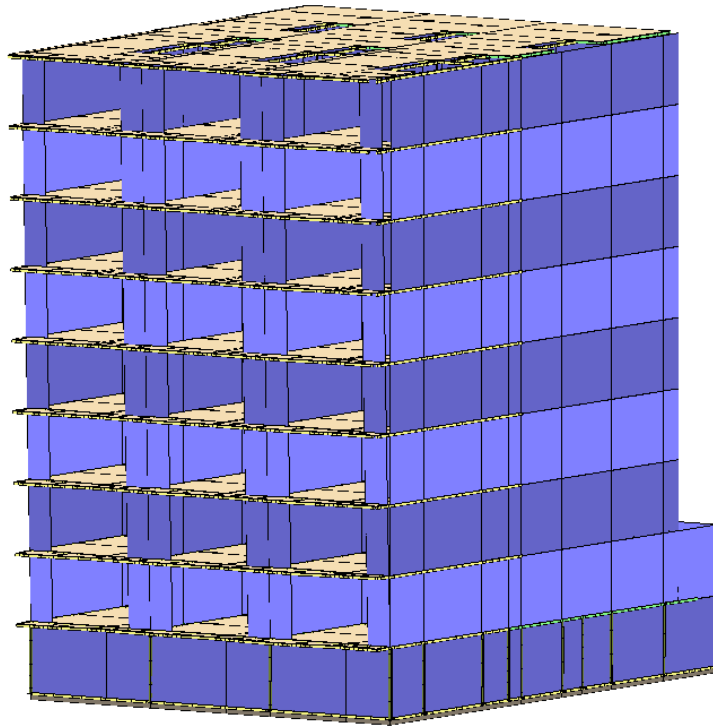
Load Case: Pushover – X Acc



Load Case: Pushover – X Acc + e



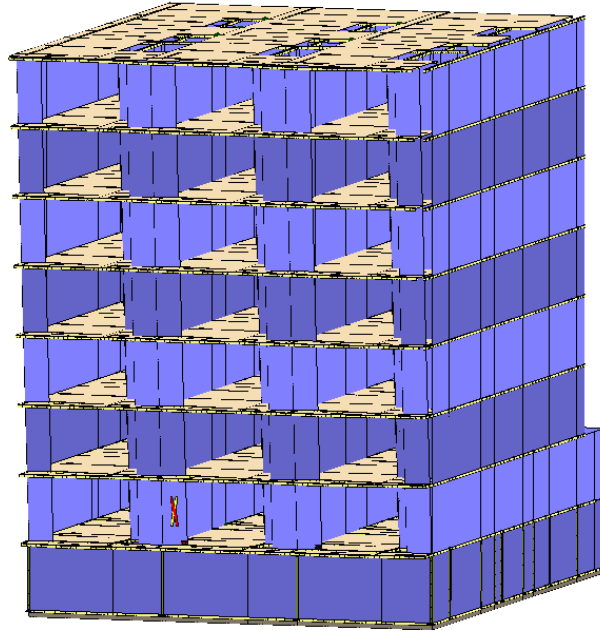
Load Case: Pushover – Ex + 0.3Ey Acc



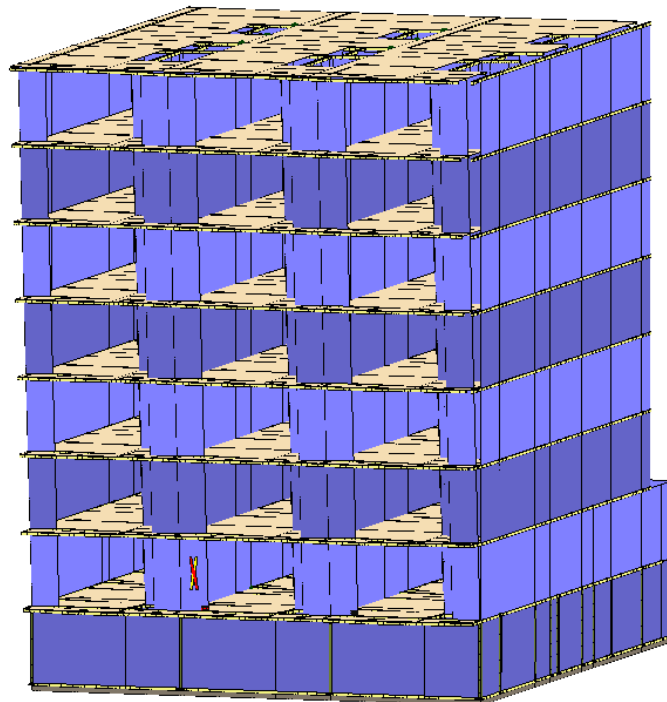


**35% of  $K_m$  Sway Stiffness in Steel Frames**

Load Case: Pushover – X Acc

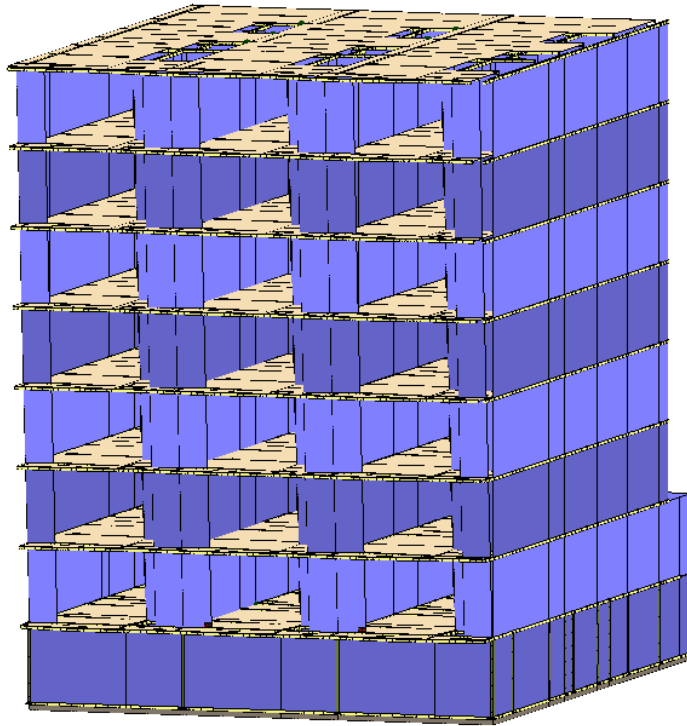


Load Case: Pushover – X Acc + e

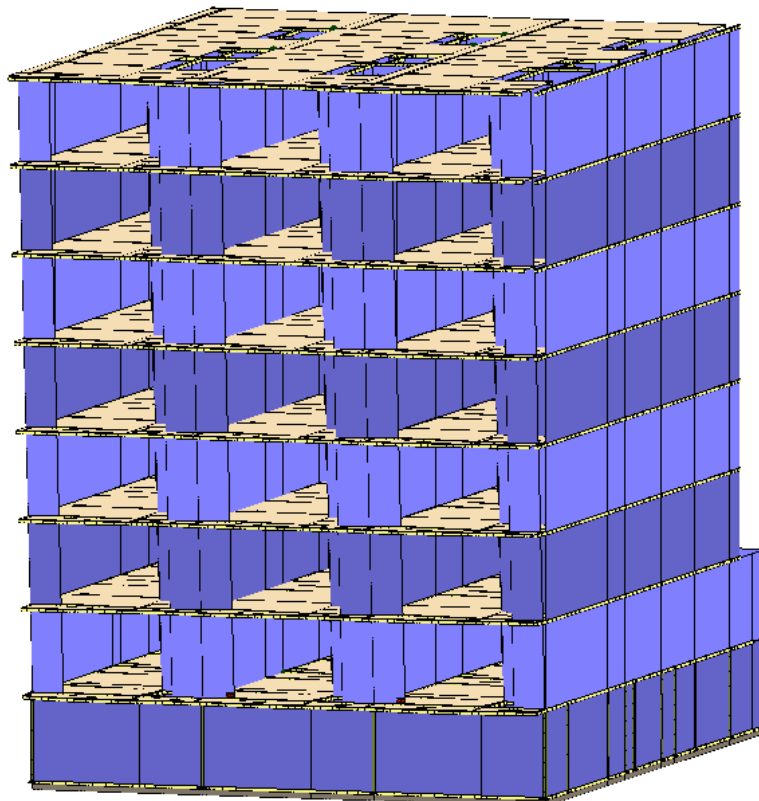


**50% of  $K_m$  Sway Stiffness in Steel Frames**

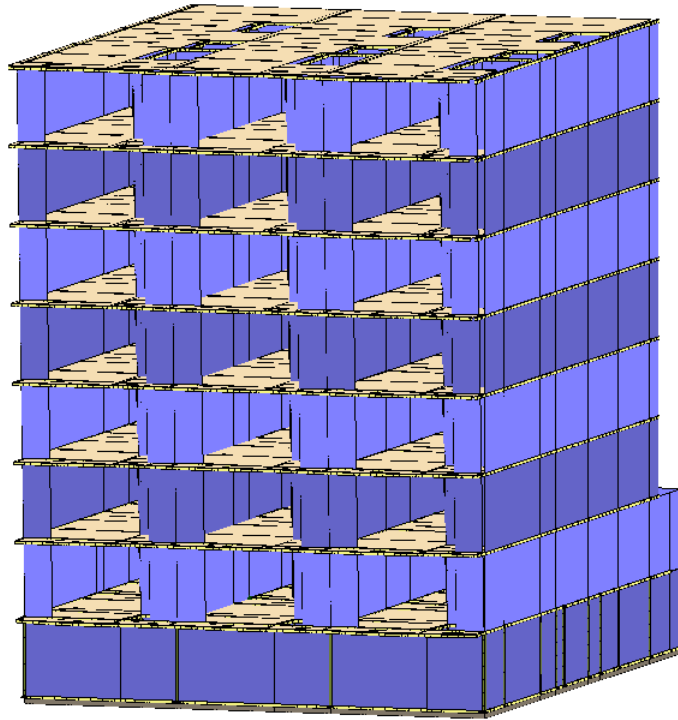
Load Case: Pushover – X Acc



Load Case: Pushover – X Acc + e



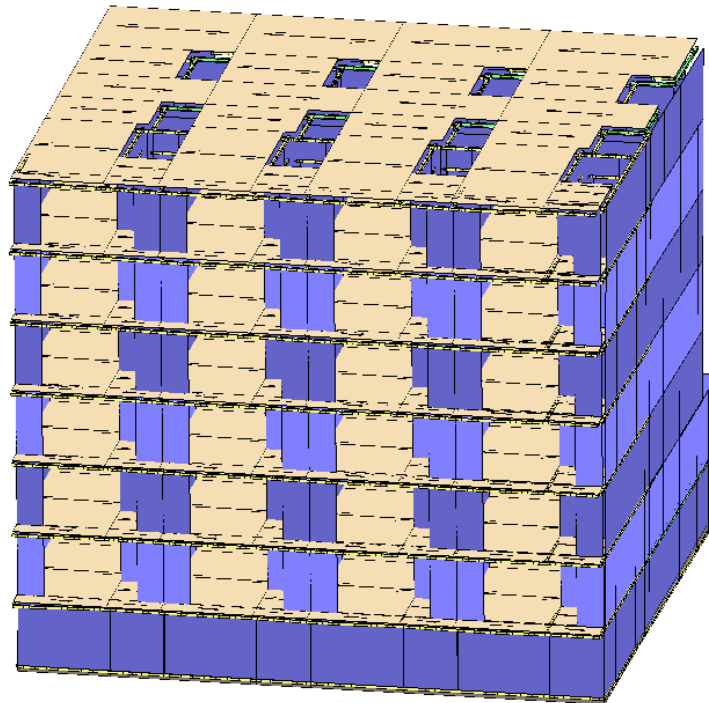
Load Case: Pushover – Ex + 0.3Ey Acc



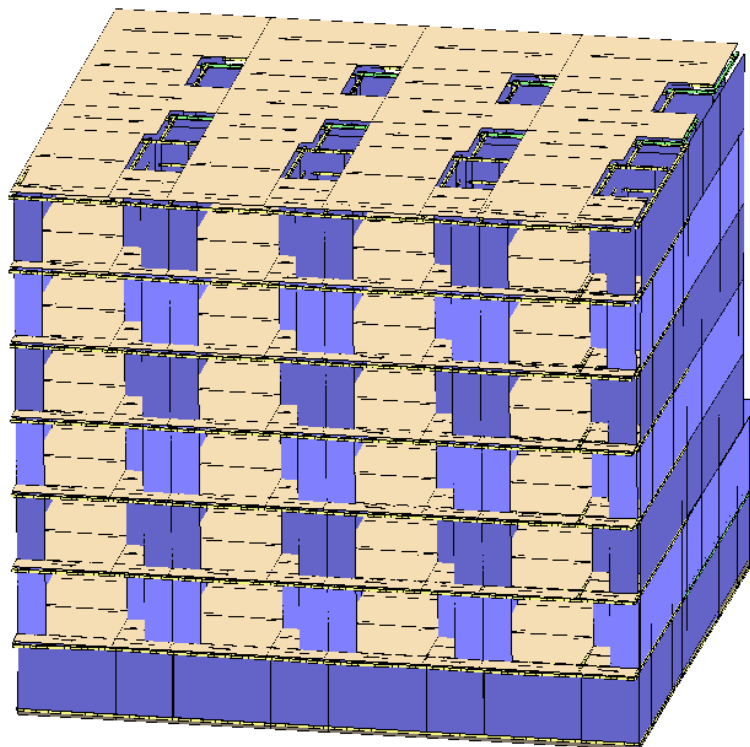
## Appendix C.6 Four-Unit Aggregate, Type A

### No Retrofitting

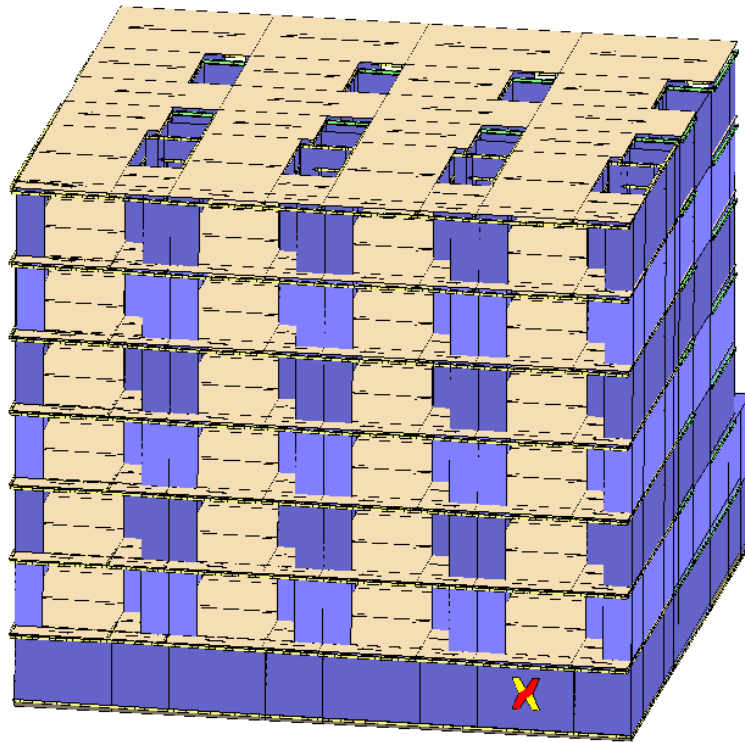
Load Case: Pushover + Y Acc



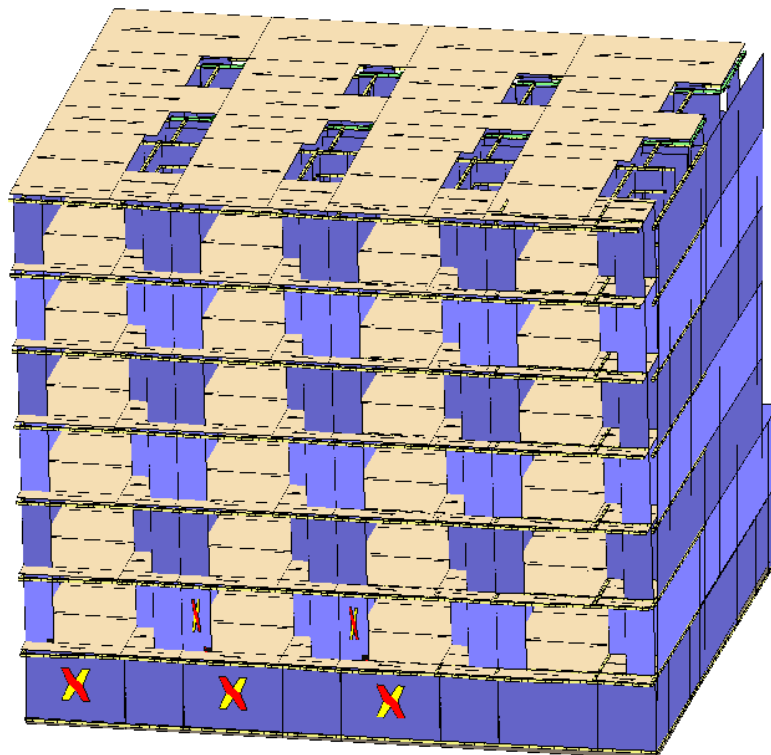
Load Case: Pushover + Y Acc + e



Load Case: Pushover  $0.3E_x + E_y$  Acc

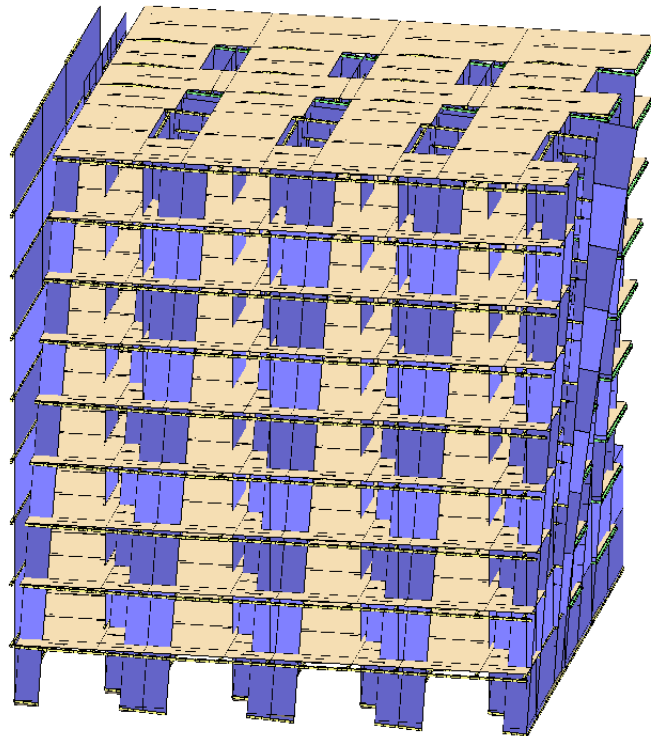


Load Case: Pushover  $-0.3E_x + E_y$  Acc

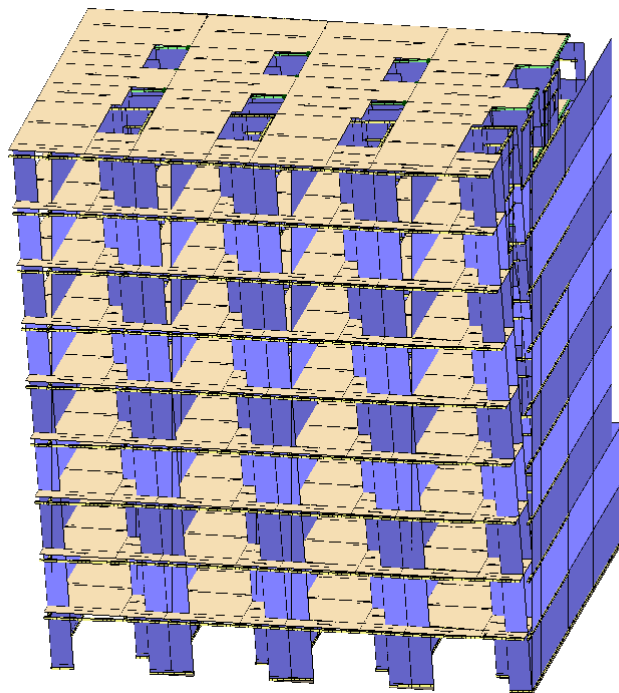


**Repeated Ground Floor**

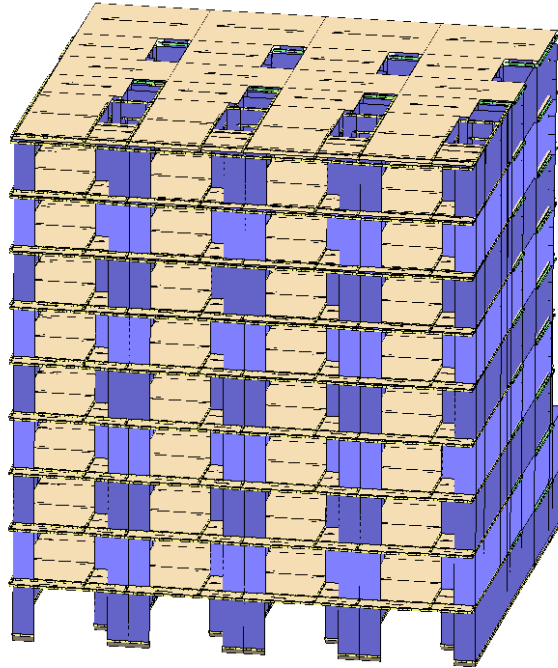
Load Case: Pushover + X Acc



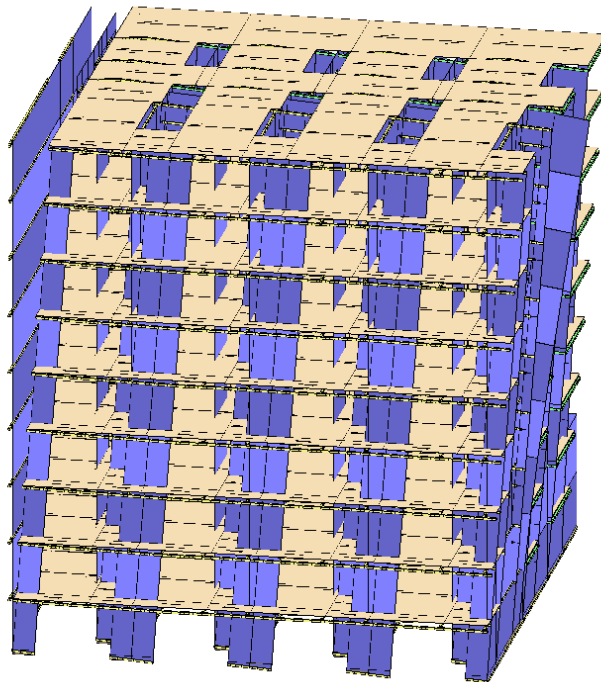
Load Case: Pushover – X Acc



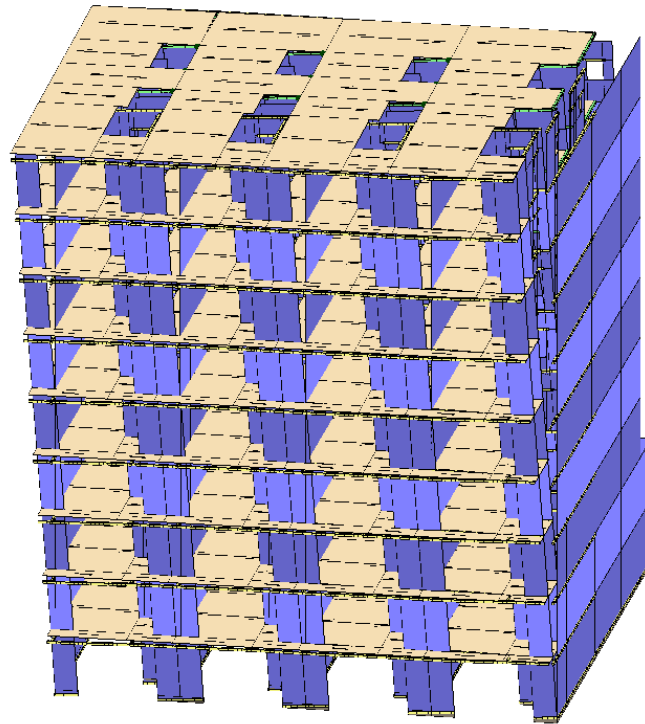
Load Case: Pushover + Y Acc



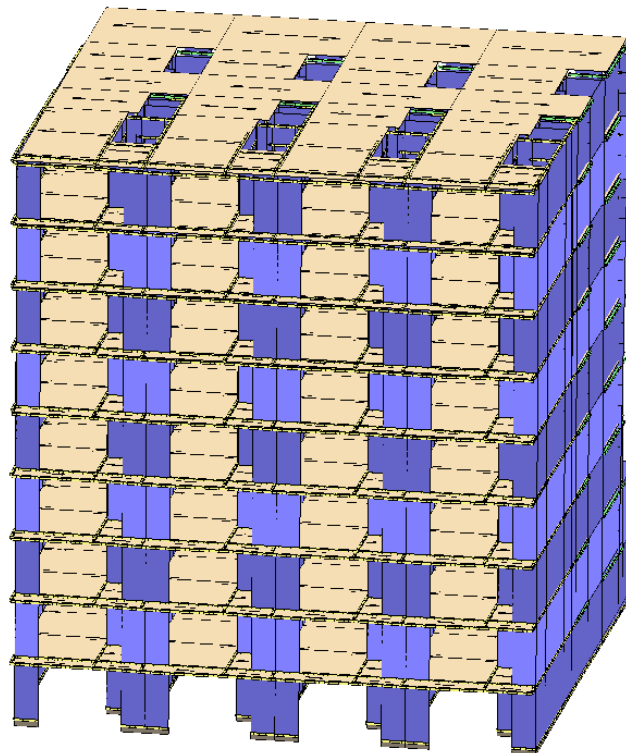
Load Case: Pushover + X Acc + e



Load Case: Pushover – X Acc + e

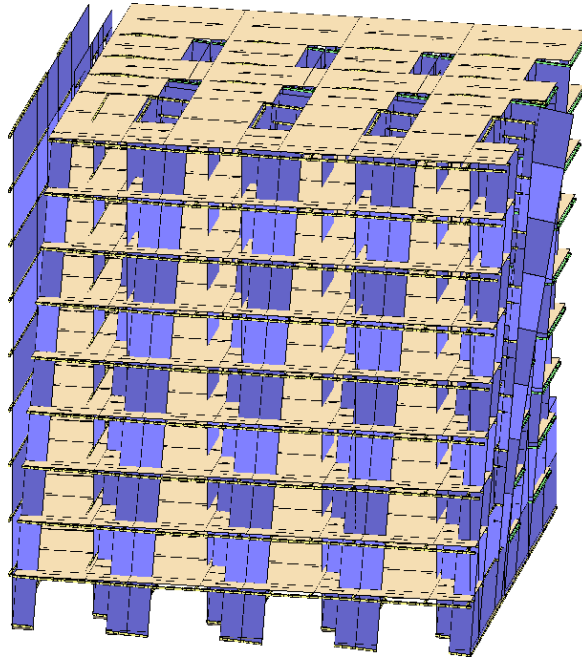


Load Case: Pushover + Y Acc + e

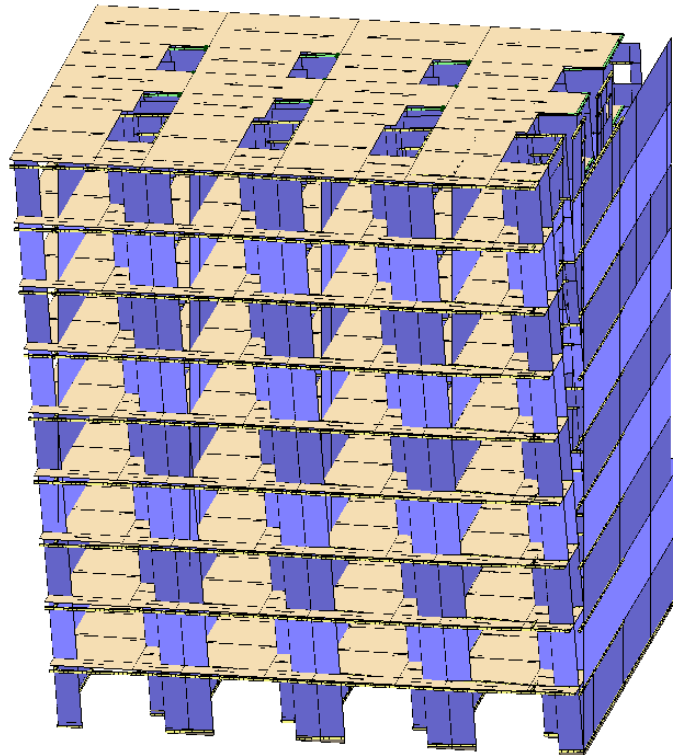




Load Case: Pushover  $E_x + 0.3E_y$  Acc

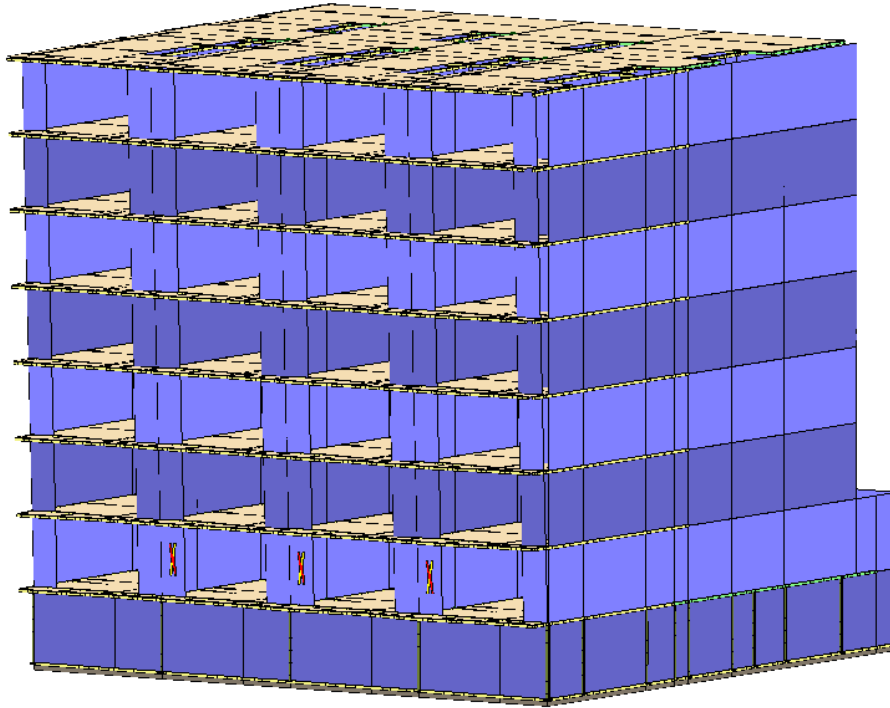


Load Case: Pushover  $-E_x + 0.3E_y$  Acc

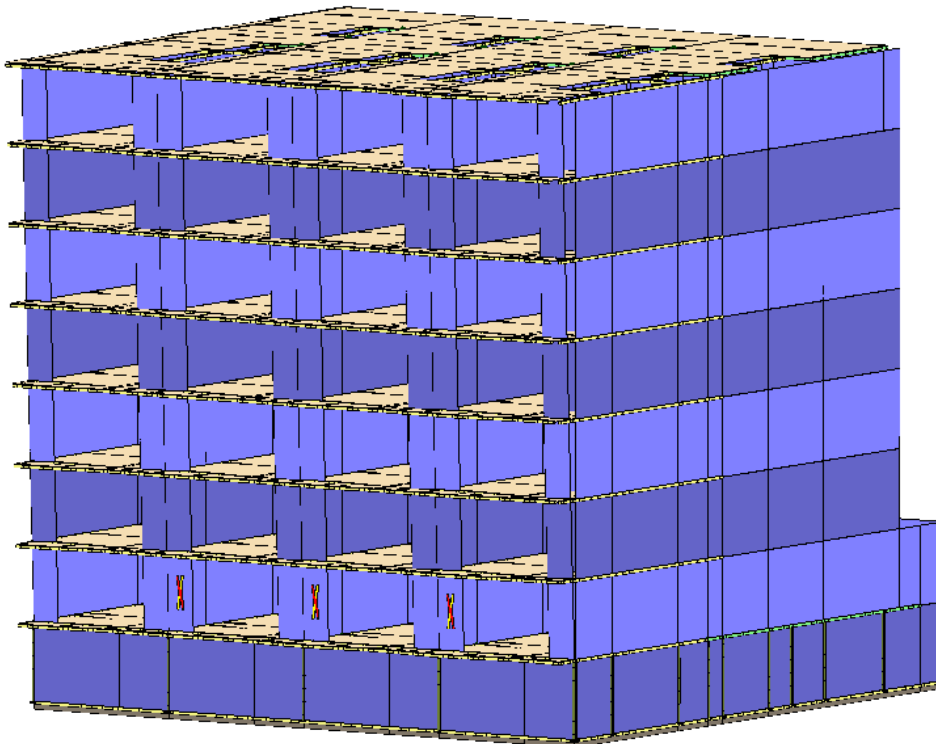


**35% of  $K_m$  Sway Stiffness in RC Frames**

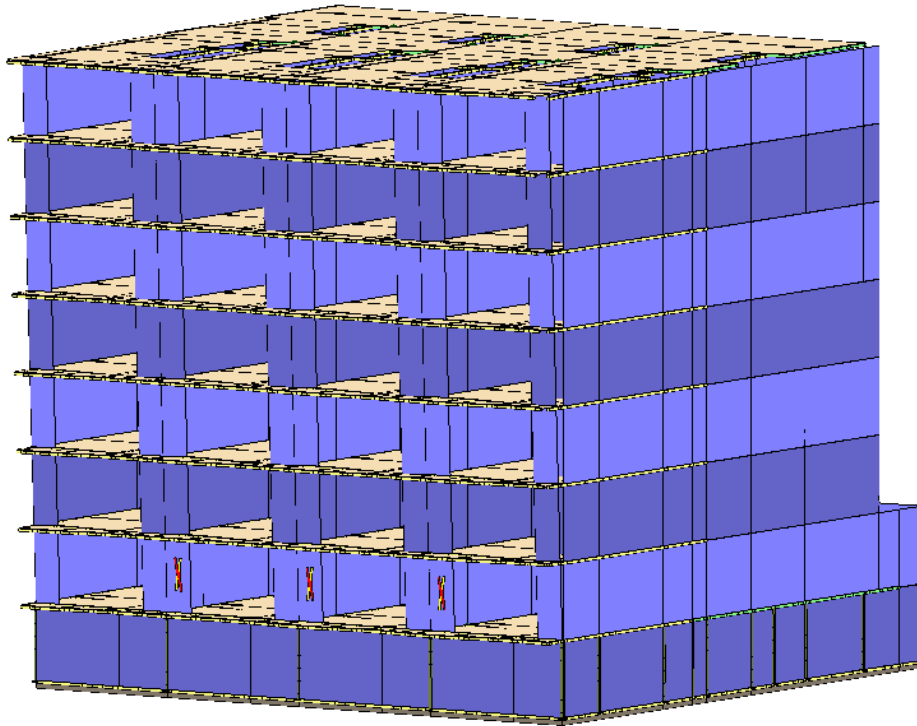
Load Case: Pushover – X Acc



Load Case: Pushover – X Acc + e

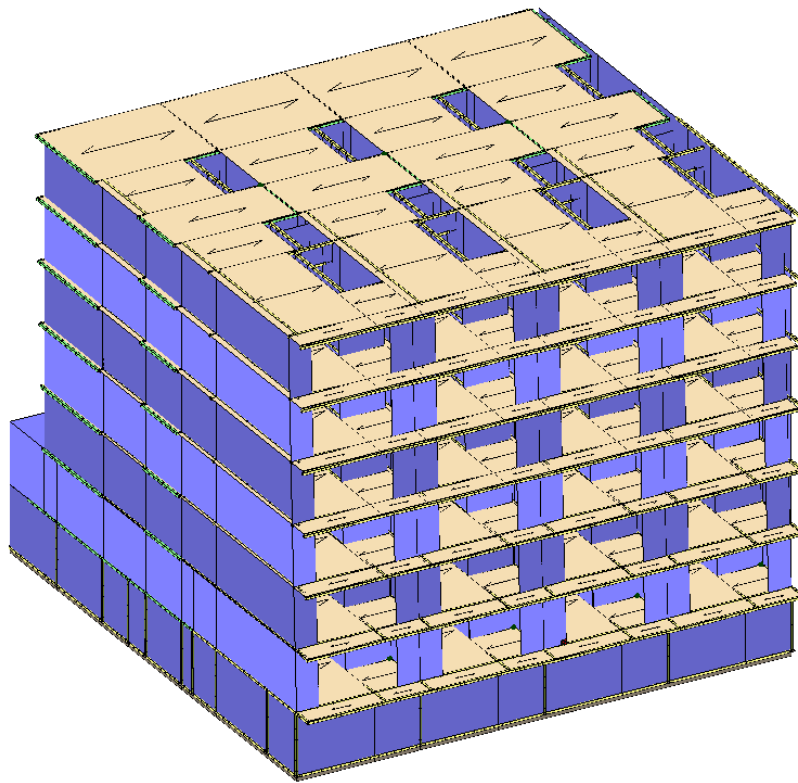


Load Case: Pushover -Ex + 0.3Ey Acc



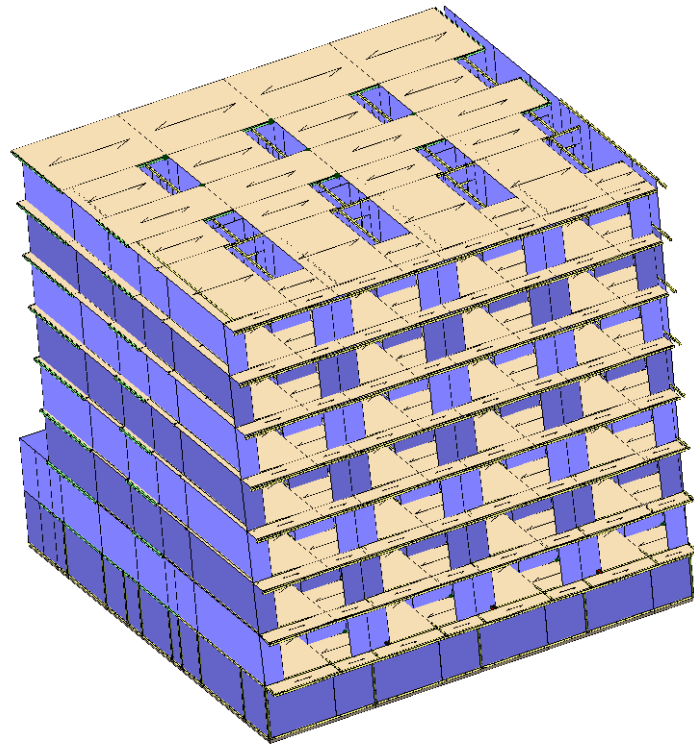
**50% of  $K_m$  Sway Stiffness in RC Frames**

Load Case: Pushover – Ex + 0.3Ey Acc

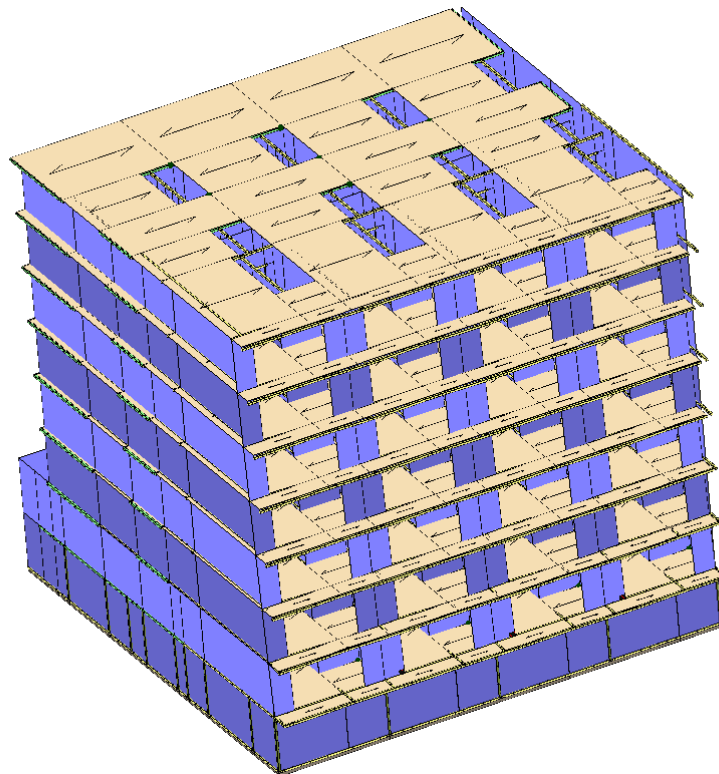


**35% of  $K_m$  Sway Stiffness in Steel Frames**

Load Case: Pushover – X Acc

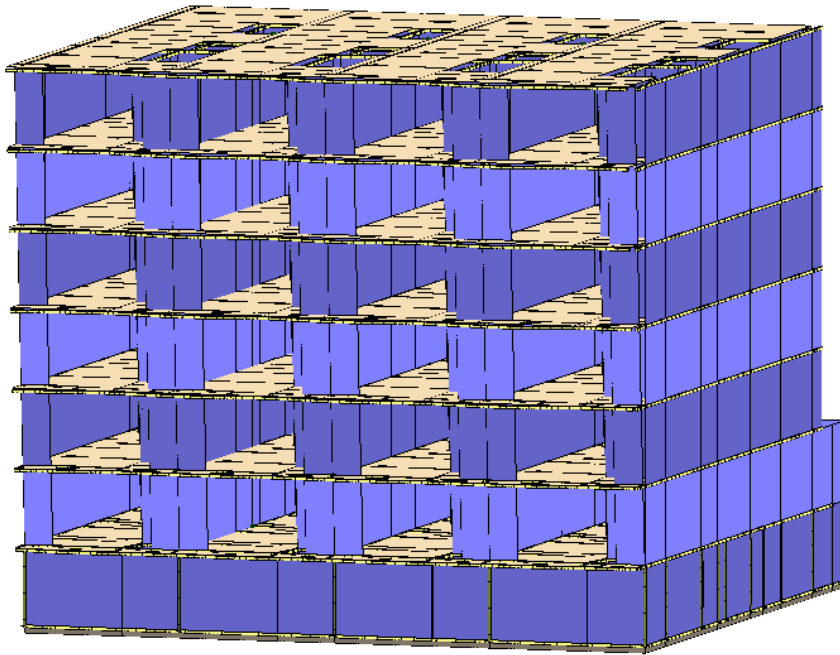


Load Case: Pushover – X Acc + e

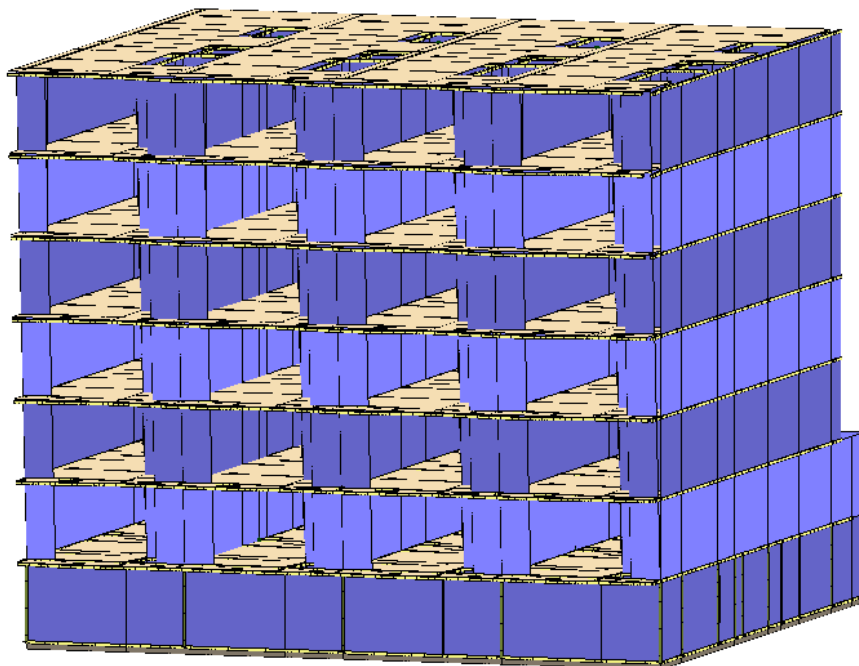


**50% of  $K_m$  Sway Stiffness in Steel Frames**

Load Case: Pushover – X Acc



Load Case: Pushover – X Acc + e



## Appendix D: Typical Example of how all $\alpha$ – values were extracted from 3DMacro

### Appendix D.1 Single-Unit Type A

Any values marked in green are the minimum alpha-values which still pass the seismic capacity check, whilst the values marked in red are the load cases which failed the seismic capacity check.

#### No Retrofitting

3 Floors									
Analysis	Limit state	Demand						Capacity	$\alpha$
		PGA/g	S	q*	de*max	d*max	dmax	dsl	
Pushover+X Acc	SLD	0.036941	1	1	0.22673	0.22673	0.285654	1.543667	5.403984
Pushover+X Acc	SLV	0.099956	1	1	0.915861	0.915861	1.15388	5.145557	4.459351
Pushover+X Acc	SLC	0.132733	1	1	1.291364	1.291364	1.626971	6.895047	4.237965
Pushover-X Acc	SLD	0.036941	1	1	0.226532	0.226532	0.285404	1.165066	4.082162
Pushover-X Acc	SLV	0.099956	1	1	0.915061	0.915061	1.152873	1.747599	1.515864
Pushover-X Acc	SLC	0.132733	1	1	1.290237	1.290237	1.625551	2.330132	1.433441
Pushover+Y Acc	SLD	0.036941	1	0.053605	0.013915	0.013915	0.017531	0.299338	17.07434
Pushover+Y Acc	SLV	0.099956	1	0.127734	0.033158	0.033158	0.041775	1.596469	38.21567
Pushover+Y Acc	SLC	0.132733	1	0.16849	0.043738	0.043738	0.055105	2.195144	39.83593
Pushover-Y Acc	SLD	0.036941	1	0.055021	0.013612	0.013612	0.01715	0.300662	17.53153
Pushover-Y Acc	SLV	0.099956	1	0.130347	0.032248	0.032248	0.040629	1.202649	29.60104
Pushover-Y Acc	SLC	0.132733	1	0.171944	0.042539	0.042539	0.053594	1.700995	31.73855
Pushover+X Acc + e	SLD	0.036941	1	1	0.226738	0.226738	0.285664	1.543667	5.403778
Pushover+X Acc + e	SLV	0.099956	1	1	0.915896	0.915896	1.153924	5.248469	5.48365
Pushover+X Acc + e	SLC	0.132733	1	1	1.291413	1.291413	1.627033	7.100869	4.364305
Pushover-X Acc + e	SLD	0.036941	1	1	0.225276	0.225276	0.283822	1.165066	4.104918
Pushover-X Acc + e	SLV	0.099956	1	1	0.909989	0.909989	1.146482	1.747599	1.524315
Pushover-X Acc + e	SLC	0.132733	1	1	1.283084	1.283084	1.61654	2.330132	1.441432
Pushover+Y Acc + e	SLD	0.036941	1	0.053024	0.013718	0.013718	0.017283	0.299338	17.31994
Pushover+Y Acc + e	SLV	0.099956	1	0.125872	0.032564	0.032564	0.041027	1.496689	36.4802
Pushover+Y Acc + e	SLC	0.132733	1	0.166039	0.042956	0.042956	0.054119	2.095365	38.7174
Pushover-Y Acc + e	SLD	0.036941	1	0.055829	0.01364	0.01364	0.017185	0.300662	17.49529
Pushover-Y Acc + e	SLV	0.099956	1	0.132334	0.032332	0.032332	0.040735	0.801766	19.68248
Pushover-Y Acc + e	SLC	0.132733	1	0.174564	0.04265	0.04265	0.053734	1.139232	21.20127
PushoverEx+0.3Ey Acc	SLD	0.036941	1	1	0.218486	0.218486	0.275267	1.539151	5.591484
PushoverEx+0.3Ey Acc	SLV	0.099956	1	1	0.882559	0.882559	1.111924	4.617452	4.152668
PushoverEx+0.3Ey Acc	SLC	0.132733	1	1	1.244409	1.244409	1.567813	6.259212	3.99232
Pushover0.3Ex+Ey Acc	SLD	0.036941	1	0.107649	0.044346	0.044346	0.055871	0.402395	7.202195
Pushover0.3Ex+Ey Acc	SLV	0.099956	1	0.297979	0.122753	0.122753	0.154655	1.710179	11.05806
Pushover0.3Ex+Ey Acc	SLC	0.132733	1	0.402774	0.165923	0.165923	0.209044	2.313771	11.06833
Pushover-0.3Ex+Ey Acc	SLD	0.036941	1	0.093525	0.051509	0.051509	0.064896	0.494981	7.627359
Pushover-0.3Ex+Ey Acc	SLV	0.099956	1	0.258882	0.14258	0.14258	0.179634	0.593978	3.306592
Pushover-0.3Ex+Ey Acc	SLC	0.132733	1	0.349927	0.192723	0.192723	0.242809	0.890966	3.669408
Pushover-Ex+0.3Ey Acc	SLD	0.036941	1	1	0.216178	0.216178	0.272359	1.26449	4.642727
Pushover-Ex+0.3Ey Acc	SLV	0.099956	1	1	0.873237	0.873237	1.100179	1.556295	1.414584
Pushover-Ex+0.3Ey Acc	SLC	0.132733	1	1	1.231264	1.231264	1.551253	2.139906	1.37947

4 Floors									
Analysis	Limit state	Demand						Capacity	$\alpha$
		PGA/g	S	q*	de*max	d*max	dmax	dsl	
Pushover+X Acc	SLD	0.036941	1	1	0.290108	0.290108	0.378946	2.41453	6.371703
Pushover+X Acc	SLV	0.099956	1	1	1.171875	1.171875	1.530729	5.983836	3.909142
Pushover+X Acc	SLC	0.132733	1	1	1.652344	1.652344	2.158328	7.978448	3.696588
Pushover-X Acc	SLD	0.036941	1	1	0.290345	0.290345	0.379255	1.520327	4.008718
Pushover-X Acc	SLV	0.099956	1	1	1.172832	1.172832	1.531979	1.900409	1.240493
Pushover-X Acc	SLC	0.132733	1	1	1.653693	1.653693	2.16009	2.565552	1.187706
Pushover+Y Acc	SLD	0.036941	1	0.063034	0.026361	0.026361	0.034433	0.498436	14.47551
Pushover+Y Acc	SLV	0.099956	1	0.174481	0.072968	0.072968	0.095313	1.594995	16.73435
Pushover+Y Acc	SLC	0.132733	1	0.235843	0.09863	0.09863	0.128833	2.189721	16.99662
Pushover-Y Acc	SLD	0.036941	1	0.065713	0.025338	0.025338	0.033097	0.501564	15.15414
Pushover-Y Acc	SLV	0.099956	1	0.181897	0.070138	0.070138	0.091616	1.80563	19.70874
Pushover-Y Acc	SLC	0.132733	1	0.244601	0.094316	0.094316	0.123198	2.407507	19.54182
Pushover+X Acc + e	SLD	0.036941	1	1	0.292114	0.292114	0.381566	2.41453	6.327949
Pushover+X Acc + e	SLV	0.099956	1	1	1.179978	1.179978	1.541313	5.983836	3.882299
Pushover+X Acc + e	SLC	0.132733	1	1	1.663769	1.663769	2.173251	7.978448	3.671204
Pushover-X Acc + e	SLD	0.036941	1	1	0.287902	0.287902	0.376064	1.520327	4.042732
Pushover-X Acc + e	SLV	0.099956	1	1	1.162964	1.162964	1.519089	1.900409	1.251019
Pushover-X Acc + e	SLC	0.132733	1	1	1.639779	1.639779	2.141916	2.565552	1.197784
Pushover+Y Acc + e	SLD	0.036941	1	0.062488	0.026136	0.026136	0.034139	0.498436	14.60023
Pushover+Y Acc + e	SLV	0.099956	1	0.172969	0.072345	0.072345	0.094498	1.594995	16.87854
Pushover+Y Acc + e	SLC	0.132733	1	0.2338	0.097788	0.097788	0.127732	2.183576	17.09495
Pushover-Y Acc + e	SLD	0.036941	1	0.065925	0.025547	0.025547	0.03337	0.501564	15.03032
Pushover-Y Acc + e	SLV	0.099956	1	0.182485	0.070716	0.070716	0.09237	1.80563	19.54771
Pushover-Y Acc + e	SLC	0.132733	1	0.245998	0.095328	0.095328	0.124519	2.407507	19.33441
PushoverEx+0.3Ey Acc	SLD	0.036941	1	1	0.283868	0.283868	0.370795	2.612058	7.044489
PushoverEx+0.3Ey Acc	SLV	0.099956	1	1	1.146667	1.146667	1.497802	5.642045	3.766883
PushoverEx+0.3Ey Acc	SLC	0.132733	1	1	1.616801	1.616801	2.111901	7.62721	3.611537
Pushover0.3Ex+Ey Acc	SLD	0.036941	1	0.121476	0.077577	0.077577	0.101332	0.606501	5.98526
Pushover0.3Ex+Ey Acc	SLV	0.099956	1	0.336252	0.214737	0.214737	0.280494	1.718421	6.126406
Pushover0.3Ex+Ey Acc	SLC	0.132733	1	0.454507	0.290257	0.290257	0.37914	2.317976	6.113776
Pushover-0.3Ex+Ey Acc	SLD	0.036941	1	0.12594	0.087836	0.087836	0.114733	0.688398	5.999993
Pushover-0.3Ex+Ey Acc	SLV	0.099956	1	0.348609	0.243134	0.243134	0.317587	0.688398	2.167584
Pushover-0.3Ex+Ey Acc	SLC	0.132733	1	0.47121	0.328641	0.328641	0.429279	0.983425	2.290879
Pushover-Ex+0.3Ey Acc	SLD	0.036941	1	1	0.277397	0.277397	0.362343	1.525528	4.210181
Pushover-Ex+0.3Ey Acc	SLV	0.099956	1	1	1.12053	1.12053	1.463661	1.811564	1.237694
Pushover-Ex+0.3Ey Acc	SLC	0.132733	1	1	1.579947	1.579947	2.063762	2.478982	1.201196



5 Floors									
Analysis	Limit state	Demand						Capacity	$\alpha$
		PGA/g	S	q*	de*max	d*max	dmax	dsl	
Pushover+X Acc	SLD	0.036941	1	1	0.358431	0.358431	0.479946	3.220506	6.710148
Pushover+X Acc	SLV	0.099956	1	1	1.447859	1.447859	1.938711	7.085112	3.654548
Pushover+X Acc	SLC	0.132733	1	1	2.041482	2.041482	2.733583	9.554166	3.495108
Pushover-X Acc	SLD	0.036941	1	1	0.358212	0.358212	0.479653	2.038296	4.249526
Pushover-X Acc	SLV	0.099956	1	1	1.446976	1.446976	1.937528	2.038296	1.052009
Pushover-X Acc	SLC	0.132733	1	1	2.040236	2.040236	2.731914	2.779495	1.017417
Pushover+Y Acc	SLD	0.036941	1	0.070475	0.045995	0.045995	0.061588	0.796694	12.93576
Pushover+Y Acc	SLV	0.099956	1	0.195079	0.127317	0.127317	0.17048	1.692974	9.930609
Pushover+Y Acc	SLC	0.132733	1	0.263686	0.172093	0.172093	0.230436	2.290494	9.939832
Pushover-Y Acc	SLD	0.036941	1	0.079413	0.042129	0.042129	0.056412	0.702893	12.46009
Pushover-Y Acc	SLV	0.099956	1	0.219819	0.116615	0.116615	0.15615	2.409919	15.43332
Pushover-Y Acc	SLC	0.132733	1	0.297126	0.157628	0.157628	0.211066	3.313638	15.69952
Pushover+X Acc + e	SLD	0.036941	1	1	0.361979	0.361979	0.484697	3.220506	6.644364
Pushover+X Acc + e	SLV	0.099956	1	1	1.462194	1.462194	1.957905	7.085112	3.61872
Pushover+X Acc + e	SLC	0.132733	1	1	2.061694	2.061694	2.760647	9.554166	3.460843
Pushover-X Acc + e	SLD	0.036941	1	1	0.354827	0.354827	0.47512	2.038296	4.290068
Pushover-X Acc + e	SLV	0.099956	1	1	1.433301	1.433301	1.919217	2.038296	1.062045
Pushover-X Acc + e	SLC	0.132733	1	1	2.020955	2.020955	2.706097	2.779495	1.027123
Pushover+Y Acc + e	SLD	0.036941	1	0.070359	0.045088	0.045088	0.060373	0.796694	13.19609
Pushover+Y Acc + e	SLV	0.099956	1	0.194758	0.124806	0.124806	0.167117	1.692974	10.13046
Pushover+Y Acc + e	SLC	0.132733	1	0.263252	0.168698	0.168698	0.22589	2.290494	10.13987
Pushover-Y Acc + e	SLD	0.036941	1	0.079819	0.042833	0.042833	0.057354	0.702893	12.25538
Pushover-Y Acc + e	SLV	0.099956	1	0.220944	0.118563	0.118563	0.158759	2.409919	15.17976
Pushover-Y Acc + e	SLC	0.132733	1	0.298646	0.160261	0.160261	0.214592	3.303142	15.39267
PushoverEx+0.3Ey Acc	SLD	0.036941	1	1	0.349547	0.349547	0.468049	3.518775	7.517955
PushoverEx+0.3Ey Acc	SLV	0.099956	1	1	1.411972	1.411972	1.890657	6.504402	3.440286
PushoverEx+0.3Ey Acc	SLC	0.132733	1	1	1.990881	1.990881	2.665827	8.743622	3.279891
Pushover0.3Ex+Ey Acc	SLD	0.036941	1	1	0.111471	0.111471	0.149262	0.914794	6.128776
Pushover0.3Ex+Ey Acc	SLV	0.099956	1	0.38473	0.343562	0.343562	0.460036	2.439452	5.302744
Pushover0.3Ex+Ey Acc	SLC	0.132733	1	0.520034	0.464388	0.464388	0.621824	3.371771	5.42239
Pushover-0.3Ex+Ey Acc	SLD	0.036941	1	1	0.11861	0.11861	0.158822	0.878381	5.530613
Pushover-0.3Ex+Ey Acc	SLV	0.099956	1	0.471189	0.388977	0.388977	0.520848	0.878381	1.686443
Pushover-0.3Ex+Ey Acc	SLC	0.132733	1	0.636899	0.525775	0.525775	0.704023	1.171174	1.663545
Pushover-Ex+0.3Ey Acc	SLD	0.036941	1	1	0.342681	0.342681	0.458857	1.862859	4.059783
Pushover-Ex+0.3Ey Acc	SLV	0.099956	1	1	1.384241	1.384241	1.853525	1.862859	1.005036
Pushover-Ex+0.3Ey Acc	SLC	0.132733	1	1	1.95178	1.95178	2.61347	2.608003	0.997908

## Repeated Ground Floor

5 Floors									
Analysis	Limit state	Demand						Capacity	$\alpha$
		PGA/g	S	q*	de*max	d*max	dmax	dsl	
Pushover+X Acc	SLD	0.043957	1	1	0.389762	0.389762	0.567346	3.740855	6.593606
Pushover+X Acc	SLV	0.099963	1	1	1.741842	1.741842	2.535464	5.380898	2.122254
Pushover+X Acc	SLC	0.123455	1	1	2.437043	2.437043	3.547413	7.267441	2.048659
Pushover-X Acc	SLD	0.043957	1	1	0.368779	0.368779	0.536803	2.962173	5.51818
Pushover-X Acc	SLV	0.099963	1	1	1.64807	1.64807	2.398967	2.962173	1.23477
Pushover-X Acc	SLC	0.123455	1	1	2.305844	2.305844	3.356437	4.068362	1.212107
Pushover+Y Acc	SLD	0.043957	1	0.079316	0.036928	0.036928	0.067554	0.826064	12.22826
Pushover+Y Acc	SLV	0.099963	1	0.169825	0.079067	0.079067	0.14464	1.905847	13.17645
Pushover+Y Acc	SLC	0.123455	1	0.204785	0.095344	0.095344	0.174416	2.627007	15.06174
Pushover-Y Acc	SLD	0.043957	1	0.085382	0.036425	0.036425	0.066633	0.77407	11.61685
Pushover-Y Acc	SLV	0.099963	1	0.182098	0.077685	0.077685	0.142112	1.921914	13.52393
Pushover-Y Acc	SLC	0.123455	1	0.2196	0.093684	0.093684	0.171379	2.697122	15.73774
Pushover+X Acc + e	SLD	0.043957	1	1	0.387926	0.387926	0.564674	3.689298	6.533498
Pushover+X Acc + e	SLV	0.099963	1	1	1.73364	1.73364	2.523524	5.209094	2.064214
Pushover+X Acc + e	SLC	0.123455	1	1	2.425567	2.425567	3.530709	7.189909	2.036393
Pushover-X Acc + e	SLD	0.043957	1	1	0.370087	0.370087	0.538707	2.991236	5.552626
Pushover-X Acc + e	SLV	0.099963	1	1	1.653916	1.653916	2.407476	2.991236	1.242478
Pushover-X Acc + e	SLC	0.123455	1	1	2.314023	2.314023	3.368343	4.12804	1.22554
Pushover+Y Acc + e	SLD	0.043957	1	0.080486	0.036497	0.036497	0.066765	0.811477	12.15424
Pushover+Y Acc + e	SLV	0.099963	1	0.171752	0.077882	0.077882	0.142473	2.405372	16.88306
Pushover+Y Acc + e	SLC	0.123455	1	0.207121	0.093921	0.093921	0.171812	3.307614	19.25133
Pushover-Y Acc + e	SLD	0.043957	1	0.087553	0.036687	0.036687	0.067113	0.747469	11.13744
Pushover-Y Acc + e	SLV	0.099963	1	0.187112	0.078405	0.078405	0.143429	1.620277	11.29673
Pushover-Y Acc + e	SLC	0.123455	1	0.225638	0.094549	0.094549	0.172961	2.197918	12.70761
PushoverEx+0.3Ey Acc	SLD	0.043957	1	1	0.35655	0.35655	0.477838	3.557004	7.443947
PushoverEx+0.3Ey Acc	SLV	0.099963	1	1	1.593418	1.593418	2.135457	4.967149	2.326036
PushoverEx+0.3Ey Acc	SLC	0.123455	1	1	2.229379	2.229379	2.987756	6.688849	2.238754
Pushover0.3Ex+Ey Acc	SLD	0.043957	1	0.078797	0.079866	0.079866	0.132565	1.662498	12.54103
Pushover0.3Ex+Ey Acc	SLV	0.099963	1	0.185194	0.187707	0.187707	0.311564	2.434934	7.815199
Pushover0.3Ex+Ey Acc	SLC	0.123455	1	0.236037	0.23924	0.23924	0.397102	3.361271	8.464508
Pushover-0.3Ex+Ey Acc	SLD	0.043957	1	0.097445	0.071352	0.071352	0.121065	1.211045	10.00326
Pushover-0.3Ex+Ey Acc	SLV	0.099963	1	0.229023	0.167697	0.167697	0.284536	1.372973	4.825298
Pushover-0.3Ex+Ey Acc	SLC	0.123455	1	0.2919	0.213737	0.213737	0.362654	1.859638	5.12786
Pushover-Ex+0.3Ey Acc	SLD	0.043957	1	1	0.334999	0.334999	0.44578	2.784026	6.245293
Pushover-Ex+0.3Ey Acc	SLV	0.099963	1	1	1.497106	1.497106	1.992187	2.784026	1.397472
Pushover-Ex+0.3Ey Acc	SLC	0.123455	1	1	2.094628	2.094628	2.787305	3.893978	1.397041

6 Floors									
Analysis	Limit state	Demand						Capacity	$\alpha$
		PGA/g	S	q*	de*max	d*max	dmax	dsl	
Pushover+X Acc	SLD	0.043957	1	1	0.476637	0.476637	0.754785	4.546654	6.02377
Pushover+X Acc	SLV	0.099963	1	1	2.130088	2.130088	3.373131	6.395135	1.895905
Pushover+X Acc	SLC	0.123455	1	1	2.980244	2.980244	4.719408	8.990777	1.905065
Pushover-X Acc	SLD	0.043957	1	1	0.448913	0.448913	0.710883	3.539427	4.978916
Pushover-X Acc	SLV	0.099963	1	1	2.00619	2.00619	3.176931	3.539427	1.114102
Pushover-X Acc	SLC	0.123455	1	1	2.806897	2.806897	4.444901	4.975492	1.119371
Pushover+Y Acc	SLD	0.043957	1	0.103998	0.064925	0.064925	0.120431	1.128796	9.372929
Pushover+Y Acc	SLV	0.099963	1	0.244425	0.152593	0.152593	0.283047	2.178855	7.697846
Pushover+Y Acc	SLC	0.123455	1	0.31153	0.194486	0.194486	0.360756	2.949563	8.176059
Pushover-Y Acc	SLD	0.043957	1	0.112664	0.065237	0.065237	0.121009	1.040991	8.602592
Pushover-Y Acc	SLV	0.099963	1	0.264792	0.153325	0.153325	0.284405	2.315144	8.140316
Pushover-Y Acc	SLC	0.123455	1	0.337488	0.195419	0.195419	0.362486	3.333999	9.197592
Pushover+X Acc + e	SLD	0.043957	1	1	0.473232	0.473232	0.749394	4.944996	6.598665
Pushover+X Acc + e	SLV	0.099963	1	1	2.114871	2.114871	3.349034	6.221787	1.857786
Pushover+X Acc + e	SLC	0.123455	1	1	2.958954	2.958954	4.685694	9.121714	1.946716
Pushover-X Acc + e	SLD	0.043957	1	1	0.450079	0.450079	0.712729	3.571582	5.011136
Pushover-X Acc + e	SLV	0.099963	1	1	2.0114	2.0114	3.185181	3.571582	1.121312
Pushover-X Acc + e	SLC	0.123455	1	1	2.814186	2.814186	4.456443	4.982349	1.11801
Pushover+Y Acc + e	SLD	0.043957	1	0.103448	0.064287	0.064287	0.119248	1.116559	9.36337
Pushover+Y Acc + e	SLV	0.099963	1	0.243132	0.151093	0.151093	0.280265	2.354757	8.401904
Pushover+Y Acc + e	SLC	0.123455	1	0.309882	0.192574	0.192574	0.35721	3.175303	8.889189
Pushover-Y Acc + e	SLD	0.043957	1	0.114676	0.065542	0.065542	0.121574	1.027179	8.448987
Pushover-Y Acc + e	SLV	0.099963	1	0.269521	0.154041	0.154041	0.285733	2.243169	7.850576
Pushover-Y Acc + e	SLC	0.123455	1	0.343516	0.196332	0.196332	0.364179	3.100717	8.514261
PushoverEx+0.3Ey Acc	SLD	0.043957	1	1	0.432622	0.432622	0.631008	4.096813	6.492486
PushoverEx+0.3Ey Acc	SLV	0.099963	1	1	1.933384	1.933384	2.819971	4.999439	1.772869
PushoverEx+0.3Ey Acc	SLC	0.123455	1	1	2.705033	2.705033	3.945473	7.175691	1.818715
Pushover0.3Ex+Ey Acc	SLD	0.043957	1	1	0.131667	0.131667	0.221842	2.07644	9.360017
Pushover0.3Ex+Ey Acc	SLV	0.099963	1	0.257155	0.323403	0.323403	0.544891	2.714085	4.98097
Pushover0.3Ex+Ey Acc	SLC	0.123455	1	0.327755	0.412191	0.412191	0.694487	3.664299	5.276269
Pushover-0.3Ex+Ey Acc	SLD	0.043957	1	0.129111	0.12162	0.12162	0.209023	1.604061	7.674098
Pushover-0.3Ex+Ey Acc	SLV	0.099963	1	0.303447	0.285841	0.285841	0.491261	1.671432	3.402328
Pushover-0.3Ex+Ey Acc	SLC	0.123455	1	0.386756	0.364317	0.364317	0.626134	2.252189	3.596977
Pushover-Ex+0.3Ey Acc	SLD	0.043957	1	1	0.406474	0.406474	0.58819	3.204939	5.448819
Pushover-Ex+0.3Ey Acc	SLV	0.099963	1	1	1.816528	1.816528	2.628615	3.204939	1.21925
Pushover-Ex+0.3Ey Acc	SLC	0.123455	1	1	2.541537	2.541537	3.677743	4.537576	1.233794

7 Floors									
Analysis	Limit state	Demand						Capacity	$\alpha$
		PGA/g	S	q*	de*max	d*max	dmax	dsl	
Pushover+X Acc	SLD	0.043957	1	1	0.552591	0.552591	0.950417	5.482778	5.768812
Pushover+X Acc	SLV	0.099963	1	1	2.469527	2.469527	4.247407	6.260664	1.473997
Pushover+X Acc	SLC	0.123455	1	1	3.455159	3.455159	5.942623	8.699476	1.463912
Pushover-X Acc	SLD	0.043957	1	1	0.527525	0.527525	0.907304	4.248263	4.682293
Pushover-X Acc	SLV	0.099963	1	1	2.357503	2.357503	4.054735	4.248263	1.047729
Pushover-X Acc	SLC	0.123455	1	1	3.298425	3.298425	5.673052	5.844798	1.030274
Pushover+Y Acc	SLD	0.043957	1	0.13011	0.105083	0.105083	0.195824	1.457353	7.442165
Pushover+Y Acc	SLV	0.099963	1	0.305794	0.246975	0.246975	0.46024	2.187	4.751866
Pushover+Y Acc	SLC	0.123455	1	0.389748	0.314781	0.314781	0.586596	3.043453	5.188328
Pushover-Y Acc	SLD	0.043957	1	0.137075	0.106525	0.106525	0.198511	1.445673	7.282596
Pushover-Y Acc	SLV	0.099963	1	0.322165	0.250364	0.250364	0.466555	2.977949	6.382847
Pushover-Y Acc	SLC	0.123455	1	0.410613	0.3191	0.3191	0.594645	4.136207	6.955764
Pushover+X Acc + e	SLD	0.043957	1	1	0.549889	0.549889	0.945769	5.37684	5.685153
Pushover+X Acc + e	SLV	0.099963	1	1	2.457449	2.457449	4.226634	6.091824	1.441295
Pushover+X Acc + e	SLC	0.123455	1	1	3.438261	3.438261	5.913558	8.65	1.46274
Pushover-X Acc + e	SLD	0.043957	1	1	0.529131	0.529131	0.910067	4.297536	4.722221
Pushover-X Acc + e	SLV	0.099963	1	1	2.364682	2.364682	4.067081	4.297536	1.056664
Pushover-X Acc + e	SLC	0.123455	1	1	3.308469	3.308469	5.690327	5.746211	1.009821
Pushover+Y Acc + e	SLD	0.043957	1	0.128961	0.104166	0.104166	0.194114	1.485118	7.650737
Pushover+Y Acc + e	SLV	0.099963	1	0.303093	0.244819	0.244819	0.456223	2.36494	5.183743
Pushover+Y Acc + e	SLC	0.123455	1	0.386305	0.312033	0.312033	0.581475	3.286822	5.652555
Pushover-Y Acc + e	SLD	0.043957	1	0.139305	0.106928	0.106928	0.199262	1.404164	7.046828
Pushover-Y Acc + e	SLV	0.099963	1	0.327406	0.251311	0.251311	0.46832	2.804066	5.987494
Pushover-Y Acc + e	SLC	0.123455	1	0.417293	0.320307	0.320307	0.596895	3.856199	6.460434
PushoverEx+0.3Ey Acc	SLD	0.043957	1	1	0.505319	0.505319	0.800787	5.06012	6.318934
PushoverEx+0.3Ey Acc	SLV	0.099963	1	1	2.258265	2.258265	3.578711	5.727057	1.600313
PushoverEx+0.3Ey Acc	SLC	0.123455	1	1	3.159579	3.159579	5.007038	8.042786	1.606296
Pushover0.3Ex+Ey Acc	SLD	0.043957	1	1	0.165446	0.165446	0.280197	2.552653	9.110193
Pushover0.3Ex+Ey Acc	SLV	0.099963	1	0.337017	0.510627	0.510627	0.86479	2.739664	3.16801
Pushover0.3Ex+Ey Acc	SLC	0.123455	1	0.429542	0.650816	0.650816	1.102213	3.768964	3.419453
Pushover-0.3Ex+Ey Acc	SLD	0.043957	1	1	0.155119	0.155119	0.267687	1.940352	7.248577
Pushover-0.3Ex+Ey Acc	SLV	0.099963	1	0.388953	0.448867	0.448867	0.774607	1.940352	2.504949
Pushover-0.3Ex+Ey Acc	SLC	0.123455	1	0.495738	0.572101	0.572101	0.987271	2.640025	2.674064
Pushover-Ex+0.3Ey Acc	SLD	0.043957	1	1	0.477565	0.477565	0.750309	3.914514	5.2172
Pushover-Ex+0.3Ey Acc	SLV	0.099963	1	1	2.134236	2.134236	3.353127	3.914514	1.167422
Pushover-Ex+0.3Ey Acc	SLC	0.123455	1	1	2.986048	2.986048	4.691421	5.358449	1.142181

8 Floors									
Analysis	Limit state	Demand						Capacity	$\alpha$
		PGA/g	S	q*	de*max	d*max	dmax	dsl	
Pushover+X Acc	SLD	0.043957	1	1	0.620993	0.620993	1.16238	5.715178	4.91679
Pushover+X Acc	SLV	0.099963	1	1	2.775214	2.775214	5.194668	5.715178	1.100201
Pushover+X Acc	SLC	0.123455	1	1	3.882851	3.882851	7.267952	7.894783	1.086246
Pushover-X Acc	SLD	0.043957	1	1	0.603474	0.603474	1.129587	4.482832	3.968557
Pushover-X Acc	SLV	0.099963	1	1	2.69692	2.69692	5.048118	4.482832	0.888021
Pushover-X Acc	SLC	0.123455	1	1	3.77331	3.77331	7.062912	6.667536	0.944021
Pushover+Y Acc	SLD	0.043957	1	1	0.142107	0.142107	0.264251	1.85436	7.017416
Pushover+Y Acc	SLV	0.099963	1	0.366375	0.37672	0.37672	0.700521	2.21717	3.165029
Pushover+Y Acc	SLC	0.123455	1	0.466961	0.480146	0.480146	0.892844	3.133847	3.509959
Pushover+Y Acc	SLD	0.043957	1	1	0.144903	0.144903	0.269451	1.928373	7.156681
Pushover-Y Acc	SLV	0.099963	1	0.374524	0.391691	0.391691	0.72836	3.563085	4.891926
Pushover-Y Acc	SLC	0.123455	1	0.477347	0.499228	0.499228	0.928327	5.197762	5.599067
Pushover+X Acc + e	SLD	0.043957	1	1	0.618591	0.618591	1.157884	5.634242	4.865982
Pushover+X Acc + e	SLV	0.099963	1	1	2.764478	2.764478	5.174573	5.634242	1.088832
Pushover+X Acc + e	SLC	0.123455	1	1	3.867832	3.867832	7.239839	7.865352	1.086399
Pushover-X Acc + e	SLD	0.043957	1	1	0.605124	0.605124	1.132676	4.518156	3.98892
Pushover-X Acc + e	SLV	0.099963	1	1	2.704295	2.704295	5.061922	4.518156	0.892577
Pushover-X Acc + e	SLC	0.123455	1	1	3.783628	3.783628	7.082226	6.622992	0.935157
Pushover+Y Acc + e	SLD	0.043957	1	1	0.141556	0.141556	0.263228	1.898143	7.211032
Pushover+Y Acc + e	SLV	0.099963	1	0.364846	0.373808	0.373808	0.695105	2.389457	3.437547
Pushover+Y Acc + e	SLC	0.123455	1	0.465012	0.476434	0.476434	0.885942	3.357724	3.790007
Pushover-Y Acc + e	SLD	0.043957	1	1	0.145209	0.145209	0.270019	1.865431	6.90851
Pushover-Y Acc + e	SLV	0.099963	1	0.379539	0.393346	0.393346	0.731437	3.647869	4.987261
Pushover-Y Acc + e	SLC	0.123455	1	0.483738	0.501337	0.501337	0.932248	4.909429	5.266223
Pushover0.3Ex+Ey Acc	SLD	0.043957	1	1	0.201767	0.201767	0.341087	2.903628	8.51286
Pushover0.3Ex+Ey Acc	SLV	0.099963	1	0.429971	0.759433	0.759433	1.283823	2.903628	2.261704
Pushover0.3Ex+Ey Acc	SLC	0.123455	1	0.548016	0.967931	0.967931	1.636288	3.888896	2.376657
Pushover-0.3Ex+Ey Acc	SLD	0.043957	1	1	0.189032	0.189032	0.325413	2.16645	6.657547
Pushover-0.3Ex+Ey Acc	SLV	0.099963	1	0.484105	0.66659	0.66659	1.147516	2.16645	1.887948
Pushover-0.3Ex+Ey Acc	SLC	0.123455	1	0.617013	0.849598	0.849598	1.462559	2.916552	1.994144
Pushover-Ex+0.3Ey Acc	SLD	0.043957	1	1	0.546527	0.546527	0.934204	4.240975	4.539669
Pushover-Ex+0.3Ey Acc	SLV	0.099963	1	1	2.442425	2.442425	4.174949	4.240975	1.015815
Pushover-Ex+0.3Ey Acc	SLC	0.123455	1	1	3.417241	3.417241	5.841247	6.229467	1.066462
Pushover-Ex-0.3Ey Acc	SLD	0.043957	1	1	0.553621	0.553621	0.955088	4.320601	4.523773
Pushover-Ex-0.3Ey Acc	SLV	0.099963	1	1	2.47413	2.47413	4.268281	4.320601	1.012258
Pushover-Ex-0.3Ey Acc	SLC	0.123455	1	1	3.461599	3.461599	5.971827	6.293272	1.053827

35% of  $K_m$  Sway Stiffness in RC Frames

5 Floors									
Analysis	Limit state	Demand						Capacity	$\alpha$
		PGA/g	S	q*	de*max	d*max	dmax	dsl	
Pushover+X Acc	SLD	0.036941	1	1	0.210983	0.210983	0.287876	1.638297	5.690984
Pushover+X Acc	SLV	0.099956	1	1	0.852252	0.852252	1.162857	2.444512	2.10216
Pushover+X Acc	SLC	0.132733	1	1	1.201675	1.201675	1.639629	3.358195	2.048144
Pushover-X Acc	SLD	0.036941	1	1	0.215149	0.215149	0.29356	0.364179	1.240558
Pushover-X Acc	SLV	0.099956	1	1	0.869081	0.869081	1.18582	1.888714	1.59275
Pushover-X Acc	SLC	0.132733	1	1	1.225404	1.225404	1.672006	2.720147	1.626877
Pushover+Y Acc	SLD	0.036941	1	0.077459	0.021103	0.021103	0.028795	0.299781	10.41103
Pushover+Y Acc	SLV	0.099956	1	0.207238	0.056461	0.056461	0.077039	3.197662	41.50728
Pushover+Y Acc	SLC	0.132733	1	0.273184	0.074428	0.074428	0.101554	4.396785	43.2952
Pushover-Y Acc	SLD	0.036941	1	0.072197	0.013131	0.013131	0.017917	0.200146	11.17055
Pushover-Y Acc	SLV	0.099956	1	0.16943	0.030817	0.030817	0.042048	3.60263	85.67934
Pushover-Y Acc	SLC	0.132733	1	0.223511	0.040653	0.040653	0.055469	4.90358	88.40173
Pushover+X Acc + e	SLD	0.036941	1	1	0.210472	0.210472	0.287178	1.629976	5.67583
Pushover+X Acc + e	SLV	0.099956	1	1	0.850187	0.850187	1.16004	2.427727	2.092796
Pushover+X Acc + e	SLC	0.132733	1	1	1.198764	1.198764	1.635657	3.333474	2.038003
Pushover-X Acc + e	SLD	0.036941	1	1	0.216194	0.216194	0.294986	0.365258	1.238221
Pushover-X Acc + e	SLV	0.099956	1	1	0.873301	0.873301	1.191578	1.923091	1.613902
Pushover-X Acc + e	SLC	0.132733	1	1	1.231355	1.231355	1.680126	2.732883	1.626594
Pushover+Y Acc + e	SLD	0.036941	1	0.078068	0.019503	0.019503	0.026611	0.299781	11.26522
Pushover+Y Acc + e	SLV	0.099956	1	0.204171	0.051006	0.051006	0.069596	3.297589	47.38198
Pushover+Y Acc + e	SLC	0.132733	1	0.269175	0.067246	0.067246	0.091754	4.496712	49.00854
Pushover-Y Acc + e	SLD	0.036941	1	0.072692	0.013064	0.013064	0.017826	0.200146	11.22791
Pushover-Y Acc + e	SLV	0.099956	1	0.170362	0.030618	0.030618	0.041777	3.60263	86.23466
Pushover-Y Acc + e	SLC	0.132733	1	0.224743	0.040392	0.040392	0.055113	4.90358	88.97398
PushoverEx+0.3Ey Acc	SLD	0.036941	1	1	0.196442	0.196442	0.268036	1.247131	4.652858
PushoverEx+0.3Ey Acc	SLV	0.099956	1	1	0.793515	0.793515	1.082713	2.702118	2.495691
PushoverEx+0.3Ey Acc	SLC	0.132733	1	1	1.118856	1.118856	1.526626	3.741394	2.45076
Pushover0.3Ex+Ey Acc	SLD	0.036941	1	0.166948	0.040469	0.040469	0.055218	0.303352	5.49367
Pushover0.3Ex+Ey Acc	SLV	0.099956	1	0.462123	0.112021	0.112021	0.152848	1.11229	7.277112
Pushover0.3Ex+Ey Acc	SLC	0.132733	1	0.624645	0.151418	0.151418	0.206602	1.617877	7.83088
Pushover-0.3Ex+Ey Acc	SLD	0.036941	1	0.144014	0.041974	0.041974	0.057272	0.098749	1.724201
Pushover-0.3Ex+Ey Acc	SLV	0.099956	1	0.398638	0.116188	0.116188	0.158532	0.592492	3.737355
Pushover-0.3Ex+Ey Acc	SLC	0.132733	1	0.538834	0.157049	0.157049	0.214286	0.888738	4.147437
Pushover-Ex+0.3Ey Acc	SLD	0.036941	1	1	0.197728	0.197728	0.269791	0.384129	1.423803
Pushover-Ex+0.3Ey Acc	SLV	0.099956	1	1	0.798711	0.798711	1.089803	1.632547	1.49802
Pushover-Ex+0.3Ey Acc	SLC	0.132733	1	1	1.126182	1.126182	1.536622	2.304772	1.499895

6 Floors									
Analysis	Limit state	Demand						Capacity	$\alpha$
		PGA/g	S	q*	de*max	d*max	dmax	dsl	
Pushover+X Acc	SLD	0.036941	1	1	0.262261	0.262261	0.363408	2.33691	6.430532
Pushover+X Acc	SLV	0.099956	1	1	1.059386	1.059386	1.467967	2.971898	2.0245
Pushover+X Acc	SLC	0.132733	1	1	1.493735	1.493735	2.069833	4.192297	2.025427
Pushover-X Acc	SLD	0.036941	1	1	0.272537	0.272537	0.377649	0.374028	0.990413
Pushover-X Acc	SLV	0.099956	1	1	1.100899	1.100899	1.525489	2.12469	1.392792
Pushover-X Acc	SLC	0.132733	1	1	1.552267	1.552267	2.15094	2.944622	1.368993
Pushover+Y Acc	SLD	0.036941	1	0.092793	0.025783	0.025783	0.035726	0.299732	8.389618
Pushover+Y Acc	SLV	0.099956	1	0.256858	0.071368	0.071368	0.098893	3.896512	39.40131
Pushover+Y Acc	SLC	0.132733	1	0.347191	0.096467	0.096467	0.133672	5.295259	39.61376
Pushover-Y Acc	SLD	0.036941	1	0.08169	0.01662	0.01662	0.02303	0.200179	8.692235
Pushover-Y Acc	SLV	0.099956	1	0.204247	0.041554	0.041554	0.05758	4.203756	73.0073
Pushover-Y Acc	SLC	0.132733	1	0.269342	0.054797	0.054797	0.075931	5.705099	75.13525
Pushover+X Acc + e	SLD	0.036941	1	1	0.262644	0.262644	0.36394	2.326889	6.393607
Pushover+X Acc + e	SLV	0.099956	1	1	1.060935	1.060935	1.470113	2.949071	2.006016
Pushover+X Acc + e	SLC	0.132733	1	1	1.495919	1.495919	2.07286	4.246448	2.048593
Pushover-X Acc + e	SLD	0.036941	1	1	0.27239	0.27239	0.377445	0.374761	0.99289
Pushover-X Acc + e	SLV	0.099956	1	1	1.100304	1.100304	1.524665	2.118632	1.389572
Pushover-X Acc + e	SLC	0.132733	1	1	1.551428	1.551428	2.149778	2.863074	1.3318
Pushover+Y Acc + e	SLD	0.036941	1	0.093117	0.025374	0.025374	0.035161	0.299732	8.524634
Pushover+Y Acc + e	SLV	0.099956	1	0.257754	0.070238	0.070238	0.097327	3.896512	40.0354
Pushover+Y Acc + e	SLC	0.132733	1	0.346756	0.09449	0.09449	0.130933	5.295259	40.44246
Pushover-Y Acc + e	SLD	0.036941	1	0.081212	0.016664	0.016664	0.02309	0.200179	8.669402
Pushover-Y Acc + e	SLV	0.099956	1	0.203199	0.041693	0.041693	0.057774	4.203756	72.76263
Pushover-Y Acc + e	SLC	0.132733	1	0.267959	0.054981	0.054981	0.076186	5.705099	74.88374
PushoverEx+0.3Ey Acc	SLD	0.036941	1	1	0.246486	0.246486	0.34155	1.688516	4.943693
PushoverEx+0.3Ey Acc	SLV	0.099956	1	1	0.995665	0.995665	1.379669	3.588098	2.600694
PushoverEx+0.3Ey Acc	SLC	0.132733	1	1	1.403887	1.403887	1.945334	4.854485	2.495451
Pushover0.3Ex+Ey Acc	SLD	0.036941	1	0.183711	0.059105	0.059105	0.0819	0.40634	4.961418
Pushover0.3Ex+Ey Acc	SLV	0.099956	1	0.508522	0.163605	0.163605	0.226704	1.42219	6.273343
Pushover0.3Ex+Ey Acc	SLC	0.132733	1	0.687362	0.221143	0.221143	0.306432	1.930115	6.298669
Pushover-0.3Ex+Ey Acc	SLD	0.036941	1	0.16761	0.061409	0.061409	0.085093	0.098251	1.154629
Pushover-0.3Ex+Ey Acc	SLV	0.099956	1	0.463953	0.169984	0.169984	0.235542	0.687756	2.919885
Pushover-0.3Ex+Ey Acc	SLC	0.132733	1	0.627118	0.229764	0.229764	0.318379	0.982509	3.085971
Pushover-Ex+0.3Ey Acc	SLD	0.036941	1	1	0.256261	0.256261	0.355095	0.377674	1.063585
Pushover-Ex+0.3Ey Acc	SLV	0.099956	1	1	1.035151	1.035151	1.434385	1.982788	1.382326
Pushover-Ex+0.3Ey Acc	SLC	0.132733	1	1	1.459563	1.459563	2.022483	2.643718	1.307164

7 Floors									
Analysis	Limit state	Demand						Capacity	$\alpha$
		PGA/g	S	q*	de*max	d*max	dmax	dsl	
Pushover+X Acc	SLD	0.036941	1	1	0.318895	0.318895	0.446893	2.793195	6.250253
Pushover+X Acc	SLV	0.099956	1	1	1.288156	1.288156	1.805198	3.660831	2.027939
Pushover+X Acc	SLC	0.132733	1	1	1.816301	1.816301	2.545329	5.174012	2.032747
Pushover-X Acc	SLD	0.036941	1	1	0.333614	0.333614	0.46752	0.38981	0.833781
Pushover-X Acc	SLV	0.099956	1	1	1.347614	1.347614	1.88852	1.981575	1.049274
Pushover-X Acc	SLC	0.132733	1	1	1.900135	1.900135	2.662814	3.148138	1.18226
Pushover+Y Acc	SLD	0.036941	1	0.109214	0.037815	0.037815	0.052993	0.399575	7.540194
Pushover+Y Acc	SLV	0.099956	1	0.302312	0.104673	0.104673	0.146687	4.495215	30.64504
Pushover+Y Acc	SLC	0.132733	1	0.40863	0.141485	0.141485	0.198274	6.093514	30.73277
Pushover-Y Acc	SLD	0.036941	1	0.09149	0.024589	0.024589	0.034458	0.300319	8.715464
Pushover-Y Acc	SLV	0.099956	1	0.253249	0.068063	0.068063	0.095382	5.005316	52.47643
Pushover-Y Acc	SLC	0.132733	1	0.3375	0.090706	0.090706	0.127114	6.707124	52.7646
Pushover+X Acc + e	SLD	0.036941	1	1	0.318925	0.318925	0.446935	2.766454	6.189835
Pushover+X Acc + e	SLV	0.099956	1	1	1.288277	1.288277	1.805367	3.621468	2.005946
Pushover+X Acc + e	SLC	0.132733	1	1	1.816471	1.816471	2.545568	5.303486	2.08342
Pushover-X Acc + e	SLD	0.036941	1	1	0.333656	0.333656	0.467579	0.390515	0.835185
Pushover-X Acc + e	SLV	0.099956	1	1	1.347783	1.347783	1.888757	1.978423	1.047473
Pushover-X Acc + e	SLC	0.132733	1	1	1.900374	1.900374	2.663148	3.136897	1.17789
Pushover+Y Acc + e	SLD	0.036941	1	0.108675	0.037962	0.037962	0.053199	0.399575	7.51089
Pushover+Y Acc + e	SLV	0.099956	1	0.300819	0.105081	0.105081	0.147259	4.495215	30.52594
Pushover+Y Acc + e	SLC	0.132733	1	0.406613	0.142037	0.142037	0.199048	6.093514	30.61333
Pushover-Y Acc + e	SLD	0.036941	1	0.091705	0.024479	0.024479	0.034305	0.300319	8.754373
Pushover-Y Acc + e	SLV	0.099956	1	0.253845	0.06776	0.06776	0.094958	5.005316	52.71071
Pushover-Y Acc + e	SLC	0.132733	1	0.337845	0.090183	0.090183	0.126381	6.707124	53.07067
PushoverEx+0.3Ey Acc	SLD	0.036941	1	1	0.301917	0.301917	0.4231	2.2528	5.324506
PushoverEx+0.3Ey Acc	SLV	0.099956	1	1	1.219574	1.219574	1.709088	4.5056	2.63626
PushoverEx+0.3Ey Acc	SLC	0.132733	1	1	1.719599	1.719599	2.409814	6.114743	2.537433
Pushover0.3Ex+Ey Acc	SLD	0.036941	1	0.210156	0.089983	0.089983	0.1261	0.51047	4.048141
Pushover0.3Ex+Ey Acc	SLV	0.099956	1	0.581725	0.249077	0.249077	0.349052	1.735599	4.972327
Pushover0.3Ex+Ey Acc	SLC	0.132733	1	0.786309	0.336674	0.336674	0.471808	2.348164	4.976944
Pushover-0.3Ex+Ey Acc	SLD	0.036941	1	0.187333	0.086922	0.086922	0.121811	0.097711	0.802148
Pushover-0.3Ex+Ey Acc	SLV	0.099956	1	0.518549	0.240606	0.240606	0.337181	0.781686	2.318299
Pushover-0.3Ex+Ey Acc	SLC	0.132733	1	0.700915	0.325224	0.325224	0.455763	1.074819	2.358286
Pushover-Ex+0.3Ey Acc	SLD	0.036941	1	1	0.325334	0.325334	0.455917	0.370661	0.813002
Pushover-Ex+0.3Ey Acc	SLV	0.099956	1	1	1.314167	1.314167	1.841649	2.223967	1.207596
Pushover-Ex+0.3Ey Acc	SLC	0.132733	1	1	1.852975	1.852975	2.596725	2.965289	1.141934



8 Floors									
Analysis	Limit state	Demand						Capacity	$\alpha$
		PGA/g	S	q*	de*max	d*max	dmax	dsl	
Pushover+X Acc	SLD	0.036941	1	1	0.378706	0.378706	0.535258	3.866183	7.223023
Pushover+X Acc	SLV	0.099956	1	1	1.529759	1.529759	2.162143	4.505136	2.083644
Pushover+X Acc	SLC	0.132733	1	1	2.15696	2.15696	3.048623	6.367167	2.088539
Pushover-X Acc	SLD	0.036941	1	1	0.397441	0.397441	0.561739	0.285168	0.507652
Pushover-X Acc	SLV	0.099956	1	1	1.605439	1.605439	2.269109	2.154912	0.949673
Pushover-X Acc	SLC	0.132733	1	1	2.263669	2.263669	3.199444	3.412374	1.066552
Pushover+Y Acc	SLD	0.036941	1	0.127686	0.045348	0.045348	0.064094	0.499384	7.791424
Pushover+Y Acc	SLV	0.099956	1	0.353443	0.125525	0.125525	0.177416	4.893966	27.58468
Pushover+Y Acc	SLC	0.132733	1	0.477744	0.169671	0.169671	0.239811	6.629057	27.64286
Pushover-Y Acc	SLD	0.036941	1	0.100676	0.033109	0.033109	0.046797	0.400493	8.558166
Pushover-Y Acc	SLV	0.099956	1	0.278677	0.091649	0.091649	0.129535	5.707018	44.05758
Pushover-Y Acc	SLC	0.132733	1	0.376684	0.123881	0.123881	0.175091	7.709482	44.03122
Pushover+X Acc + e	SLD	0.036941	1	1	0.377776	0.377776	0.533944	3.849856	7.210227
Pushover+X Acc + e	SLV	0.099956	1	1	1.526002	1.526002	2.156834	4.484781	2.079336
Pushover+X Acc + e	SLC	0.132733	1	1	2.151663	2.151663	3.041136	6.319258	2.077927
Pushover-X Acc + e	SLD	0.036941	1	1	0.397608	0.397608	0.561975	0.285667	0.508326
Pushover-X Acc + e	SLV	0.099956	1	1	1.606115	1.606115	2.270064	2.171916	0.956764
Pushover-X Acc + e	SLC	0.132733	1	1	2.264622	2.264622	3.20079	3.369144	1.052598
Pushover+Y Acc + e	SLD	0.036941	1	0.126009	0.047334	0.047334	0.066901	0.499384	7.464544
Pushover+Y Acc + e	SLV	0.099956	1	0.348801	0.131022	0.131022	0.185185	4.993843	26.96674
Pushover+Y Acc + e	SLC	0.132733	1	0.471469	0.177101	0.177101	0.250312	6.687406	26.71624
Pushover-Y Acc + e	SLD	0.036941	1	0.100855	0.033054	0.033054	0.046718	0.400493	8.57252
Pushover-Y Acc + e	SLV	0.099956	1	0.279172	0.091495	0.091495	0.129319	5.707018	44.13148
Pushover-Y Acc + e	SLC	0.132733	1	0.377352	0.123673	0.123673	0.174798	7.709482	44.10507
PushoverEx+0.3Ey Acc	SLD	0.036941	1	1	0.358144	0.358144	0.506196	2.837317	5.605169
PushoverEx+0.3Ey Acc	SLV	0.099956	1	1	1.446701	1.446701	2.04475	5.456379	2.668482
PushoverEx+0.3Ey Acc	SLC	0.132733	1	1	2.039848	2.039848	2.883098	7.311547	2.536004
Pushover0.3Ex+Ey Acc	SLD	0.036941	1	1	0.112735	0.112735	0.159339	0.718448	4.508939
Pushover0.3Ex+Ey Acc	SLV	0.099956	1	0.641675	0.351397	0.351397	0.49666	2.052709	4.133024
Pushover0.3Ex+Ey Acc	SLC	0.132733	1	0.867343	0.474978	0.474978	0.671329	2.873793	4.280753
Pushover-0.3Ex+Ey Acc	SLD	0.036941	1	1	0.110749	0.110749	0.156532	0.097139	0.620569
Pushover-0.3Ex+Ey Acc	SLV	0.099956	1	0.604837	0.339125	0.339125	0.479315	0.874247	1.823951
Pushover-0.3Ex+Ey Acc	SLC	0.132733	1	0.81755	0.45839	0.45839	0.647884	1.165663	1.799186
Pushover-Ex+0.3Ey Acc	SLD	0.036941	1	1	0.406265	0.406265	0.57421	0.363219	0.632554
Pushover-Ex+0.3Ey Acc	SLV	0.099956	1	1	1.641081	1.641081	2.319485	2.451725	1.057013
Pushover-Ex+0.3Ey Acc	SLC	0.132733	1	1	2.313925	2.313925	3.270474	3.268967	0.999539

**50% of  $K_m$  Sway Stiffness in RC Frames**

5 Floors									
Analysis	Limit state	Demand						Capacity	$\alpha$
		PGA/g	S	q*	de*max	d*max	dmax	dsl	
Pushover+X Acc	SLD	0.036941	1	1	0.211796	0.211796	0.291662	1.601031	5.489336
Pushover+X Acc	SLV	0.099956	1	1	0.855536	0.855536	1.178151	2.401843	2.038654
Pushover+X Acc	SLC	0.132733	1	1	1.206306	1.206306	1.661194	3.250076	1.95647
Pushover-X Acc	SLD	0.036941	1	1	0.219328	0.219328	0.302035	0.426585	1.412369
Pushover-X Acc	SLV	0.099956	1	1	0.885962	0.885962	1.220051	1.928372	1.580566
Pushover-X Acc	SLC	0.132733	1	1	1.249207	1.249207	1.720273	2.692264	1.565022
Pushover+Y Acc	SLD	0.036941	1	0.081484	0.025539	0.025539	0.035169	0.399772	11.36714
Pushover+Y Acc	SLV	0.099956	1	0.225553	0.070693	0.070693	0.09735	3.29812	33.87896
Pushover+Y Acc	SLC	0.132733	1	0.304025	0.095287	0.095287	0.131219	4.497436	34.27424
Pushover-Y Acc	SLD	0.036941	1	0.078689	0.0138	0.0138	0.019004	0.200114	10.52995
Pushover-Y Acc	SLV	0.099956	1	0.187096	0.032812	0.032812	0.045186	3.702109	81.9313
Pushover-Y Acc	SLC	0.132733	1	0.246796	0.043282	0.043282	0.059604	5.002849	83.93504
Pushover+X Acc + e	SLD	0.036941	1	1	0.213047	0.213047	0.293386	1.607588	5.479432
Pushover+X Acc + e	SLV	0.099956	1	1	0.860592	0.860592	1.185115	2.398934	2.024221
Pushover+X Acc + e	SLC	0.132733	1	1	1.213435	1.213435	1.671012	3.262462	1.952387
Pushover-X Acc + e	SLD	0.036941	1	1	0.221112	0.221112	0.304491	0.355581	1.167787
Pushover-X Acc + e	SLV	0.099956	1	1	0.893168	0.893168	1.229975	1.954939	1.589414
Pushover-X Acc + e	SLC	0.132733	1	1	1.259367	1.259367	1.734265	2.74163	1.58086
Pushover+Y Acc + e	SLD	0.036941	1	0.082947	0.022716	0.022716	0.031282	0.299829	9.584681
Pushover+Y Acc + e	SLV	0.099956	1	0.226763	0.062102	0.062102	0.08552	3.29812	38.56538
Pushover+Y Acc + e	SLC	0.132733	1	0.298889	0.081855	0.081855	0.112722	4.497436	39.89864
Pushover-Y Acc + e	SLD	0.036941	1	0.078196	0.013883	0.013883	0.019118	0.200114	10.46717
Pushover-Y Acc + e	SLV	0.099956	1	0.186217	0.033061	0.033061	0.045529	3.702109	81.31397
Pushover-Y Acc + e	SLC	0.132733	1	0.245635	0.043611	0.043611	0.060056	5.002849	83.30338
PushoverEx+0.3Ey Acc	SLD	0.036941	1	1	0.200247	0.200247	0.275758	1.244608	4.513407
PushoverEx+0.3Ey Acc	SLV	0.099956	1	1	0.808884	0.808884	1.113907	2.800368	2.514004
PushoverEx+0.3Ey Acc	SLC	0.132733	1	1	1.140527	1.140527	1.57061	3.733823	2.377308
Pushover0.3Ex+Ey Acc	SLD	0.036941	1	0.174464	0.041962	0.041962	0.057785	0.303203	5.247095
Pushover0.3Ex+Ey Acc	SLV	0.099956	1	0.482926	0.116152	0.116152	0.159952	1.111744	6.95049
Pushover0.3Ex+Ey Acc	SLC	0.132733	1	0.652764	0.157001	0.157001	0.216205	1.516014	7.01194
Pushover-0.3Ex+Ey Acc	SLD	0.036941	1	0.152341	0.038646	0.038646	0.05322	0.098828	1.856979
Pushover-0.3Ex+Ey Acc	SLV	0.099956	1	0.421689	0.106975	0.106975	0.147315	0.592967	4.025161
Pushover-0.3Ex+Ey Acc	SLC	0.132733	1	0.569991	0.144597	0.144597	0.199124	0.88945	4.466823
Pushover-Ex+0.3Ey Acc	SLD	0.036941	1	1	0.19862	0.19862	0.273518	0.385005	1.407603
Pushover-Ex+0.3Ey Acc	SLV	0.099956	1	1	0.802315	0.802315	1.104861	1.732524	1.568092
Pushover-Ex+0.3Ey Acc	SLC	0.132733	1	1	1.131264	1.131264	1.557854	2.310032	1.482829

6 Floors									
Analysis	Limit state	Demand						Capacity	$\alpha$
		PGA/g	S	q*	de*max	d*max	dmax	dsl	
Pushover+X Acc	SLD	0.036941	1	1	0.311008	0.311008	0.436407	2.333906	5.348
Pushover+X Acc	SLV	0.099956	1	1	1.256298	1.256298	1.762841	2.907082	1.649089
Pushover+X Acc	SLC	0.132733	1	1	1.77138	1.77138	2.485606	4.305336	1.732107
Pushover-X Acc	SLD	0.036941	1	1	0.343073	0.343073	0.4814	0.121627	0.252652
Pushover-X Acc	SLV	0.099956	1	1	1.385821	1.385821	1.944588	1.825554	0.938787
Pushover-X Acc	SLC	0.132733	1	1	1.954008	1.954008	2.741869	2.678053	0.976725
Pushover+Y Acc	SLD	0.036941	1	0.133669	0.043002	0.043002	0.06034	0.399489	6.620613
Pushover+Y Acc	SLV	0.099956	1	0.370005	0.119031	0.119031	0.167025	4.094759	24.51586
Pushover+Y Acc	SLC	0.132733	1	0.50013	0.160893	0.160893	0.225765	5.49297	24.33045
Pushover-Y Acc	SLD	0.036941	1	0.119526	0.024032	0.024032	0.033722	0.200256	5.938357
Pushover-Y Acc	SLV	0.099956	1	0.330856	0.066523	0.066523	0.093345	4.405624	47.19697
Pushover-Y Acc	SLC	0.132733	1	0.43793	0.088052	0.088052	0.123555	5.907542	47.81318
Pushover+X Acc + e	SLD	0.036941	1	1	0.311082	0.311082	0.436511	2.322815	5.321322
Pushover+X Acc + e	SLV	0.099956	1	1	1.256596	1.256596	1.763259	3.237756	1.836234
Pushover+X Acc + e	SLC	0.132733	1	1	1.7718	1.7718	2.486196	4.401662	1.770441
Pushover-X Acc + e	SLD	0.036941	1	1	0.343627	0.343627	0.482178	0.121862	0.252733
Pushover-X Acc + e	SLV	0.099956	1	1	1.388059	1.388059	1.947728	1.825477	0.937234
Pushover-X Acc + e	SLC	0.132733	1	1	1.957163	1.957163	2.746297	2.631136	0.958067
Pushover+Y Acc + e	SLD	0.036941	1	0.132528	0.043432	0.043432	0.060944	0.399489	6.555053
Pushover+Y Acc + e	SLV	0.099956	1	0.366845	0.120222	0.120222	0.168695	4.094759	24.27309
Pushover+Y Acc + e	SLC	0.132733	1	0.495859	0.162502	0.162502	0.228023	5.49297	24.08952
Pushover-Y Acc + e	SLD	0.036941	1	0.119858	0.024088	0.024088	0.0338	0.200256	5.92478
Pushover-Y Acc + e	SLV	0.099956	1	0.331773	0.066676	0.066676	0.093559	4.405624	47.08906
Pushover-Y Acc + e	SLC	0.132733	1	0.439443	0.088314	0.088314	0.123922	5.907542	47.67141
PushoverEx+0.3Ey Acc	SLD	0.036941	1	1	0.295813	0.295813	0.415086	1.81725	4.378004
PushoverEx+0.3Ey Acc	SLV	0.099956	1	1	1.194921	1.194921	1.676716	3.741396	2.231383
PushoverEx+0.3Ey Acc	SLC	0.132733	1	1	1.684838	1.684838	2.36417	5.024161	2.125127
Pushover0.3Ex+Ey Acc	SLD	0.036941	1	0.268116	0.091215	0.091215	0.127993	0.40785	3.186508
Pushover0.3Ex+Ey Acc	SLV	0.099956	1	0.74216	0.252487	0.252487	0.354291	1.529436	4.316894
Pushover0.3Ex+Ey Acc	SLC	0.132733	1	1.003167	0.341283	0.341924	0.479789	2.039248	4.250301
Pushover-0.3Ex+Ey Acc	SLD	0.036941	1	0.241628	0.089748	0.089748	0.125935	0	0
Pushover-0.3Ex+Ey Acc	SLV	0.099956	1	0.668839	0.248428	0.248428	0.348594	0.586818	1.683385
Pushover-0.3Ex+Ey Acc	SLC	0.132733	1	0.904061	0.335796	0.335796	0.47119	0.880228	1.868095
Pushover-Ex+0.3Ey Acc	SLD	0.036941	1	1	0.329806	0.329806	0.462785	0.093033	0.201028
Pushover-Ex+0.3Ey Acc	SLV	0.099956	1	1	1.332232	1.332232	1.869392	1.767619	0.945558
Pushover-Ex+0.3Ey Acc	SLC	0.132733	1	1	1.878448	1.878448	2.635844	2.418848	0.917675

35% of  $K_m$  Sway Stiffness in Steel Frames

5 Floors									
Analysis	Limit state	Demand						Capacity	$\alpha$
		PGA/g	S	q*	de*max	d*max	dmax	dsl	
Pushover+X Acc	SLD	0.036941	1	1	0.194486	0.194486	0.264792	1.482507	5.598765
Pushover+X Acc	SLV	0.099956	1	1	0.785614	0.785614	1.06961	1.746827	1.633143
Pushover+X Acc	SLC	0.132733	1	1	1.107717	1.107717	1.508151	2.393643	1.587137
Pushover-X Acc	SLD	0.036941	1	1	0.215874	0.215874	0.293912	0.404275	1.375496
Pushover-X Acc	SLV	0.099956	1	1	0.872012	0.872012	1.18724	1.519309	1.279698
Pushover-X Acc	SLC	0.132733	1	1	1.229536	1.229536	1.674008	2.091979	1.249683
Pushover+Y Acc	SLD	0.036941	1	0.059173	0.05123	0.05123	0.069749	1.099074	15.75757
Pushover+Y Acc	SLV	0.099956	1	0.163794	0.141807	0.141807	0.193069	3.497055	18.11297
Pushover+Y Acc	SLC	0.132733	1	0.221399	0.191678	0.191678	0.260969	4.79596	18.37753
Pushover-Y Acc	SLD	0.036941	1	0.055782	0.020181	0.020181	0.027476	0.400337	14.57024
Pushover-Y Acc	SLV	0.099956	1	0.147324	0.053299	0.053299	0.072567	4.203535	57.92645
Pushover-Y Acc	SLC	0.132733	1	0.194218	0.070265	0.070265	0.095665	5.687585	59.4529
Pushover+X Acc + e	SLD	0.036941	1	1	0.19354	0.19354	0.263504	1.354233	5.139332
Pushover+X Acc + e	SLV	0.099956	1	1	0.781793	0.781793	1.064407	1.742027	1.636617
Pushover+X Acc + e	SLC	0.132733	1	1	1.102328	1.102328	1.500814	2.378751	1.584974
Pushover-X Acc + e	SLD	0.036941	1	1	0.216341	0.216341	0.294547	0.407104	1.382136
Pushover-X Acc + e	SLV	0.099956	1	1	0.873896	0.873896	1.189806	1.525374	1.282036
Pushover-X Acc + e	SLC	0.132733	1	1	1.232194	1.232194	1.677626	2.101866	1.252881
Pushover+Y Acc + e	SLD	0.036941	1	0.058924	0.050561	0.050561	0.068838	1.099074	15.96609
Pushover+Y Acc + e	SLV	0.099956	1	0.163106	0.139955	0.139955	0.190548	3.497055	18.35266
Pushover+Y Acc + e	SLC	0.132733	1	0.220468	0.189175	0.189175	0.25756	4.79596	18.62071
Pushover-Y Acc + e	SLD	0.036941	1	0.055524	0.021206	0.021206	0.028872	0.500421	17.33215
Pushover-Y Acc + e	SLV	0.099956	1	0.148764	0.056817	0.056817	0.077357	4.203535	54.33977
Pushover-Y Acc + e	SLC	0.132733	1	0.196101	0.074897	0.074897	0.101972	5.691926	55.81854
PushoverEx+0.3Ey Acc	SLD	0.036941	1	1	0.184282	0.184282	0.250899	0.928134	3.699233
PushoverEx+0.3Ey Acc	SLV	0.099956	1	1	0.744396	0.744396	1.013491	1.753142	1.729804
PushoverEx+0.3Ey Acc	SLC	0.132733	1	1	1.049598	1.049598	1.429023	2.371898	1.659804
Pushover0.3Ex+Ey Acc	SLD	0.036941	1	0.171501	0.035623	0.035623	0.0485	0.201735	4.159495
Pushover0.3Ex+Ey Acc	SLV	0.099956	1	0.474725	0.098605	0.098605	0.13425	0.706073	5.25937
Pushover0.3Ex+Ey Acc	SLC	0.132733	1	0.641679	0.133283	0.133283	0.181464	1.008675	5.558529
Pushover-0.3Ex+Ey Acc	SLD	0.036941	1	0.147573	0.036037	0.036037	0.049064	0.098978	2.017342
Pushover-0.3Ex+Ey Acc	SLV	0.099956	1	0.408492	0.099751	0.099751	0.135811	0.49489	3.643969
Pushover-0.3Ex+Ey Acc	SLC	0.132733	1	0.552152	0.134832	0.134832	0.183573	0.791824	4.313391
Pushover-Ex+0.3Ey Acc	SLD	0.036941	1	1	0.239949	0.239949	0.326689	0.387311	1.185565
Pushover-Ex+0.3Ey Acc	SLV	0.099956	1	1	0.969258	0.969258	1.31964	1.549243	1.173989
Pushover-Ex+0.3Ey Acc	SLC	0.132733	1	1	1.366654	1.366654	1.860693	2.130209	1.144848

6 Floors									
Analysis	Limit state	Demand						Capacity	$\alpha$
		PGA/g	S	q*	de*max	d*max	dmax	dsl	
Pushover+X Acc	SLD	0.036941	1	1	0.243973	0.243973	0.337404	1.735385	5.143342
Pushover+X Acc	SLV	0.099956	1	1	0.985514	0.985514	1.362924	2.134735	1.566291
Pushover+X Acc	SLC	0.132733	1	1	1.389575	1.389575	1.921723	3.016339	1.569601
Pushover-X Acc	SLD	0.036941	1	1	0.268167	0.268167	0.370864	0.44454	1.198663
Pushover-X Acc	SLV	0.099956	1	1	1.083245	1.083245	1.498081	1.675363	1.118339
Pushover-X Acc	SLC	0.132733	1	1	1.527376	1.527376	2.112295	2.410184	1.141026
Pushover+Y Acc	SLD	0.036941	1	0.104827	0.017677	0.017677	0.024447	0.199785	8.172236
Pushover+Y Acc	SLV	0.099956	1	0.266629	0.044962	0.044962	0.062181	0.899031	14.45834
Pushover+Y Acc	SLC	0.132733	1	0.351571	0.059286	0.059286	0.08199	1.198709	14.62012
Pushover-Y Acc	SLD	0.036941	1	0.071582	0.017605	0.017605	0.024348	0.300323	12.33482
Pushover-Y Acc	SLV	0.099956	1	0.181864	0.044729	0.044729	0.061858	5.105487	82.53558
Pushover-Y Acc	SLC	0.132733	1	0.239804	0.058979	0.058979	0.081565	6.807317	83.45855
Pushover+X Acc + e	SLD	0.036941	1	1	0.243304	0.243304	0.336479	1.920718	5.70829
Pushover+X Acc + e	SLV	0.099956	1	1	0.982811	0.982811	1.359185	2.341088	1.72242
Pushover+X Acc + e	SLC	0.132733	1	1	1.385764	1.385764	1.916452	3.128535	1.632462
Pushover-X Acc + e	SLD	0.036941	1	1	0.268575	0.268575	0.371427	0.445714	1.200004
Pushover-X Acc + e	SLV	0.099956	1	1	1.084891	1.084891	1.500358	1.682293	1.121261
Pushover-X Acc + e	SLC	0.132733	1	1	1.529697	1.529697	2.115505	2.453069	1.159567
Pushover+Y Acc + e	SLD	0.036941	1	0.083055	0.027042	0.027042	0.037398	0.39957	10.68414
Pushover+Y Acc + e	SLV	0.099956	1	0.229902	0.074855	0.074855	0.103521	4.395265	42.45779
Pushover+Y Acc + e	SLC	0.132733	1	0.310755	0.10118	0.10118	0.139928	5.893651	42.11928
Pushover-Y Acc + e	SLD	0.036941	1	0.071356	0.018585	0.018585	0.025702	0.300323	11.68478
Pushover-Y Acc + e	SLV	0.099956	1	0.184073	0.047942	0.047942	0.066302	5.205595	78.5135
Pushover-Y Acc + e	SLC	0.132733	1	0.242696	0.063211	0.063211	0.087418	7.007533	80.16163
PushoverEx+0.3Ey Acc	SLD	0.036941	1	1	0.232313	0.232313	0.321279	1.357355	4.224847
PushoverEx+0.3Ey Acc	SLV	0.099956	1	1	0.938415	0.938415	1.297788	2.297062	1.769983
PushoverEx+0.3Ey Acc	SLC	0.132733	1	1	1.323165	1.323165	1.82988	3.132358	1.711783
Pushover0.3Ex+Ey Acc	SLD	0.036941	1	0.256271	0.083146	0.083146	0.114988	0.404935	3.521551
Pushover0.3Ex+Ey Acc	SLV	0.099956	1	0.709372	0.230153	0.230153	0.318292	0.80987	2.544422
Pushover0.3Ex+Ey Acc	SLC	0.132733	1	0.958848	0.311095	0.311095	0.430231	1.113571	2.588308
Pushover-0.3Ex+Ey Acc	SLD	0.036941	1	0.18061	0.058246	0.058246	0.080552	0.098569	1.223667
Pushover-0.3Ex+Ey Acc	SLV	0.099956	1	0.49994	0.161229	0.161229	0.222972	0.689982	3.094471
Pushover-0.3Ex+Ey Acc	SLC	0.132733	1	0.675761	0.217931	0.217931	0.301389	0.985688	3.270488
Pushover-Ex+0.3Ey Acc	SLD	0.036941	1	1	0.295912	0.295912	0.409233	0.382115	0.933735
Pushover-Ex+0.3Ey Acc	SLV	0.099956	1	1	1.195317	1.195317	1.653072	1.815048	1.097985
Pushover-Ex+0.3Ey Acc	SLC	0.132733	1	1	1.685397	1.685397	2.330832	2.48375	1.065607

7 Floors									
Analysis	Limit state	Demand						Capacity	$\alpha$
		PGA/g	S	q*	de*max	d*max	dmax	dsl	
Pushover+X Acc	SLD	0.036941	1	1	0.304436	0.304436	0.461999	1.202311	2.60241
Pushover+X Acc	SLV	0.099956	1	1	1.22975	1.22975	1.866218	1.202311	0.64425
Pushover+X Acc	SLC	0.132733	1	1	1.733948	1.733948	2.631367	1.740523	0.661452
Pushover-X Acc	SLD	0.036941	1	1	0.342372	0.342372	0.51957	0.343893	0.661881
Pushover-X Acc	SLV	0.099956	1	1	1.382992	1.382992	2.098771	2.155198	1.026886
Pushover-X Acc	SLC	0.132733	1	1	1.950019	1.950019	2.959268	2.878351	0.972656
Pushover+Y Acc	SLD	0.036941	1	0.173852	0.025474	0.025474	0.044856	0.199731	4.452734
Pushover+Y Acc	SLV	0.099956	1	0.481233	0.070514	0.070514	0.124163	0.399461	3.217229
Pushover+Y Acc	SLC	0.132733	1	0.648164	0.094973	0.094973	0.167233	0.639542	3.824252
Pushover-Y Acc	SLD	0.036941	1	0.11512	0.025802	0.025802	0.045434	0.300404	6.61192
Pushover-Y Acc	SLV	0.099956	1	0.318659	0.071422	0.071422	0.125763	1.802425	14.33191
Pushover-Y Acc	SLC	0.132733	1	0.430727	0.09654	0.09654	0.169992	2.503368	14.72637
Pushover+X Acc + e	SLD	0.036941	1	1	0.303415	0.303415	0.460451	0.849236	1.844358
Pushover+X Acc + e	SLV	0.099956	1	1	1.225628	1.225628	1.859962	0.849236	0.456588
Pushover+X Acc + e	SLC	0.132733	1	1	1.728135	1.728135	2.622547	1.232441	0.46994
Pushover-X Acc + e	SLD	0.036941	1	1	0.342938	0.342938	0.520428	0.346111	0.665049
Pushover-X Acc + e	SLV	0.099956	1	1	1.385277	1.385277	2.102239	1.853714	0.88178
Pushover-X Acc + e	SLC	0.132733	1	1	1.953241	1.953241	2.964158	2.824622	0.952926
Pushover+Y Acc + e	SLD	0.036941	1	0.166262	0.02379	0.02379	0.04189	0.199731	4.767968
Pushover+Y Acc + e	SLV	0.099956	1	0.460221	0.065852	0.065852	0.115954	0.499326	4.306242
Pushover+Y Acc + e	SLC	0.132733	1	0.607329	0.086901	0.086901	0.153018	0.699057	4.568454
Pushover-Y Acc + e	SLD	0.036941	1	0.115316	0.026235	0.026235	0.046196	0.400539	8.670464
Pushover-Y Acc + e	SLV	0.099956	1	0.319201	0.07262	0.07262	0.127873	1.802425	14.09548
Pushover-Y Acc + e	SLC	0.132733	1	0.431459	0.09816	0.09816	0.172843	2.501541	14.47287
PushoverEx+0.3Ey Acc	SLD	0.036941	1	1	0.284003	0.284003	0.395094	0.740801	1.875
PushoverEx+0.3Ey Acc	SLV	0.099956	1	1	1.147212	1.147212	1.595958	0.740801	0.464173
PushoverEx+0.3Ey Acc	SLC	0.132733	1	1	1.617569	1.617569	2.2503	1.095808	0.486961
Pushover0.3Ex+Ey Acc	SLD	0.036941	1	0.218754	0.051225	0.051225	0.082083	0.304908	3.714647
Pushover0.3Ex+Ey Acc	SLV	0.099956	1	0.605523	0.141795	0.141795	0.22721	0.304908	1.34197
Pushover0.3Ex+Ey Acc	SLC	0.132733	1	0.818477	0.191662	0.191662	0.307116	0.475372	1.547858
Pushover-0.3Ex+Ey Acc	SLD	0.036941	1	0.211368	0.065124	0.065124	0.106056	0.098117	0.925139
Pushover-0.3Ex+Ey Acc	SLV	0.099956	1	0.585079	0.180267	0.180267	0.293569	0.88305	3.007978
Pushover-0.3Ex+Ey Acc	SLC	0.132733	1	0.790843	0.243665	0.243665	0.396814	1.1774	2.967137
Pushover-Ex+0.3Ey Acc	SLD	0.036941	1	1	0.358055	0.358055	0.498896	0.376389	0.754442
Pushover-Ex+0.3Ey Acc	SLV	0.099956	1	1	1.446343	1.446343	2.015262	2.164235	1.073922
Pushover-Ex+0.3Ey Acc	SLC	0.132733	1	1	2.039345	2.039345	2.84152	2.917012	1.026567

50% of  $K_m$  Sway Stiffness in Steel Frames

5 Floors									
Analysis	Limit state	Demand						Capacity	$\alpha$
		PGA/g	S	q*	de*max	d*max	dmax	dsl	
Pushover+X Acc	SLD	0.036941	1	1	0.218569	0.218569	0.297981	1.380316	4.632221
Pushover+X Acc	SLV	0.099956	1	1	0.882896	0.882896	1.203678	1.65493	1.374894
Pushover+X Acc	SLC	0.132733	1	1	1.244883	1.244883	1.697186	2.238123	1.318726
Pushover-X Acc	SLD	0.036941	1	1	0.237119	0.237119	0.323271	0.327747	1.013846
Pushover-X Acc	SLV	0.099956	1	1	0.957828	0.957828	1.305836	1.32089	1.011528
Pushover-X Acc	SLC	0.132733	1	1	1.350538	1.350538	1.841229	1.832641	0.995336
Pushover+Y Acc	SLD	0.036941	1	0.069929	0.027989	0.027989	0.038158	0.499665	13.09473
Pushover+Y Acc	SLV	0.099956	1	0.193567	0.077474	0.077474	0.105623	3.497654	33.1146
Pushover+Y Acc	SLC	0.132733	1	0.261642	0.104721	0.104721	0.142769	4.796783	33.59827
Pushover-Y Acc	SLD	0.036941	1	0.063144	0.012678	0.012678	0.017284	0.200134	11.57929
Pushover-Y Acc	SLV	0.099956	1	0.146833	0.02948	0.02948	0.040191	4.102747	102.0808
Pushover-Y Acc	SLC	0.132733	1	0.193712	0.038892	0.038892	0.053023	5.503685	103.7982
Pushover+X Acc + e	SLD	0.036941	1	1	0.218351	0.218351	0.297684	1.38063	4.637905
Pushover+X Acc + e	SLV	0.099956	1	1	0.882014	0.882014	1.202477	1.654399	1.375826
Pushover+X Acc + e	SLC	0.132733	1	1	1.24364	1.24364	1.695492	2.236612	1.319152
Pushover-X Acc + e	SLD	0.036941	1	1	0.237549	0.237549	0.323857	0.328096	1.01309
Pushover-X Acc + e	SLV	0.099956	1	1	0.959563	0.959563	1.308201	1.325323	1.013088
Pushover-X Acc + e	SLC	0.132733	1	1	1.352984	1.352984	1.844564	1.836389	0.995568
Pushover+Y Acc + e	SLD	0.036941	1	0.069406	0.029346	0.029346	0.040009	0.499665	12.48885
Pushover+Y Acc + e	SLV	0.099956	1	0.192118	0.081233	0.081233	0.110747	3.497654	31.58243
Pushover+Y Acc + e	SLC	0.132733	1	0.259684	0.109801	0.109801	0.149695	4.796783	32.04372
Pushover-Y Acc + e	SLD	0.036941	1	0.062569	0.012792	0.012792	0.01744	0.200134	11.47589
Pushover-Y Acc + e	SLV	0.099956	1	0.145836	0.029815	0.029815	0.040648	4.102747	100.9339
Pushover-Y Acc + e	SLC	0.132733	1	0.192393	0.039334	0.039334	0.053625	5.601842	104.464
PushoverEx+0.3Ey Acc	SLD	0.036941	1	1	0.209093	0.209093	0.285063	1.244117	4.364363
PushoverEx+0.3Ey Acc	SLV	0.099956	1	1	0.844618	0.844618	1.151493	1.451469	1.260511
PushoverEx+0.3Ey Acc	SLC	0.132733	1	1	1.190912	1.190912	1.623606	2.073527	1.277113
Pushover0.3Ex+Ey Acc	SLD	0.036941	1	0.152741	0.041872	0.041872	0.057085	0.303141	5.310325
Pushover0.3Ex+Ey Acc	SLV	0.099956	1	0.422796	0.115904	0.115904	0.158015	0.606282	3.836862
Pushover0.3Ex+Ey Acc	SLC	0.132733	1	0.571487	0.156665	0.156665	0.213587	0.808376	3.784767
Pushover-0.3Ex+Ey Acc	SLD	0.036941	1	0.130627	0.041612	0.041612	0.056731	0.09883	1.742072
Pushover-0.3Ex+Ey Acc	SLV	0.099956	1	0.361583	0.115185	0.115185	0.157035	0.39532	2.517394
Pushover-0.3Ex+Ey Acc	SLC	0.132733	1	0.488746	0.155694	0.155694	0.212263	0.59298	2.793616
Pushover-Ex+0.3Ey Acc	SLD	0.036941	1	1	0.224192	0.224192	0.305647	0.28886	0.945078
Pushover-Ex+0.3Ey Acc	SLV	0.099956	1	1	0.905608	0.905608	1.234643	1.251728	1.013838
Pushover-Ex+0.3Ey Acc	SLC	0.132733	1	1	1.276908	1.276908	1.740847	1.733161	0.995585

6 Floors									
Analysis	Limit state	Demand						Capacity	$\alpha$
		PGA/g	S	q*	de*max	d*max	dmax	dsl	
Pushover+X Acc	SLD	0.036941	1	1	0.267884	0.267884	0.370923	1.980187	5.338533
Pushover+X Acc	SLV	0.099956	1	1	1.082102	1.082102	1.498323	1.980187	1.321603
Pushover+X Acc	SLC	0.132733	1	1	1.525764	1.525764	2.112635	2.876138	1.361398
Pushover-X Acc	SLD	0.036941	1	1	0.293885	0.293885	0.406925	0.265135	0.651558
Pushover-X Acc	SLV	0.099956	1	1	1.187132	1.187132	1.643751	1.617162	0.983825
Pushover-X Acc	SLC	0.132733	1	1	1.673856	1.673856	2.317688	2.159301	0.931661
Pushover+Y Acc	SLD	0.036941	1	0.086964	0.028128	0.028128	0.038947	0.399668	10.26182
Pushover+Y Acc	SLV	0.099956	1	0.240721	0.07786	0.07786	0.107808	4.396352	40.77952
Pushover+Y Acc	SLC	0.132733	1	0.325379	0.105242	0.105242	0.145722	5.89511	40.4544
Pushover-Y Acc	SLD	0.036941	1	0.07201	0.016064	0.016064	0.022243	0.300249	13.4987
Pushover-Y Acc	SLV	0.099956	1	0.178365	0.03979	0.03979	0.055095	5.104228	92.64494
Pushover-Y Acc	SLC	0.132733	1	0.235224	0.052474	0.052474	0.072657	6.90572	95.04503
Pushover+X Acc + e	SLD	0.036941	1	1	0.267475	0.267475	0.370357	1.974174	5.330457
Pushover+X Acc + e	SLV	0.099956	1	1	1.080451	1.080451	1.496036	1.974174	1.319603
Pushover+X Acc + e	SLC	0.132733	1	1	1.523436	1.523436	2.109411	2.866145	1.358742
Pushover-X Acc + e	SLD	0.036941	1	1	0.295581	0.295581	0.409273	0.265471	0.648639
Pushover-X Acc + e	SLV	0.099956	1	1	1.193981	1.193981	1.653235	1.414809	0.855782
Pushover-X Acc + e	SLC	0.132733	1	1	1.683513	1.683513	2.331061	2.172201	0.931851
Pushover+Y Acc + e	SLD	0.036941	1	0.085811	0.029576	0.029576	0.040952	0.399668	9.759392
Pushover+Y Acc + e	SLV	0.099956	1	0.237531	0.081868	0.081868	0.113358	4.396352	38.78292
Pushover+Y Acc + e	SLC	0.132733	1	0.321067	0.11066	0.11066	0.153224	5.995026	39.12581
Pushover-Y Acc + e	SLD	0.036941	1	0.071834	0.015797	0.015797	0.021873	0.300249	13.72698
Pushover-Y Acc + e	SLV	0.099956	1	0.177115	0.038949	0.038949	0.05393	5.104228	94.64491
Pushover-Y Acc + e	SLC	0.132733	1	0.233581	0.051366	0.051366	0.071124	6.805637	95.68708
PushoverEx+0.3Ey Acc	SLD	0.036941	1	1	0.256032	0.256032	0.354512	1.575756	4.444854
PushoverEx+0.3Ey Acc	SLV	0.099956	1	1	1.034226	1.034226	1.432031	1.890907	1.320437
PushoverEx+0.3Ey Acc	SLC	0.132733	1	1	1.458259	1.458259	2.019165	2.62626	1.300667
Pushover0.3Ex+Ey Acc	SLD	0.036941	1	0.16883	0.058874	0.058874	0.08152	0.405784	4.977728
Pushover0.3Ex+Ey Acc	SLV	0.099956	1	0.46733	0.162968	0.162968	0.225652	0.710121	3.146983
Pushover0.3Ex+Ey Acc	SLC	0.132733	1	0.631683	0.220281	0.220281	0.30501	1.014459	3.325986
Pushover-0.3Ex+Ey Acc	SLD	0.036941	1	0.147301	0.05719	0.05719	0.079188	0.098402	1.242643
Pushover-0.3Ex+Ey Acc	SLV	0.099956	1	0.407738	0.158305	0.158305	0.219196	0.590412	2.693537
Pushover-0.3Ex+Ey Acc	SLC	0.132733	1	0.551134	0.213979	0.213979	0.296284	0.787216	2.656965
Pushover-Ex+0.3Ey Acc	SLD	0.036941	1	1	0.287527	0.287527	0.398122	0.189808	0.476758
Pushover-Ex+0.3Ey Acc	SLV	0.099956	1	1	1.16145	1.16145	1.608191	1.518464	0.944206
Pushover-Ex+0.3Ey Acc	SLC	0.132733	1	1	1.637644	1.637644	2.267549	2.087888	0.920769